Diastereoselective Transformations of Macrocyclic 1,4-Diketones for the Synthesis of Cyclobutane-containing Natural Products

by

Kara F. Johnson

A dissertation submitted to the Graduate Faculty of
Auburn University
in partial fulfillment of the
requirements for the Degree of
Doctor of Philosophy

Auburn, Alabama
December 12, 2020

Keywords: Diastereoselective, macrocyclic diketone, cyclobutane,
transannular McMurry, Grignard addition

Approved by

Bradley L. Merner, Chair, Associate Professor of Chemistry and Biochemistry
Doug Goodwin, Professor and Chair of Chemistry and Biochemistry
Ming Chen, Assistant Professor of Chemistry and Biochemistry
Rashad Karimov, Assistant Professor of Chemistry and Biochemistry

Abstract

CHAPTER 1

Macrocyclic conformation has been investigated since the 1950s. The understanding of this phenomenon has been applied to predict and explain diastereoselective reactions to macrocyclic systems since this time, and correlation is observed between the low-energy conformation of a macrocycle and the diastereoselectivity of reactions to that system. High levels of diastereoselectivity have been observed for Grignard reactions of macrocyclic 1,4-diketones. In all of the macrocycles investigated, ring size proved to be the greatest contributor to diastereoselectivity. As the size of the macrocyclic 1,4-diketone system employed decreases, the observed diastereoselectivity of the 1,2-addition increases. For vinyl Grignard additions other factors affecting the observed diastereoselectivity include Grignard halide, solvent, and bridging motif.

CHAPTER 2

Based on the results obtained from the studies of the Grignard reaction to macrocyclic 1,4-diketones, an investigation of enolate alkylations to these same macrocyclic diketones as a means to alkylate the α and α' positions diastereoselectively was undertaken. High levels of diastereoselectivity where obtained in these vicinal alkylation reactions, and the resulting macrocyclic 1,4-diketones were subsequently subjected to a five step sequence, featuring a transannular McMurry reaction, to afford di-*O*-methylendiandrin A as well as other lignan-type cyclobutane-containing compounds.

Acknowledgments

I would like to acknowledge those who have both pushed and supported me in my journey to this point. Firstly, I would like to express my gratitude to Prof. Bradley L. Merner for providing me the opportunity to learn under his guidance. He has taught me more than I could have imagined and has pushed me to grow as a scientist beyond the bounds of which I felt capable. I will carry these lessons with me into future endeavors as I continue to learn and grow throughout my life. I also wish to thank my committee members: Prof. Doug Goodwin, Prof. Rashad Karimov, Prof. Ming Chen, and Prof. Angela Calderón for their time, support, and suggestions.

I also would like to thank the Auburn University department of Chemistry and Biochemistry for the opportunity to learn from so many incredible professors and mentors both in classes and as a teaching assistant. My gratitude especially goes to Dr. Michael Meadows and Dr. Alvaro Herrera for teaching me so much about NMR spectroscopy and instrumentation. I have gained valuable knowledge and experience from both of these men as I served under them in the NMR facility. Also, a special thanks to Dr. Melissa Boersma for her help and instruction in mass spectrometry.

My deepest gratitude also belongs to my lab mates throughout my time in the Merner group. Nirmal, Ana, Caroline, Nirob, Sydney, Hank, Meng, and Jacob have all been a source of encouragement and have pushed me to grow as a leader and scientist. Other friends within the department, especially Jessica Krewall, Julie Niklas, and Ethan Hiti, have made my time here so much better, and I am so grateful for your friendship.

Lastly, I need to thank my church families at Auburn and Rose Hill for praying with me and for me and serving as constant support to keep going; my parents and siblings who have been both spiritually and physically present to support me; Rylie and Calum who have blessed my life beyond understanding with joy and perspective; and my loving husband, Scott, who has stood beside me, pushed me forward, and held me up every step of the way. God gave me these people to help strengthen me for this journey. It is only through His strength that I am here, and I could not be more grateful for His provision, salvation, and strength.

Table of Contents

List of Tables

List of Figures

List of Schemes

List of Abbreviations

Å	Angstroms
Ac	Acetyl
add'n	Addition
alk.	Alkylation
Ar	Aromatic
aq.	Aqueous
BArF	Tetrakis[3,5-bis(trifluoromethyl)phenyl]boron
BHT	2,6-Di-*tert*-butyl-*p*-hydroxytoluene
BINAL-H	Binaphthyllithium aluminum hydride
BINAM	2,2'-Bis(diphenylphosphinoamino)-1,1'-binaphthyl
Bn	Benzyl
BOM	Benzyloxymethyl
bpm	2,2'-bipyrimidine
brsm	Based on recovered starting material
Bz	Benzoyl
°C	Degrees celcius
cat.	Catalytic
CCl_4	Carbon tetrachloride
C_6D_6	Deuterated benzene
$CDCl_3$	Deuterated chloroform
CFL	Compact fluorescent lamp
C_6H_{14}	*n*-hexane
CH_2Cl_2	dichloromethane
cm	centimeters
cod	Cyclooctadiene
dCPA	2,2-Dicyclohexyl-2-phenylacetic acid
d	doublet
dd	doublet of doublets
ddd	doublet of doublet of doublets
DDQ	2,3,-Dichloro-5,6-dicyano-1,4-benzoquinone
DFT	Density functional theory
DMDO	Dimethyldioxirane
DME	Dimethyl ether
DMF	Dimethyl formamide
DMP	Dess-Martin periodinane

DMSO	Dimethyl sulfoxide
D_2O	Deuterium oxide
dpm	Bis(diphenylphosphino)methane
d.r.	Diastereomeric ratio
E^+	Electrophile
e^-	Electron
EDC	1-Ethyl-3-(3-dimethylaminopropyl)carbodiimide
e.e.	Enantiomeric excess
EE	Ethoxyethyl
ESI	Electrospray ionization
Et	Ethyl
Et_3N	Triethyl amine
Et_2O	Diethyl ether
EtOAc	Ethyl acetate
EtOH	Ethanol
equiv.	Equivalents
g	Gram
Grubbs II	Grubbs 2nd generation catalyst
h	hour
HG II	Hoveyda-Grubbs 2nd generation catalyst
HK	Hydroxyketone
HMPA	Hexamethylphosphoramide
$h\nu$	Light
HOMO	Highest occupied molecular orbital
HPLC	High-performance liquid chromatography
HRMS	High-resolution mass spectrometry
Hz	Hertz
IBX	2-Iodoxybenzoic acid
*i*Pr	Isopropyl
i-PrOH	Isopropanol
J	Coupling constant
kcal	Kilo-calories
KHMDS	Potassium hexamethyl disilazide
LDA	Lithium diisopropyl amide
LiHMDS	Lithium hexamethyl disilazide
LUMO	Lowest unoccupied molecular orbital
m	Multiplet

M	Molar
*m*CPBA	*meta*-Chloroperoxybenzoic acid
MD	Molecular dynamics
Me	Methyl
MeCN	Acetonitrile
MeOH	Methanol
MHz	Megahertz
Min.	Minute
mL	Milliliter
MM	Molecular mechanics
mmol	Millimole
mol	Mole
MOM	Methoxymethyl
MOPS	3-(N-morpholino)propanesulfonic acid
MS	Molecular sieves
MsCl	Methanesulfonyl chloride
NaHMDS	Sodium hexamethyldisilazide
nm	nanometers
NMR	Nuclear magnetic resonance
NOE	Nuclear Overhauser effect
Np	Naphthalene
NTTL	tetrakis[*N*-naphthaloyl-(*S*)-*tert*-leucinate]
Nuc.	Nucleophile
OAc	Acetate
oba	4,4'-oxybis(benzoate)
OsO_4	Osmium tetroxide
OTf	Trifluoromethanesulfonate
p	Pentet
PCC	Pyridinium chlorochromate
Ph	Phenyl
Ph_2CO	Benzophenone
PhH	Benzene
PhMe	Toluene
PMB	*para*-methoxybenzyl
p-OMeTPT	2,4,6- tris(4-methoxyphenyl)pyrylium tetrafluoroborate
PPh_3	Triphenylphosphine
ppm	Parts per million

ppy	2-phenylpyridinyl
pyr	Pyridine
QDs	Quantum dots
Q-TOF	Quadrupole time-of-flight
quant.	Quantitative
RCM	Ring closing metathesis
r.r.	Regiomeric ratio
s	singlet
S_0	Singlet ground state
S_1	Single excited state
SAMP	(*S*)-(–)-1-amino-2-(methoxymethyl)pyrrolidine
salen	Ethylenebis(salicylimine)
SEM	Trimethylsilylethoxymethyl
st-DNA	Salmon testes deoxyribonucleic acid
t	Triplet
T_1	Triplet excited state
TBAF	Tetra-n-butylammonium fluoride
TBAI	Tetrabutylammonium iodide
TBDPS	*tertiary*- butyl diisopropylsilyl
TBS	*tertiary*-butyldimethylsilyl
^{t}Bu	*tertiary*-butyl
^{t}BuOOH	*tertiary*-butyl hydrogen peroxide
td	triplet of doublets
temp.	Temperature
TfOH	Trifluoromethanesulfonic acid
THF	Tetrahydrofuran
$Ti(O^{i}Pr)_4$	Titanium isopropoxide
TLC	Thin-layer chromatography
TMEDA	Tetramethylethylenediamine
TMS	Trimethylsilyl
TsOH	*para*-Toluenesufonic acid
UV	Ultraviolet light
vic.	Vicinal
VT-NMR	Variable temperature nuclear magnetic resonance
W2 Ra Ni	Raney Nickel

CHAPTER 1 Stereoselective Reactions of Macrocycles

1. Introduction

For over six decades, scientists have been seeking to understand how ring conformation contributes to the outcome of organic reactions that involve macrocyclic systems (8-membered rings and larger). Before this time the works of Odd Hassel[1] and Derek Barton[2] on smaller rings (5, 6, and 7-membered) showed that there are obvious preferences for certain ring conformations and orientations of substituents. Through these efforts the field of conformational analysis – the study of energetic differences between rotamers – was born. Researchers like A. J. Hubert,[3] Johannes Dale,[3–5] and Frank Anet[6,7] were among the first to explore the conformations of medium and large rings in order to understand the preferred conformations of cycloalkanes, alkenes, and alkynes. Later studies by W. Clark Still,[8,9] E. J. Corey,[10] Takeyoshi Takahashi,[11,12] and E. Vedejs[13,14] set out to understand how the conformational preferences of a macrocycle could affect the stereoselectivity of a reaction to the macrocyclic backbone using reactions such as epoxidations,[8,10,12,13] enolate alkylations,[9,11] conjugate additions,[9] reductions,[9,11] and *syn*-dihydroxylations[13,14] on everything from 8-16 membered rings. What was seen repeatedly is that the low-energy starting conformation or that of the transition state dictates the observed stereoselectivity of the reactions.

This chapter will look first at the developments made toward understanding macrocyclic conformation, followed by an outline of how these conformational preferences have led to several stereoselective reactions and a better understanding of the role of conformation in reactivity. These advances have led to much of the work pursued by our research group, in which macrocyclic 1,4-diketones are employed for the synthesis of strained compounds.[15–18] Here the discussion will focus on the diastereoselective nature of 1,2-additions to macrocyclic 1,4-diketones, including trends observed based on macrocyclic size and preliminary computational studies on the conformations of these macrocycles in an effort to ascertain the true origin of the observed diastereoselectivity of these reactions.

1.1 Conformations of Macrocycles

1.1.1 General Observations

Hubert and Dale were among the very first to analyze macrocyclic conformation, looking at everything from 8- to 30-membered macrocyclic systems (only even-numbered) using what they knew about structure and analyzing melting points and transition points of different sized alkanes, alkenes, and alkynes.[5] What they found in their studies was that macrocycles between 8-14 carbons are necessarily strained because no possible conformation permitted the relief of unfavorable transannular interactions. However, larger cycloalkanes (more than 14 atoms), when in a con-

formation that limits transannular interactions, are not strained. Dale also suggested that odd-numbered systems always have some strain because of their lack of symmetry, and although, Still does not explicitly support this claim, he does note that odd-numbered ring systems have more low-energy conformations than do even-numbered systems, attributing this also to the lack of symmetry.[9]

In order to optimize the structures of various macrocycles, parameters such as angle strain and transannular strain should be limited, but the structure is also less favorable if it contains a cavity within the cycle,[5] so finding the balance between limiting transannular interactions and too great an opening at the center of the macrocycle can be challenging. Of course, not all macrocycles are simply cycloalkanes, but introducing unsaturation in the form of alkenes, alkynes, or double bond character (*i.e.* lactones, lactams, etc.) necessarily perturbs the system and generally causes the conformation to change to accommodate changes in hybridization and the incorporation of heteroatoms.[4,5,9] Introducing a single sp^2-hybridized center does not necessitate much change in the conformation, and depending on its placement within the cycle can actually serve to relieve some of the unfavorable transannular interactions.[4,7] Similarly, replacing a CH_2 group with an –O– or –NH– group does not generally perturb the ring, but it can serve to eliminate transannular interactions.[19] Specific examples of these considerations are outlined in the sections that follow.

1.1.2 Conformations of Medium-Sized Ring Systems

Medium-sized rings (8- to 11-membered systems) were among the first macrocycles to receive in-depth studies of both conformation and reactivity. A lot of what was first understood about these medium-sized rings, translated well to larger macrocycles, although, each macrocycle has some of its own considerations. Each of these will be discussed below.

Cyclooctane, the smallest of the medium-sized rings, prefers to maintain a boat-chair conformation (**1a**, **Figure 1**) in order to alleviate as much transannular strain as possible; however, the twist boat-chair (**1b**), crown (**1c**), and boat-boat (**1d**) conformations have also been calculated to be similar enough in energy that these conformations are also somewhat populated.[20] Even in the lowest energy boat-chair conformation, however, there is still some transannular strain between the hydrogens on carbons

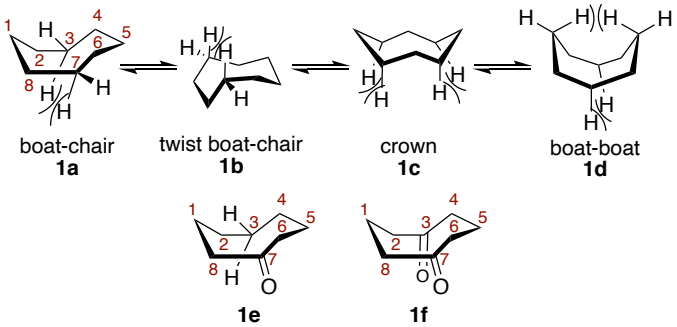

Figure 1: Conformations of cyclooctane (**1a-1d**), cyclooctanone (**1e**), and 1,5-cyclooctadione (**1f**).[7,20]

labeled C3 and C7 (**1a**, **Figure 1**); however, placement of a ketone at either the C3 or C7 positions alleviates this unfavorable transannular interaction because of the planar sp^2 nature now present at this position (**1e**, **Figure 1**). For the same reason, when the 8-membered ring has a 1,5-dicarbonyl, the macrocycle preferentially places the ketones at the C3 and C7 positions (**1f**, **Figure 1**). The same preferential placement of carbonyls that allows for transannular strain relief is also observed in the 9-, 10-, and 11-membered rings,[4,7] and it is this strain-relieving positioning of the ketones that makes them somewhat unreactive to borohydride reductions and hydrogen cyanide additions.[7] Such additions introduces the transannular strain that is absent in the ketone starting materials. The equilibrium of the addition reaction thus favors the ketone starting material rather than the addition product.

For cyclononane, many low-energy conformations have been determined computationally (8 by molecular mechanics,[21] and 7 by DFT[20]), but variable temperature nuclear magnetic resonance (VT-NMR) spectroscopy studies on the 9-membered cycloalkane, show that only two low-energy conformations are observed at temperatures as low as −173 °C (**Figure 2**, **2a** and **2b**) and three conformations at room temperature (also **2c**).[7,22,23] The energy difference between **2a** and **2b** is only 2.8 kcal/mol at −173 °C,[22] but this difference causes 95% of the molecules in solution to assume the twist-boat-chair conformation (**2a**).[24] As the temperature increases to room temperature, the energy gap closes to only about 1 kcal/mol,[20] and 50% of the solution assumes the twist-chair-boat conformation (**2b**), 40% the twist-boat-chair (**2a**), and 10% the twist-chair-chair conformation (**2c**), which is not observed at temperatures below −95 °C during VT-NMR studies.[24] However, placement of a single ketone unit within the 9-membered ring structure reduces the number of observed conformations, with the twist-boat-chair conformation (**3a**, **Figure 3**) being favored over the twist-chair-boat (**3b**) by *ca.* 5-6.5 kcal/mol.[7] Incorporating additional substitution around the ring increases the barrier for interconversion still further. For example, 4,4,7,7-tetramethylcyclononanone assumes the twist-boat-chair conformation (**3c**, **Figure 3**), with a barrier of interconversion of 14 kcal/mol. 4,4,8,8-Tetramethyl-1,2-cyclononanedione, however, assumes the twist-chair-boat conformation (**3e**, **Figure 3**) with a barrier of interconversion of 21 kcal/mol.[7]

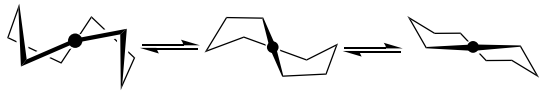

Figure 2: Lowest-energy conformations for cyclononane.[24]

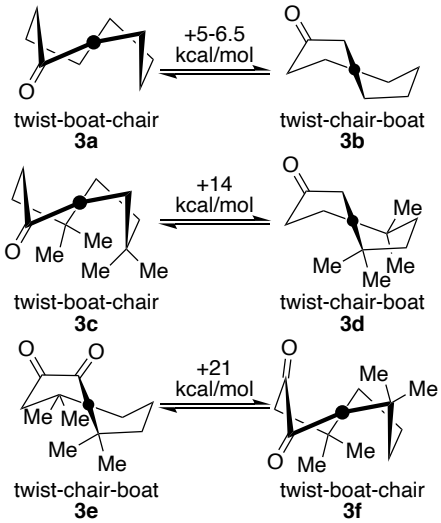

Figure 3: Conformations of substituted cyclononanes.[7]

Cyclodecane is generally thought to have one predominant conformation, the boat-chair-boat (**4a**, **Figure 4**), and while this is the lowest energy conformation based on DFT calculations, there are actually 6 different conformations that exist at room temperature with similar energies (less than 2 kcal/mol of difference between the lowest energy **4a** and **4c** and the highest energy **4e**) and in similar proportions (**Figure 4**).[20,25] Adding substitution, as seen for the 9-membered rings, reduces the number of ring conformations available at room temperature. Cyclodecanone (**4g**, **Figure 4**), for example, predominantly assumes the boat-chair-boat conformation at room temperature, positioning the ketone in such a way as to eliminate unfavorable transannular interactions (similar to that seen in **Figure 1**, **1b**).[7,26] Similarly, a *Z*-configured endocyclic olefin restricts the conformation of the 10-membered ring to only 1 conformation (boat-chair-boat) at room temperature (**4h**, **Figure 4**).[27,28] An *E*-alkene in a 10-membered ring, however, introduces strain such that no one conformation is preferred. In fact, *E*-cyclodecene has five different low-energy conformations interconverting at −155 °C with a barrier of 6.5-6.6 kcal/mol, but the exact conformations of these have not been elucidated.[27,29]

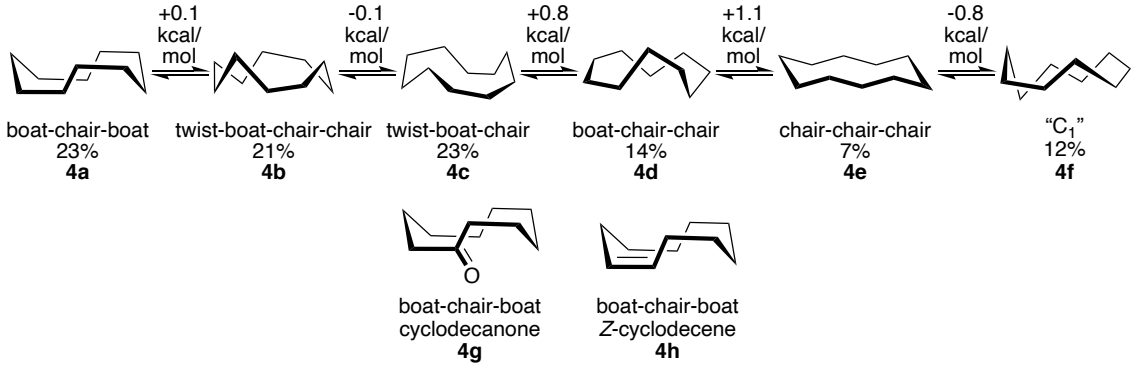

Figure 4: Lowest-energy conformations of cyclodecane (**4a**-**4f**), cyclodecanone (**4g**), and *Z*-cyclodecene (**4h**). Relative energy values and population calculated with b3lyp at room temperature.[20,25]

Cycloundecane is the most understudied of the medium-sized rings, so much less is understood about its structure. Both MM2 and MM3 calculations of cycloundecane indicate that there are many similar energy conformations (41 and 32 conformations, respectively);[21] When coupled with VT-NMR studies only two low-energy conformations emerge at low temperatures (−183 °C), and these two interconvert easily even at these low temperatures (**Figure 5**).[27,30] As the temperature increases, though, many additional conformations are seen for cycloundecane.[31] Similar to cyclodecanone, cycloundecanone only seems to have a single, unsymmetrical conformation, that of **5b**.[7,32] Unlike the other medium-sized rings, however,

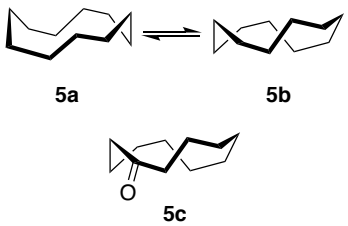

Figure 5: The two lowest energy conformations of cycloundecane (**5a** and **5b**) and cycloundecanone (**5c**).[25]

cycloundecane has some additional flexibility, as indicated by the number of possible conformations it possesses. It is not until 11 atoms are present in the cycle that a *trans* olefin is not only supported, but preferred. In smaller rings, the *trans* double bond may be possible but it increases the strain energy of the cycle.[4]

1.1.3 Conformations of Large Ring Systems

Macrocycles with 12 or more members are considered large ring systems. These systems are less conformationally restricted than small- and medium-ring systems; however, they do still exhibit conformational preferences as saturated cycloalkanes, and these conformational preferences become more pronounced with increased substitution, which will be addressed in the paragraphs that follow. Despite these preferences, because of their more flexible structures, the presence of a single functional group, such as a single ketone, does not impose the same conformational restrictions or preferences in a large macrocycle as it does in medium-sized macrocyle. The presence of dicarbonyl functional groups (diketone, dilactones, dilactams, etc.), however, can have significant effects on the structure due to the dipole interactions and the addition of partial double bond character (dilactones and dilactams).[4] Other rigidifyling elements such as olefins can affect the shape of the macrocyle, and even stereogenic centers can themselves affect the shape of the macrocycle because of non-bonded interactions.[33] In the paragraphs that follow, the details of each large macrocycle's conformational preferences will be laid out.

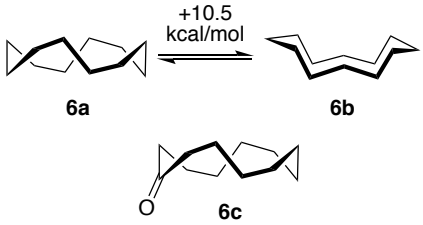

Figure 6: Lowest energy conformations of cyclododecane (**6a-b**)[35] and cyclododecanone (**6c**)[36]

Because of the increasing number of possible conformations with each additional CH_2 group throughout the medium-sized rings, it is no surprise that for cyclododecane MM2 calculations predict 121 possible conformations and MM3 predicts 97.[21] Despite all of the possible conformations, VT-NMR studies indicate only two interconverting conformations at room temperature (**Figure 6**).[34] Combining this with electron diffraction and computational techniques has shown that in fact there is only one low-energy conformation (**6a**). The next lowest energy conformation is 10.5 kcal/mol higher in energy (**6b**).[35] Cyclododecanone is believed to have only one conformation (**6c**, **Figure 6**) at low temperatures, but at room temperature and above, population of other conformations is possible.[5,36] Introducing an *E*-configured olefin into the backbone of the macrocycle, however, increases the number of low-energy conformations to four (**Figure 7**, **7a**-**7d**),[27,34] and likewise a *Z*-configured olefin has two interconverting conformations (**Figure 7**, **7e**-**7f**).[37]

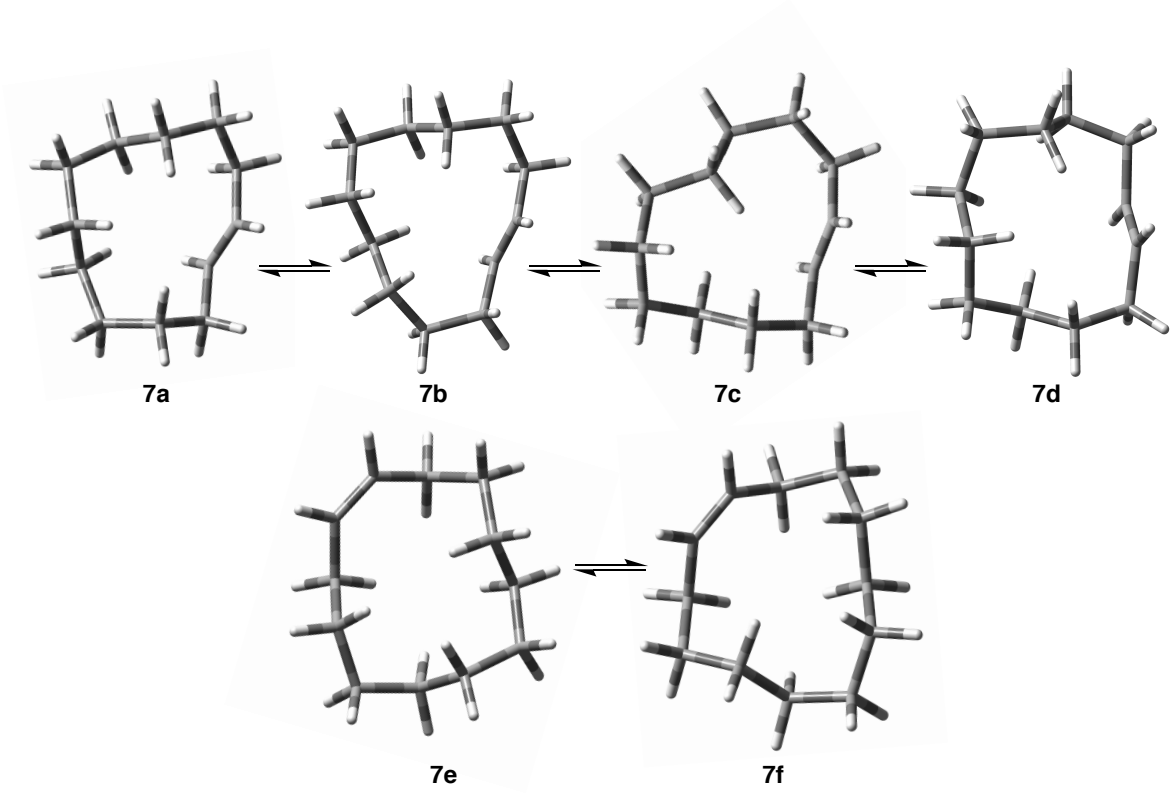

Figure 7: Lowest energy conformations of *E*-cyclododecene (**7a**-**7d**)[27,34] and *Z*-cyclododecene (**7e**-**7f**)[37]

Cyclotridecane, and other 13-membered ring systems have not been studied extensively. Even at low temperatures, NMR studies show that cyclotridecane interconverts too quickly to definitively identify its structures, but computational studies indicate that cyclotridecane has five low-energy conformations (**Figure 8**),[38–40] three of which are predicted to be significantly populated at room temperature, including **8a**, **8b**, and one of the triangular structures **8c-e**, but which of these triangular structures is still unclear.[39] Several NMR and computational studies agree that **8a** is the lowest energy conformation for cyclotridecane, accounting for about 80% of the conformational population at room temperature.[38,41] Others, however, argue that **8b** is the preferred conformation of cyclotridecane because of structural similarities between x-ray and computational data, and the calculated relative energy difference between **8a** and **8b** is close to 0.5 kcal/mol.[40] But in all of these studies, the calculated free energy and strain energy of quinquangular comformations **8a** and **8b** are lowest in energy than the triangular structures of **8c**, **8d**, and **8e**. Much like the parent cyclotridecane, cyclotridecanone's true conformation has been difficult to ascertain. It is suspected of only having a single conformation based on VT-NMR studies, but some uncertainty still remains because some of the methylene signals still overlap at low temperatures.[6] In early studies on cyclotridecanone oxime and cyclotridecanone phenylsemicarbazone, Groth describes the structure as an ordered triangular conformation yet a

different triangular structure than has otherwise been reported for cyclotridecane.[42,43] A more recent study of the crystal structure of cyclotridecanone 2,4-dinitrophenylhydrazone reports the same triangular conformation as Groth.[44] However, in these three works as well as those of Weiss[45] and Allinger[41], the crystal structures are very similar to that of **8b**; thus, this is the currently proposed structure of cyclotridecanone.[40]

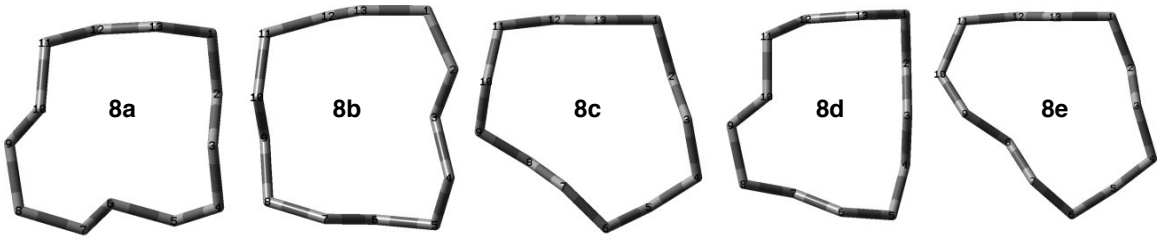

Figure 8: Predicted conformations of cyclotridecane using MP2/6-31G(d,p).[40] **8a** [13333], **8b** [12433], **8c** [445], **8d** [355], **8e** [346]

As macrocyclic size increases, the understanding of the cycloalkanes diminishes, but more complex structures that incorporate greater functionality and substitution are utilized and understood. Peczuh and coworkers studied 13-membered macrodilactones as a model for understanding macrocyclic conformation more generally (**Figure 9**), but what they found for the systems investigated was that these particular macrodilactones prefer to be in a ribbon conformation, orienting the two carbonyl units anti-periplanar to one another (**Figure 9B** and **C**). Also, because of the presence of the *trans* olefin, the structure arranges itself in such a way as to create a pair of enantiomers – it exhibits planar chirality (**Figure 9C**). However, substituting the backbone of the macrodilactone forces the ring into a single planar chirality because of non-bonded interactions. Depending on the placement of the substituent and its absolute configuration, **p***S* or **p***R* may be preferred. Additional substitution can either reinforce the established handedness of the macrocycle or compete with one another, causing the ring system to assume an alternate conformation altogether in order to accommodate the substituents in the most energy-efficient orientation (generally pseudo-equatorial).[33]

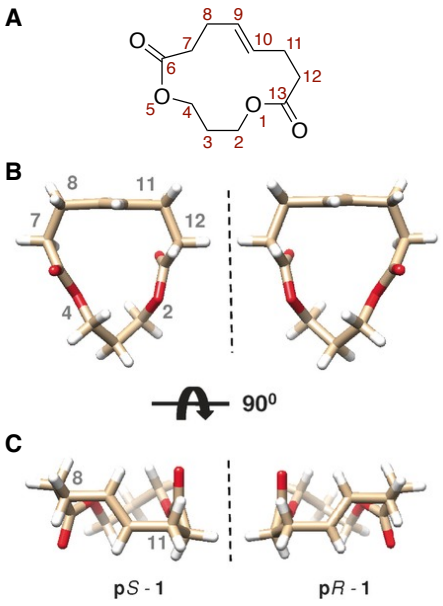

Figure 9: [13]macrodilactone. (a) numbered bond-line structure; (b) X-ray crystal structures, triangular view; (c) X-ray crystal structures, planar ribbon view.[33]

In Dale's early work on macrocylic conformation, he suggested that cyclotetradecane preferred to be in a rectangular, diamond-lattice structure in both the solid and solution phases, which allows it to be completely strain free (**Figure 10**, **10a**).[4,22] Later analysis showed that while this is the lowest energy conformation and the most populated in both the solid and solution state, two quadrangular structures are only 1.1 and 2.4 kcal/mol higher in energy than the rectangular, diamond-lattice conformation in the solution state (**10b** and **10c**, respectively).[46] Incorporating one double bond does not perturb the macrocycle greatly and the same diamond-lattice is accomodated (**10d-e**, **Figure 10**). Similarly when two alkenes or alkynes are diametrically placed in a 14-membered ring, the macrocycle has the potential to be unstrained. This is true for 1,8-diynes (**10f**), but for the 1,8-diene, this is only true when both double bonds are *trans* (**10g**). The *cis,cis*-isomer (**10i**) forces unfavorable transannular interactions, destabilizing it. The *cis,trans*-isomer (**10h**) also introduces some strain into the macrocyclic backbone, which is why at room temperature, 92% of a mixture of isomers will be *trans,trans*, 6% will be *cis,trans*, and only 2% will be *cis,cis* (**Figure 10**).[4] The preference for the rectangular, diamond lattice (**10a**) is also seen in the 14-membered macrocyclic ketone, monolactone, and monolactam.[46,47] However, a substituted macrolide system or an α,β-unsaturated ketone leads to additional conformational possibilities; thus, it should not be assumed that the diamond lattice is always preferred. Unsaturation and heavy substitution, as can be seen in compounds like erythromycin A (**Figure 11**, **11a**), changes the preferred conformation to accommodate these additions while limiting unfavorable transannular interactions,[46] as is predicted by Peczuh and coworkers from their work with the [13]macrodilactones.[33] When Dugat and coworkers studied 14-membered dilactam diketones, they observed that the ring could accommodate the *trans* lactams well, but as was mentioned for the [13]macrodilactones and for other substituted 14-membered systems, the additional substitution around the macrocyclic ring predominantly dictates the preferred conformation of the ring system.[47]

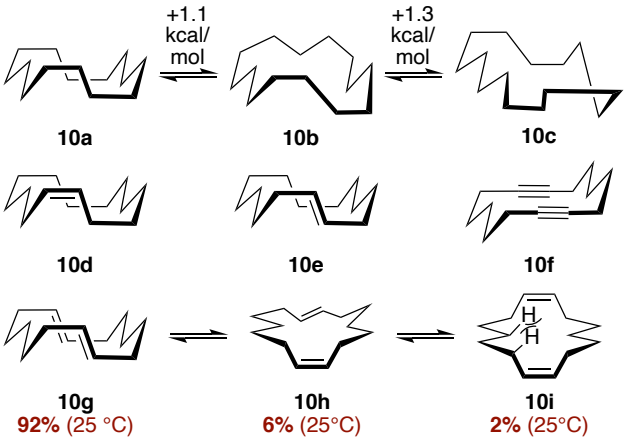

Figure 10: Lowest-energy conformations of cyclotetradecane (**10a-c**),[46] *cis*-cyclotetradecene (**10d**), *trans*-cyclotetradecene (**10e**), 1,8-cyclotetradecadiyne (**10f**), and 1,8-cyclotetradecadiene (**10g-i**).[4]

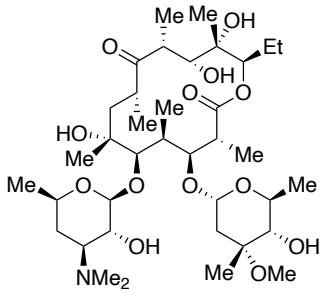

erythromycin A (**11a**)

Figure 11: Structure of erythromycin A

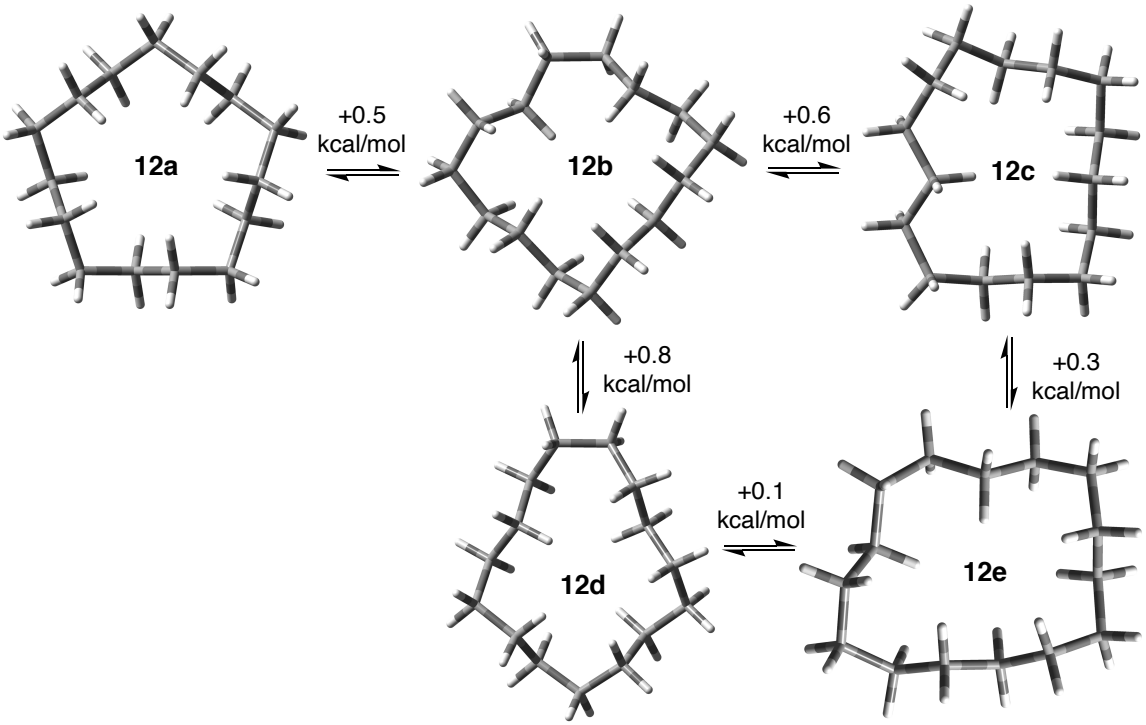

Figure 12: Lowest-energy conformations of cyclopentadecane.[38]

Very little is known about 15-membered macrocyclic systems. Early computational studies of cyclopentadecane indicated 5 similar energy conformations (less than 1.5 kcal/mol of strain energy between them) all with quinquangular shapes (**Figure 12**).[38,39] Similar to the methods used to understand cyclotridecane, attempts have been made at understanding cyclopentadecanone as a way to understand the conformation of this 15-membered ring system. Cyclopentadecanone's crystal structure (**Figure 13**) was observed to be the same quinquangular structure which was shown to have the highest amount of strain energy in Anet and Rawdah's previous study, **12e** (although it is still only 1.5 kcal/mol higher in energy than the lowest computed energy structure, **12a**).[38,48] Other studies on cyclopentadecanone phenylsemicarbazone and cyclopentadecanone 2,4-dinitrophenylhydrazone have been undertaken using x-ray crystallography. The phenylsemicarbazone derivative shows a ring structure similar to that calculated for cyclopentadecane with only minor deviations at two carbons to accommodate the sp^2 nature of the hydrazone but still different than that later found for cyclopentadecanone.[49] The 2,4-dinitrophenylhydrazone derivative was more similar to that seen for cyclopentadecanone than the phenylsemicarbonzone derivative was; however, this structure also had its own conformation that differed from other conformations observed.[50] These results show

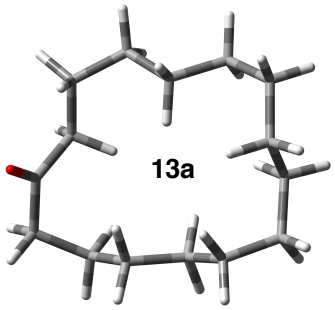

Figure 13: Structure of cyclopentadecanone.[48]

just how difficult it can be to identify and articulate the structure of large macrocycles because of the many possible conformations such structures can assume.

Cyclohexadecane's lowest energy conformation is a square diamond-lattice structure (**Figure 14**, **14a**),[22] as confirmed by both computational and NMR studies. However, it is expected to have at least 18 different conformers within 3.5 kcal/mol of one another.[51] Early NMR and computational studies suggest that in the solid state from low temperatures to those as high as 30 °C and as a liquid, the mixture of conformations is predominantly the square diamond-lattice structure (at least 70% at room temperature and at least 90% at lower temperatures);[52,53] however, because of extensive line broadening, experimental IR studies have sometimes been interpretted such that the square diamond-lattice structure can only comprise a maximum of 15% of the conformations at room temperature.[51] Others have explained this by observing that the flexibility of this molecule may be extensive (perturbations of 10°), thus causing this line broadening.[39,52] The next lowest energy conformation is a rectangular-lattice and has been calculated to be only 1.9 kcal/mol higher in strain energy than the square diamond-lattice structure.[52] Cyclohexadecanone and some of its methylated derivatives do not seem to be consistent with the square diamond-lattice, so the rectangular lattice structure has been proposed as the conformation for these compounds based on spectral data.[52] 1,9-cyclohexadecanedione has also been calculated to predominantly assume the rectangular lattice structure.[52,54] Even still, the dione is so flexible that at least 19 other conformations were found to be within 2.5 kcal/mol.[54]

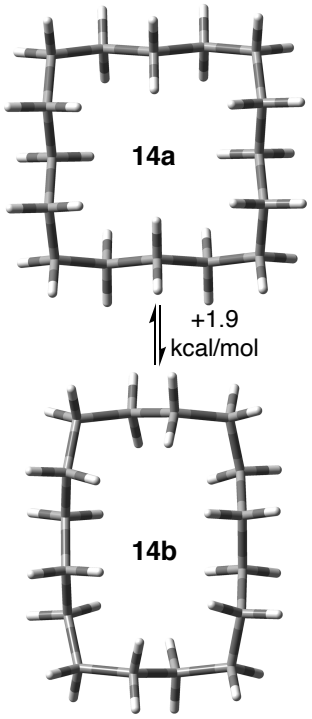

Figure 14: Lowest-energy conformations of cyclohexadecane.[52]

As was mentioned previously, with increasing macrocycle size, the number of similar-energy conformations increases, thus making conformational analyses of completely saturated systems more challenging. While smaller rings accept angular strain in order to push bonds outward and relieve transannular interactions between the hydrogens across the ring, larger rings have the capability of spreading out until a hole or cavity is created in the center of the ring. However, attractive van der Waals forces can lower the overall energy of the ring by bringing the ring system into a more confined, rectangular shape.[55]

Compounds like cycloheptadecane and larger do not have only a single low-energy conformation that can be understood through spectral analysis.[31] Cycloheptadecane itself has been computed to have at least 262 conformations within 3 kcal/mol.[21,56] For cyclooctadecane, a long rectangular conformation (**Figure 15**, **15a**) has been computed to be the lowest energy conformation, with a more square conformation (**15b**) only being 0.3 kcal/mol higher in energy. Additional low-energy conformations for cyclooctadecane incorporate bends, called nicks, and these nicks are seen more frequently in larger macrocycles.[55] For cyclooctadecane, 96 different conformations have been found to be within 3 kcal/mol of the lowest energy conformation.[55] Cyclononadecane has 254 calculated conformations that are within 3 kcal/mol, and cycloicosane has 63 conformations within 3 kcal/mol of the lowest energy conformation.[55] Much like in Peczuh's analysis of [13]macrodilactones,[33] Dolata notes that as cyclic systems get larger, they generally assume a more ribbon-like structure, as well (*i.e.* **15a** vs. **15b**).[55]

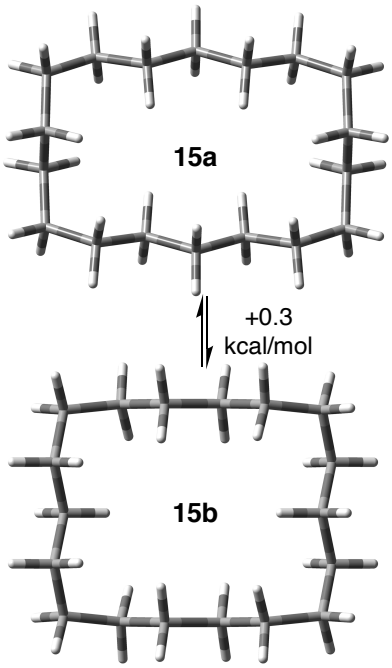

Figure 15: Structures of the lowest-energy conformations of cyclooctadecane.[55]

It is this understanding of conformation for macrocyclic cycloalkanes and their simply substituted derivatives that evolved into much of the work that was done in understanding the stereoselectivity of reactions performed on macrocycles, but much still had to be reexamined for each substrate, as was seen to be the case with the simple cycloalkanes described above.

1.2 Early Examples of Stereoselective Reactions of Macrocycles

Much time and effort have been spent understanding the conformations of macrocyclic cycloalkanes, such that these systems could be better utilized as synthetic intermediates for completing the total syntheses of stereochemically rich macrocyclic natural products. Still and co-workers were amongst the first to explore how simple reactions performed on macrocycles could exhibit high levels of diastereoselectivity. After observing that addition reactions of macrocyclic olefins occur with high, and in some cases, complete facial selectivity, he layed out the principles of the peripheral attack model, which is still widely accepted today.[8] Some of the different types of stereoselective reactions of macrocycles that have been explored include enolate alkylations,[9,11,57,58] conjugate additions,[9,57] reductions,[9,11,58,59] epoxidations,[8,10,13,58,60–63] and osmylations.[13,14]

1.2.1 Kinetic enolate alkylations

In Still's study of the general reactivity of macrocyclic ring systems, he found that kinetic enolate alkylations of 2-methylcyclooctanone give high levels of diastereoselectivity (**Scheme 1**, **1.1** to **1.5**, and **1.2** to **1.6**), but simply increasing the size of the macrocycle to 9- and 10-membered cycloalkanones eliminates the observed diastereoselectivity (**Scheme 1**, **1.3** to **1.7** and **1.4** to **1.8**). However, when 9- and 10-membered lactones are used for kinetic enolate alkylations instead of the cycloalkanones, high levels of diastereoselectivity are again observed (**Scheme 1, 1.9** to **1.16**, and **1.12** to **1.19**). This is observed because of the additional rigidity offered to the macrocyclic backbone through the partial double bond character of the lactone. It should be noted, though, that the closer the substitution is to the reactive center, the greater the effect of the remote asymmetric induction (compare the observed diastereoselectivities for **1.10** to **1.17**, *50:50* with **1.11** to **1.18**, *86:14* with **1.12** to **1.19**, *>99:1*). Still found that the best way to understand the observed diastereoselectivity was by modeling an early transition state. **Figure 16** shows this for the 10-membered lactones, in which the *Z*-configured enolate is formed preferentially, and the degree of preference at each position around the ring for the substituent to assume the pseudo-axial or pseudo-equatorial positions in this transition state dictates the relative stereochemistry of the product (**Figure 16**, C7, C8, and C9, preferred position represented by a filled circle). The C9 position has a preference for the larger substituent to occupy the pseudo-axial position to eliminate interactions with the carbonyl oxygen. Substituents on the C8 carbon, though, will prefer to assume the pseudo-equatorial position, but little preference is observed for the substituents at the C7 position because the corner position allows the pseudo-axial and pseudo-equatorial positions to be almost equivalent. Thus, even though the alkylation reaction occurs from the same diastereoface of the enolate, the orientation of the methyl groups at the other positions dictate whether the final product has relative *syn* or *anti* stereochemistry. Even for the larger 11-, 12-, and 13-membered macrocyclic lactones, kinetic enolate alkylations of these systems still gave

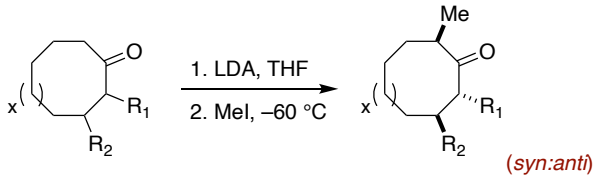

1.1: x=1, R_1=Me, R_2=H
1.2: x=1, R_1=H, R_2=Me
1.3: x=2, R_1=Me, R_2=H
1.4: x=3, R_1=Me, R_2=H
1.5: x=1, R_1=Me, R_2=H, (*5:95*)
1.6: x=1, R_1=H, R_2=Me, (*98:2*)
1.7: x=2, R_1=Me, R_2=H, (*52:48*)
1.8: x=3, R_1=Me, R_2=H, (*50:50*)

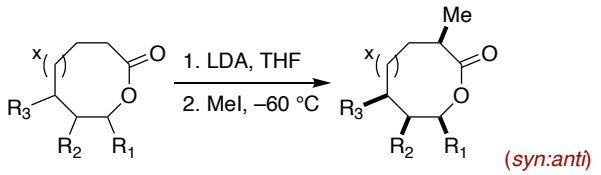

1.9: x=2, R_1=Me, R_2=R_3=H
1.10: x=3, R_1=R_2=H, R_3=Me
1.11: x=3, R_1=R_3=H, R_2=Me
1.12: x=3, R_1=Me, R_2=R_3=H
1.13: x=4, R_1=Me, R_2=R_3=H
1.14: x=5, R_1=Me, R_2=R_3=H
1.15: x=6, R_1=Me, R_2=R_3=H
1.16: x=2, R_1=Me, R_2=R_3=H, (*98:2*)
1.17: x=3, R_1=R_2=H, R_3=Me, (*50:50*)
1.18: x=3, R_1=R_3=H, R_2=Me, (*86:14*)
1.19: x=3, R_1=Me, R_2=R_3=H, (*>99:1*)
1.20: x=4, R_1=Me, R_2=R_3=H, (*98:2*)
1.21: x=5, R_1=Me, R_2=R_3=H, (*92:8*)
1.22: x=6, R_1=Me, R_2=R_3=H, (*92:8*)

Scheme 1: Still's kinetic enolate alkylations of 8- to 13-membered macrocycles.[9]

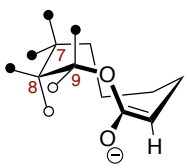

Figure 16: Early transition state of kinetic enolate alkylation to 10-membered lactone.[9]

high levels of diastereoselectivity (**Scheme 1**, **1.13** to **1.20**, **1.14** to **1.21**, and **1.15** to **1.22**, respectively).[9]

Takahashi also made use of macrocyclic conformation to do a stereoselective enolate alkylation of a 10-membered ring in the synthesis of 3-oxygenated 13-norheliangolides. (**Scheme 2**, **2.4**). This reaction furnished a single diastereomeric product due to the exclusive formation of *Z*-configured enolate **2.2**, which when the peripheral attack model is employed to explain the observed diastereoselectivity, does quite nicely show that the only product that should be formed is **2.3**.[11]

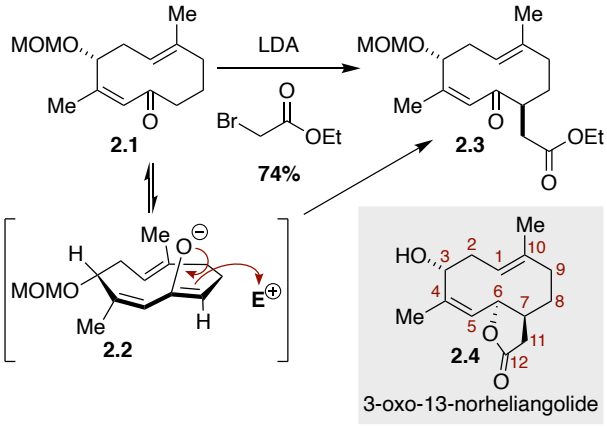

Scheme 2: Takahashi's stereoselective enolate alkylation in the synthesis of 3-oxygenated 13-norheliangolides (**2.4**).[11]

Still was able to perform three consecutive regio- and diastereoselective enolate alkylations to a 16-membered macrocycle in his synthesis of (±)-3-deoxyrosaranolide **17a**, an aglycon of rosaramicin **17b** (**Figure 17**). The first enolate alkylation (**Scheme 3, 3.1** to **3.2**) was completely regioselective and gave >20:1 diastereoselection. Still explains this diastereoselection because the conformation of **3.1**, as seen by x-ray crystallography, is similar to that observed crystallographically in rosaramicin. The second alkylation showed >20:1 regioselectivity and 6-10:1 diastereoselectivity (**Scheme 3**, **3.2** to **3.3**). The third alkylation had >40:1 diastereoselectivity for the β-methyl group (**Scheme 3**, **3.3** to **3.4**), but this was the undesired relative configuration. Therefore, Still obtained the correct relative configuration of the C-methyl stereogenic center through an alkylidentation, which was accomplished by installing a hydroxymethyl group (62% yield) and eliminating via the mesylate to give **3.5**. A subsequent conjugate addition installed a thioether (71% yield) that was then cleaved with Raney nickel to give the α-methyl group in >25:1 diastereoselection (**3.5** to **3.6**).[58]

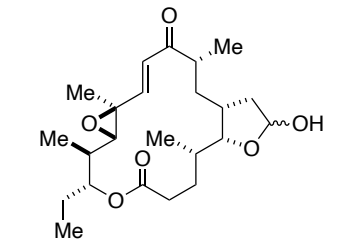

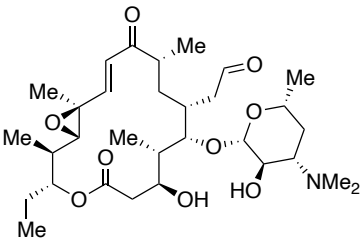

Figure 17: Structures of the (±)-3-deoxyrosaranolide and rosaramicin

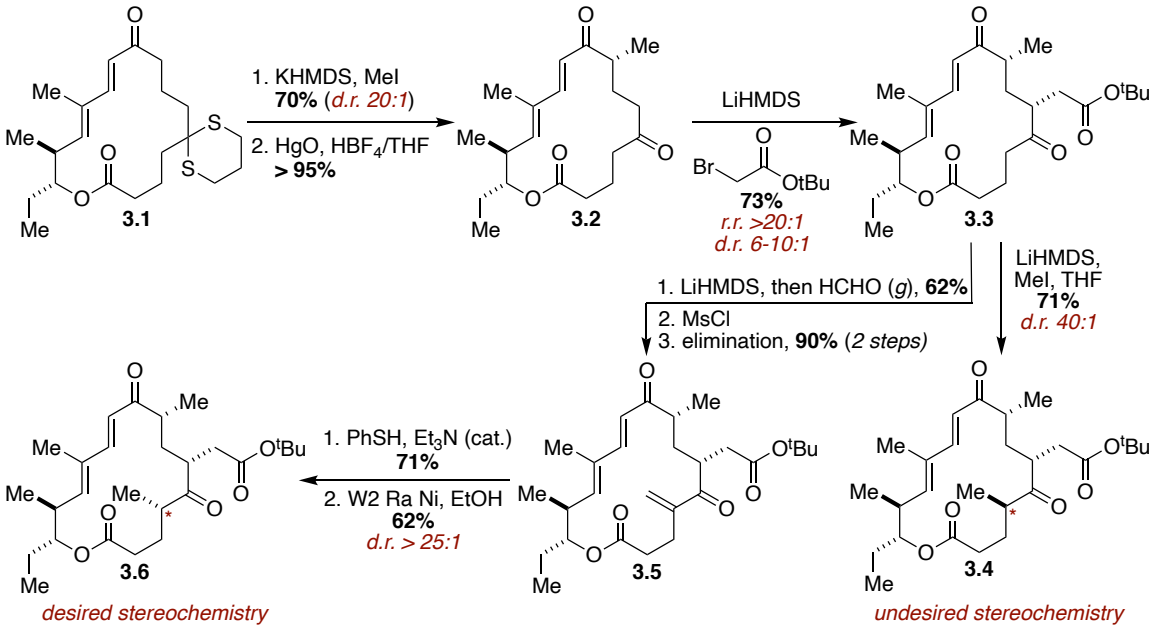

Scheme 3: Still's regio- and diastereoselective enolate alkylations in the synthesis of (±)-3-deoxyroaranolide (**17a**).[58]

1.2.2 Conjugate Additions

Similar to the kinetic enolate alkylations, Still found that conjugate additions of substituted 8- to 10-membered cycloalkenones and 8- to 12-membered α,β-unsaturated lactones also give high levels of diastereoselectivity (**Scheme 4**). For (*Z*)-2-methylcyclooctenone **4.1**, (*Z*)-2-methylcyclononenone **4.2**, and (*E*)-2-methylcyclononenone **4.3**, high diastereoselectivity was observed, preferring the *anti*-relative stereochemistry in the product. However, the observed product for the conjugate addition of 2-methylcyclodecenone depended on the configuration of the double bond. When the starting macrocycle contained a *Z*-configured olefin, the product was *anti* (**4.4** to **4.10**) with high diastereoselection, but when the starting olefin was *E*-configured, the *syn* product

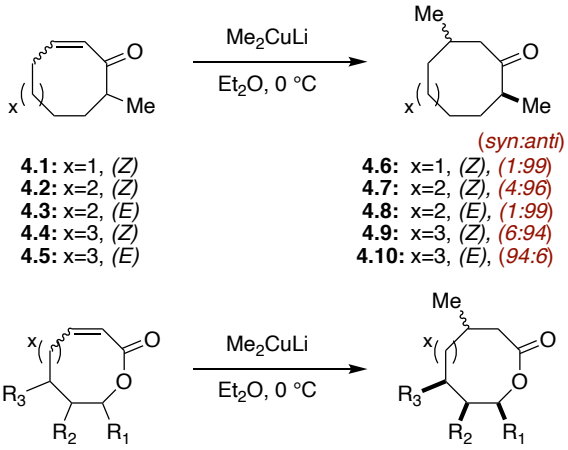

Scheme 4: Still's stereospecific conjugate additions of 8- to 12-membered macrocycles.[9]

was observed with the same selectivity (**4.5** to **4.10**). Similarly, the conjugate addition product for the 12-membered α,β-unsaturated lactones also depended on the configuration of the olefin (**4.16** to **4.23** and **4.17** to **4.24**). Also, as was observed for the kinetic enolate alkylations, the proximity of the other substituents around the ring can greatly affect both the observed diastereoselection of the reaction and the relative stereochemistry of the products. When the methyl group was immediately beside the lactone oxygen, the highest diastereoselectivity was observed (**4.12** to **4.19**). Removing the methyl only one position further, decreases the diastereoselectivity from *99:1* to *80:20* in favor of the *syn* product (**4.13** to **4.20**). And one position still further and the preferred stereochemistry of the product switches to give the *anti* methyl groups preferentially (**4.14** to **4.21**).[9]

In Still's synthesis of the C30-C43 segment of Palytoxin (**Scheme 5**, **5.6**), he utilizes a 9-membered macrocycle to do a completely stereoselective conjugate addition to establish the necessary relative stereochemistry around the ring (**Scheme 5**, **5.1** to **5.2**). The observed *syn* relative stereochemistry of the methyl groups was predicted based on the previously observed results of a conjugate addition a to 9-membered macrolactone (see **Scheme 4**, **4.11** to **4.18**), but this outcome is understood computationally by modeling the lowest energy conformations of both the macrocyclic starting material and the β-methyl enolate, a late-stage transition state structure (**Figure 18**, **18a** and **18b**, respectively). In modeling both of these structures, the preferred *syn*-addition product was easily predicted. The product of the conjugate addition (**5.2**) then underwent saponification to **5.3** followed by iodolactonization through intermediate **5.4** to establish the relative stereochemistry seen in compound **5.5**.[57]

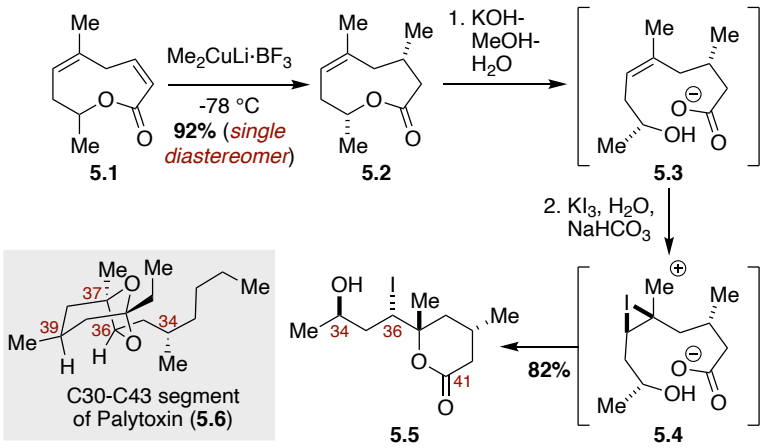

Scheme 5: Still's stereospecific synthesis of C30-C43 segment of Palytoxin (**5.6**).[57]

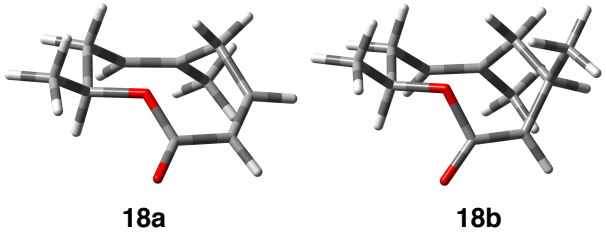

18a **18b**

Figure 18: Reactive conformation of Still's palytoxin precursor (enone) **18a** and β-methyl enolate **18b**.[57]

Still explained the observed diastereoselectivity of these reactions by using the peripheral attack model of the ground state conformation for 8-membered rings (**Scheme 4**, **4.1** to **4.6**), but he used late-transition states (β-methyl enolates) for 9-membered systems (**Scheme 4**, **4.2** to **4.7** and **4.3** to **4.8**). In the 10-, 11-, and 12-membered systems, the observed diastereoselectivity is explained by reasoning that the reactive conformation is the one in which the double bond and ketone are in conjugation, and therefore planar. Although these systems are slightly higher in energy than the lowest energy conformation, he reasons that this still must be the reactive conformation. And while Still notes this in his computational analysis in 1981, such a rule is not explicitly set out, nor is it consistent for all systems under consideration.[9] Choosing at which point the conformation of the macrocycle will dictate the product under the peripheral attack model is thus challenging and ambiguous. In his dissertation Wzorek tries to correlate the peripheral attack model to more modern computational methods (MM-DFT). In the study of conjugate additions, he notes that for many of the systems he analyzed, the lowest-energy conformation does not have these components in conjugation, and therefore concludes that the results of the peripheral attack model did not correlate well to those found experimentally.[64] However, because Still does note this discrepancy also, Wzorek's findings are less novel. Nevertheless, Wzorek's suggestion to plot the entire course of the reaction, noting both transition state energies and local minima to gain a better understanding of why the particular outcome is achieved is valid.

1.2.3 Reductions

In Still's studies, catalytic hydrogenations of olefins in 8- to 10-membered macrocycles also gave high levels of diastereoselectivity (**Scheme 6**). Both the reduction of an exocyclic olefin (**Scheme 6**, **6.1** to **6.2**) and of endocyclic olefins of lactones **6.3**-**6.6** gave complimentary results to those seen in previous conjugate additions. For the 9-membered lactone **4.11** (**Scheme 4**, R_1=Me, R_2=R_3=H), the conjugate addition product has *syn*-relative stereochemistry of the methyl groups, indicating that the methyl nucleophile attacks from the top face (as drawn in **Schemes 4** and **6**). For the hydrogenation of **6.3**, the *anti*-relative stereochemistry of the methyl groups is observed, indicating that the hydrogen is also attacking from the top face. The same trend is seen for the other sized macrocycles, indicating that it is the conformation of the ring that dictates from which face

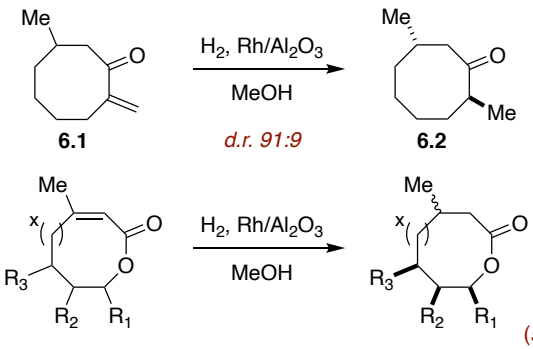

6.1 **6.2**

(*syn:anti*)

6.3: x=2, R_1=Me, R_2=R_3=H
6.4: x=3, R_1=Me, R_2=R_3=H
6.5: x=3, R_2=Me, R_1=R_3=H
6.6: x=3, R_3=Me, R_1=R_2=H

6.7: x=2, R_1=Me, R_2=R_3=H, (*6:94*)
6.8: x=3, R_1=Me, R_2=R_3=H, (*9:91*)
6.9: x=3, R_2=Me, R_1=R_3=H, (*17:83*)
6.10: x=3, R_3=Me, R_1=R_2=H, (*83:17*)

Scheme 6: Still's stereoselective reductions of 8- to 10-membered olefins, both exocyclic (**6.1**) and endocyclic (**6.3**-**6.6**).[9]

the nucleophile (in the case of the conjugate addition) or hydrogen (in catalytic hydrogenations) can attack, and thus the diastereoselectivity observed in the product.[9]

The observed diastereoselectivity for reductions on macrocyclic systems is not limited to alkenes. Takahashi also finds in his synthesis of 3-oxygenated 13-norheliangolides (**2.4**) that reducing the ketone of 10-membered macrocycle **7.1** is stereospecific, giving only a single diastereomer because of the conformation of the macrocycle (**Scheme 7A**).[11] Still utilizes a similar diastereoselective reduction of 10-membered macrocyclic ketones in his synthesis of eucannabinolide (**Figure 19**). In this case, though, Still is able to use the same reagents to reduce two ketones in separate steps, giving an α-hydroxyl group (**Scheme 7B**, **7.3** to **7.4**) and a β-hydroxyl group (**Scheme 7B**, **7.5** to **7.6**).[59] Also, in Still's synthesis of (±)-3-deoxyrosaranolide (**Figure 17**, **17a**), he stereoselectively reduces the ketone at C5 (**7.7**) to give the α-hydroxy group in **7.8** (**Scheme 7C**). This was only accessible because of the presence of the neighboring anhydride (present after steps 1 and 2 in **Scheme 7C**). When the *t*-butyl ester was present (**7.7**), the β-hydroxy was formed with *>20:1* selectivity.[58]

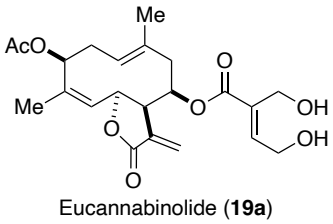

Eucannabinolide (**19a**)

Figure 19: Structure of cytotoxic germacranolide eucannabinolide.[59]

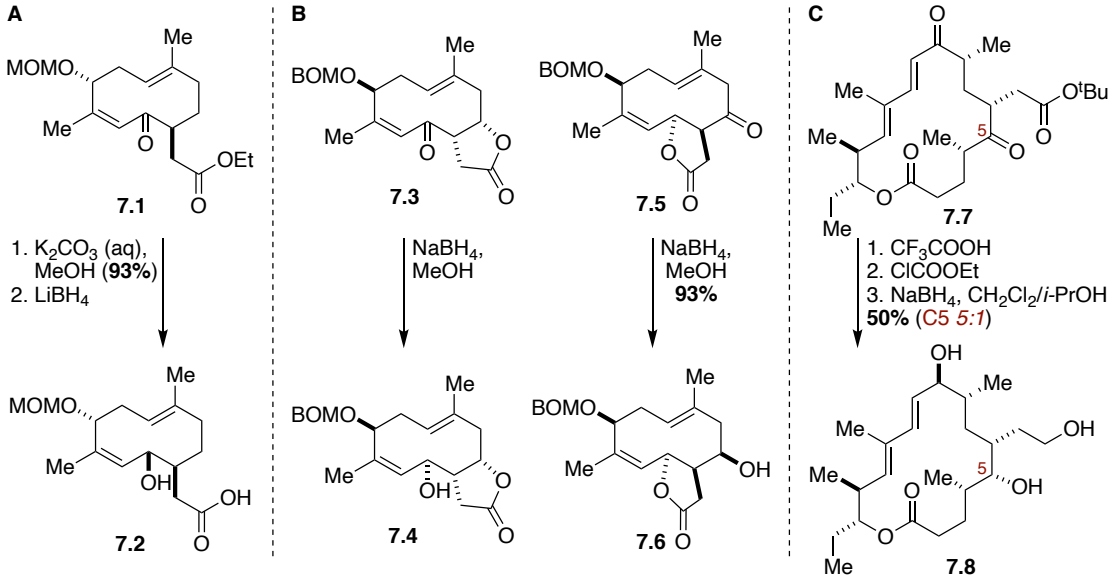

Scheme 7: A. Takahashi's stereoselective reduction of a ketone in the synthesis of 3-oxygenated 13-norheliangolides (**2.4**);[11] **B.** Still's diastereoselective reductions of ketones in the synthesis of eucannabinolide (**19a**);[59] **C.** Still's stereoselective reduction of C5 ketone in the synthesis of (±)-3-deoxyrosaranolide (**17a**).[58]

1.2.4 Epoxidations

Epoxidations of macrocyclic olefins are one of the most frequently used diastereocontrolled reactions of macrocycles, and in most of these cases the peripheral attack model is used to either

predict or explain the observed diastereoselectivity of these reactions.[8,10,13,58,60–63] Based on the work of Evans and coworkers this is the only reaction type in which it is acceptable to truly rely on the peripheral attack model as a reliable method for predicting the outcome of reactions.[64] Different types of reactions – including epoxidations, conjugate additions, hydrogenations, and 1,2-additions to carbonyls – were investigated using exclusively molecular mechanics (MM) and a combined MM-DFT approach, and what was observed is that the peripheral attack model is not universally applicable to macrocycles of all sizes or reactions of all types, and while it does seem to agree with experiment the majority of the time (usually >70% of cases tested), it does not agree sufficiently often (>90%) for it to be relied upon. Epoxidation reactions, however, showed to be reliably predicted by the peripheral attack model; however, conjugate additions, hydrogenations, and 1,2-additions were not.

Much earlier than the work of Evans and coworkers, however, Vedejs and Gapinski studied epoxidations, comparing the observed diastereocontrol of *Z*- and *E*-configured olefins, both di- and trisubstituted, looking for whether local conformational preferences dictated the stereochemical outcome of a reaction.[13] In their studies they observed that *Z*-configured olefins showed greater diastereoselectivity when reacted with *m*-CPBA (**Table 1**, entries 1, 3, 5, and 7) and attributed this to only a single conformational preference for the olefinic region of the macrocycle (**Figure 20**, **20a**). The trisubstituted *E*-configured alkene (**Table 1**, entry 4) also gave exclusively one diastereomer, but when the *E*-configured alkene was only a disubstituted system, a mixture of diastereomers were observed (**Table 1**, entries 2, 6, and 8). This is attributed to more low-energy conformations for the *E*-configured olefin (**Figure 20**, **20b** and **20c**) existing than for the *Z*-configured olefin. Such a trend was also observed for unsubstituted cyclodecenes.[27–29]

Table 1: Stereoselective epoxidations of 10- to 15-membered macrocyclic olefins.[13]

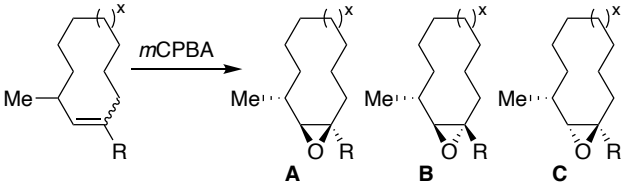

entry	x	ring size	olefin geometry	R	product ratios a	b	c
1	1	10	*Z*	H	**100%**	—	—
2	1	10	*E*	H	—	**85%**	**15%**
3	3	12	*Z*	Me	**100%**	—	—
4	3	12	*E*	Me	—	**100%**	—
5	3	12	*Z*	H	**100%**	—	—
6	3	12	*E*	H	—	**86%**	**14%**
7	6	15	*Z*	H	**100%**	—	—
8	6	15	*E*	H	—	**75%**	**25%**

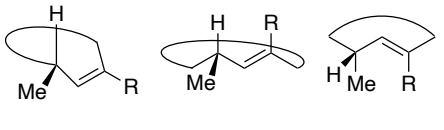

20a **20b** **20c**

Figure 20: Local geometries of macrocyclic olefins.[13]

W. Clark Still performed one of the first known conformationally controlled epoxidation reactions of a macrocycle in his synthesis of periplanone B (**8.5**). The epoxidation with *t*-butyl hydrogen peroxide of α,β-unsaturated ketone **8.1** gave only a single epoxidation product **8.2**

(**Scheme 8**). However, because the relative stereochemistry did not correctly match the natural source, another diastereomer was prepared. This time instead of the protected methyl alcohol in **8.1**, an exocyclic olefin was incorporated, changing the conformation of the macrocycle and promoting addition from the other face (**8.3** to **8.4**). Still explains the observed stereoselectivity of both of these additions as peripheral attack to the macrocyclic olefin.[8]

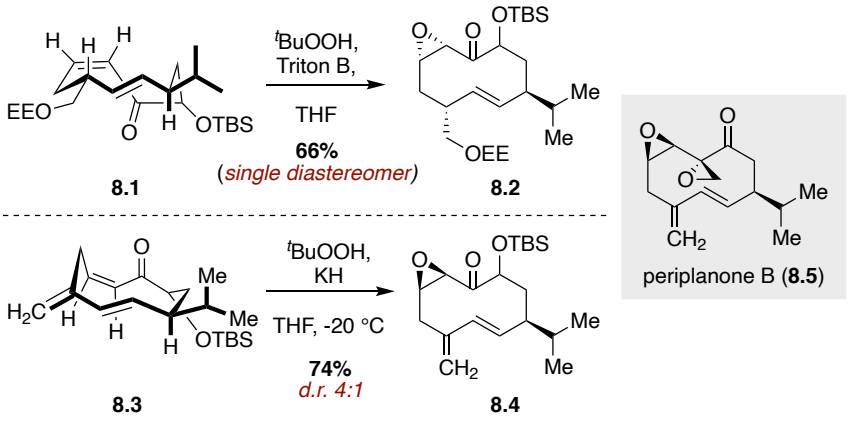

Scheme 8: Still's stereospecific epoxidations in the synthesis of periplanone B (**8.5**).[8]

Takahashi and coworkers wanted to predict which structural features of the macrocycle in their synthesis of periplanone B (**Scheme 8**, **8.5**) contribute to the observed diastereoselectivity of the epoxidation step and developed a means to predict this when planning the synthesis instead of simply trying reactions. What they found was that MM2 calculations comparing strain and conformational distributions aligned well with the observed conformers of the starting materials seen by NMR. This allowed for the definitive determination of the reactive conformation(s) of both their proposed starting material (**Scheme 9**, **9.1** and **9.2**) and other similar compounds (like Still's intermediate in **Scheme 8**, **8.3**), such that when they performed the epoxidation, only a single stereoisomer **9.3** was obtained, where previously reported syntheses had reported diastereoselectivity as high as 4:1.[12]

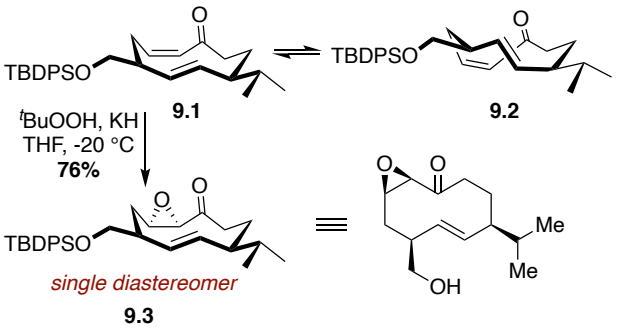

Scheme 9: Takahashi's stereospecific epoxidation for the synthesis of periplanone B (**8.5**).[12]

In E.J. Corey's synthesis of erythronolide A (14-membered macrocycle **10.3**), most of the stereochemistry was set before the macrocyclization; however, one of the final steps was a stereospecific epoxidation of the macrocyclic backbone with *m*-CPBA to form exclusively the β-epoxide **10.2** (**Scheme 10**).[10] It is conceivable that the stereochemistry of the epoxidation reaction not only dictated by the macrocyclic conformation but is also assisted through a

hydroxyl-directed process. However, in a similar synthesis of erythronolide B (10-epi-12-deoxy erythronolide A), there is no hydroxyl group at C12 and C9 is a ketone instead of a β-hydroxyl group and the same β-epoxide is observed to form,[65] thus it is presumable that the macrocycle helps dictate the stereochemistry of the epoxidation reaction.

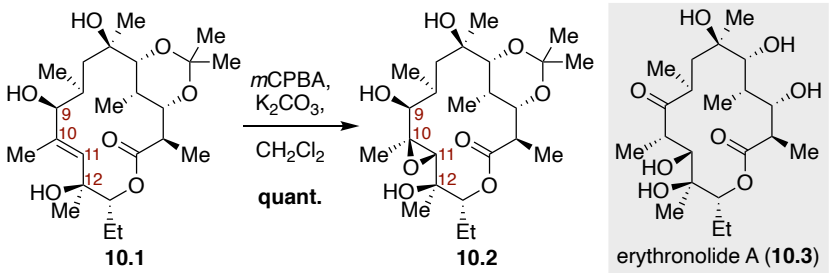

Scheme 10: Corey's stereospecific epoxidation in the synthesis of erythronolide A (**10.3**).[10]

In addition to Still's most famous example of conformationally controlled epoxidation of a macrocycle in the synthesis of periplanone B (**Scheme 8**). He employs three other conformationally controlled epoxidations in the syntheses of (±)-3-deoxyrosaranolide,[58] baccarin B5,[60] and a portion of the monensin B backbone.[61] In the synthesis of (±)-3-deoxyrosaranolide (**Figure 17**, **17a**), he completes the synthesis that has showcased many conformationally controlled reactions of the macrocycle with a stereospecific epoxidation of **11.1** to give **11.2** with a diastereomeric ratio of >15:1 (**Scheme 11A**), which then only required an oxidation to complete the total synthesis.[58] In his synthesis of baccharin B5 (**11.3**), Still and coworkers also accomplish a stereospecific double epoxidation of 18-membered macrocycle **11.4** with greater than 15:1 diastereoselectivity (**Scheme 11B**). The epoxide on the six-membered ring has the natural stereochemistry, but further manipulation was needed on the macrocyclic epoxide, including an elimination to open the epoxide, an allylic alcohol epoxidation, and then a subsequent inversion of the stereochemistry using a Mitsunobu reaction.[60] Still continued to showcase the usefulness of macrocyclic conformational control, though, when he used 16-membered macrocycle **11.6** in the synthesis of a portion of the backbone of monensin B (**11.8**). The starting macrocycle **11.6** was a 4:1 mixture of diastereomers, but Still and coworkers were able to simultaneously install 6 stereocenters through a triple epoxidation with *m*-CPBA to give a single diastereoisomeric product **11.7** (**Scheme 11C**).[61]

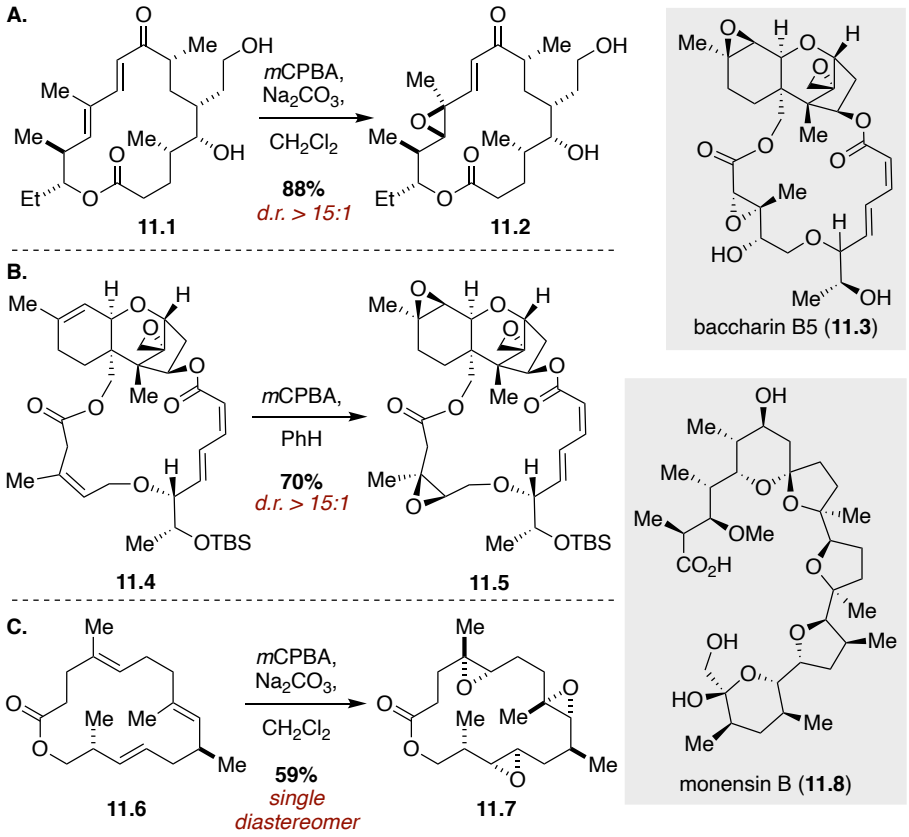

Scheme 11: A. Still's stereospecific epoxidation in the synthesis of (±)-3-deoxyrosaranolide (**17a**);[58] **B.** Still's stereospecific epoxidation in the synthesis of baccharin B5 (**11.3**);[60] **C.** Still's stereospecific triple epoxidation toward the formation of the monensin B backbone (**11.8**).[61]

In Vedejs' synthesis of *d,l*-methynolide, a stereospecific epoxidation of 12-membered keto-lactone **12.1** with *m*-CPBA gave β-epoxide **12.2** as a single diastereomer, which had the desired stereochemistry necessary for completion of the synthesis of the natural product. (**Scheme 12**).[62]

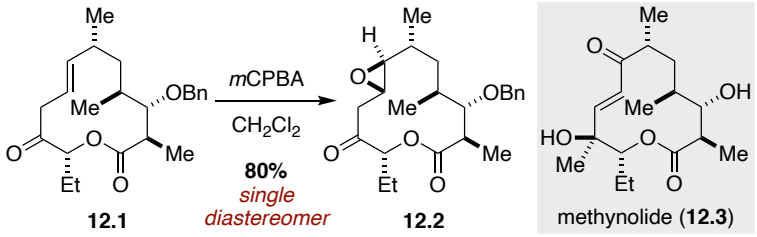

Scheme 12: Vedejs' stereospecific epoxidation in the synthesis of *d,l*-methynolide (**12.3**).[62]

In Evans' synthesis of Ionomycin A (**Scheme 13**, **13.4**), two epoxides are installed in one pot with 9:1 diastereoselectivity because of the conformation of 12-membered macrolactone **13.1** (**Scheme 13**). Evans found that two low-energy conformations of **13.1** (differing in energy by only 1.1 kcal/mol) caused the observed diastereoselectivity. The olefin at C4/C5 reacts first, but is less

rigid, allowing the two diastereomers to be formed in a ratio of 9:1 (**13.2:13.3**). Then the olefin at C8/C9 reacts with 97:3 selectivity because in both low-energy conformations, this olefin at this position maintains a more rigid local conformation.[63]

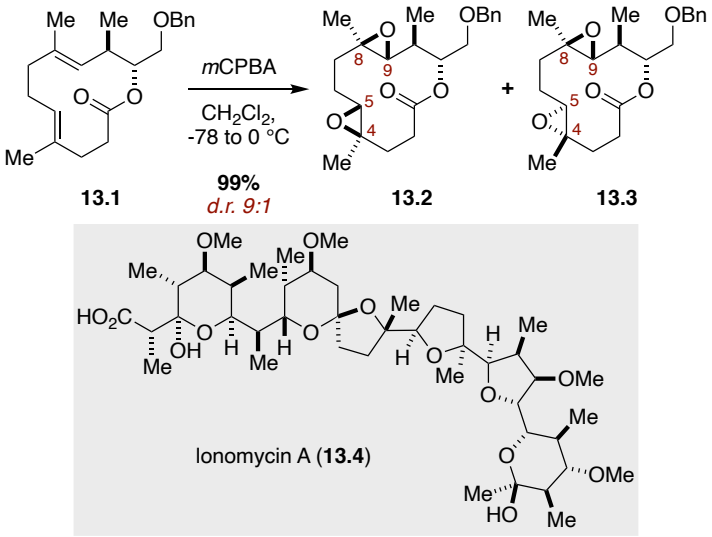

Scheme 13: Evans' diastereospecific double epoxidation in the synthesis of Ionomycin A (**13.4**).[63]

1.2.5 Syn-dihydroxylations with OsO_4

Syn-dihydroxylations with OsO_4 have also been utilized as an efficient means to install new functionality on a macrocyclic backbone.[13,14] Vedejs and Gapinski studied these types of reactions in conjunction with epoxidations to understand the influence that neighboring groups and local conformational preferences have on diastereoselective reactions (**Table 2**). It was observed that while generally stereoselective, dihydroxylations with OsO_4 are not as selective as epoxidations. Similar to the epoxidations, both *E* and *Z* tri-substituted olefins (**Table 2**, entries 3 and 4) and *Z* di-substituted olefins (**Table 2**, entries 1 and 5) give high diastereoselection (with the exception of the 15-membered ring, which gave only a *d.r.* of 4:1, **Table 2**, entry 7). However, dihydroxylation does not work well with di-substituted *(E)*-3-methyl cycloalkenes (**Table 2**, entries 2, 6, and 8) because the interconversion between to two conformers (**Figure 20**, **20b** and **20c**) happens too rapidly

Table 2: Stereoselective osmylations of 10- to 15-membered macrocyclic olefins.[13]

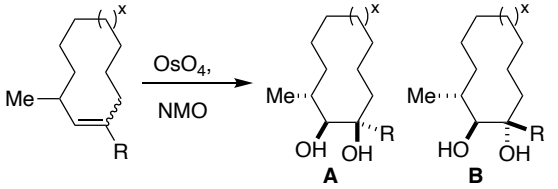

entry	x	ring size	olefin geometry	R	product ratios A	B
1	1	10	*Z*	H	**100%**	—
2	1	10	*E*	H	**50%**	**50%**
3	3	12	*Z*	Me	**100%**	—
4	3	12	*E*	Me	—	**100%**
5	3	12	*Z*	H	**100%**	—
6	3	12	*E*	H	**66%***	**34%***
7	6	15	*Z*	H	**80%***	**20%***
8	6	15	*E*	H	**67%***	**33%***

*Unknown selectivity for product **A** or **B**

to allow the bulky osmium reagent to add to only one face of the olefin.[13]

However, in a later paper, Vedejs showcases the utility of these *syn*-dihydroxylations with OsO_4 when 3 different macrocycles (**Scheme 14**, **14.1**, **14.4**, and **14.7**), all formed from a common starting material, are subjected to OsO_4. In this paper, the goal was to synthesize the C1-C9 segment of erythronolide A (**14.10**) using **14.2** as an intermediate, but to showcase the utility of the *syn*-dihydroxylation, **14.4** and **14.7** were also synthesized and subjected to OsO_4. Each addition gives only a single product; although, **14.5** and **14.8** were not isolated because they rapidly undergo *S* to *O* acyl transfer to give **14.6** and **14.9**, respectively. The conformation of the individual macrocycles dictates how the osmium can approach, leading to the different diastereomeric products **14.3**, **14.6**, and **14.9**.[14]

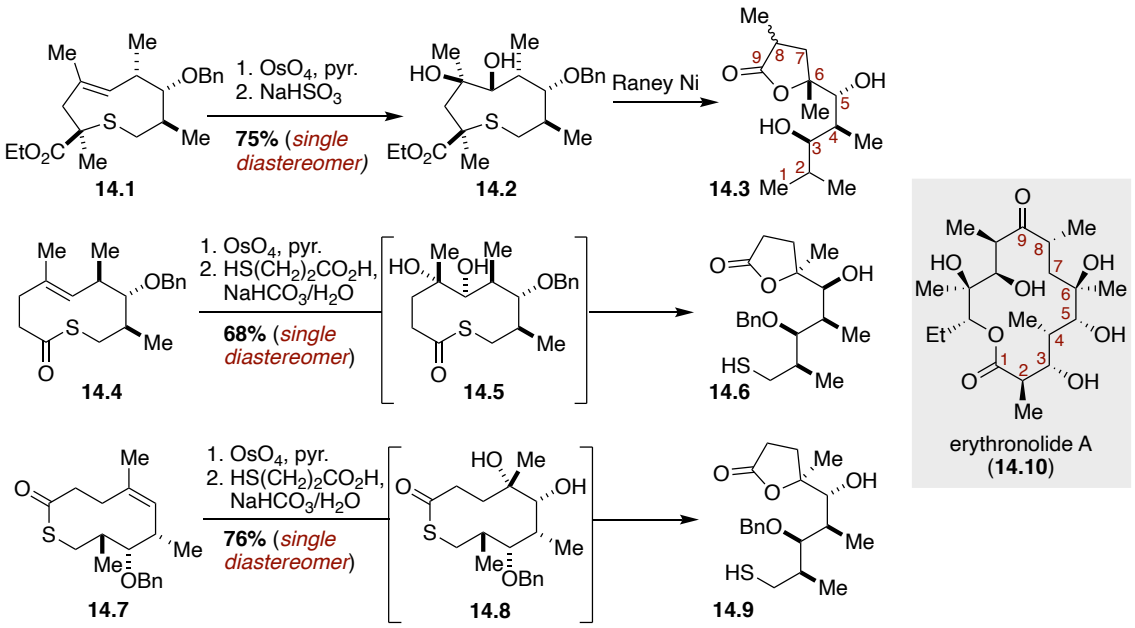

Scheme 14: Vedejs' work in diastereospecific osmylations of 9- and 10-membered macrocycles for the C_1-C_9 segment of the erythronolides.[14]

1.2.6 Other Conformationally Controlled Transformations

In Evans' synthesis of (+)-miyakolide **15.4**, he uses 22-membered macrocycle **15.2** to set up for a transannular aldol reaction, giving a new 16-membered macrocycle **15.3** with complete stereoselectivity (**Scheme 15**). In this transformation, enaminone **15.1** needed to be converted into 1,3-diketone (enol/keto tautomer) **15.2**, so it could undergo the desired cyclization step to give **15.3**. The OMe that was present in **15.1** was also hydrolyzed under the same conditions. Subjecting **15.3**, then, to DDQ to deprotect the PMB ether gave the final product (+)-miyakolide. One of the interesting things that was found during the synthesis of this compound was that in different solvents systems (in this case benzene and dioxane/water), the macrocycle has different

preferred conformations, as observed by NOE. For **15.1**, the macrocycle assumes a more compressed conformation when in benzene and a more open conformation in dioxane/water.[66]

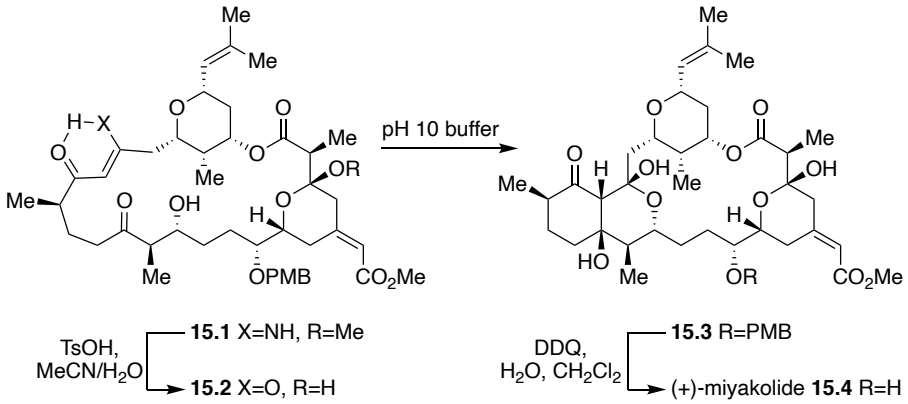

Scheme 15: Evans' transannular aldol reaction in the synthesis of (+)-miyakolide (**15.4**).[66]

1.3 More Recent Examples of Stereoselective Reactions of Macrocycles

Interest in the development of diastereoselective transformations of macrocylic systems has reduced over the past 20 years; however, there is still much to understand, and a few have used stereocontrolled elements afforded by macrocyclic conformation to accomplish late-stage installation of stereogenic centers.

In 2001, Danishefsky and co-workers revisited stereoselective epoxidations that they had reported on during the synthesis of the epothilones.[67] In these investigations they test the parameters of previous epoxidations due to difficulty with reproducing results. Although careful attention must be paid to the temperature and set-up of these reactions, Danishefsky again found that at low temperatures, dimethyldioxirane (DMDO) works very well to give the desired epoxide in high diastereoselectivities (**Scheme 16A**, **16.1** to **16.2**, *d.r. >96:4* at –78 °C).

In 2002, Panek and coworkers performed an epoxidation on an exocyclic olefin of 14-membered macrolactone **16.3** in the synthesis of oleandolide to give a single diastereomer **16.4** (**Scheme 16B**). Using Monte Carlo MM2 energy minimizations, they were able to see that one side of the olefin was blocked by the bulky silyl ether at C9, and the hydroxyl-group at C11 was positioned close enough to do a hydroxyl-directed epoxidation. Both of these ensured that only a single diastereomer was accessible.[68] Then again in 2003, Panek and coworkers used stereoselective epoxidations for both di- and tri-substituted olefins in 16-membered macrocycles (**Scheme 16C**).[69] For the disubstituted olefins of **16.5**, a mixture of diastereomers were formed (*d.r. 83:17*, diastereomeric at C3-C4, but only a single side was attacked at C11-C12). When the tri-substituted olefins of **16.7** were subjected to *m*-CPBA, only a single diastereomer was isolated

(**16.8**). This correlates well to that observed by Vedejs and coworkers in their studies of local stereocontrol. Trisubstituted olefins gave a single diastereomeric product in that study, while *E*-configured disubstituted olefins gave a mixture of diastereomers.[13]

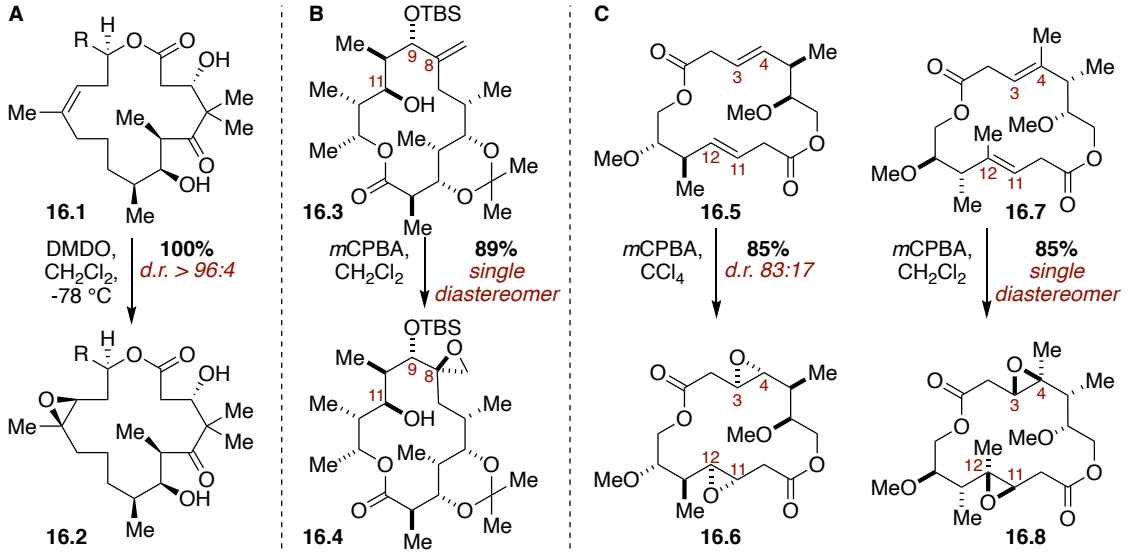

Scheme 16: Stereoselective epoxidations of macrocycles: **A.** Danishefsky's epoxidation of 16-membered macrolactone in the synthesis of the epothilones;[67] **B.** Panek's epoxidation of exocyclic olefinin the synthesis of oleandolide;[68] **C.** Panek's epoxidations of di-substituted olefins **16.5** and tri-substituted olefins **16.7**.[69]

Stereoselective reductions of macrocyclic systems have also been employed in recent years. Blüme and coworkers reduced a trisubstituted olefin of a 14-membered macrocycle catalytically to get a *d.r.* of *8:1* (**Scheme 17A**, **17.1** to **17.2**).[70] The observed diastereo-selectivity is attributed to the rigid nature of the molecule at the olefin, in which one side is blocked by the rest of the macrocycle. Similarly, Vilarrasa and coworkers reduced trisubstituted olefins **17.3** and **17.4**, and in both cases high selectivity for the *S* configured

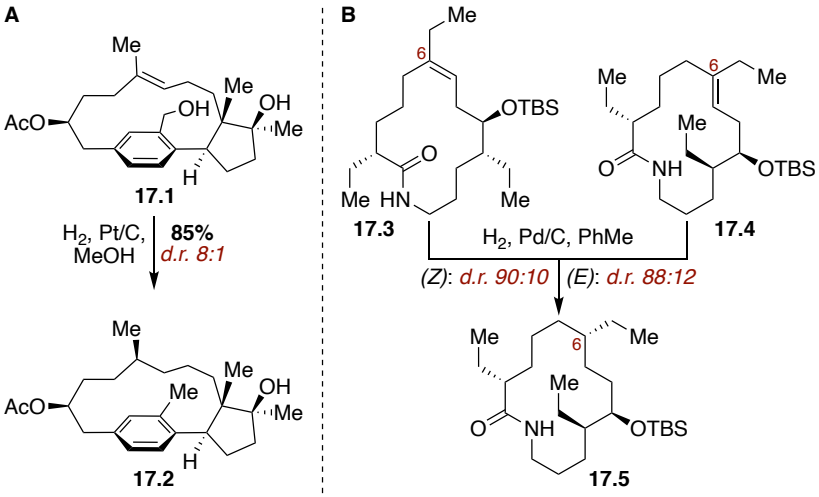

Scheme 17: A. Blüme's stereoselective reduction of 14-membered macrocyclic olefin;[70] **B.** Vilarrasa's stereoselective reduction of both *E* and *Z* isomers of 14-membered olefins **17.3** and **17.4** to give the same diastereomeric product.[71]

stereocenter at C6 was generated (**Scheme 17B**). Modeling of both the *E* and *Z*-configured starting materials showed the lowest-energy conformers of each having the same preference for addition to give the *S* configured center.[71]

Paterson, Zhai, and Nicolaou have all stereoselectively reduced ketones that are part of macrocyclic systems (**Scheme 18**). Paterson and coworkers reduced the ketone in 22-membered macrolactone **18.1** to give only a single product **18.2** in 70% yield with a Luche reduction using the macrocyclic conformation to direct the hydride addition.[72] Zhai and coworkers had more difficulty stereoselectively reducing the ketone in their 14-membered macrolactone system to give the desired product (**Scheme 18B**). Similarly to when Paterson applied the Luche reduction conditions, when these were applied to Zhai's system, only a single diastereomer **18.4** was isolated. However, **18.5** is the desired diastereomer; thus, (*S*)-BINAL-H was employed to give **18.5** preferentially (*d.r. 1:2.5* **18.4**:**18.5**), and **18.4** was recycled through oxidation with IBX and re-reduced to obtain more of the desired **18.5**.[73] Nicolaou was able to apply simple borohydride reduction conditions to epimers **18.6** and **18.8** (**Scheme 18C**) that had been obtained in the macrocyclization step to get a single diastereomeric product for each (**18.7** and **18.9**, respectively).[74] Manual modeling of the starting materials showed that only one face of each of the carbonyls was accessible for hydride attack.

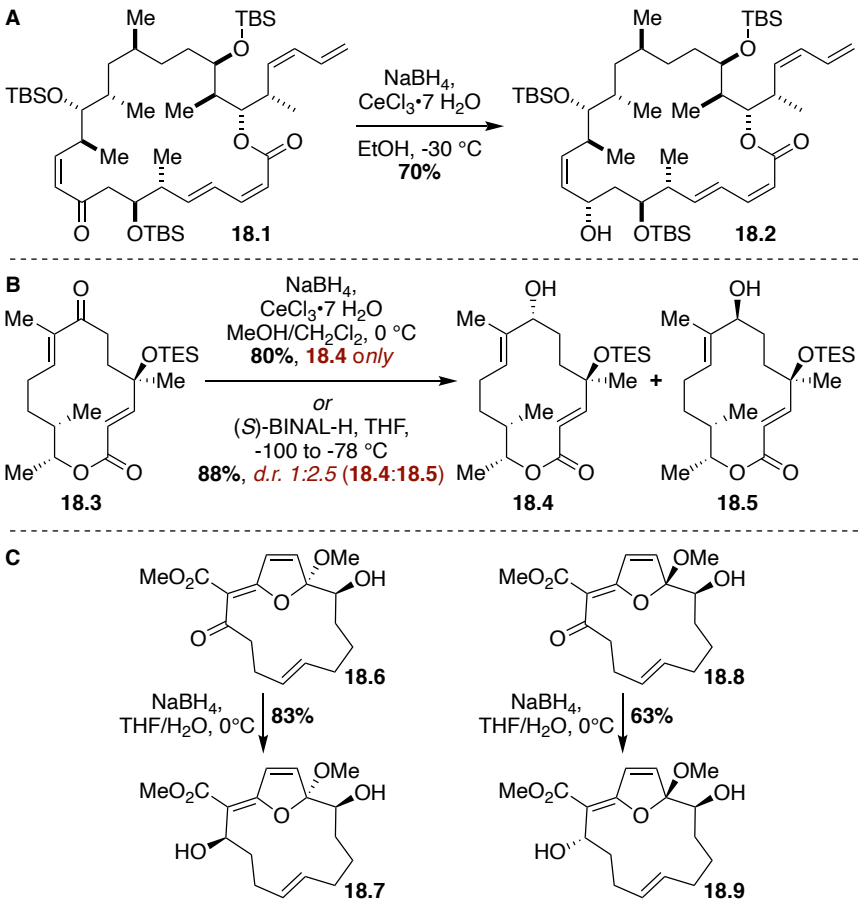

Scheme 18: Stereoselective reductions of macrocyclic ketones. **A.** Paterson's reduction of 22-membered macrocyclic ketone;[72] **B.** Zhai's stereoselective reduction of 14-membered macrocyclic ketone;[73] **C.** Nicolaou's stereoselective reduction of ketones in 13-membered macrocyclic epimers **18.6** and **18.8** to give diastereomers **18.7** and **18.9**.[74]

1.4 Diastereoselective Grignard Reactions of Macrocyclic 1,4-Diketones

Using macrocyclic 1,4-diketones as building blocks for the synthesis of strained benzenoid macrocycles has been a major thrust in the Merner laboratory. A streamlined synthetic approach to macrocyclic 1,4-diketones that are [*n*.4]metacylophane derivatives has been developed. The application of this approach to bent *para*-phenylene synthesis has resulted in the development of mild aromatization protocols and π-extension reaction strategies that lead to the synthesis of larger, curved polycyclic aromatic hydrocarbons, which represent substructures of carbon nanobelts.[15,75] During the devlopment of their synthetic approach to strained *p*-terphenyl-containg macrocyles (**Scheme 19**), it was noticed that the addition of Grignard reagents (*e.g.*, vinylmagnesium bromide or chloride) to the macrocyclic 1,4-diketone was diastereoselective, with a strong preference for the *syn* diastereoemer. This proved to be advantageous for the syntheis of bent *para*-phenylene units, as only the *syn*-bis-allylic-1,4-diols **19.11** to **19.15** undergo a ring-closing metathesis reaction (**Scheme 19**).[15–18] To further understand this diastereoselectivity, a detailed investigation that looked at several reaction parameters – including macrocyclic ring size, reagent, solvent, temperature, and bridging motif in the 1,4-diketone-containing macrocycle – was undertaken.

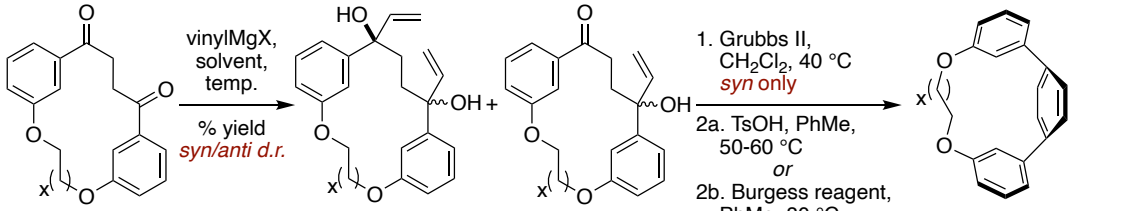

Scheme 19: Grignard addition to macrocyclic 1,4-diketones, followed by RCM (only of the *syn* addition product), and dehydrative aromatization.

It should be noted that some of the data that is presented here was carried out by other members of the Merner laboratory, particularly Nirob Saha and Nirmal Mitra; however, these data have been included here to provide context for the chemistry that will be presented. The earliest reaction screenings were performed using vinylmagnesium chloride and vinylmagnesium bromide in THF at 60 °C, somewhat standard Grignard reaction conditions, to determine if the Grignard halide counter ion influenced the diastereoselectivity of the addition. What was immediately apparent was when vinylmagnesium *bromide* was used (**Table 3**, entries 1, 3, 5, 7, and 9), significantly more of a hydroxyketone by-product **19.11**-**19.15** was obtained than when vinylmagnesium *chloride* was employed (**Table 3**, entries 2, 4, 6, 8, and 10). Comparing only the 19-membered macrocyclic systems, when bromide was the counter ion, 61% of the product

mixture was hydroxyketone; however, when chloride was the counter ion for the same system, only 38% of the product mixture was hydroxyketone (**Table 3**, entries 1 and 2, respectively). Additionally, the diastereoselectivity obtained when vinylmagnesium *chloride* was employed was greater for all ring sizes examined (**Table 3**, entries 2, 4, 6, 8, and 10). For the 18-membered macrocyclic system, when bromide was the counter ion, no observable preference for one diastereomer over the other is observed; however, when chloride is the counter ion, the diastereoselectivity increases to 2:1 in favor of the *syn*-1,4-diol product (**Table 3**, entries 3 and 4, respectively). The preference for diol formation and diastereoselectivity favoring the *syn* product is observed for all of the macrocycles presented in Table 3. It was also observed that larger macrocycles produce more of the hydroxyketone by-product and result in lower levels of diastereoselectivity when compared to smaller macrocycles. When vinylmagnesium chloride was employed for each of the macrocycles, the 19-membered macrocycle gave 62% diol (**Table 3**, entry 2: 2:1 *syn:anti*), the 18-membered 67% (entry 4: 2:1 *syn:anti*), the 17-membered 72% (entry 6: 5:1 *syn:anti*), the 16-membered 70% (entry 8: 20:1 *syn:anti*), and the 15-membered 72% (entry 10: 20:1 *syn:anti*).

Table 3: Reagent and Size Dependence – [*n*.4]*meta*-cyclophanes

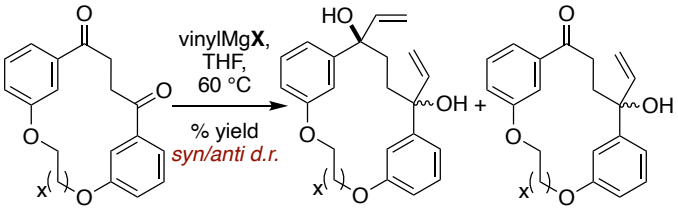

19.1: x=2
19.2: x=3
19.3: x=4
19.4: x=5
19.5: x=6

19.6: x=2
19.7: x=3
19.8: x=4
19.9: x=5
19.10: x=6

19.11: x=2
19.12: x=3
19.13: x=4
19.14: x=5
19.15: x=6

entry	**n** (x)	ring size	vinylMg**X**	1,4-diol	*d.r.*[(a)] *(syn/anti)*	HK
1	**9** (6)	19	**Br**	39%	1:2	61%
2	**9** (6)	19	**Cl**	62%	2:1	38%
3	**8** (5)	18	**Br**	48%	1:1	52%
4	**8** (5)	18	**Cl**	67%	2:1	33%
5	**7** (4)	17	**Br**	55%	2:1	45%
6	**7** (4)	17	**Cl**	72%	5:1	28%
7	**6** (3)	16	**Br**	58%	9:1	42%
8	**6** (3)	16	**Cl**	70%	20:1	30%
9	**5** (2)	15	**Br**	50%	9:1	40%
10	**5** (2)	15	**Cl**	72%	20:1	28%

(a) Yields/product ratios and *d.r.* were determined by ^{1}H NMR analysis (crude mixtures). These reactions were performed by Nirmal and Nirob.

Additional screenings were done of different solvents (**Table 4**) and temperatures (**Table 5**) to see if the results could be optimized still further in favor of formation of the *syn*-diol. The solvent was found to make a substantial difference. Although ethereal solvents are typical for Grignard reactions, the highest incidence of hydroxyketone formation and the lowest levels of diastereoselectivity were both observed when THF was the solvent (**Table 4**, entry 1). Both dichloromethane and benzene, however, gave both high diastereoselectivity and very little hydroxyketone (**Table 4**, entries 3 and 4, respectively). The temperature made less difference in the observed diastereoselectivity for the Grignard addition, but with increased temperatures, additional diol formation was observed in preference to the hydroxyketone (**Table 5**). This was observed to the greatest degree in going from -40 °C to 0°C, in which only 35% of the product mixture was observed to be diol at -40 °C but 89% of the product mixture was the diol at 0 °C (**Table 5**, entries 1 and 2, respectively). Although, both the solvent and the temperature made a difference in the observed diastereoselectivity of the reaction, the size of the macrocycle seemed to make the largest difference.

Table 4: Solvent Dependence – [*n*.4]*meta*-cyclophanes

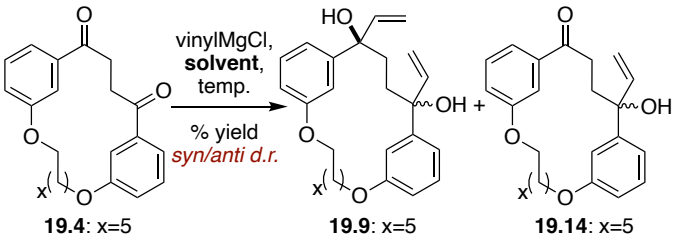

19.4: x=5 **19.9**: x=5 **19.14**: x=5

entry	**n** (x)	ring size	**solvent**	temp. (°C)	1,4-diol	*d.r.*[(a)] *(syn/anti)*	HK
1	**8** (5)	18	**THF**	60	67%[(b)]	67:33	33%[(b)]
2	**8** (5)	18	**PhMe**	23	82%[(b)]	79:21	18%[(b)]
3	**8** (5)	18	**CH_2Cl_2**	23	95%	83:17	5%
4	**8** (5)	18	**PhH**	23	96%	83:17	4%

(a) Product ratios and *d.r.* were determined by ^{1}H NMR analysis (crude mixtures); (b) Product ratios are isolated. These reactions were performed by Nirmal and Nirob.

Table 5: Temperature Dependence – [8.4]-*meta*-cyclophanes

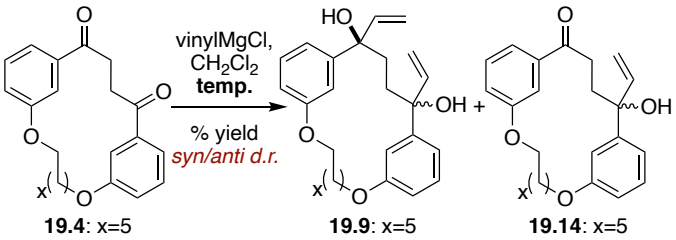

19.4: x=5 **19.9**: x=5 **19.14**: x=5

entry	**n** (x)	ring size	solvent	**temp. (°C)**	1,4-diol	*d.r.*[(a)] *(syn/anti)*	HK
1	**8** (5)	18	CH_2Cl_2	**-40**	35%	74:26	65%
2	**8** (5)	18	CH_2Cl_2	**0**	89%	83:17	11%
3	**8** (5)	18	CH_2Cl_2	**23**	95%	83:17	5%
4	**8** (5)	18	CH_2Cl_2	**40**	97%	79:21	3%

(a) Product ratios and *d.r.* were determined by ^{1}H NMR analysis (crude mixtures). These reactions were performed by Nirmal and Nirob.

The next parameter investigated was that of the bridging motif of the macrocyle. Before this point, all of the macrocycles investigated have been *meta*-cyclophanes, but it was hypothesized that reducing the ridgidity of the macrocycle by eliminating two of the sp^2-hybridized positions could affect the observed diastereoselectivity. This series of compounds was synthesized using the same four-step protocol employed in the syntheses of the *meta*-cyclophanes, but starting with salicylaldehyde (**20.1**) instead of 3-hydroxybenzaldehyde (**Scheme**

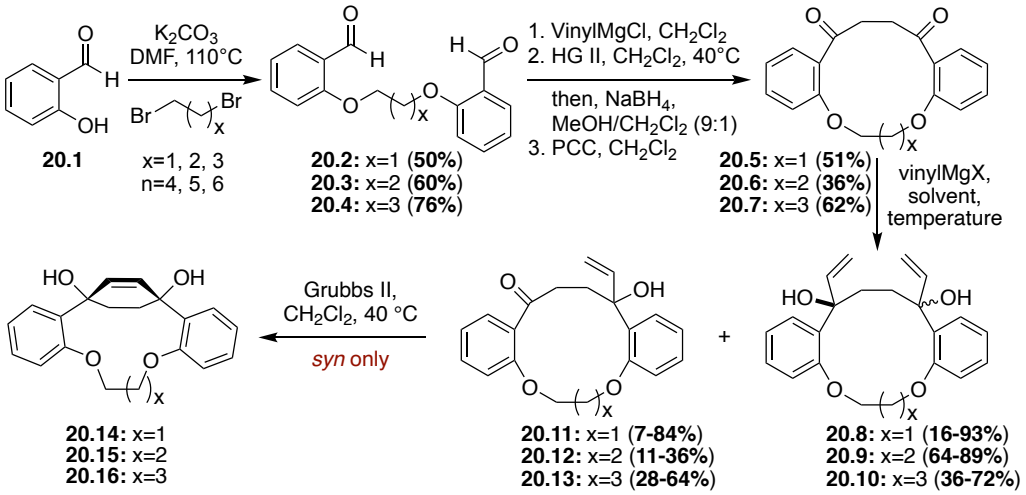

Scheme 20: Synthesis of [*n*.4]*ortho*-cyclophanes

20). When these macrocyclic 1,4-diketones were subjected to the same reaction conditions, lower levels of diastereoselection were indeed observed as was hypothesized, but more hydroxyketone was also observed in these reactions (**Table 6**). As in the *meta*-cyclophanes, as the macrocylic size decreased so did the formation of the hydroxyketone, and the diastereoselectivity increased. Also similar to that observed in the *meta*-cyclophanes, when vinylmagnesium *bromide* was used (**Table 6**, entry 13), much more hydroxyketone was observed than when *chloride* was the counterion (compare to **Table 6**, entry 10). Differently than the *meta*-cyclophanes, however, less distinction was observed between reactions performed in different solvents or at different temperatures for the *ortho*-cyclophanes than was observed for the *meta*-cyclophanes. Benzene and dichloromethane were again seen to be the most optimal

Table 6: Solvent and Temperature Dependence – [*n*.4]*ortho*-cyclophanes

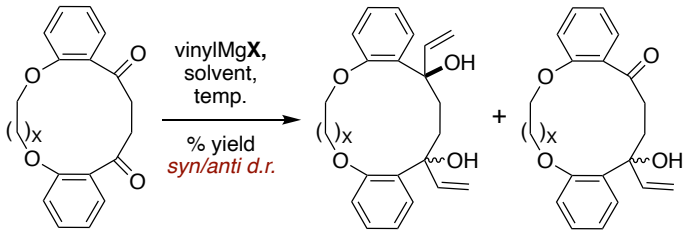

entry	**n** (x)	ring size	vinylMg***X***	solvent	temp. (°C)	1,4-diol	*d.r.*[(a)] (*syn*/*anti*)	HK
1	**6** (3)	14	**Cl**	THF	23	36%	29:71	64%
2	**5** (2)	13	**Cl**	THF	23	64%	75:25	36%
3	**4** (1)	12	**Cl**	THF	23	69%	83:17	31%
4	**4** (1)	12	**Cl**	THF	60	73%	71:29	27%
5	**6** (3)	14	**Cl**	PhH	40	72%	38:62	28%
6	**5** (2)	13	**Cl**	PhH	40	89%	76:24	11%
7	**4** (1)	12	**Cl**	PhH	40	90%	69:31	10%
8	**6** (3)	14	**Cl**	CH_2Cl_2	23	47%	42:58	53%
9	**5** (2)	13	**Cl**	CH_2Cl_2	23	76%	63:37	24%
10	**4** (1)	12	**Cl**	CH_2Cl_2	23	90%	74:26	10%
11	**4** (1)	12	**Cl**	CH_2Cl_2	40	91%	76:24	9%
12	**4** (1)	12	**Cl**	CH_2Cl_2	0	88%	80:20	12%
13	**4** (1)	12	**Br**	CH_2Cl_2	23	16%	74:26	84%
14	**4** (1)	12	**Cl**	PhMe	60	93%	70:30	7%

(a) Yields/product ratios and *d.r.* were determined by ^{1}H NMR analysis (crude mixtures).

solvents for suppressing hydroxyketone formation, but THF and toluene showed similar diastereoselectivities to benzene and dichloromethane.

To try to understand what other factors could also be contributing to the observed diastereoselectivity, other Grignard reagents were employed and other metal cations were tested. For easier comparison to the bulk of the data gathered, these reactions were performed on the *meta*-cyclophanes. What is immediately apparent from both the phenylmagnesium chloride (**Table 7**, entry 2, 90% diol, *d.r. 61:39*) and ethylmagnesium chloride (**Table 8**, entry 3, 87% diol, *d.r. 78:22*) reactions is that less of the material is converted to the 1,4-diol (although the discrepancy is not great) and the diastereoselectivities are lower. When vinylmagnesium chloride was used for the 18-membered macrocyclic diketone, 95% of the product mixture was diol, and the *d.r.* was *83:17* (**Table 4**, entry 3). The phenylmetal reactions (**Table 7**) showed that temperature and solvent affected the amount of diol that was obtained, but the *d.r.*'s remained similar and showed little selectivity for one diastereomer over the other. For the ethyl Grignard reagents, dichloromethane is the preferred solvent over THF for the formation of the 1,4-diol and for getting the desired *syn* diastereomer (compare **Table 8**, entry 3 to 8 and 4 to 9), similar to that which was observed in the reactions employing vinylmagnesium reagents. When comparing the ethylmetal reagents themselves, ethyl lithium gave the greatest conversion to the 1,4-diol in THF (**Table 8**, entry 7, 94% diol). Ethylmagnesium chloride and bromide in THF only gave 57 and 58% diol, respectively

Table 7: Phenyl-metal Derivatives – [8.4]-*meta*-cyclophanes

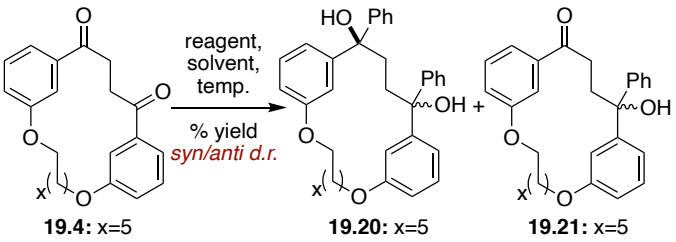

entry	reagent	solvent	temp. (°C)	1,4-diol	*d.r.*[(a)] *(syn/anti)*	HK
1	PhMgCl	CH_2Cl_2	0	45%	54:46	55%
2	PhMgCl	CH_2Cl_2	23	90%	61:39	10%
3	PhMgCl	CH_2Cl_2	40	69%	68:32	31%
4	PhMgCl	PhH	60	64%	68:32	36%
5	PhLi	THF	0–23	60%	70:30	40%

(a) Yields/product ratios and *d.r.* were determined by ^{1}H NMR analysis (crude mixtures).

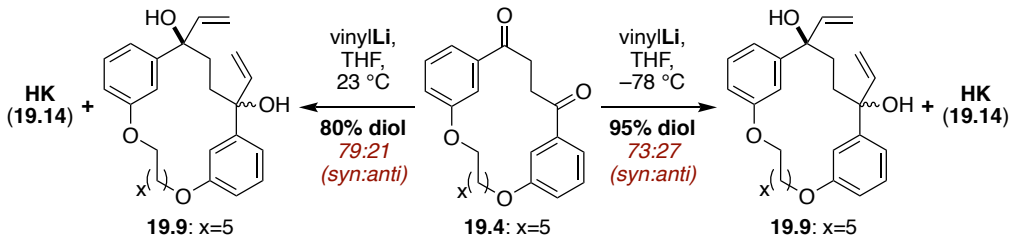

Scheme 21: Addition of vinylLi to 18-membered macrocyclic 1,4-diketone at –78 and 23 °C.

(**Table 8**, entries 8 and 9, respectively). In both THF and dichloromethane, the diethyl zinc reagents did not add at all to the diketone. Instead, the diketone was simply returned unreacted. The final organometallic reagent that was tested was was vinyllithium (**Scheme 21**). These tests were run in THF, and at both -78 °C (95% diol, *d.r. 73:27*) and room temperature (80% diol, *d.r. 79:21*), more of the product mixture was diol and the diastereoselectivities are higher than were observed with vinylmagnesium bromide or chloride reactions in THF (**Table 3**, entry 3, **Br**, 48% diol, *d.r. 1:1* and entry 4, **Cl**, 67% diol, *d.r. 2:1*).

Table 8: Reagent Dependence – EtM Derivatives – [*n*.4]*meta*-cyclophanes

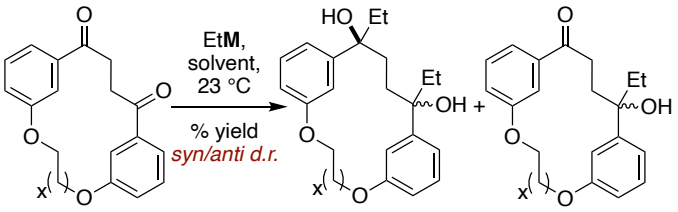

19.3: x=4 **19.4:** x=5 **19.16:** x=4 **19.17:** x=5 **19.18:** x=4 **19.19:** x=5

entry	**n** (x)	ring size	Et**M**	solvent	1,4-diol	*d.r.*[(a)] (syn/anti)	HK
1	**7** (4)	17	Et**MgCl**	CH_2Cl_2	96%	90:10	4%
2	**7** (4)	17	Et**MgBr**	CH_2Cl_2	93%	90:10	7%
3	**7** (4)	17	Et_2**Zn**	CH_2Cl_2	0%	—:—	0%
4	**7** (4)	17	Et_2**Zn**[(b)]	CH_2Cl_2	0%	—:—	0%
5	**7** (4)	17	Et**Li**	THF	86%	73:27	27%
6	**7** (4)	17	Et**MgCl**	THF	83%	89:11	17%
7	**7** (4)	17	Et**MgBr**	THF	81%	80:20	19%
8	**7** (4)	17	Et_2**Zn**	THF	0%	—:—	0%
9	**7** (4)	17	Et_2**Zn**[(b)]	THF	0%	—:—	0%
10	**8** (5)	18	Et**MgCl**	CH_2Cl_2	94%	81:19	6%
11	**8** (5)	18	Et**MgBr**	CH_2Cl_2	91%	85:15	9%
12	**8** (5)	18	Et_2**Zn**	CH_2Cl_2	0%	—:—	0%
13	**8** (5)	18	Et_2**Zn**[(b)]	CH_2Cl_2	0%	—:—	0%
14	**8** (5)	18	Et**Li**	THF	95%	49:51	5%
15	**8** (5)	18	Et**MgCl**	THF	85%	77:23	15%
16	**8** (5)	18	Et**MgBr**	THF	87%	75:25	13%
17	**8** (5)	18	Et_2**Zn**	THF	0%	—:—	0%
18	**8** (5)	18	Et_2**Zn**[(b)]	THF	0%	—:—	0%

(a) Yields/product ratios and *d.r.* were determined by ^{1}H NMR analysis (crude mixtures). (b) $Ti(O^iPr)_4$ was also added to this reaction.

The trends shown in the tables above indicate that there are many factors that contribute to the diastereoselectivity of 1,2-additions to macrocyclic 1,4-diketones. However, the data is consistent in showing that smaller macrocycles have higher observed diastereoselectivities despite the other conditions' contributions, and this is true for both the *meta*-cyclophanes and *ortho*-cyclophanes investigated. Such results are consistent with that described earlier in the

chapter relating to the observed low-energy conformations of macrocyclic systems. When cycloalkanes, exclusively, are compared, it becomes evident that as the macrocycle gets larger, the system takes on greater degrees of freedom and thus has more similar energy conformations available to it. The macrocyclic 1,4-diketones dealt with in this section are comparable because the only difference between one macrocycle and the next (within each system, *meta* and *ortho*, considered separately) is the number of CH_2 groups in the tether between the aromatic rings. The degrees of unsaturation and the placement of the sp^2-hybridized carbon atoms and heteroatoms remain consistent throughout each series.

To investigate how much difference such an effect makes, a determination of the number of low-energy conformers for each cycle is necessary. A thorough investigation of such a conformational search requires the use of molecular dynamics simulations, such as Monte Carlo or MMFF. Such an investigation is beyond the computational expertise available within our group and department, so to try to make a start at understanding the conformations at play in these reactions, gas-phase DFT calculations were carried out using b3lyp/6-31g(d) to determine (1) one or two low-energy conformations of the starting diketone, (2) the lowest energy conformations of the hydroxyketones that would most likely lead to the *syn* and *anti* diasteromers, and (3) the conformations of the *syn* and *anti* diastereomers. The structures investigated were optimized from the x-ray crystal structure coordinates of [8.4]*meta*-cyclophane **19.4**, and CH_2 groups were added or removed accordingly to obtain each macrocycle. Additionally, based on the work of Peczuh and coworkers,[33] ribbon conformations of the diketones were investigated and included if a similar low-energy conformation was also found. **Figure 21** shows the computed structures for the [5.4]*meta*-cyclophane series. **21A** represents the lowest-energy conformation of the 15-membered 1,4-diketone, but **21B**, which assumes a ribbon conformation, is only 0.6 kcal/mol higher in energy than **21A**; thus, either of these conformations can be assumed as possible starting conformations. As shown by **21C** and **21D**, the lowest computed energy conformers for the hydroxyketones assume a similar ribbon conformation to that of **21B**. **21C** leads to the *syn* diastereomer (**21E**), and **21D** leads to the *anti* diastereomer (**21F**). These conformations of hydroxyketone have essentially the same energy value (only 0.1 kcal/mol difference). Structures **21E** and **21F** show the lowest-energy conformations for the *syn* and *anti* 1,4-diols, respectively. The computed energy difference for these compounds is 1.5 kcal/mol, which is in relatively good agreement with experiment. For a diastereomeric ratio of 20:1, the energy

Table 9: Relative computed energies of compounds **21A**-**21F**

compound	structure type	relative energy (kcal/mol)	experimental *d.r.* *(syn/anti)*
21A	open	0.0	
21B	ribbon	0.6	
21C	ribbon	-2.1	
21D	ribbon	-2.2	
21E	ribbon	26.0	20:1[(a)]
21F	open	27.5	9:1[(b)]

(a) *d.r.* from **Table 3**, entry 10; (b) *d.r.* from **Table 3**, entry 9

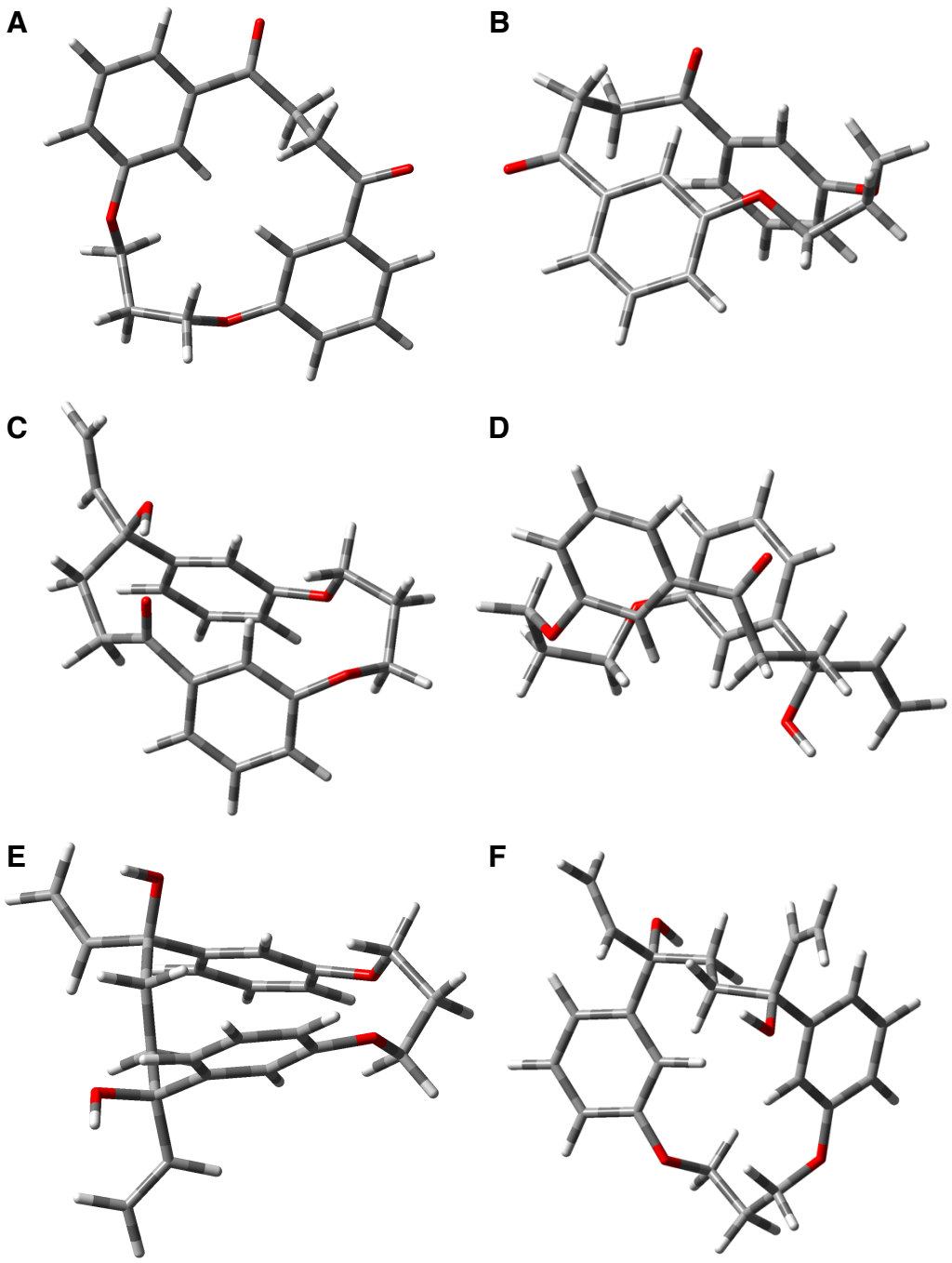

Figure 21: DFT computed structure for [5.4]*meta*-cyclophane series. **A.** Lowest-energy conformation of [5.4]*meta*-diketone based on X-ray structures; **B.** Ribbon conformation of [5.4]*meta*-diketone; **C.** Hydroxyketone conformer leading to *syn* diastereomer; **D.** Hydroxyketone conformer leading to *anti* diastereomer; **E.** *Syn* [5.4]*meta*-1,4-diol; **F.** *Anti* [5.4]*meta*-1,4-diol.

difference is expected to be 1.8 kcal/mol, and for a ratio of 9:1, the expected energy difference is 1.3 kcal/mol. Although, these computed energy values do not give the full picture, they do begin to give some understanding as to potentially why these macrocycles react diastereoselectively.

1.5 Future Directions

To truly understand what drives the diastereoselectivity of reactions to macrocycles, more investigation is needed. As Wzorek points out, it is not sufficient to generalize reactions of macrocycles by pointing to either the starting material configuration or a particular transition state model. Understanding a type of reaction to a particular system requires extensive modeling of the entire reaction sequence.[64] To accomplish this for the macrocyclic diketones described above, molecular dynamics (MD) calculations need to be performed to determine what other low-energy conformations exist for each of the macrocyclic systems. Doing so will allow for a better understanding of the conformations that are contributing to the observed reactivity of the systems. This is especially true for the hydroxyketone intermediates, since it is at this stage when the diastereoselectivity of the reactions is determined. Additionally, once the low-energy conformations have been identified, modeling the transition states for each conformation to the product will help determine which reaction pathways are feasible, because even though a conformation is low-energy, it may not be a reactive conformation. The barrier it must overcome to give the product could be too high for the reaction conditions used.

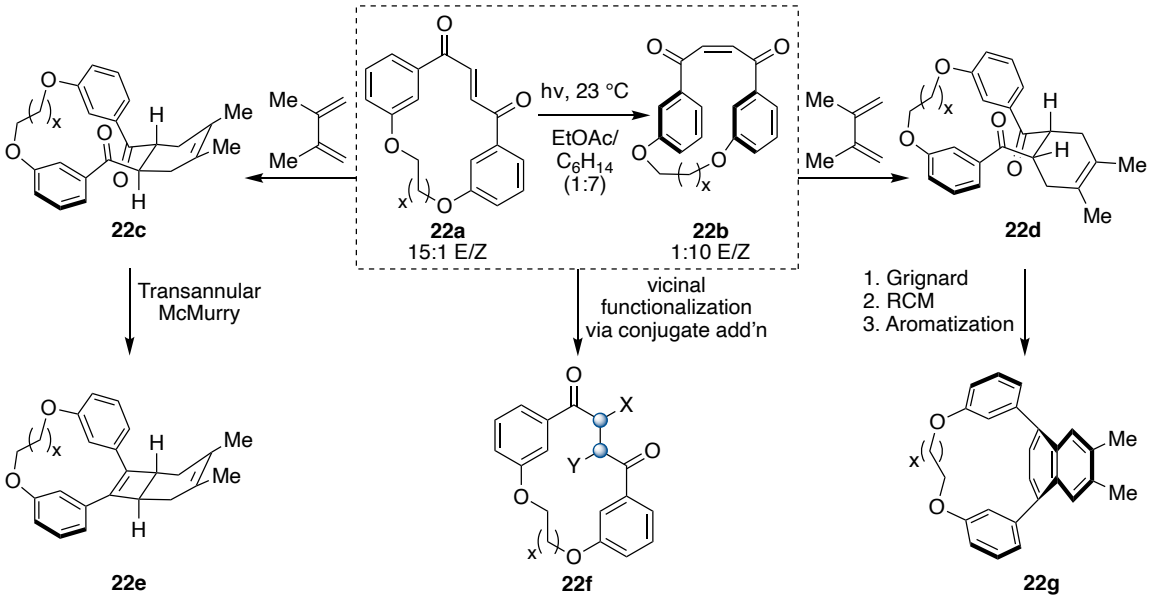

Figure 22: Proposed reactions to install new stereocenters and/or functionality to the macrocyclic backbone from macrocyclic ene-diones **22a** and **22b**.

In addition to computational studies on the systems and reactions described above, the macrocyclic ketones can serve as handles for adding additional functionality to the macrocyclic backbone. The Merner group has already shown that we can make bent aromatic rings using the diastereoselective Grignard additions shown above,[15–18] and that these can be used to do Scholl

reactions to extend the π-system for the ground up synthesis of carbon nanobelts and tubes.[75] However, it is also feasible that an unsaturated ene-dione could be used as a handle for [4+2] addition reactions (**Figure 22**, **22a** to **22c** or **22b** to **22d**). This allows for the installation of 2 new stereogenic centers. Then if **22d** is subjected to the previously described aromatization sequence, followed by an additional aromatization with DDQ, a napthyl group to be installed instead of simply a phenyl (**22g**), which continues the π-extension further than it has currently been accomplished. Alternatively, the product of the [4+2], either **22c** or **22d** could be subjected to a transannular McMurry reaction to form a cyclobutene ring (**22e** and its *syn* diastereomer). In addition to these possibilities, subjecting the ene-dione (either **22a** or **22b**) to a conjugate addition could allow for the installation of two new stereocenters where X and Y could be the same or different (**22f**). The saturated 1,4-diketone can also serve as a handle to do enolate alkylations diastereoselectively for the synthesis of natural products (as will be described in detail in the following chapter, **Figure 23**).

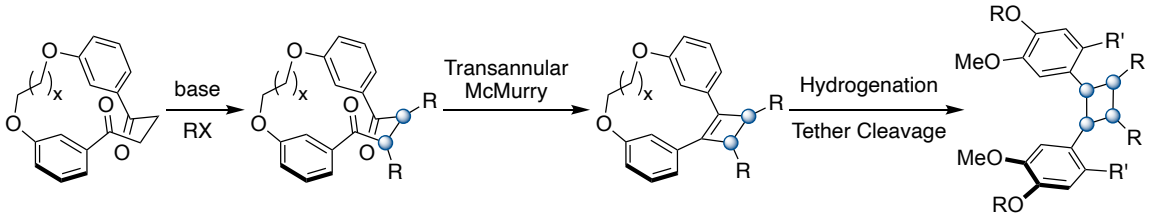

Figure 23: Double enolate alkylation to macrocyclic 1,4-diketone for the synthesis of lignan natural products **23e**.

1.6 Conclusions

Reactions of macrocycles have been observed for more than 50 years to give interesting and high diastereoselectivity. Early investigations led to the understanding that although macrocyclic systems may appear to be floppy, they generally adopt only a few low-energy conformations. Models such as the peripheral attack model have been used to predict and explain reaction outcomes, but computational modeling is still the most effective way to explain the observed diastereoselectivity of reactions.

The diastereoselective nature of 1,2-additions to macrocyclic 1,4-diketones has been investigated, and while many factors contribute to the diastereoselectivity of these reactions, the size of the macrocycle influences the observed diastereoselectivity to the greatest extent. This seems to be predominantly because with each additional CH_2 group making the ring larger, additional degrees of freedom are introduced and thus the possibility for additional similar energy

conformations exists. Other factors such as solvent effects, temperature dependence, bridging motif, and reagent dependence were also investigated and their effects noted, but still none played as influential a roll as the macrocyclic size itself.

References

(1) Hassel, O.; Ottar, B. *Acta Chem. Scand.* **1947**, *1*, 929–943

(2) Barton, D. H. R. *Experientia* **1950**, *6*, 316–320.

(3) Hubert, A. J.; Dale, J. *J. Chem. Soc.* **1963**, 86–93.

(4) Dale, J. *Angew. Chemie Int. Ed. English* **1966**, *5*, 1000–1021.

(5) Dale, J. *J. Chem. Soc.* **1963**, 93–111.

(6) Anet, F. A. L.; Cheng, A. K.; Krane, J. *J. Am. Chem. Soc.* **1973**, *95*, 7877–7878.

(7) Anet, F. A. L.; St. Jacques, M.; Henrichs, P. M.; Cheng, A. K.; Krane, J.; Wong, L. *Tetrahedron* **1974**, *30*, 1629–1637.

(8) Still, W. C. *J. Am. Chem. Soc.* **1979**, *101*, 2493–2495.

(9) Still, W. C.; Galynker, I. *Tetrahedron* **1981**, *37*, 3981–3996.

(10) Corey, E. J.; Hopkins, P. B.; Sunggak, K.; Sung-eun, Y.; Nambiar, K. P.; Falck, J. R. *J. Am. Chem. Soc.* **1979**, *101*, 7131–7134.

(11) Kuroda, C.; Hirota, H.; Takahashi, T. *Chem. Lett.* **1982**, *11*, 249–252.

(12) Takahashi, T.; Kanda, Y.; Nemoto, H.; Kitamura, K.; Tsuji, J.; Fukazawa, Y. *J. Org. Chem.* **1986**, *51*, 3393–3394.

(13) Vedejs, E.; Gapinski, D. M. *J. Am. Chem. Soc.* **1983**, *105*, 5058–5061.

(14) Vedejs, E.; Dolphin, J. M.; Mastalerz, H. *J. Am. Chem. Soc.* **1983**, *105*, 127–130.

(15) Mitra, N. K.; Corzo, H. H.; Merner, B. L. *Org. Lett.* **2016**, *18*, 3278–3281.

(16) Mitra, N. K.; Merryman, C. P.; Merner, B. L. *Synlett* **2017**, *28*, 2205–2211.

(17) Mitra, N. K.; Meudom, R.; Gorden, J. D.; Merner, B. L. *Org. Lett.* **2015**, *17*, 2700–2703.

(18) Mitra, N. K.; Meudom, R.; Corzo, H. H.; Gorden, J. D.; Merner, B. L. *J. Am. Chem. Soc.* **2016**, *138*, 3235–3240.

(19) Anet, F. A. L.; Degen, P. J.; Yavari, I. *J. Org. Chem.* **1978**, *43*, 3021–3023.

(20) Wiberg, K. B. *J. Org. Chem.* **2003**, *68*, 9322–9329.

(21) Weinberg, N.; Wolfe, S. *J. Am. Chem. Soc.* **1994**, *116*, 9860–9868.

(22) Dale, J.; Ryde-Petterson, G.; Strand, U.; Jalonen, H.; Lüning, B.; Swahn, C.-G. *Acta Chemica Scandinavica*, 1973, 1115–1129.

(23) Pawar, D. M.; Miggins, S. D.; Smith, S. V; Noe, E. A. *J. Org. Chem* **1999**, *64*, 2418–2421.

(24) Anet, F. A. L.; Krane, J. *Isr. J. Chem.* **1980**, *20*, 72–83.

(25) Pawar, D. M.; Cain, D.; Gill, G.; Bain, A. D.; Sullivan, R. H.; Noe, E. A. *J. Org. Chem.* **2007**, *72*, 25–29.

(26) Rawdah, T. N. *Tetrahedron* **1989**, *45*, 7405–7410.

(27) Casarini, D.; Lunazzi, L.; Mazzanti, A. *European J. Org. Chem.* **2010**, *2*, 2035–2056.

(28) Pawar, D. M.; Noe, E. A. *J. Am. Chem. Soc.* **1998**, *120*, 5312–5314.

(29) Pawar, D. M.; Noe, E. A. *J. Am. Chem. Soc.* **1996**, *118*, 12821–12825.

(30) Pawar, D. M.; Brown II, J.; Chen, K.-H.; Allinger, N. L.; Noe, E. A. *J. Org. Chem.* **2006**, *71*, 6512–6515.

(31) Dragojlovic, V. *ChemTexts* **2015**, *1*, 1–30.

(32) Allinger, N. L.; Dale, J. *Topics in Stereochemistry*; 1967.

(33) Magpusao, A. N.; Rutledge, K.; Hamlin, T. A.; Lawrence, J. M.; Mercado, B. Q.; Leadbeater, N. E.; Peczuh, M. W. *Chem. - A Eur. J.* **2016**, *22*, 6001–6011.

(34) Pawar, D. M.; Davis, K. L.; Brown, B. L.; Smith, S. V; Noe, E. A. *J. Org. Chem.* **1999**, *64*, 4580–4585.

(35) Atavin, E. G.; Mastryukov, V. S.; Allinger, N. L.; Almenningen, A.; Seip, R. *J. Mol. Struct.* **1989**, *212* (C), 87–95.

(36) Rawdah, T. N.; Zamil El-Faer, M. *Tetrahedron* **1990**, *46*, 4101–4108.

(37) Anet, F. A. L.; Rawdah, T. N. *Tetrahedron Lett.* **1979**, *20*, 1943–1946.

(38) Anet, F. A. L.; Rawdah, T. N. *J. Am. Chem. Soc.* **1978**, *100*, 7810–7814.

(39) Winnik, M. A. *Chem. Rev* **1981**, *81*, 491–524.

(40) Dos Santos, H. F.; Franco, M. L.; Venâncio, M. F.; Ferreira, D. E. C.; Anconi, C. P. A.; Rocha, W. R.; De Almeida, W. B. *Int. J. Quantum Chem.* **2012**, *112*, 3188–3197.

(41) Rubin, B. H.; Williamson, M.; Takeshita, M.; Menger, F. M.; Anet, F. A. L.; Bacon, B.; Allinger, N. L. *J. Am. Chem. Soc.* **1984**, *106*, 2088–2092.

(42) Groth, P. *Acta Chem. Scand. A* **1979**, *33*, 503–513.

(43) Groth, P. *Acta Chem. Scand. A* **1980**, *34*, 609–620.

(44) Valente, E. J.; Pawar, D. M.; Fronczek, F. R.; Noe, E. A. *Acta Crystallogr. Sect. C* **2008**, *C64*, o447–o449.

(45) Samuel, G.; Weiss, R. *Tetrahedron Lett.* **1969**, *10*, 2803–2806.

(46) Keller, T. H.; Neeland, E. G.; Rettig, S.; Trotter, J.; Weiler, L. *J. Am. Chem. Soc.* **1988**, *110*, 7858–7868.

(47) Dugat, D.; Valade, A. G.; Combourieu, B.; Guyot, J. *Tetrahedron* **2005**, *61*, 5641–5653.

(48) Noe, E. A.; Pawar, D. M.; Fronczek, F. R. *Acta Crystallogr. Sect. C Cryst. Struct. Commun.* **2008**, *64*, 67–68.

(49) van den Hoek, W. G. M.; Oonk, H. A. J.; Kroon, J. *Acta Crystallogr. Sect. B Struct. Crystallogr. Cryst. Chem.* **1979**, *35*, 1858–1861.

(50) Noe, E. A.; Pawar, D. M.; Fronczek, F. R. *Acta Crystallogr. Sect. C Cryst. Struct. Commun.* **2008**, *64*, 139–141.

(51) Shannon, V. L.; Strauss, H. L.; Snyder, R. G.; Elliger, C. A.; Mattice, W. L. *J. Am. Chem. Soc.* **1989**, *111*, 1947–1958.

(52) Anet, F. A. L.; Cheng, A. K. *J. Am. Chem. Soc.* **1975**, *97*, 2420–2424.

(53) Allinger, N. L.; Gorden, B.; Profeta, S. O. *Tetrahedron* **1980**, *36*, 859–864.

(54) Gudmundsdottir, A. D.; Lewis, T. J.; Randall, L. H.; Scheffer, J. R.; Rettig, S. J.; Trotter, J.;

Wu, C.-H. *J. Am. Chem. Soc.* **1996**, *118*, 6167–6184.
(55) Shah, A. V.; Dolata, D. P. *J. Comput. Aided. Mol. Des.* **1993**, *7*, 103–124.
(56) Kolossváry, I.; Guida, W. C. *J. Comput. Chem.* **1999**, *20*, 1671–1684.
(57) Still, W. C.; Galynker, I. *J. Am. Chem. Soc.* **1982**, *104*, 1774–1776.
(58) Still, W. C.; Novack, V. J. *J. Am. Chem. Soc.* **1984**, *106*, 1148–1149.
(59) Still, W. C.; Murata, S.; Revial, G.; Yoshihara, K. *J. Am. Chem. Soc.* **1983**, *105*, 625–627.
(60) Still, W. C.; Gennari, C.; Noguez, J. A.; Pearson, D. A. *J. Am. Chem. Soc.* **1984**, *106*, 260–262.
(61) Still, W. C.; Romero, A. G. *J. Am. Chem. Soc.* **1986**, *108*, 2105–2106.
(62) Vedejs, E.; Buchanan, R. A.; Watanabe, Y. *J. Am. Chem. Soc.* **1989**, *111*, 8430–8438.
(63) Evans, D. A.; Ratz, A. M.; Huff, B. E.; Sheppard, G. S. *J. Am. Chem. Soc.* **1995**, *117*, 3448–3467.
(64) Wzorek Jr., Joseph Stanley. 2012. Macrocyclic Stereocontrol in Organic Synthesis: I. Efforts Toward the Synthesis of (-)-Tetracycline. II. Analysis of the Peripheral Attack Model. Doctoral dissertation, Harvard University.
(65) Corey, E. J.; Kim, S.; Yoo, S.; Nicolaou, K. C.; Melvin Jr., L. S.; Brunelle, D. J.; Falck, J. R.; Trybulski, E. J.; Lett, R.; Sheldrake, P. W. *J. Am. Chem. Soc.* **1978**, *100*, 4620–4622.
(66) Evans, D. A.; Ripin, D. H. B.; Halstead, D. P.; Campos, K. R. *J. Am. Chem. Soc.* **1999**, *121*, 6816–6826.
(67) Stachel, S. J.; Danishefsky, S. J. *Tetrahedron Lett.* **2001**, *42*, 6785–6787.
(68) Hu, T.; Takenaka, N.; Panek, J. S. *J. Am. Chem. Soc.* **2002**, *124*, 12806–12815.
(69) Su, Q.; Beeler, A. B.; Lobkovsky, E.; Porco, Jr., J. A.; Panek, J. S. *Org. Lett.* **2003**, *5*, 2149–2152.
(70) Bäurle, S.; Blume, T.; Mengel, A.; Parchmann, C.; Skuballa, W.; Bäsler, S.; Schäfer, M.; Sülzle, D.; Wrona-Metzinger, H. P. *Angew. Chemie - Int. Ed.* **2003**, *42*, 3961–3964.
(71) Llàcer, E.; Urpí, F.; Vilarrasa, J. *Org. Lett.* **2009**, *11*, 3198–3201.
(72) Paterson, I.; Britton, R.; Delgado, O.; Meyer, A.; Poullennec, K. G. *Angew. Chemie - Int. Ed.* **2004**, *43*, 4629–4633.
(73) Li, G.; Yang, X.; Zhai, H. *J. Org. Chem.* **2009**, *74*, 1356–1359.
(74) Nicolaou, K. C.; Adsool, V. A.; Hale, C. R. H. *Angew. Chemie - Int. Ed.* **2011**, *50*, 5149–5152.
(75) Saha, N. K.; Mitra, N. K.; Johnson, K. F.; Merner, B. L. *Org. Lett.* **2018**, *20*, 6855–6858.

CHAPTER 2 Regioselective Formation of 1,2,3,4-Tetrasubstituted Cyclobutanes

2. Introduction

Cyclobutanes, four-membered carbocyclic rings, are a strained ring that have been receiving growing interest amongst the scientific community to exploit the possibilities these structures offer in practical applications but also for the synthetic challenge they present because of their inherent strain (27 kcal/mol).[1] From a pharmacological standpoint, cyclobutane-containing natural products show robust cardiovascular,[2,3] anti-tumor,[3–7] anti-inflammatory,[3,8] anti-microbial,[3,6,9,10] and insecticidal activities.[3] Additionally, cyclobutane rings have also found use in materials science. They have been tested as tunable energetic materials with uses as both explosives and propellants[11] and as a more sustainable alternative in polymer synthesis. Polymers containing cyclobutane rings display similar thermal and chemical stability to more well-known polymers like polyethylene terephthalate, a common polymer found in plastic bottles, but with the advantage of their building blocks being derived from biomass-based sources.[12,13]

In addition to these applications, however, compounds featuring a cyclobutane ring have received attention as interesting and challenging synthetic targets.[1,14,15] Because of the strained nature of these compounds, the number of approaches that have led to their syntheses are relatively limited. However, creative and new techniques are constantly being pursued.[1] Both historically and presently the [2+2] photocycloaddition reaction is generally the method of choice when approaching the formation of a four-membered ring. However well explored these [2+2] photocycloadditions have been, there is still room for improvement and investigation to create different regio- and stereoisomers and incorporate new functional groups around the ring. In addition, other methods that have been utilized to try to overcome some of the issues presented by [2+2] cycloadditions will be highlighted below.

2.1 [2+2] Photocycloaddition Reactions for Assembling 1,2,3,4-Tetrasubstituted Cyclobutane Rings

Several review articles have been written on the topics of [2+2] cycloaddition reactions and on photochemical reactions in general, so the following sections will highlight some examples of the formation of stand-alone 1,2,3,4-tetrasubstituted cyclobutane rings formed through [2+2] cycloaddition reactions.

Photocycloaddition reactions are fascinating because of the way in which high-energy intermediates are accessed and tolerated because of the absorption of light. Fundamentally, when an olefin is photo-excited, a single electron moves from the highest occupied molecular orbital (HOMO) to an excited state, the lowest unoccupied molecular orbital (LUMO), but this can be accomplished through several different mechanisms. The most straightforward of these is a direct excitation of the olefin (**Figure 24A**), and this most often occurs in conjugated π-systems (like stilbenes and styrenes).[16] If the LUMO is in the singlet state (S_1), the reaction needs to occur rapidly because the S_1 state is generally short-lived (**Figure 24A**, *pathway a*). This is most commonly seen in intramolecular reactions, although it does not have to be.[16] Having the excited electron instead in a triplet excited state with ππ* character allows the electron to remain excited for a longer time, allowing an intermolecular reaction to more feasibly take place, but competition with *E/Z* olefin isomerization becomes an added challenge (**Figure 24A**, *pathway b*).[16] This is seen in starting materials that contain α,β-unsaturated carbonyl units. The triplet state is long-lived enough to allow for an intermolecular reaction to occur, but the stereoselectivity of the reaction can be diminished. This has been overcome, however, by employing 5- and 6-membered enones, which maintain their starting olefin geometry while the reaction takes place.[17] Other ways to assist in the excitation, however, include complexing the olefin to a transition metal, especially copper (**Figure 24B**).[16] The transition metal catalyst (or its attached ligands) can directly excite the olefin through a charge transfer complex/reaction. Otherwise, a triplet sensitizer can be employed which undergoes an electron exchange mechanism (Dexter mechanism) with the olefin.[16] This only works if the sensitizer is both in close proximity to the olefin (frequently accomplished by making the sensitizer the

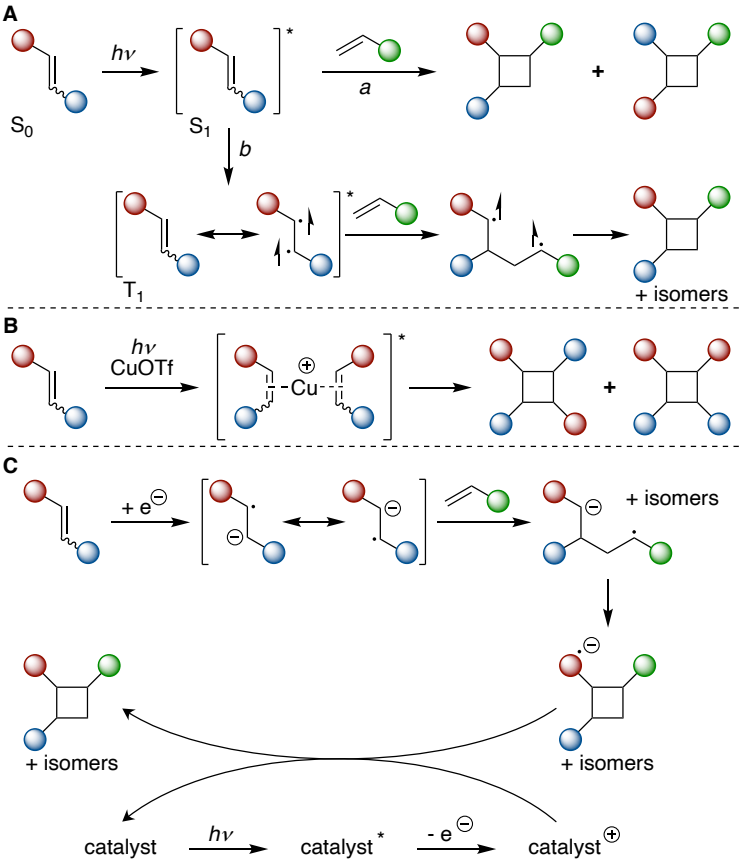

Figure 24: General mechanisms of [2+2] cycloaddition reactions. **A.** Direct photochemical excitation of olefin: *pathway a* goes through singlet excited state, *pathway b* through triplet excited state; **B.** Copper-mediated excitation; **C.** Single electron transfer mechanism (only radical anionic mechanism shown).[16]

solvent or a prominent component in the reaction solution) and has a higher energy triplet state than does the olefin to which the electron is being transferred. This mechanism is similar to *pathway b* (**Figure 24A**), but it is the energy from the sensitizer that excites the olefin to the excited triplet state. Because sensitization requires the transfer of two electrons, sometimes it is preferred to use a photoredox catalyst to accomplish a single electron transfer to the olefin, which is then back-transferred to the catalyst at the completion of the cycloaddition (**Figure 24C**).[16] Such a process creates a series of radical intermediates, either cationic or anionic radical intermediates, that are able to accomplish the cycloaddition.

Regardless of the mechanism through which the cycloaddition proceeds, there are three different parameters that must be taken into consideration (**Figure 25**). The first is the distance (*d*) between the olefin pairing partners, which must be no more than 4.2 Å apart in order for the cycloaddition to take place. The second is the angle τ, which indicates how close to parallel the reacting olefins are. This optimal angle for the desired reaction to occur is 0°. Finally, the slip angle (α) shows how well aligned the olefins are, which is optimal at 90°.[18,19] With these parameters met, however, photocycloadditions are exceptionally useful because they can allow for access to highly strained and/or sterically congested compounds that other methods fail to accomplish, and they do it through a single step.[20]

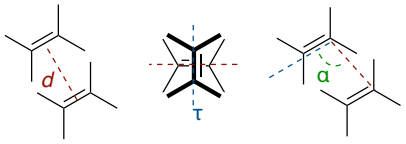

Figure 25: Schmidt's parameters for potential photoreactivity.[19]

2.1.1 [2+2] Photocycloaddition Reactions with No Added Catalysts

One of the most common ways [2+2] photocycloadditions have been made selective is through solid-state reactions. Such reactions frequently do not require any kind of catalyst and are both regio- and stereospecific. The crystal packing determines if the olefins align head-to-head or head-to-tail, and the olefin pairing partners do not isomerize in the solid-state the way they can in solution. Feldman and co-workers utilized this strategy by synthesizing alkene components that hydrogen-bond in a head-to-tail fashion and crystallize,

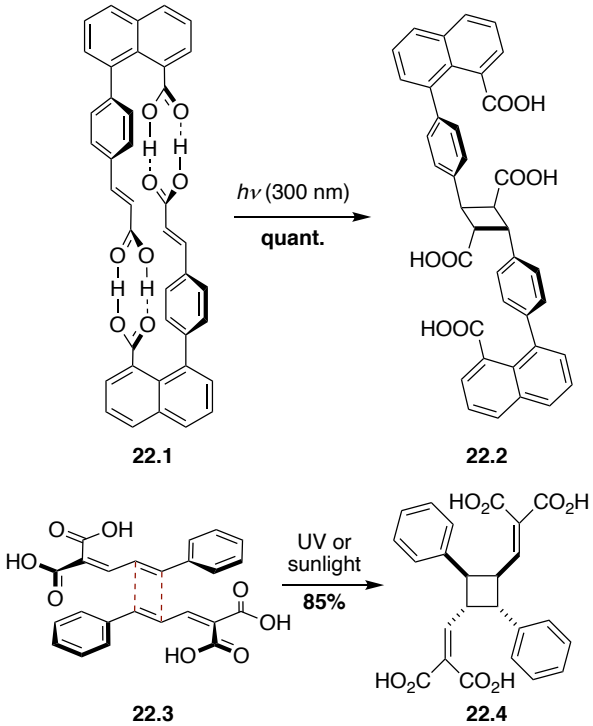

Scheme 22: Feldman (**22.1** to **22.2**)[21] and Dinkelmeyer's (**22.3** to **22.4**)[22] solid-state [2+2] photocycloadditions

as such, in the solid-state, giving a single product (**22.2**, **Scheme 22**). However, the same olefin pairing partners upon irradiation in solution give no characterizable products, although starting material is consumed.[21] Dinkelmeyer and co-workers also exploited the usefulness of solid-state reactions to accomplish a regio- and stereospecific dimerization of cinnamylidene malonic acid (**Scheme 22**).[22] In this synthesis, the cinnamylidene malonic acid molecules string together in a head-to-tail fashion through hydrogen bonding. These pre-organized molecules then stack through Van der Waals forces upon crystallization (**22.3, Scheme 22**). When irradiated using UV or sunlight, the crystals crack and fragment into a powder that is cyclobutane product **22.4**.

In general, intramolecular [2+2] cycloaddition reactions are more selective than their intermolecular counterparts. This has been critical to many syntheses' plans and was instrumental in MacMillan and co-workers' synthesis of (–)-littoralisone, an iridoid glycoside. In the final step of the synthesis, two olefin components (**Scheme 23A**, **23.1**) are irradiated without any additional catalysts or photosensitizers to create highly functionalized cyclobutane **23.2** as a single diastereomer.[23] Thomas and Evanno also use an intramolecular dimerization to bring together the olefins of anchinopeptolide C (**23.3**) to form cycloanchinopeptolide C (**23.4**) in the same manner as it is presumed to occur biosynthetically.[24] This reaction, which was run in deuterated water, gave the natural stereochemistry of the product in 24% yield (**Scheme 23B**). Similarly, following the isolation of gaditanone (**23.6**), Hernández-Galán and co-workers performed a transannular [2+2] cycloaddition reaction almost quantitatively on **23.5**, another

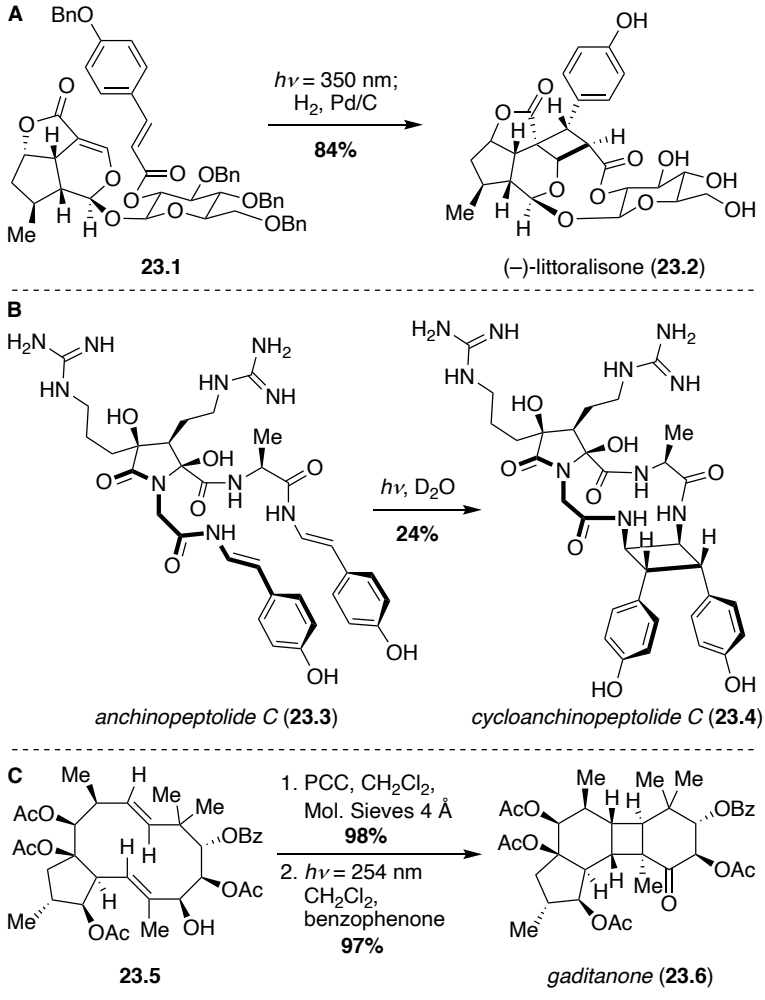

Scheme 23: Intramolecular [2+2] photocycloadditions. **A.** MacMillan's synthesis of (–)-littoralisone;[23] **B.** Thomas and Evanno's synthesis of cycloanchinopeptolide C;[24] and **C.** Hernández-Galán's synthesis of gaditanone.[25]

compound isolated from the same natural source and hypothesized to be the natural precursor of gaditanone.[25] For this particular transformation, oxidation with PCC to furnish the enone of **23.5** was followed by photocycloaddition in the presence of benzophenone as a sensitizer to give the natural product as a single stereoisomer (**Scheme 23C**). For each of these, the cyclobutane ring was part of a polycyclic system, thereby making an intramolecular or transannular cycloaddition reaction a logical choice, but Mizuno and co-workers took a slightly different approach and tested the usefulness of tethering the olefin pairing partners with a silyl tether (**Figure 26**).[26] Doing so allowed the desired photocycloaddition to take place, which, in the absence of the silicon-based tether (*i.e.*, intermolecularly), gave only the photoisomerized olefin. With only a single tether, the cycloaddition did take place, but the stereoselectivity for these reactions was low due to the competing photoisomerization (**Figure 26**, **26A** to **26B**). By converting the silyl tethered stilbazoles to a macrocyclic stilbazolium carboxylate (**26C**), though, the stereoselectivity of the reaction improved such that only a single stereoisomeric product was observed (**26D**).

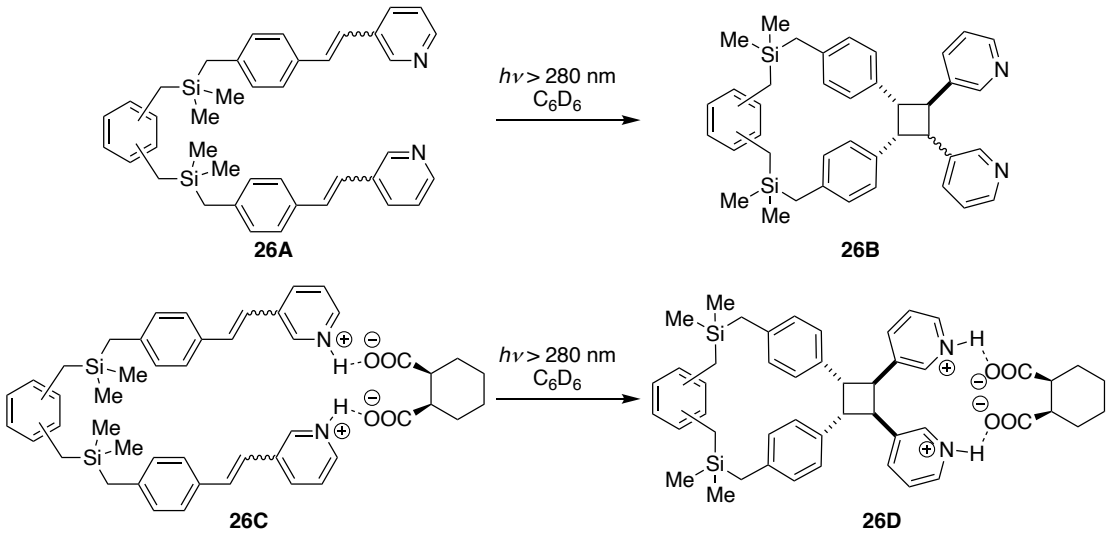

26A **26B** **26C** **26D**

Figure 26: Mizuno's intramolecular [2+2] photocycloadditions.[26]

Intermolecular [2+2] cycloaddition reactions can be difficult to control without adding a catalyst or templating agent. During Dickschat and co-workers' total synthesis of the oroidin-based alkaloid sceptrin (**24.5**, **Scheme 24**), enantiopure **24.1**, synthesized in 3 steps, was subjected to a photodimerization. The desired head-to-head diastereomer **24.2** was only obtained in 37% yield. Head-to-tail cycloaddition product **24.3** was produced in 32% yield, and the undesired head-to-head diastereomer **24.4** in 5% yield.[27] Birman and co-workers also synthesized sceptrin utilizing a [2+2] cycloaddition reaction (**Scheme 24B**), and eliminated regiochemical challenges by using symmetrical olefin pairing partners, maleic anhydride (**24.6**) and *trans*-1,4-dichloro-2-butene (**24.7**).[28] Although this transformation afforded the unnatural stereochemistry for the cy-

clobutane product (**24.8**), it did give a single diastereomeric product, and the desired stereochemistry was addressed at a later stage in the synthesis.

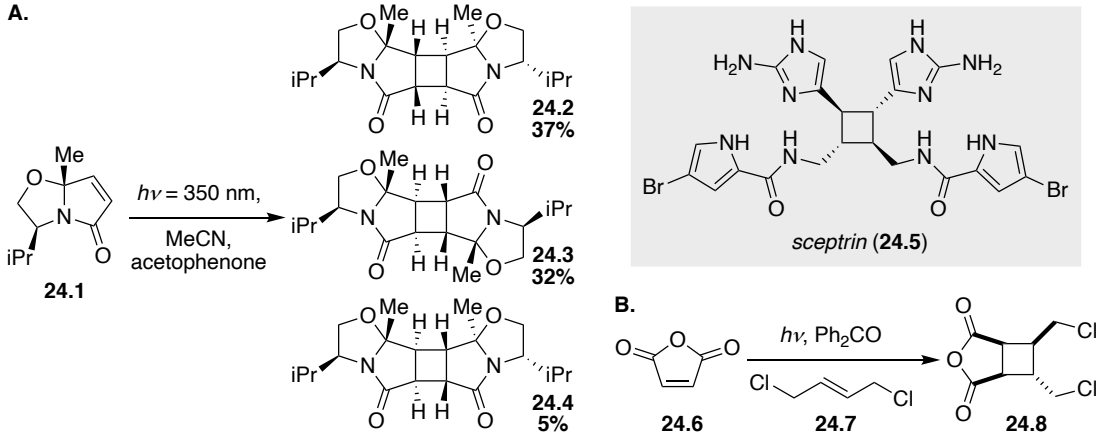

Scheme 24: [2+2] Cycloadditions in the syntheses of sceptrin (**24.5**) from **A.** Dickschat and co-workers[27] and **B.** Birman and co-workers.[28]

Baran and co-workers also employed symmetrical π-systems for intermolecular cycloadditions, thus avoiding issues with regiochemistry, and were able perform two different intermolecular [2+2] cycloaddition reactions in a diastereoselective manner (**Scheme 25A**).[11] Fedorova and co-workers were also able to successfully perform a regio- and stereoselective dimerization with quinoxaline styrene derivatives (**25.6**). The presence of quinoxaline instead of pyridine promoted the intermolecular [2+2] cycloaddition instead of an intramolecular photochemical cyclization.[29] By ^{1}H NMR analysis, a single diastereomer was isolated (**25.7**, **Scheme 25B**), with the only other by-product being that of olefin isomerization. Munshi and co-workers used the electronic properties of the olefin pairing partners to overcome the regiochemical difficulties associated with intermolecular [2+2] cycloadditions (**Scheme 25C**). Using "push-pull" olefins, the electron-rich end of one olefin unit aligns preferentially with the electron-deficient end of its cycloaddition partner to give (exclusively) the head-to-tail dimerization product (**25.9**). The observed stereochemistry of these cycloadditions is attributed to the steric interactions. *Z*-configured olefins were added to the reactions, but the product of the reaction is the result of an *E*-configured olefin pairing with a *Z*-configured olefin. If the starting olefin did not succumb to *Z* to *E*-isomerization (as observed through fluorescence spectroscopy), it also did not dimerize, but when both the (*Z*) and (*E*) olefins were observed, dimerization was also observed.[30] Tang and co-workers also achieved a regio- and stereoselective dimerization intermolecularly in solution through molecular aggregation (**Scheme 25D**).[31] Due to the insolubility of the olefins (**25.10**) in water, the olefins could be dissolved in acetonitrile and when water was added until the suspension was 90+% aqueous, the molecules aggregated sufficiently that when irradiated with UV light, dimerization occurred. Less than 90% water led to isomerization and cyclization instead of dimerization.

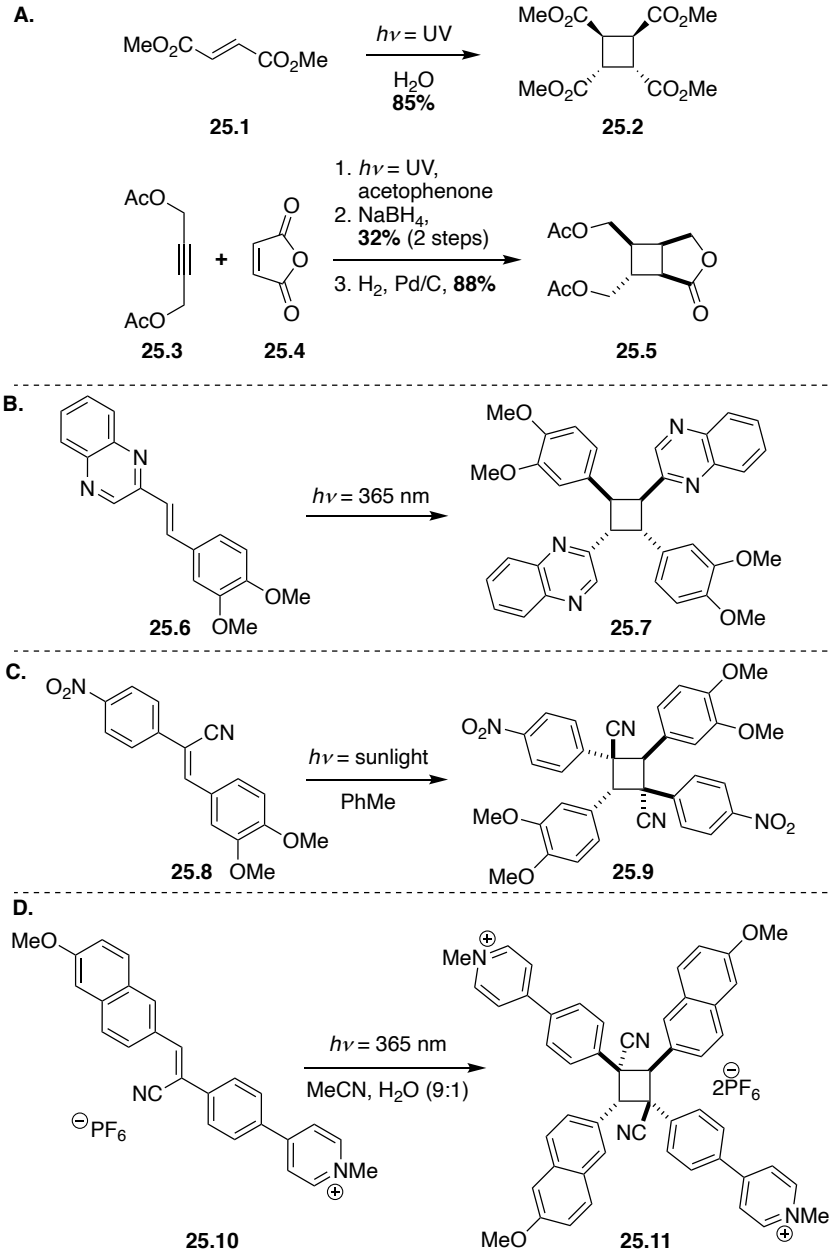

Scheme 25: Intermolecular [2+2] cycloaddition reactions without catalysts by **A.** Baran and co-workers;[11] **B.** Fedorova and co-workers;[29] **C.** Munshi and co-workers;[30] **D.** Tang and co-workers.[31]

2.1.2 Templated [2+2] Photocycloaddition Reactions

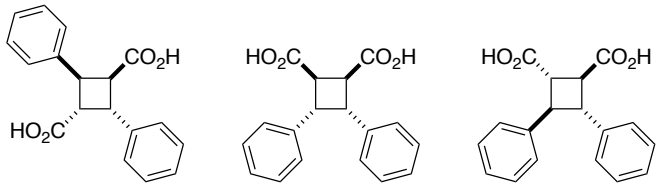

α-truxillic acid (**27a**) β-truxinic acid (**27b**) δ-truxinic acid (**27c**)

Figure 27: Dimerization products of *trans*-cinnamic acid

Another approach to regio- and stereoselective [2+2] cycloaddition reactions is templating olefin pairing partners, both orienting them head-to-head or head-to-tail and bringing them into the necessary proximity to perform the cycloaddition. The earliest example of a photochemical template effect was performed by Neckers and co-workers with *trans*-cinnamate esters.[32] Three polymers were designed to template these cinnamate esters for cycloaddition to form α-truxillic acid (**Figure 27**, **27a**), β-truxinic acid (**27b**), or δ-truxinic acid (**27c**). α-Truxillic acid (**27a**) was the only one to be formed exclusively and in quantitative yields. The β-truxinic acid (**27b**) polymer gave 53% of the desired product and 47% of the α-truxillic acid. In the absence of a templating agent, α-truxillate (ester of **27a**) is the only product observed in solution; thus, such a competition between the head-to-head β-dimer and head-to-tail α-dimer is expected. The δ-truxinate product (ester of **27c**) is never the observed cycloaddition product in either the solid state or in solution, but with the proper template, 53% δ-truxinic acid was isolated (the other 47% was α-truxillic acid).

Instead of designing separate polymers, Ramamurthy and co-workers were able to access β-truxinic acid (**Figure 27**, **27b**) exclusively using a macromolecular cavity to direct the regio- and stereochemical outcome of a [2+2] photocycloaddition.[33] By reacting two *trans*-cinnamic acid derivatives within the cavity of either [8]cucurbituril (**Figure 28**, **28a**) or γ-cyclodextrin (**28b**)

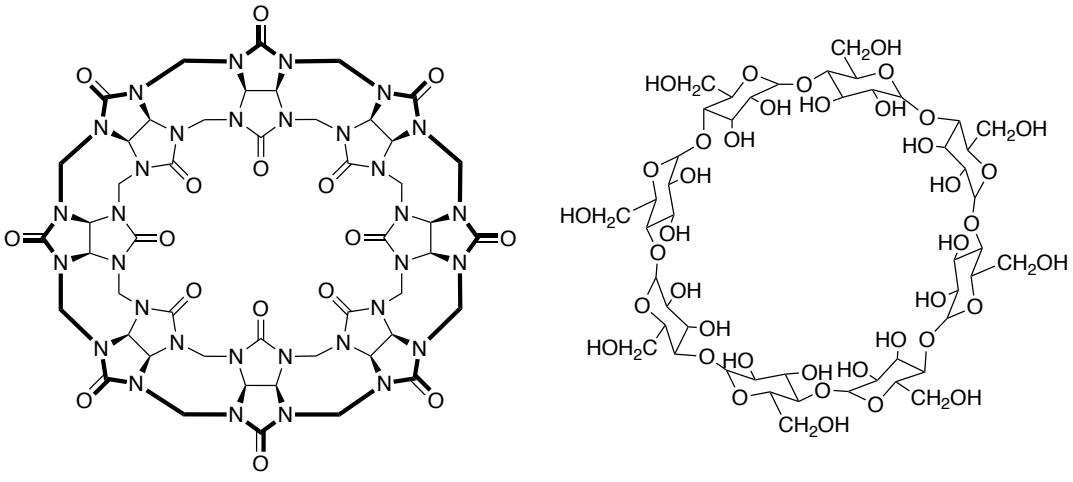

cucurbit[8]uril (**28a**) γ-cylodextrin (**28b**)

Figure 28: Macromolecular cavities employed by Ramamurthy and co-workers in the synthesis of β-truxinic acid.[33]

in an aqueous solution, the orientation of the olefin pairing partners was regiocontrolled to give the head-to-head product because of the hydrophilic and hydrophobic components of *trans*-cinnamic acid derivatives. The stereochemistry was also controlled in these reactions because within the cavity, there is insufficient space to allow for photoisomerization, thus eliminating diastereomeric side-products, and leading to exclusively the *syn*, head-to-head product of β-truxinic acid (**27b**).

Davis and co-workers were also able to effectively synthesize a derivative of β-truxinate (the ester of **27b**) using guanosine quadruplexes and potassium cations (**Figure 29**).[34] The addition of guanosine to *trans*-cinnamic acid to form *trans*-cinnamoyl guanosine (**29a**) allowed four molecules to complex in solution through H-bonding to form planar units, which then stacked with potassium cations placing the olefins only 3.3 Å apart, sufficiently close for cycloaddition. Then upon irradiation of the reaction solution, *syn* head-to-head dimerization was observed, the product of which could be easily isolated with methanol and the guanosine cleaved under acidic conditions to give exclusively β-truxinate. Although potassium was used in only catalytic amounts, its presence was necessary to promote the quadruplexing; without it, *E/Z* photoisomerization was exclusively observed. In a similar manner, Arseniyadis and co-workers were able to carry out a previously unattainable dimerization between two units of (*E*)-aplysinopsin. This was accomplished using salmon testes DNA as the templating agent.[35] Through this approach, dictazole B (**Scheme 26**, **26.3**) was synthesized by the photocycloaddition of two different aplysinopsin-derived monomers (**26.1** and **26.2**), and while low-yielding (16%), the reaction was completely stereoselective. Other aplysinopsin monomers could also be combined with this approach, and four different dictazoles were synthesized.

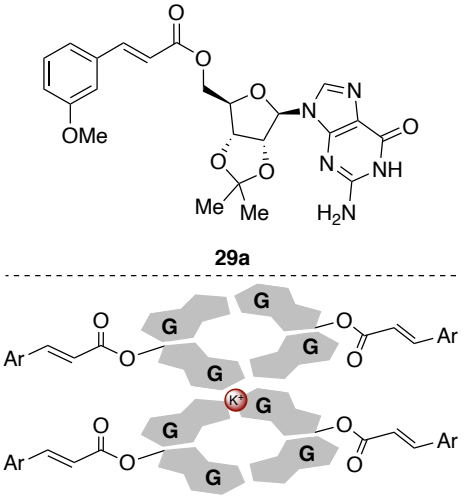

Figure 29: Synthesis of β-truxinate with guanosine quadruplexing.[34]

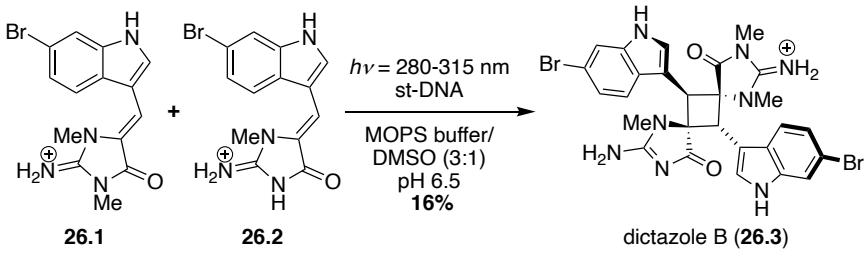

Scheme 26: Synthesis of dictazole from monomers of aplysinopsins.[35]

While in the previous examples the templating agents have been predominantly organic, metals are also frequently used to complex or template the olefin pairing partners to direct the regio- and stereochemistry of a cycloaddition. Using boron's ability to weakly coordinate with the nitrogen of a pyridine, MacGillivray and co-workers crystallized 4-stilbazole (**27.2**) in the presence of phenylboronic acid catechol ester (**27.1**). The single crystals formed oriented 4-stilbazole head-to-tail (**Scheme 27**). Upon irradiation with UV light, quantitative yields of a single diastereomer (**27.3**) were synthesized.[36] Lang and co-workers were also able to dimerize 4-stilbazole stereoselectively using templated photochemistry.[18] The template was a metal-organic framework in which Zn^{II} coordinated to 4,4'-oxybis(benzoate) to create a cavity in which two 4-stilbazole (**27.2**) derivatives fit (**Figure 30**). Using this template, the head-to-tail regioisomeric product is again observed because the stilbazole nitrogen coordinates to the zinc within the molecular framework of the cavity. Also, because of the size of the cavity (similar to that of cucurbit[8]uril and γ-cyclodextrin), photoisomerization of the olefin generally cannot occur, making the reaction stereospecific for the *syn* product. This template proved generally useful for both homo- and heterodimerizations.

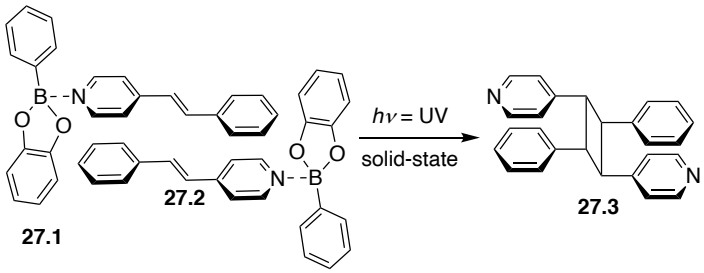

Scheme 27: MacGillivray and co-workers' dimerization of 4-stilbazole using boron as a templating agent.[36]

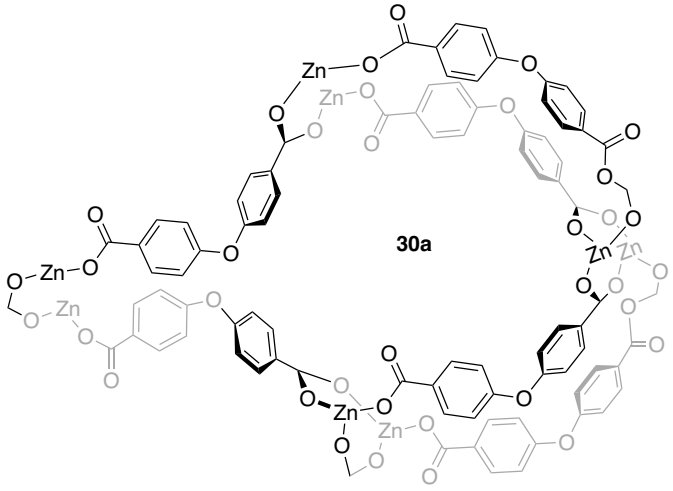

Figure 30: Zn(oba) network for Lang and co-workers' templated photocycloadditions.[18]

Metal coordination with simpler metal complexes can also be useful to pre-organize olefin pairing partners for cycloaddition. Kole and Vittal were able to coordinate *trans*-5-styrylpyrimidine (**31a**) to silver (I) salts for cycloaddtition.[37] Coordinating these and bulky triphenylphosphine groups to the silver caused the coordination polymer to assume a helical structure, which aligned the styrylpyrimidine groups head-to-tail for quantitative photocycloaddition in the solid-state. Peedikakkal and co-workers used a cadmium-containing coordination polymer to build triple-stranded ladder structures, aligning symmetrical 4-pyridylethylenes (**31b**) to give a single diastereomeric cycloaddition product in up to 100% yield in the solid-state.[38] Mir and co-workers also designed a zinc-containing coordination polymer that allowed for head-to-tail dimerization of two 4-(naphthylvinyl)pyridine (**31c**) molecules stereospecifically in the solid-state.[39]

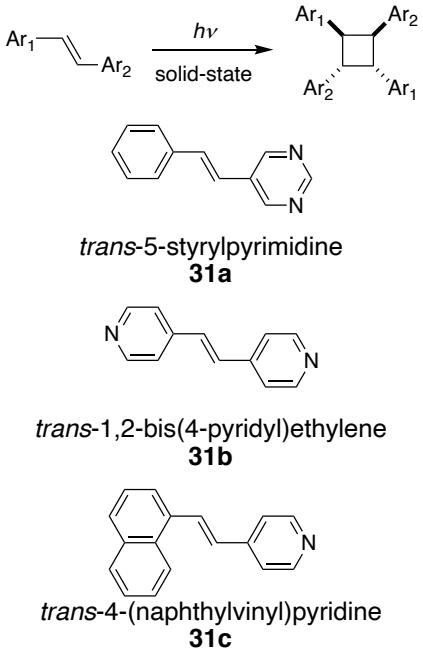

Figure 31: Metal-templated head-to-tail dimerizations of styrylpyrimidine **31a**,[37] pyridylethylene **31b**,[38] and napthylvinylpyrindine **31c**.[39]

Weiss and co-workers used quantum dots (CdSe) to effectively template different 4-vinylbenzoic acid derivatives (**Figure 32**, **32a**, **32b**, and **32c**), allowing for highly regio- and stereoselective heterodimerizations to occur.[40] The quantum dots could be tuned to preferentially accommodate heterodimerization instead of homodimerization simply by adjusting the size of the quantum dot. Such an adjustment changes the triplet energy levels, so one of the olefins can be oxidized while the other is not. Additionally, the carboxylic acid portion could be placed on either end of the olefinic partners (**Figure 32B**), driving the regiochemical outcome of the reaction. Stereochemistry for these reactions favored the *syn* product (**32d** and **32g**) with high diastereoselectivity.

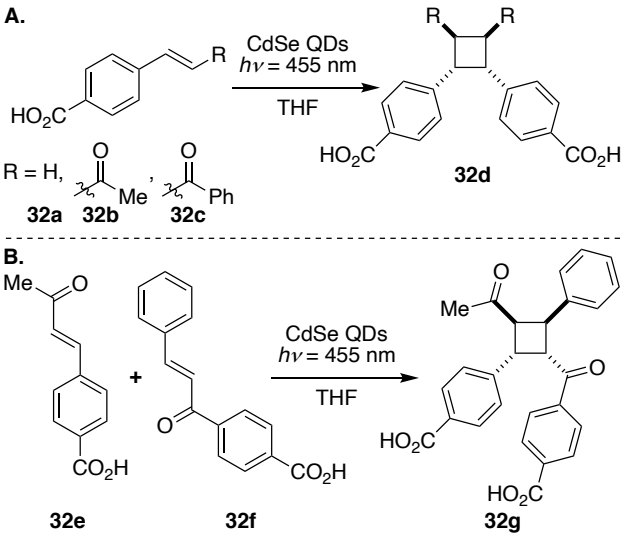

Figure 32: Weiss' photocycloadditions with CdSe quantum dots (QDs)[40]

Urriolabeitia and co-workers used C-H activation to complex palladium to different oxazolones to regio- and stereoselectively perform cycloadditions in solution to form diaminotruxillics

(**Figure 33**).[41] Oxazolones (**33a**) are notably difficult to dimerize because they isomerize instead of dimerize under photochemical conditions. However, when orthopalladated, the substrates dimerize to form a single head-to-tail diastereomer (**33c**). In solution, several different isomers of **33b** are observed, but upon irradiation, only the *transoid* complex (**33b**) is reactive, and any other isomers rearrange to this *transoid* isomer before dimerization occurs.

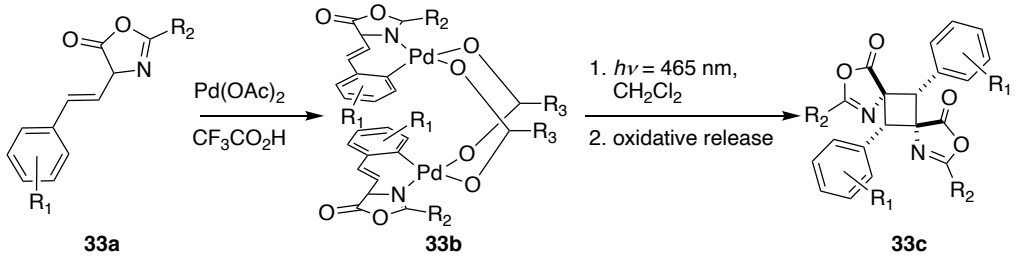

Figure 33: Urriolabeitia's ortho-palladation template for photocycloaddition of oxazolones.[41]

2.1.3 Metal-catalyzed [2+2] Photocycloaddition Reactions

Similar to metal-templated cycloadditions, metal-catalyzed cycloadditions also help control the regio- and stereochemical outcome of reactions through temporary coordination; however, metal-catalyzed reactions use the metals in catalytic amounts and generally do not require additional steps or conditions for removing the catalyst, as is sometimes the case in templated reactions.[41] Yoon and co-workers have been frequently cited for their work in photocatalyzed [2+2] cycloaddition reactions because they were the first to publish a method that overcomes oxidative cycloreversion through catalyst tuning. The catalyst has the oxidizing potential to promote the forward cycloaddition reaction, but not enough to promote the cycloreversion.[42] The optimized catalyst used for both homo- and heterodimerization for the substrates tested was $Ru(bpm)_3(BArF)_2$ (**Scheme 28A**, **28.1** and **28.2** to **28.3**). The prerequisite for this method is that one olefin must be less electron-rich than the other for heterodimerization to be favored over the homodimerization. This worked well for several styrene derivatives, giving greater than 10:1 diastereoselection in most cases and complete regiocontrol, only the head-to-head products were observed. Most of Yoon's examples give only tri-substituted cyclobutanes, but Chen and co-workers' synthesis of *ent*-sceptrin employs the same methodology using $Ir(ppy)_3$ to photocatalyze an intramolecular [2+2] cycloaddition to give a tetrasubstituted cyclobutane (**Scheme 28B**).[43] This also gives a single regioisomer. However, because the starting material was a mixture of diastereomers, upon cyclization, both epimers were isolated (**Scheme 28B**, **28.4** to **28.5**, *d.r. 1.8:1*). A transthioketalization with $TiCl_4$ was then employed to expose the cyclobutane core (**28.6**).

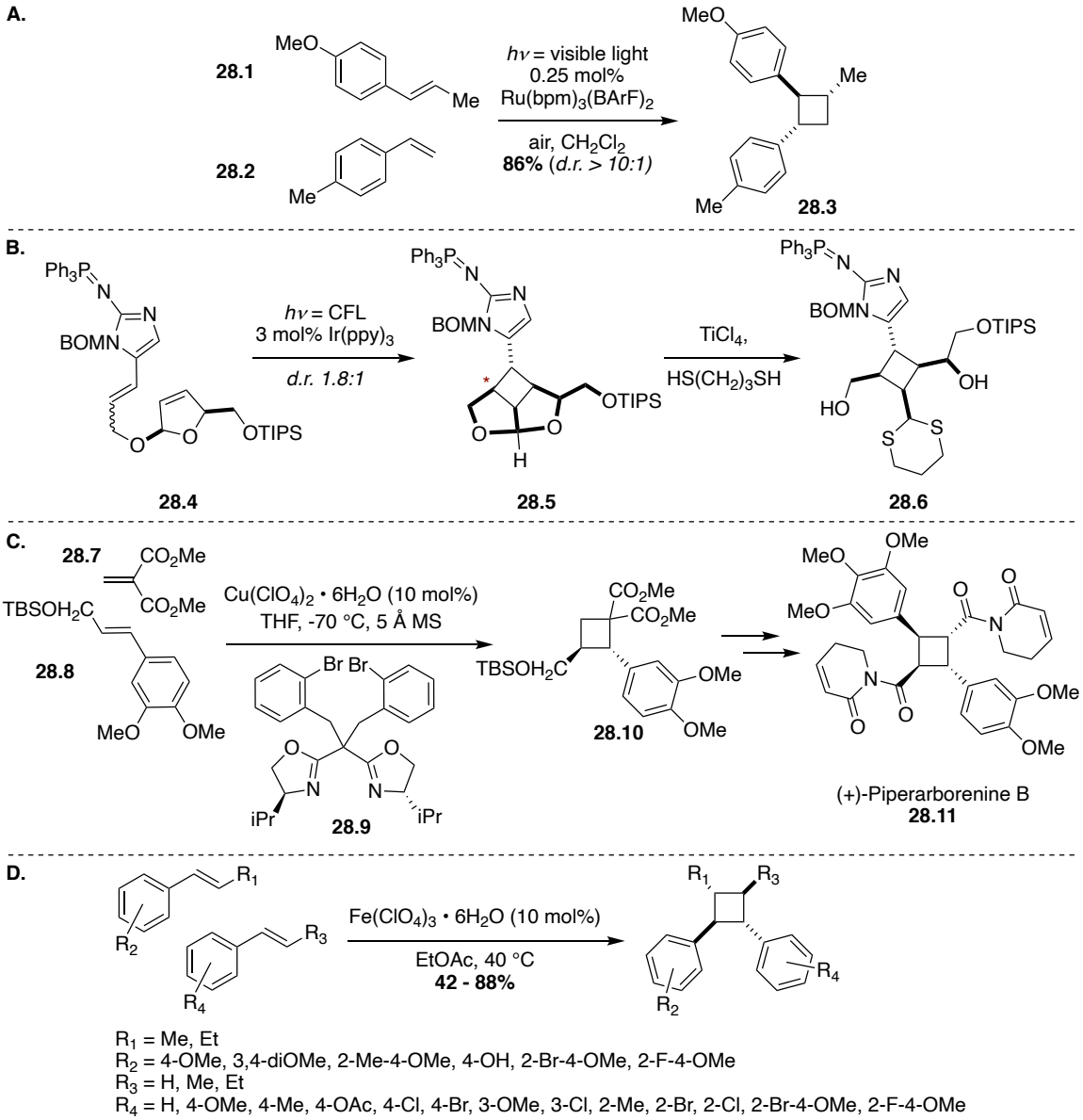

R_1 = Me, Et
R_2 = 4-OMe, 3,4-diOMe, 2-Me-4-OMe, 4-OH, 2-Br-4-OMe, 2-F-4-OMe
R_3 = H, Me, Et
R_4 = H, 4-OMe, 4-Me, 4-OAc, 4-Cl, 4-Br, 3-OMe, 3-Cl, 2-Me, 2-Br, 2-Cl, 2-Br-4-OMe, 2-F-4-OMe

Scheme 28: Metal-catalyzed [2+2] cycloaddition reactions: **A.** Yoon and co-workers' ruthenium-catalyzed intermolecular [2+2] photocycloaddition,[42] **B.** Chen and co-workers' iridium-catalyzed intramolecular [2+2] photocycloaddition and subsequent transthioketalization,[43] **C.** Xie and Tang's copper-catalyzed [2+2] cycloaddition,[44] and **D.** Zhong and co-workers' iron-catalyzed [2+2] cycloaddition.[45]

Others have performed [2+2] cycloaddition reactions but without the need for photo-induced excitations. Xie, Tang, and coworkers' synthesis of (+)-piperarborenine B (**28.11**) uses a copper-catalyzed [2+2] cycloaddition reaction to form the cyclobutane core regio-, diastereo-, and enantioselectively, but only three corners of the cyclobutane ring were functionalized through this (**Scheme 28C**, **28.7** and **28.8** to **28.10**). However, after functional group manipulations, C-H functionalization provided substitution at the final corner, and then in two short steps, the natural product was produced in 99% enantiomeric excess.[44] Zhong and co-workers similarly use iron(III) salts to catalyze both homo- and heterodimerizations of anethole and styrene derivatives regio- and diastereoselectively (**Scheme 28D**).[45] This approach worked well for a variety of substrates,

including ortho, meta, and para-substituted aromatics, both electron-withdrawing and donating, providing the all *trans* head-to-head products. This method also provides the first example of a phenol successfully undergoing direct [2+2] cycloaddition.

2.1.4 Organo-catalyzed [2+2] Photocycloaddition Reactions

Although less prominent in the literature, organic catalysts have also been found useful for promoting [2+2] photocycloaddition reactions. Nicewicz and co-workers were among the first to successfully employ an organocatalyst in a regio- and diastereoselective [2+2] cycloaddition reaction.[46] In this work 2,4,6-tris(4-methoxyphenyl)pyrylium tetrafluoroborate (*p*-OMeTPT, **Xc**) was used in a single electron transfer relay system with anthracene or naphthalene to oxidize one of the olefin pairing partners to a radical cation, which then undergoes dimerization with another olefin (homodimerizations only) to form the cyclobutane ring (**Figure 34A**). As in Yoon and co-workers' approach,[42] the catalyst was carefully tuned to promote the forward reaction (dimerization) without also being a powerful enough oxidant to promote the cycloreversion. Both magnosalin (**23d**) and endiandrin A (**23e**) were synthesized using this approach, and all of the derivatives tested gave exclusively the head-to-head, all *trans* products.

Donohoe and co-workers synthesized a series of symmetrical and unsymmetrical tri- and tetrasubstituted cyclobutanes, including (±)-nigramide R (**34g**) using hypervalent iodine as the catalyst in the [2+2] photocycloadditions (**Figure 34B**).[47] These reactions proceeded through a single electron transfer (SET) mechanism in which the hypervalent iodine source (either phenyliodine diacetate or Dess-Martin periodinane) oxidized one of the olefin pairing partners, forming a radical cationic intermediate which added to the other unoxidized olefin, forming the cyclobutane ring. This approach was unique in that it was the first example of tetrasubstituted heterodimerization through a SET mechanism, and the reaction was both regioselective (head-to-head) and stereoselective (all *trans*). Although this approach supported a variety of substrates with varying substitution around the aromatic ring, homodimerization was only accessible in reasonable yields if the olefins were electron-rich (38% for electron-deficient vs. 60-95% for electron-rich). However, heterodimerizations did not have this same stipulation: one olefin must be electron-rich for oxidation, but the other pairing partner could be either electron-rich or deficient. The same mechanism was applied later to an intramolecular diene in which the olefins were tethered by a silicon tether that could be easily cleaved after the cycloaddition took place (**Figure 34C**).[48] This approach also supported a variety of functional groups. The regiochemistry was controlled by the fact that the reactions were intramolecular, but the stereochemistry was more challenging to predict. Depending on the length of the tether, either the all *trans* relative stereochemistry was preferred (**34i**, longer tethers) or *trans-cis-trans* stereochemistry was observed (**34j**, shorter tethers). Thus, the

method allows for access to highly functionalized tetrasubstituted cyclobutanes (**34k** and **34l**) from reactants which can be tuned slightly to give different diastereomeric products.

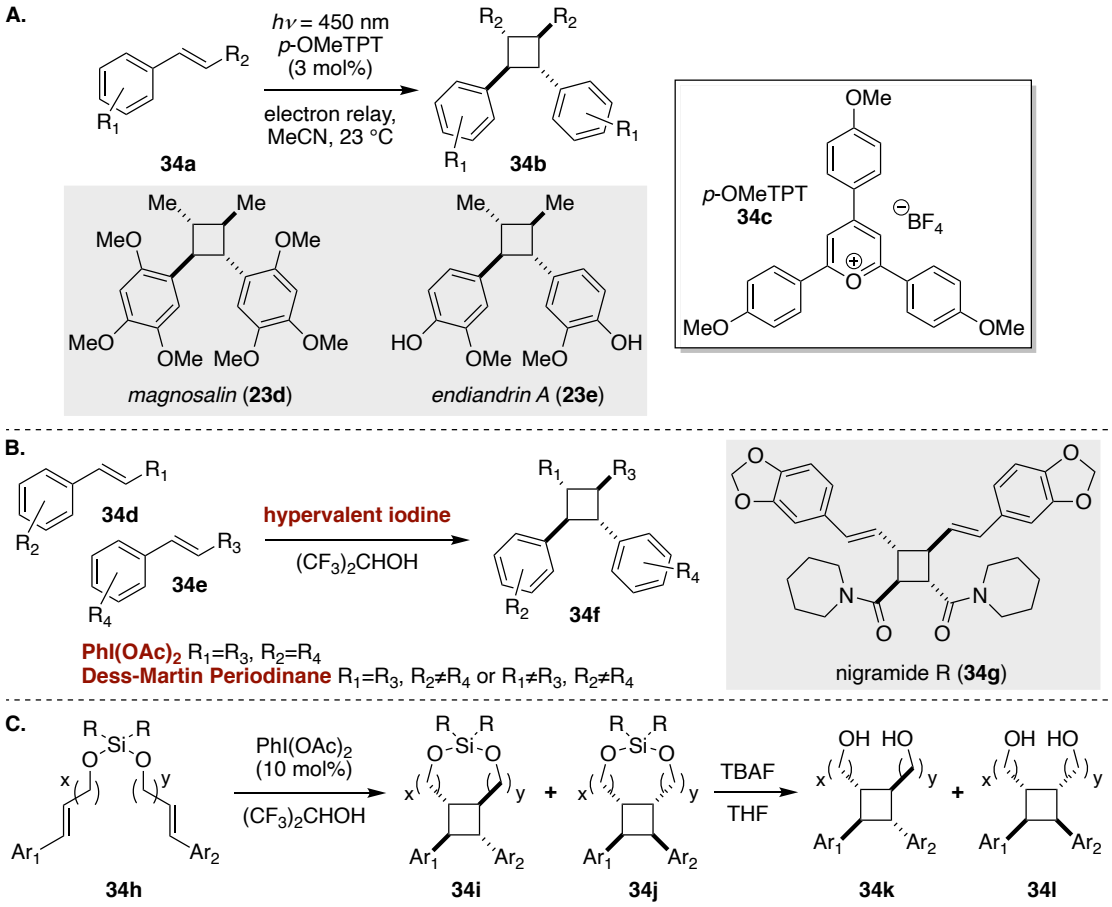

Figure 34: Organocatalyzed [2+2] cycloaddition reactions: **A.** Nicewicz's electron relay [2+2] photocycloaddition;[46] **B.** Donohoe's intermolecular hypervalent iodine-catalyzed SET cycloaddition;[47] and **C.** Donohoe's intramolecular hypervalent-iodine catalyzed cycloaddition.[48]

2.1.5 Limitations to the [2+2] Photocycloaddition

Although very useful reactions for forming carbon-carbon sigma bonds, [2+2] cycloaddition reactions also have limitations. Specifically, directing the regio- and stereochemical outcomes of intermolecular cycloadditions can be particularly challenging.[49,50] Crimmins notes in his review of enone-olefin photocycloadditions that if *E/Z*-isomerization is energetically accessible, this will occur instead of the desired cyclization reactions unless the olefins are held in position by hydrogen bonding.[51] This isomerization causes the products to be a mixture of stereoisomers, assuming that the olefins do undergo the cycloaddition. Some olefin diastereomers do not

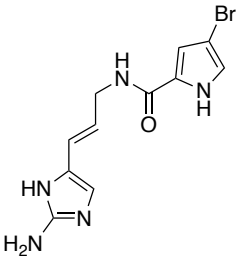

hymenidin (**35a**)

Figure 35: Structure of hymenidin, supposed biological precursor to sceptrin.[53,54]

undergo cycloaddition at all due to steric considerations.[30,52] In the synthesis of sceptrin (**24.5**), many have attempted to dimerize what would be the obvious pairing partners of hymenidin (**35a**) to form sceptrin, but because of its complex functionalization, hymenidin has yet to undergo a synthetic [2+2] cycloaddition,[53] although it is proposed that biosynthetically an enzyme takes this compound through a single electron transfer mechanism to form sceptrin.[54] Although many advances have been made in the field of [2+2] cycloadditions, some olefins still will not dimerize to give cyclobutanes.

In addition to the challenges of performing cycloadditions on certain olefin substrates, competing ring-opening reactions are also known to occur. De Mayo came up with an approach to irradiate β-diketones in the presence of another olefin to produce a 1,5-diketone (**Figure 36**, **36b**), which proceeds through a cyclobutane intermediate (**36a**), but trapping this intermediate is challenging because it rapidly and spontaneously undergoes a retro-aldol reaction to give a 1,5-diketone (**36b**).[49,51] Similarly, the functional groups at the corners of the cyclobutane ring can encourage ring opening reactions through either a Grob fragmentation mechanism (if a halide or other good leaving group are present, **Figure 36**, **36c** to **36d**) or a radical fragmentation (**36e** to **36f**).[49]

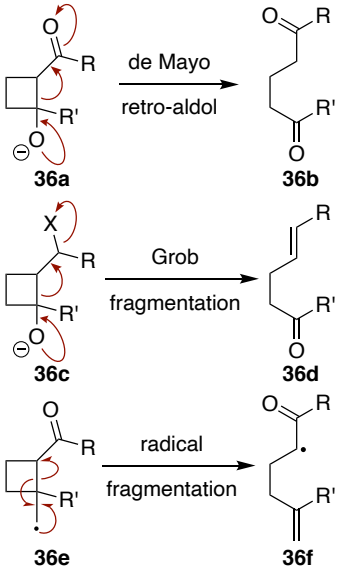

Figure 36: Ring-opening mechanisms of cyclobutane rings.[49]

Many have undertaken to improve the substrate scope and selectivity of [2+2] reactions with great success (as have been outlined in the previous sections), but several challenges still remain because most approaches can only tolerate certain electronic or steric environments. Additionally, most approaches favor only a single regiochemical or stereochemical outcome, which, while selective, is also limiting in the scope of cyclobutane molecules that can be accessed through a single route.

2.2 Other Methods for Assembling a 1,2,3,4-tetrasubstituted Cyclobutane

2.2.1 [4π]photocyclizations

Unlike a cycloaddition reaction in which two sigma bonds are formed, cyclizations form only one sigma bond, but they are still a powerful tool for introducing strain into a ring system be-

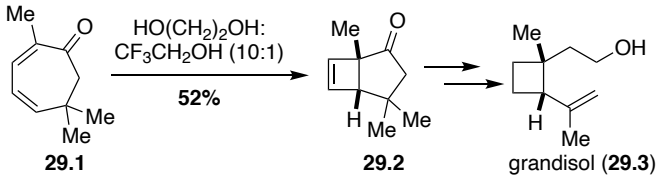

Scheme 29: Ayer and Browne's synthesis of grandisol using 4π electrocyclization.[55]

cause of the preorganization of the starting material.[1] In the synthesis of (±)-grandisol (**29.3**), a substituted cycloheptadienone (**Scheme 29**, **29.1**) was used as the starting compound for a [4π]photocyclization.[55] After 7 days in an ethylene glycol/trifluoroethanol (10:1) solvent system, the stereospecific cyclization was completed, giving a [3.2.0]bicycloheptenone (**29.2**) that could be further manipulated to the natural product.

In Baran's synthesis of piperarborenine B (**Scheme 30**, **30.4**) and D (**30.5**), the cyclobutane core was synthesized through a [4π]photocyclization of methyl coumalate (**30.1**) to form photopyrone **30.2**, which could be hydrogenated *in situ* to give a cyclobutane 1,3-dicarboxylate.[54] Because the photocyclization was done in dichloromethane, the methyl coumalate could be telescoped all the way to cyclobutane amide ester **30.3** in one-pot. Further C-H functionalization strategies were then employed to substitute each carbon of the cyclobutane ring, forming the desired tetrasubstituted cyclobutane of both piperarborenine B and D.

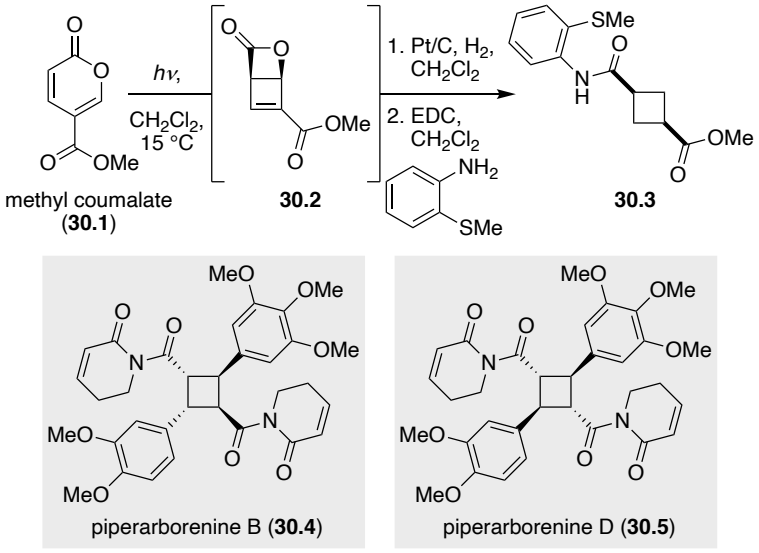

Scheme 30: Baran's 4π photocyclization for the syntheses of piperarborenine B and D.[54]

2.2.2 Intramolecular Direct Ring Closure

Although entropically disfavored, an intramolecular ring closure reaction is frequently useful and can be accomplished through nucleophilic addition, radical cyclization, or transition-metal catalyzed cyclization means.[1]

To my knowledge, nucleophilic addition reactions have not been used to synthesize a stand-alone 1,2,3,4-tetrasubstituted cyclobutane ring directly, however heavily substituted cyclobutane rings have been formed through this method. In Tanino, Miyashita, and co-workers' synthesis of solanoeclepin A (**Scheme 31A**, **31.3**), a [4.3.0]bicyclic core with bridgehead epoxide (**31.1**) was prepared and then subjected to LDA to promote an intramolecular nucleophilic addition, followed by a protection to form a highly substituted cyclobutane ring in quantitative yield.[56]

In Carreira's synthesis of (+)-dendrowardol C, a [2+2] cycloaddition approach was first attempted, but the wrong regioisomer was isolated as the only product.[57] Therefore, cyclobutane formation was accomplished through lithiation of triflate **31.4** followed by carbonyl addition, but fragmentation product **31.6** was also observed in an almost equal ratio (**Scheme 31B**).

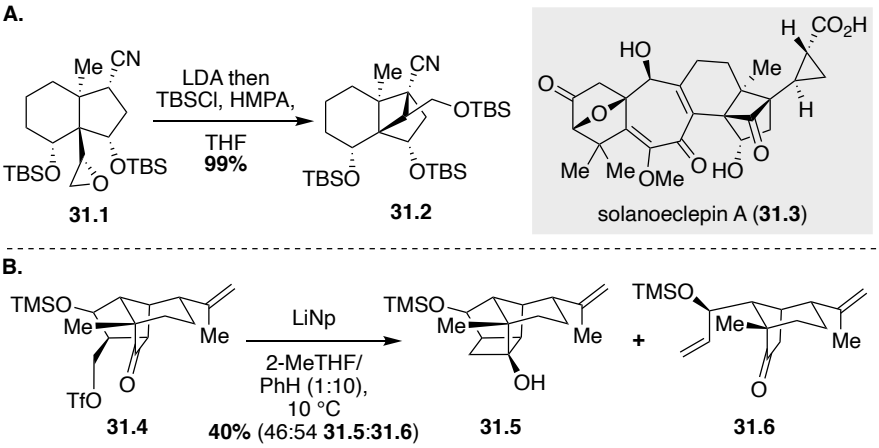

Scheme 31: Nucleophilic addition reactions for the formation of cyclobutane rings: **A.** Tanino and Miyashita's intramolecular nucleophilic addition in the synthesis of solanoeclepin A,[56] and **B.** Carreira's intramolecular nucleophilic addition in the synthesis of dendrowardol C.[57]

Baran and co-workers employ a double alkylation reaction in which the dianion of 4-methoxyphenylacetic acid (**Figure 37**, **37a**) is treated with the Grignard of epichlorohydrin (**37b**) to form cyclobutane core **37c**.[54] The magnesium chelate formed during the first addition templates the reaction for the final cyclization, dictating the observed stereochemistry in **37c**. This cyclobutane core is then further elaborated through C-H functionalization to be substituted at all of the carbons on the cyclobutane ring.

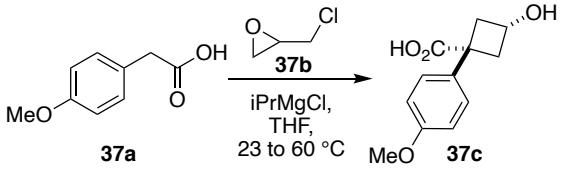

Figure 37: Baran's synthesis of cyclobutane ring **37c** through double nucleophilic addition.[54]

Radical cyclization methods are often not chosen to produce cyclobutane rings because of the ring's inherent strain; however, the presence of electron-withdrawing groups and/or geminal substitution has been used to overcome the challenges associated with this approach to cyclobutane formation.[1] The Norrish-

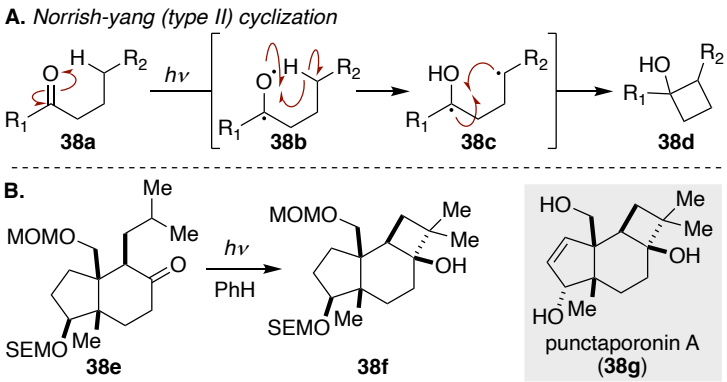

Figure 38: Norris-Yang cyclization and its application in the synthesis of punctaporonin A and D.[58,59]

Yang cyclization proceeds through a 1,4-diradical formed when the γ-hydrogen is abstracted from a molecule containing a photoexcited carbonyl group (**Figure 38A**). Such a mechanism allows for the formation of cyclobutanes, oxetanes, or azetidines.[49] In Paquette and co-workers' syntheses of (–)-punctaporonin A (**38g**) and (+)-punctaporonin D (enantiomer of **38g**), a Norrish-Yang cyclization is employed to form a highly substituted cyclobutane ring.[58,59] The stereochemistry of this cyclization is controlled by the chair-like transition state that the 1,4-diradical assumes before cyclization.

In Sabatini, Baran, and co-workers' synthesis of energetic materials, one of the cyclobutene rings was formed through a 1,4-addition in which **32.1** adds to the triphenylphosphonium cation of acetylene dicarboxylate **32.2** to make phosphonium ylide **32.3**. Subsequent intramolecular Wittig formed cyclobutene **32.4**.[11] Then, a catalytic hydrogenation allowed for the formation of a single diastereomer **32.5** in high yield.

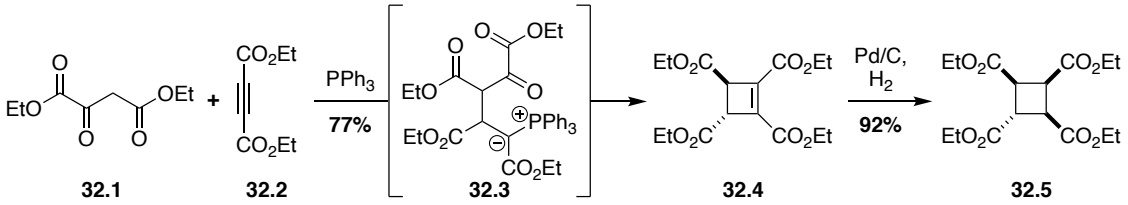

32.1 **32.2** **32.3** **32.4** **32.5**

Scheme 32: Sabatini and Baran's synthesis of *cis-cis-trans* cyclobutane **32.5** using a 1,4-addition followed by an intramolecular Wittig reaction.[11]

Hong and co-workers bring together a vinylogous ketone enolate (**Scheme 33**, enolate of **33.1**) and nitroalkene (**33.2**) through a conjugate addition catalyzed by squaramide catalyst **33.4**. The addition product then undergoes a nitro-Michael addition to produce cyclobutanes **33.3** in high yields (89-93%).[60] Because of the mechanism through which this particular reaction proceeds, the side product of a simple Michael addition product is also observed. However, the reactants dictate how efficiently the cyclobutane can be formed over the Michael addition product. Phenyl ketone **33.1** and 1,1,2-trisubstituted nitroolefins **33.2** lead to the cyclobutane product preferentially (82-91% of the product mixture) with good yields (89-93%) and high enantiomeric excess (96-98%). If, however, the ketone is a methyl ketone or the nitroalkene is 1,2-disubstituted, the Michael addition product is preferred.

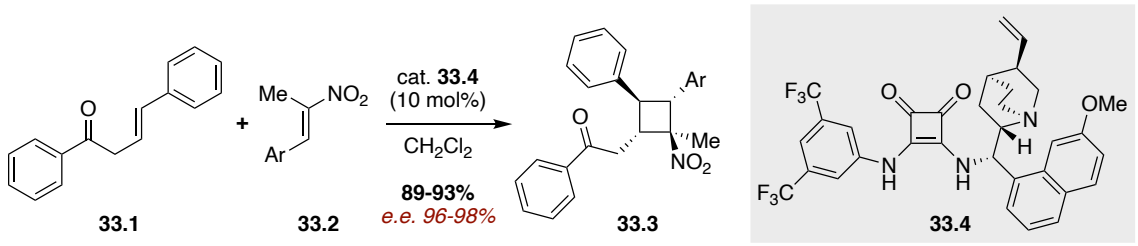

Scheme 33: Hong and co-workers' synthesis of fully substituted cyclobutanes through conjugate addition and subsequent nitro-Michael addition.[60]

2.2.3 Rearrangements

Ring contractions are an appealing approach to the synthesis of cyclobutanes because the substitution can be preinstalled before the strain is introduced into the system; however, because of the addition of strain, these reactions sometimes have steep energetic barriers to overcome. Such reactions can be initiated through electrophilic reagents or highly reactive intermediates, however.[1] Reisman and co-workers have employed a ring contraction strategy in the form of a Wolff rearrangement and subsequent ketene addition for the synthesis of natural products (+)-psiguadial B[61,62] (**Scheme 34**, **34.5**) and (+)-rumphellaone A[63] (**34.6**). The Wolff rearrangement is accomplished with (+)-cinchonine (**34.4**) as the catalyst, and cyclopentanone (**34.1**) is contracted to a cyclobutane with an exocyclic ketene (**34.2**), which then undergoes an addition reaction from 8-aminoquinoline to give the desired product (**34.3**), which is suitable for the subsequent C-H functionalization steps to the natural products.

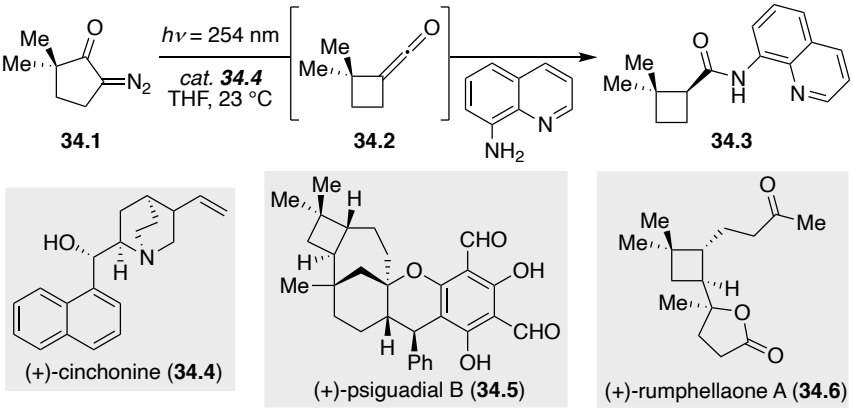

Scheme 34: Reisman's Wolff rearrangement and ketene addition to form cyclobutane core **34.3** for the synthesis of (+)-psiguadial B and (+)-rumphellaone A.[61-63]

In contrast, a ring expansion approach should be energetically favorable, due to the release of strain; however, such an approach for the formation of cyclobutanes has not been extensively explored because the cyclobutane ring has been generally presumed unstable to the conditions necessary for a ring expansion.[1] Tang and co-workers, however, have developed a strategy for performing a silver (AgOTf) catalyzed ring expansion from cyclopropane **35.1** (**Scheme 35A**) to cyclobutenoate **35.2**, rendering a single diastereomeric product in 95% yield. Subsequent aryl-

boronic acid addition gives 1,2,3,4-tetrasubstituted cyclobutane **35.3**, which was then further elaborated to the proposed structure of piperchabamide G (**35.7**).[64] Fox and co-workers employed an acyclic compound (**Scheme 35B**, **35.4**) to form bicyclobutane **35.5**, which upon conjugate addition opened to give 1,2,3-trisubstituted cyclobutane **35.6**.[65] Further functional group manipulation and C-H functionalization gave the 1,2,3,4-tetrasubstituted natural product piperarborenine B (**Scheme 30**, **30.4**).

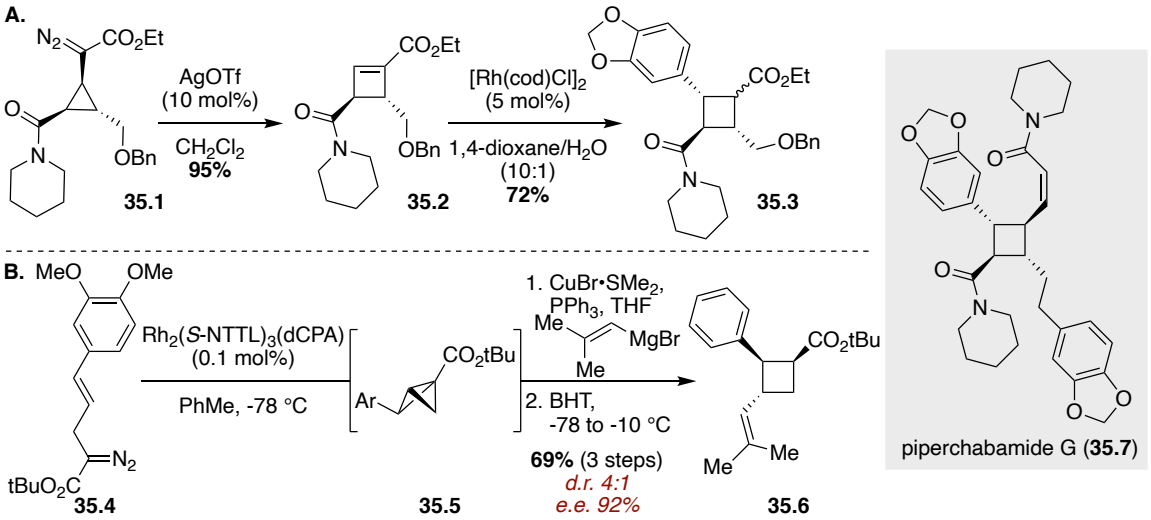

Scheme 35: Ring-expansion approaches to the synthesis of cyclobutanes: **A.** Tang and co-workers' approach in the synthesis of piperchabamide G,[64] and **B.** Fox and co-workers' approach in the synthesis of piperarborenine B.[65]

Baran and co-workers employed a straightforward yet different rearrangement for the synthesis of all *trans* 1,2,3,4-tetrasubstituted cyclobutane **36.2** in their 2004 synthesis of (±)-sceptrin (**Scheme 24**, **24.5**).[53] Here, 3-oxaquadricyclane (**Scheme 36**, **36.1**) was rearranged in the presence of sulfuric acid to give diketo diester **36.2** in 50% yield upon recrystallization. Further functional group manipulations gave racemic sceptrin in only 12 total steps. Similarly, in an enantioselective synthesis of sceptrin, the acid-catalyzed photo rearrangement of oxaquadricyclane **36.3** gave the *cis-trans-trans* cyclobutane **36.4** in 50% yield and 75% *e.e.*[66]

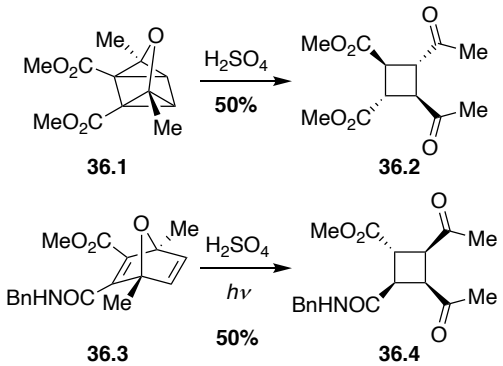

Scheme 36: Baran and coworkers' syntheses of sceptrin using oxaquadricyclane rearrangements to form the cyclobutane core.[53,66]

2.2.4 *Transannular McMurry of Macrocyclic 1,4-Diketones for the Assembly of 1,2,3,4-tetrasubstituted Cyclobutanes*

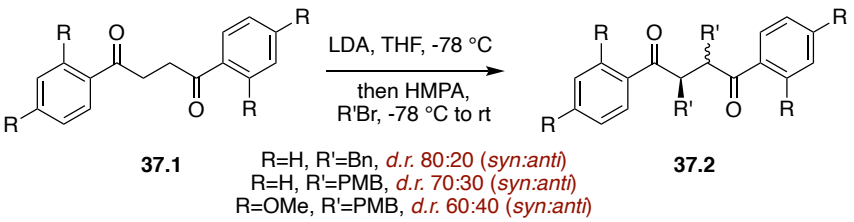

Scheme 37: Drewes and coworker's diastereoselective double enolate alkylations of non-macrocyclic 1,4-diketones.[67]

Despite all of the approaches examined so far, accessing certain stand-alone 1,2,3,4-tetrasubstituted cyclobutane rings remains challenging. For example, andamanicin (**23g**) has yet to be synthesized even though its diastereomer magnosalin (**23d**) has been synthesized.[46,47] In an attempt to develop a new and diverse approach to heavily substituted cyclobutane rings, we sought to employ macrocyclic 1,4-diketones as intermediates in such syntheses. After observing that diastereoselective organometallic addition reactions occur to the 1,4-diketone backbone of a series of macrocyclic systems, as discussed in Chapter 1, it was hypothesized that diastereoselective double alkylation reactions could also be possible. Based on a 1989 paper by Drewes and co-workers in which an acyclic 1,4-diketone was diastereoselectively alkylated using LDA, HMPA, and BnBr (with up to 4:1 diastereoselection, **Scheme 37**),[67] it was hypothesized that similar conditions could be applied to the cyclophane-based macrocyclic 1,4-diketones reported in Chapter 1 and, hopefully, still higher levels of diastereoselectivity could be achieved. This seemed especially feasible since Grignard additions performed on non-macrocyclic 1,4-diketone analogs of the systems investigated in Chapter 1 showed no diastereoselectivity (**Figure 39A**), but depending on the size of the macrocycle, >95% diastereoselection was observed under the same conditions (**Figure 39B**). Furthermore, it had been previously discovered in our laboratory that macrocyclic 1,4-diketone **19.4** could be converted into strained cyclobutene-containing

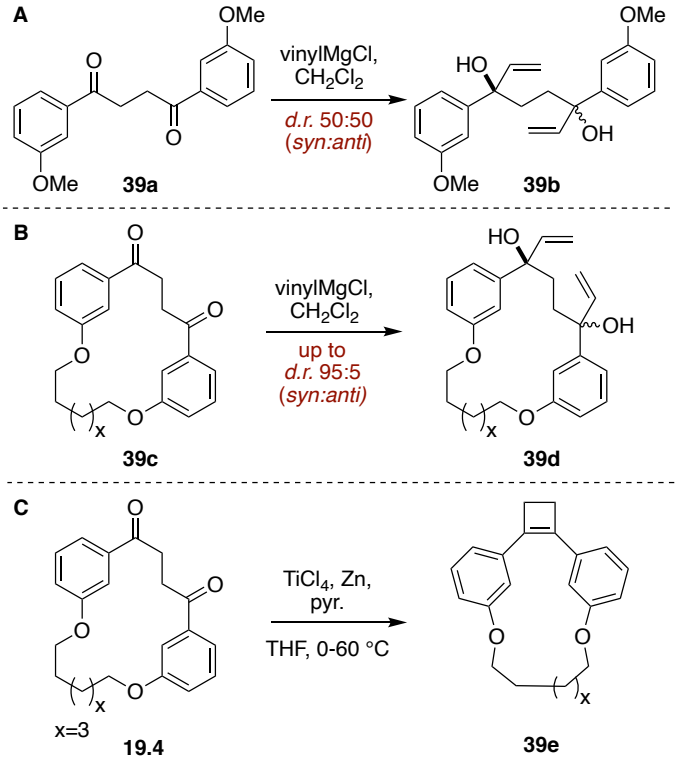

Figure 39: A. Grignard addition to a non-macrocyclic 1,4-diketone; **B.** Diastereoselective Grignard additions to macrocyclic 1,4-diketones; and **C.** Transannular McMurry of macrocyclic 1,4-diketone.

macrocycle **39e** via a transannular McMurry reaction (**Figure 39C**). With these strategies in mind, a retrosynthetic analysis for the synthesis of lignan-based natural products magnosalin (**23d**), endiandrin A (**23e**) and di-*O*-methylendiandrin A (**23f**) was proposed (**Figure 40**). It was envisioned that like the Grignard additions, macrocyclic stereocontrol could also be employed to install *C*-methyl groups to the backbone of the macrocyclic diketone (**40b**). If this could be achieved, then a transannular McMurry reaction should render a chiral macrocyclic cyclobutene **40a**, which we were optimistic could then be converted into the desired natural products. The total syntheses of these compounds would thus demonstrate the viability of this synthetic route to 1,2,3,4-tetrasubstituted cyclobutanes.

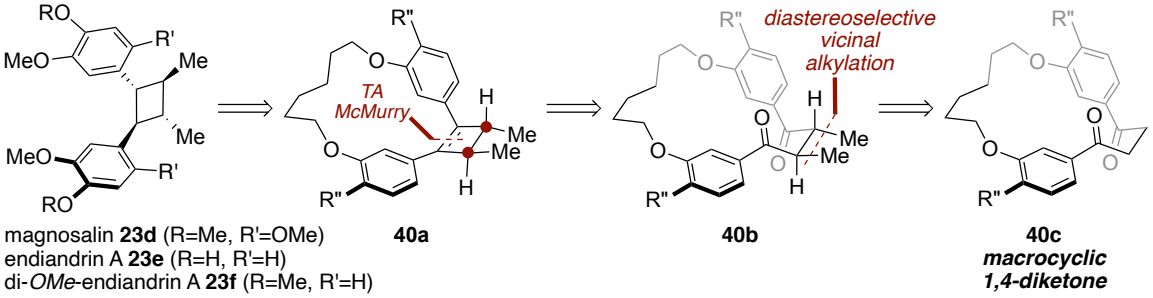

Figure 40: Retrosynthetic plan for the synthesis of lignan-type natural products magnosalin **23d**, endiandrin A **23e**, and di-OMe-endiandrin A **23f** from macrocyclic 1,4-diketones **40c**.

The conditions reported by Drewes and co-workers were applied to [8.4]*meta*cyclophane-1,4-diketone **19.4.** This macrocycle was selected as the entry point into these investigations because high levels of diastereoselectivity were obtained in the Grignard additions to this system (as reported in Chapter 1), but also it was hypothesized that this macrocycle would be able to accommodate the necessary enolate or bis-enolate without significant strain since the *para*-terphenylophane of this macrocycle (Chapter 1, **Scheme 19**, **19.19**) only has 25 kcal/mol of strain. However, initial attempts at vicinally alkylate the α and α′ positions with LDA and BnBr were not met with success. Only mono, *C*-benzylation (**41b**) and *O*-benzylation (**41c**) products

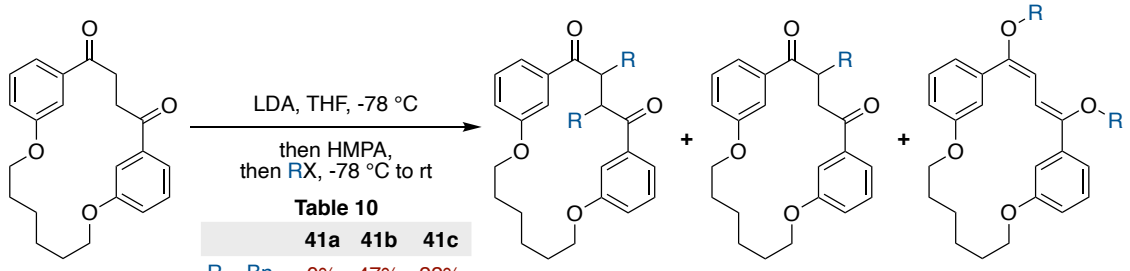

Table 10

	41a	41b	41c
R = Bn	0%	47%	22%
R = allyl	0%	10%	0%
R = Me	4%	13%	0%

Figure 41: Initial attempts to alkylate [8.4]*meta*-1,4-diketone with benzyl bromide, allyl bromide, and methyl iodide.

were observed (**Table 10**, R=Bn). The same reaction conditions were attempted with allyl bromide as the alkylation source; however, only the mono-allylated product was isolated (**Table 10, 41b,** R=allyl). Vicinal alkylation was observed under these conditions, however, when methyl iodide was employed as the alkylating agent, but the yield of the desired product was only 4% (**Table 10**, **41a**, R=Me). Under these conditions, the major product was the result of a monoalkylation reaction (**41b**, R=Me, 13%), but based on ^{1}H NMR anaylsis, the vicinal alkylation product appeared to be formed as a single diastereomer. With this result in hand, optimization of enolate alkylation conditons with methyl iodide were pursued.

Table 11: Size dependent vicinal enolate alkylations

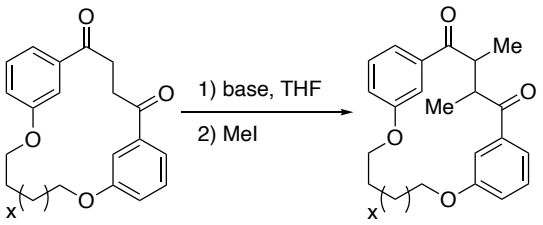

19.2: x=1
19.3: x=2
19.4: x=3
19.5: x=4

41d: x=1
41e: x=2
41a: x=3
41f : x=4

entry	**n** (x)	ring size	base	mono alk.	vic. alk.	tri-alk.	NMR ratio (vic:tri)
1	**6** (1)	16	LDA[(a)]	23%	0%	0%	—:—
2	**7** (2)	17	LDA[(a)]	32%	0%	0%	—:—
3	**8** (3)	18	LDA[(a)]	13%	4%	0%	—:—
4	**6** (1)	16	NaH	0%	12%	4%	5:1
5	**7** (2)	17	NaH	0%	46%	4%	10:1
6	**8** (3)	18	NaH	5%	53%	4%	15:1
7	**9** (4)	19	NaH	0%	43%	0%	—:—

vicinal and tri-alkylated systems are inseparable at the diketone stage, so mono-alkylation yields are isolated and vicinal and tri-alkylation yields are based on the ratio by NMR. (a) HMPA was also added

The next tests performed were on different sized macrocycles using LDA, but with methyl iodide as the alkylating agent since some of the vicinal alkylation product was obtained. However, for both [6.4]*m*-1,4-diketone **19.2** and [7.4]*m*-1,4-diketone **19.3**, none of the vicinally methylated product was observed (**Table 11**, entries 1 and 2, respectively). Because of the challenge alkylating the macrocyclic backbones, some acyclic compounds were also screened (**Table 12**). Alkylation of diketone **37.1** with ortho methoxy groups gave no product regardless of whether the alkylating agent was benzyl bromide (**Table 12**, entry 1) or methyl iodide (**Table 12**, entry 2). However, when diketone **39a** was subjected to LDA and benzyl bromide, conversion to the mono-alkylated product (**12y**) was observed. When the same diketone was subjected to LDA and methyl iodide, however, no product was again observed. However,

Table 12: Alkylation reactions on acyclic 1,4-diketones

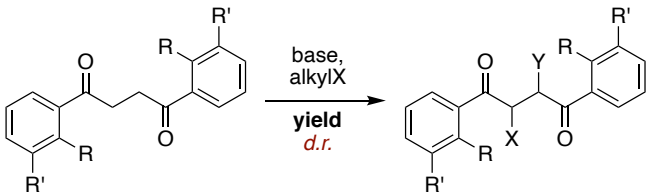

37.1: R=OMe, R'=H
39a: R=H, R'=OMe

12y: R=H, R'=OMe, X=Bn, Y=H
12z: R=H, R'=OMe, X=Y=Me

entry	R	R'	base	alkylX	*result*	yield
1	OMe	H	LDA	BnBr	*no rxn*	—
2	OMe	H	LDA	MeI	*no rxn*	—
3	H	OMe	LDA	BnBr	*X=Bn, Y=H*	36%
4	H	OMe	LDA	MeI	*no rxn*	—
5	H	OMe	NaH	MeI	*X=Y=Me, d.r. 71:29*	27%

when the base was changed to NaH, a 27% yield for the 2,3-dimethyl product (**12z**) was observed with a diastereomeric ratio 71:29. Thus, the macrocycles were again subjected to alkylation with methyl iodide, but with NaH as the base instead of LDA (**Table 11**, entries 4-7). Under these reaction conditions, for all of the macrocycles tested – [6.4], [7.4], [8.4], and [9.4]-*meta*cyclophane-1,4-diketone – vicinal alkylation was observed (**Table 11**, 12%, 46%, 56%, and 43%, respectively). The lower yields of vicinally alkylated product observed in the smaller macrocycles supports the hypothesis that enolate formation would be more challenging in smaller macrocycles because of the additional strain introduced by the unsaturation.

Additional bases, temperatures, and additives were tested on the 18-membered macrocyclic 1,4-diketone to determine if the reaction could be further optimized (**Table 13**). Although most of the reaction conditions gave a mixture of mono-, vicinal, and tri-alkylated products, most only gave a single diastereomer of the vicinally methylated product, with the exception of entries 8, 15, and 17 (**Table 13**). When NaH was used in DMF instead of THF, only *anti*-2,3-dimethyl-1,4-diketone **42a** was isolated, albeit in only a 5% yield (entry 8). The NMR data comparing the *syn* and *anti* diastereomers is shown in **Figure 42**. Additionally, when KHMDS was used with HMPA at –78 °C (entry 15, Table 13) and without HMPA, but warmed from –78 °C to room temperature (entry 17), some of the *anti*-2,3-dimethyl diketone was isolated with the *syn*-2,3-dimethyl diketone (0.5% and 3% *anti*, respectively). Alkylations carried out with hexamethyldisilazide-based reagents (LiHMDS: entries 2-3, NaHMDS: entries 10-14, and KHMDS: entries 15-17, Table 13) proved to be the best suited for preventing over-alkylation; however, the yields were lower for the desired vicinal alkylation product. Overall, NaH in THF proved to be the best suited for vicinal alkylation of **19.4**, giving the best isolated yields and greatest conversion of the starting material to alkylated products, in general. One of the drawbacks of these conditions, however, was over-alkylation, specifically the formation of a trialkylated product (entries 5 and 6, Table 13).

Table 13: Enolate alkylations of [8.4]*meta*-1,4-diketone

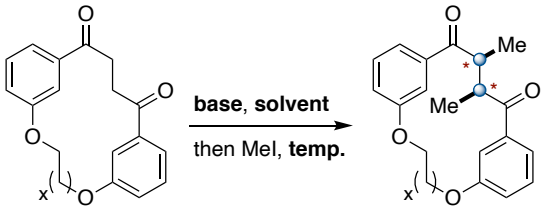

19.4: x=5 **41a:** x=5

entry	base	solvent	temp. (°C)	mono alk.	vic. alk.	tri-alk.	NMR ratio (vic: tri)
1	LDA[(a)]	THF	-78–25	36%	9%	0%	—:—
2	LiHMDS[(a)]	THF	-78–25	16%	24%	0%	—:—
3	LiHMDS	THF	-78–25	19%	16%	0%	—:—
4	NaH	THF	-20	0%	15%	3%	5.6:1
5	NaH	THF	0	0%	45%	4%	12:1
6	NaH	THF	0–25	5%	53%	4%	15:1
7	NaH	Dioxane	0–25	0%	10%	4%	2.5:1
8	NaH	DMF	0–25	0%	5%*	0%	—:—
9	NaH	Et_2O	0–25	0%	0%	0%	—:—
10	NaHMDS[(a)]	THF	-78	10%	21%	0%	—:—
11	NaHMDS[(a)]	THF	-78–25	0%	31%	0.5 %	60:1
12	NaHMDS	THF	-78–25	13%	39%	3%	12:1
13	NaHMDS[(b)]	THF	-78–25	9%	22%	0.5%	22:1
14	NaHMDS[(c)]	THF	-78–25	7%	20%	1%	24:1
15	KHMDS[(a)]	THF	-78	4%	30%†	0%	—:—
16	KHMDS	THF	-78	0%	37%	0%	—:—
17	KHMDS	THF	-78–25	9%	25%‡	0.5%	46:1

*vicinal and tri-alkylated systems are inseparable at the diketone stage, so mono-alkylation yields are isolated and vicinal and tri-alkylation yields are based on the ratio by NMR; (a) HMPA was also added; (b) base and diketone solution was warmed from -78 to 0 °C then cooled again to add MeI; (c) all reagents/reactants were added sequentially; *other vicinal diastereomer only; † also 0.5%* anti *vicinal diastereomer (inseparable from mono alkylation product); ‡ also 3%* anti *vicinal diastereomer (inseparable from mono alkylation product.*

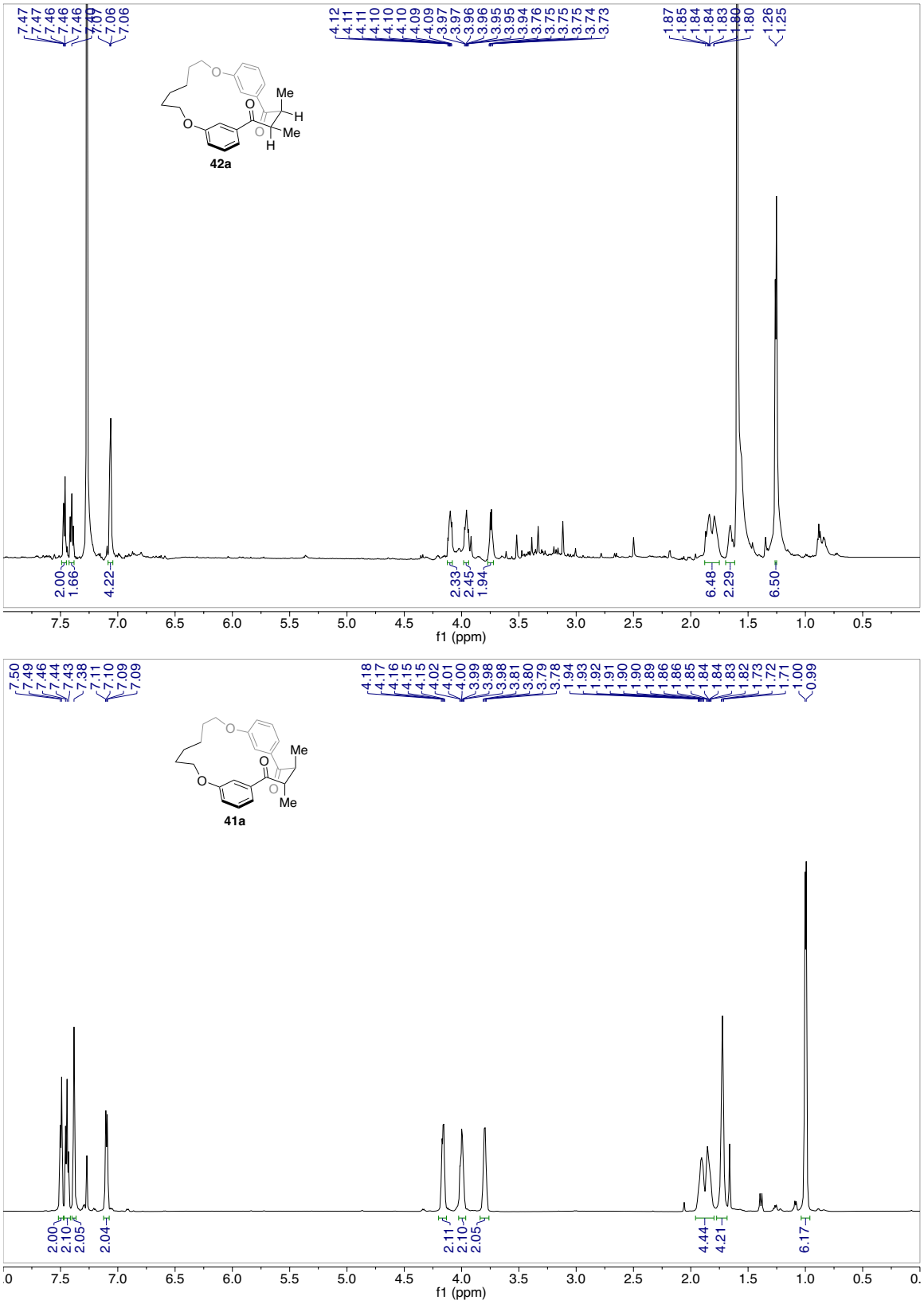

Figure 42: NMRs of *syn*-2,3-dimethyl-1,4-diketone **42a** and *anti*-2,3-dimethyl-1,4-diketone **41a**.

For magnosalin (**23d**), endiandrin A (**23e**), di-*O*-methylendiandrin A (**23f**), and andamanicin (**23g**), the relative configuration of the vicinal *C*-methyl stereogenic centers is *anti.* Thus, the relative configuration obtained during the vicinal enolate alkylation of **19.4** led to cautious optimism that the total synthesis of these natural products could be completed using the designed synthetic approach. Other related natural products such as endiandrin B (**43a**, **Figure 43**) possess a *syn* relative configuration for the vicinal *C*-methyl groups.[5] Therefore, in addition to enolate alkylations, conjugate additions were also tested to determine if perhaps under such conditions: (1) higher yields could be obtained, (2) the other diastereomer could be accessed, and/or (3) the two alkyl groups could differ. **Table 14** shows the results of these tests. The best set of conditions for the 18-membered macrocycle employed CuBr•SMe_2 to make the cuprate with methylmagnesium bromide as the nucleophile and HMPA and TMSCl as additives (20% yield, entry 5). It should be noted also, that without the TMSCl, no conversion to the mono-alkylated product was observed (entry 4). When copper (I) iodide was used instead of CuBr•SMe_2 with methylmagnesium bromide, a 14% yield was obtained (entry 2). Some of these conditions were also tested on the 16-membered macrocyclic system, but still lower conversion to the mono-alkylated product was observed. Since none of the yields obtained throughout these tests were comparable to those obtained during the double enolate alkylations, this method was abandoned, and the synthesis continued with the previously described enolate alkylations.

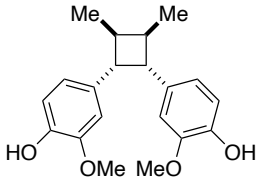

endiandrin B (**43a**)

Figure 43: Structure of endiandrin B.

Table 14: Conjugate additions to macrocyclic ene-diones

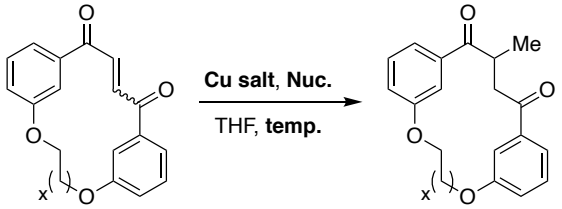

14u: x=3
14v: x=4
14w: x=5

14x: x=3
14y: x=4
14z: x=5

entry	**n** (x)	ring size	Cu salt	Nuc.	additive	temp. (°C)	Yield
1	**8** (5)	18	CuI	MeLi	—	-78	0%
2	**8** (5)	18	CuI	MeMgBr	—	0	14%
3	**8** (5)	18	CuI	MeMgBr	HMPA	-78-25	0%
4	**8** (5)	18	CuBr•SMe_2	MeMgBr	HMPA	-78	0%
5	**8** (5)	18	CuBr•SMe_2	MeMgBr	HMPA, TMSCl	-78	20%
6	**8** (5)	18	CuBr•SMe_2	MeMgBr	BF_3•OEt_2	-78-25	0%
7	**6** (3)	16	CuI	MeMgBr	—	0-25	4%
8	**6** (3)	16	CuBr•SMe_2	MeMgBr	HMPA	-78	0%

With the 2,3-dimethyl 1,4-diketone in hand, the next step in the synthesis was to perform the transannular McMurry with the Lenoir modification to form the cyclobutene ring.[68] Preliminary studies on an unsubstituted derivative gave 23% yield of the cyclobutene product (**Table 15**, entry 1). Under the same conditions, monoalkylated diketone **14z** afforded the cyclobutene-containing

macrocycle **15w** in 52% yield (entry 2), and the bisalkylated diketone **41a** gave the desired reductive coupling product **15z** in 81% yield as a single diastereomer (**Table 15**, entry 3). This trend suggests that a Thorpe-Ingold type effect facilitates the coupling. The same reductive coupling conditions were also applied to the unsubstituted 16- and 17-membered macrocyclic diketones, and 39% and 56% yields were observed, respectively (**Table 15**, entries 4 and 5). It was at this stage that the relative stereochemistry of the vicinal dimethyl groups was identified as being *anti* (as represented in **Table 15**, **41a**). Although a single diastereomer was seen before, the identity of the relative relationship between the methyl groups was uncertain. To my knowledge, this is only the second reported cyclobutene to be formed under McMurry conditions, and the first to be done transannularly and with such a high yield.

Table 15: Transannular McMurry of Macrocyclic 1,4-diketones

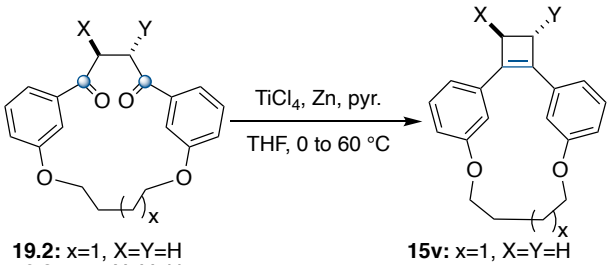

19.2: x=1, X=Y=H
19.3: x=2, X=Y=H
19.4: x=3, X=Y=H
14z: x=3, X=H, Y=Me
41a: x=3, X=Y=Me

15v: x=1, X=Y=H
15w: x=2, X=Y=H
15x: x=3, X=Y=H
15y: x=3, X=H, Y=Me
15z: x=3, X=Y=Me

entry	**n** (x)	ring size	X	Y	% Yield	*syn:anti*
1	**8** (5)	18	H	H	23%	—
2	**8** (5)	18	H	Me	52%	—
3	**8** (5)	18	Me	Me	81%	0:100
4	**7** (4)	17	H	H	56%	—
5	**6** (3)	16	H	H	39%	—

After the formation of the cyclobutene ring, the tetra-substituted olefin needs to be reduced to set the stereochemistry of the final product. Magnosalin and endiandrin A have all-*trans* relative stereochemistry, but andamanicin has *anti-syn-anti-syn* relative stereochemistry. To access these natural products, the ionic hydrogenation conditions shown in **Table 16** (entries 1-5) were attempted, hypothesizing that the all *trans* product would probably be preferred. The hydrogenations were tested on both macrocyclic and non-macrocyclic systems supposing that the strain induced by the macrocycle could cause the preferred geometry to be different than that observed for the non-macrocyclic derivatives. However, all attempts at performing an ionic hydrogenation failed and either the starting material was

Table 16: Hydrogenation conditions tested to reduce cyclobutene to cyclobutane

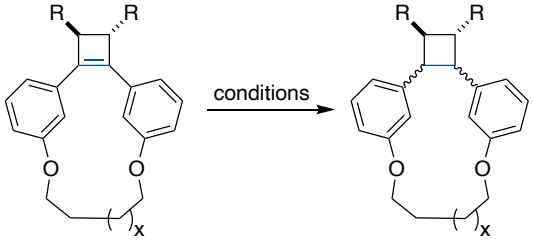

entry	**n** (x)	ring size	R	conditions	results
1	**8** (5)	18	H	Et_3SiH, TfOH, PhH	no reaction
2	**OMe**	—	Me	Et_3SiH, TfOH, CH_2Cl_2	no reaction
3	**8** (5)	18	H	TBAI, TfOH, CH_2Cl_2	no reaction
4	**8** (5)	18	H	KOH, Pd/C, H_2, EtOH/EtOAc	*syn*-Ar
5	**OMe**	—	Me	$Mn(dpm)_3$, PhSiH, ^{t}BuOOH, *i*-PrOH	no reaction
6	**8** (5)	18	Me	Pd/C, H_2, MeOH, EtOAc	*syn*-Ar

returned unchanged (entries 1, 2, 3, and 5) or the *syn*-relative stereochemistry of the aromatic groups was obtained (entry 4). Therefore, the cyclobutene ring was reduced to the cyclobutane using a catalytic hydrogenation with Pd/C and hydrogen gas (**Table 16**, entry 6) to give the *syn* configuration for the aromatic rings (*cis-cis-trans* around the ring).

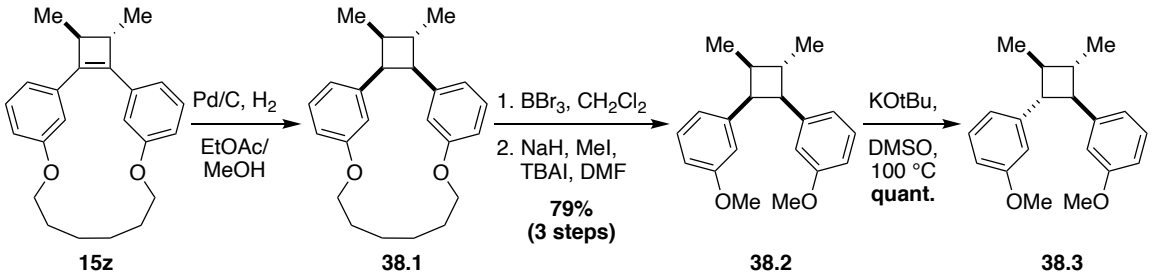

Scheme 38: Synthetic steps from macrocyclic cyclobutene **15z** to all *trans* cyclobutane **38.3**.

With the *cis-cis-trans* cyclobutane ring **38.1** in hand, the next step was to remove the macrocyclic tether to give the free lignan-type cyclobutane. This was accomplished by breaking the O-CH_2 bonds on each side of the tether with BBr_3 in dichloromethane. At this stage, the free alcohols could be left as such or converted into any number of ethers or other functional groups to contribute to a library of these lignan-type compounds. However, in pursuit of the synthesis of magnosalin or endiandrin A, the phenols were converted to *O*-methyl groups with NaH, MeI, and TBAI in DMF (**Scheme 38**, **38.1** to **38.2**). The final step in accomplishing the all *trans* stereochemistry around the cyclobutane ring was to perform an epimerization at one of the

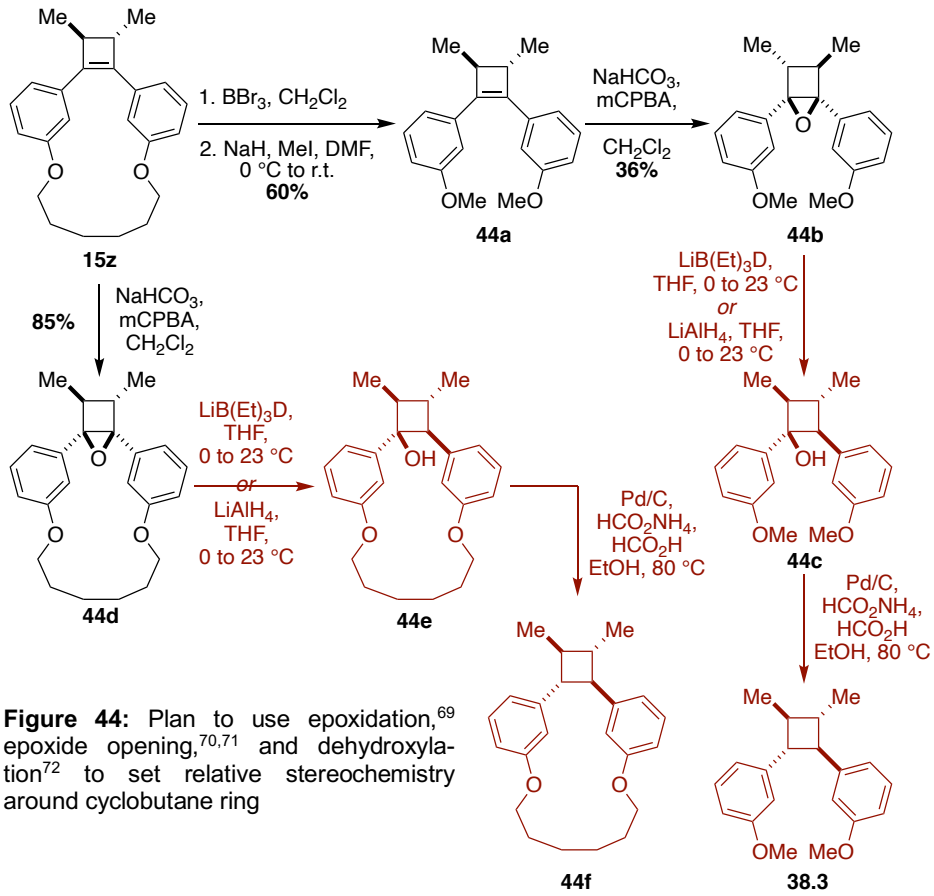

Figure 44: Plan to use epoxidation,[69] epoxide opening,[70,71] and dehydroxylation[72] to set relative stereochemistry around cyclobutane ring

benzylic positions of **38.2**. Initially, this was met with no success, so epoxiations of both the macrocyclic and non-macrocyclic cyclobutenes were attempted. The proposed approach to this method of obtaining the all-trans cyclobutane is shown in **Figure 44**. Epoxidation of both the macrocyclic and non-macrocyclic cyclobutenes (**15z** and **44a**, respectively) were accomplished to give **44d** and **44b**,[69] but attempts to open the epoxide gave inseparable mixtures of products in both cases,[70,71] and dehydroxylations were not attempted.[72] Thus, the epimerization was retried under rigorously anhydrous conditions. Happily, with excess potassium *tert*-butoxide in DMSO at 100 °C, the epimerization occurred. However, initial attempts at the epimerization still rendered only a 55% yield because of the difficulty in extracting the final product from the DMSO (aq.) phase during workup. However, when a 3:1 mixture of chloroform:isopropanol was used, the recovery of the cleanly epimerized product was quantitative (**Scheme 38**, **38.3**).

Now two different non-macrocyclic lignan-type structures have been synthesized (**38.2** and **38.3**), but the natural product still had not been formed through this route, so compound **38.3** was subjected to bromination conditions (**Scheme 39**). When Br_2 was added to the substrate in dichloromethane at 0 °C, quantitative conversion to the dibrominated compound **39.1** was isolated as the only product. Further investigation showed that when the reaction was performed at room temperature instead of 0 °C, a mixture of di-, tri-, and tetrabrominated products were isolated but were inseparable chromatographically. However, when the bromination was done in neat acetic acid at room temperature, clean and quantitative conversion to tetrabrominated **39.2** was observed. From here, Ullman-type couplings were proposed, as had been used in Nicewicz's synthesis of endiandrin A;[46] however, of the conditions tested (**Table 17**), none showed any conversion of the bromines to either alcohols or ethers. Other conditions and approaches are still under investigation in our laboratory, but another ground-up approach has also shown great promise.

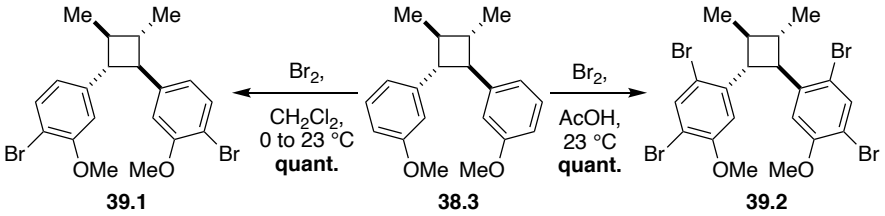

Scheme 39: Brominations of cyclobutane **38.3**

Table 17: Ullman-type coupling reactions to dibromo **39.1** and tetrabromo **39.2**.

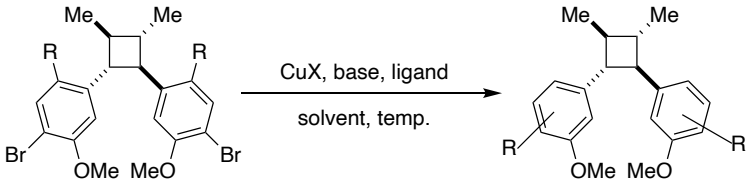

39.1: R=H
39.2: R=Br

entry	R	CuX	base	ligand	solvent	temp. (°C)	result
1	H	CuI	Cs_2CO_3	**17X**	BnOH	110	no rxn
2	H	CuI	Cs_2CO_3	**17X**	MeOH	110	no rxn
3	H	CuI	Cs_2CO_3	**17Y**	MeOH	110	no rxn
4	H	CuI	NaOMe	—	DMF/MeOH	110	no rxn
5	H	CuI	Cs_2CO_3	**17Z**	MeOH	110	no prod*
6	Br	CuI	Cs_2CO_3	**17Z**	MeOH	110	no prod*
7	Br	Cu^0	NaOH	—	H_2O	100	no rxn

* the starting material was consumed, but no product was isolated

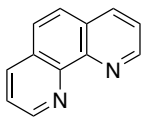

17X: 1,10-phenanthroline

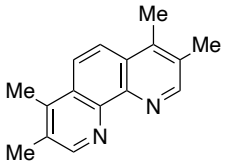

17Y: 3,4,7,8-tetramethyl-1,10-phenanthroline

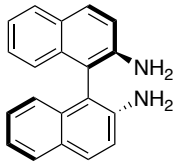

17Z: (R)-(+)-BINAM

Instead of starting with 3-hydroxybenzaldehyde, isovanillin (**40.1**) was taken through the same sequence of steps as previously described (**Scheme 40**). Although the initial formation of the macrocyclic 1,4-diketone **40.3** was lower yielding than for the sequence starting from 3-hydroxybenzaldehyde (39%),[73] the other synthetic steps had comparable yields to those seen for the 3-hydroxybenzaldehyde sequence until the final steps, and the result was the direct formation of racemic di-*O*-methyl-endiandrin A (**23f**). In the final removal of the macrocyclic tether and epimerization steps, solubility issues caused yields to be diminished. However, since this synthesis was initially completed as shown below, the enolate alkylation, *O*-methylation, and epimerization steps have been optimized further by another member of our laboratory, and these results were recently published as a communication.[74]

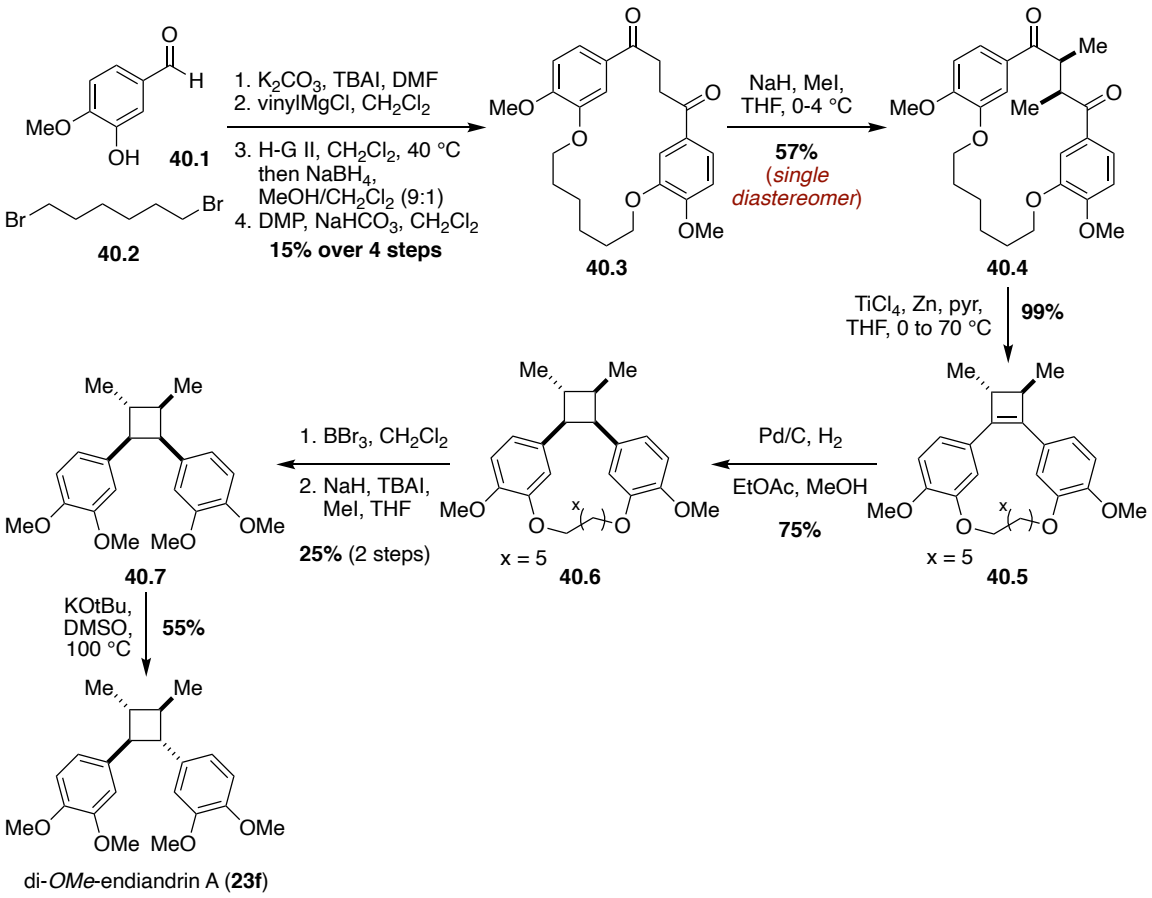

Scheme 40: Synthesis of di-*OMe*-endiandrin A (**23f**) from isovanillin (**40.1**)

2.3 Future Directions

At this point, one natural product (di-*OMe*-endiandrin A **23f**) has been accessed using the above method, and five other non-macrocyclic (**38.2**, **38.3**, **39.1**, **39.2**, and **40.7**) and two macrocyclic (**38.1** and **40.6**) lignan-type products have been formed. However, this approach's utility is best seen through the synthesis of other cyclobutane-containing natural products including magnosalin (**23d**) and endiandrin A (**23e**), which both possess the all *trans* stereochemistry around the cyclobutane. However, accessing lignan-type natural products such as andamanicin (**23g**) and endiandrin B (**43a**), which have not yet been synthesized, would showcase how useful this method could truly be in accessing a library of lignan-type products through a single macrocyclic diketone intermediate. The relative stereochemistry around the cyclobutane rings for both magnosalin and endiandrin A has been achieved through the methods described here, but the substitution of the aromatic ring has yet to be accomplished. Ullman-type reaction conditions are currently being explored to convert the brominated derivatives shown in **Scheme 39** to the functional groups of

both of these compounds. Additionally, the relative stereochemistry of the methyl groups in andamanicin (**23g**) has been achieved through the methods previously described, so adjustment to the epimerization conditions could lead to the *trans-cis-trans* stereochemistry of **23g**. Some preliminary experiments have shown that longer reactions times for the epimerization with potassium *t*-butoxide may cause the formation of another diastereomer, but significant quantities of this diastereomer have not yet been obtained, and thus its identity is not yet known. Accessing endiandrin B (**43a**) will require adjustment at the backbone alkylation stage. Perhaps adjustments and optimizations could take place to the enolate alkylation in DMF (**Table 13**, entry 8), which gave exclusively **42a** with *syn* relative stereochemistry of the *C*-methyl groups (as drawn in **Figure 42**), albeit in only 5% yield.

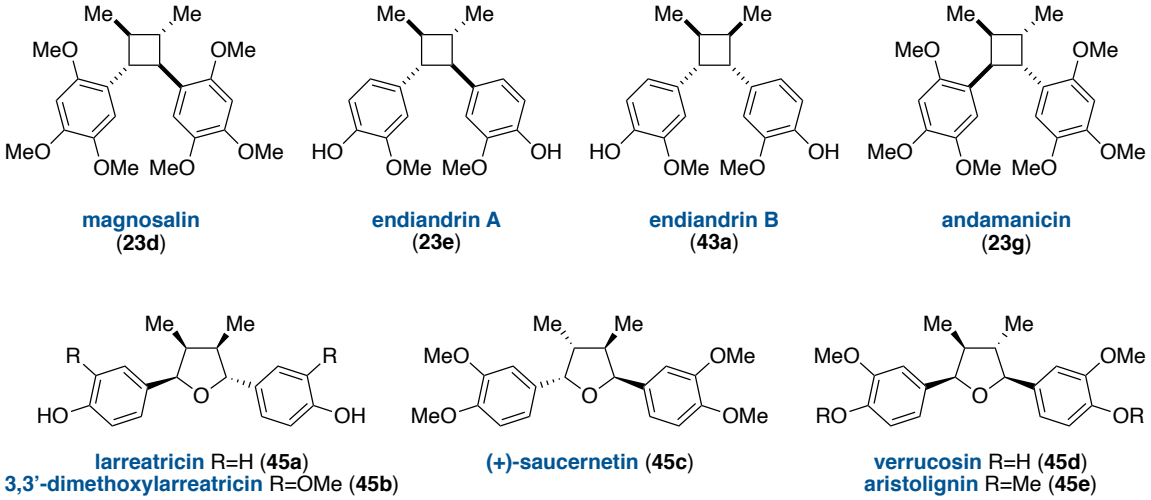

Figure 45: Lignan-type natural products that could be accessed from the macrocyclic 1,4-diketone

In addition to accessing cyclobutane-containing natural products, there are several lignan-type natural products with tetrahydrofuran rings instead of cyclobutane rings. Some examples are shown in **Figure 45** and include larreatricin (**45a**), 3,3'-dimethoxylarreatricin (**45b**), saucernetin (**45c**), verrucosin (**45d**), and aristolignin (**45e**). Some of these compounds have been accessed from non-macrocyclic 1,4-diketones using lithium aluminum hydride to form the tetrahydrofuran ring, followed by cleavage of the mesylate (**Figure 46**).[75] This approach has given a variety of diastereomers and enantiomers that are separable through chiral HPLC to give clean products. However, the yields have been relatively low (34%). As in the diastereoselective enolate alkylations and transannular McMurry reactions presented above, the yield and diastereose-

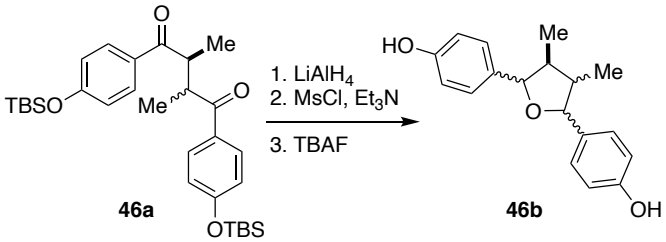

Figure 46: Lewis's approach to the synthesis of tetrahydrofuran-containing lignan natural products.[74]

lectivity could be improved by alkylating the macrocyclic backbone and performing the cyclization transannularly rather than simply intramolecularly.

Accessing racemic natural products and creating a library of compounds consisting of analogs of these using this approach is both worthwhile and meaningful to the synthetic community. Such a library could include varied *C*-alkyl groups to include more than methyl, additional substitution and functionalization around the aromatic rings, and varied stereochemistry around the cyclobutane or tetrahydrofuran rings. However, to my knowledge, these lignan natural products have not been synthesized enantioselectively, so developing an approach to efficiently access several through the same route could be very valuable. Using the approach taken here, if the alkylation could be performed enantioselectively, the retention of stereochemistry throughout the subsequent steps would allow for an enantioselective synthesis of these natural products. Chiral hydrazines such as SAMP (**47a**) and RAMP (enantiomer of **47a**) have been used in the literature to do enantioselective enolate alkylations to single ketone-containing compounds through a hydrazone intermediate.[76] Other chiral amines like **47b** could also potentially be used to direct the absolute stereochemistry of the alkylation (**Figure 47A**).[77] If these methods did not prove sufficient, chiral catalysis could also be explored. Both Jacobsen[78] and Koga[77] have em-

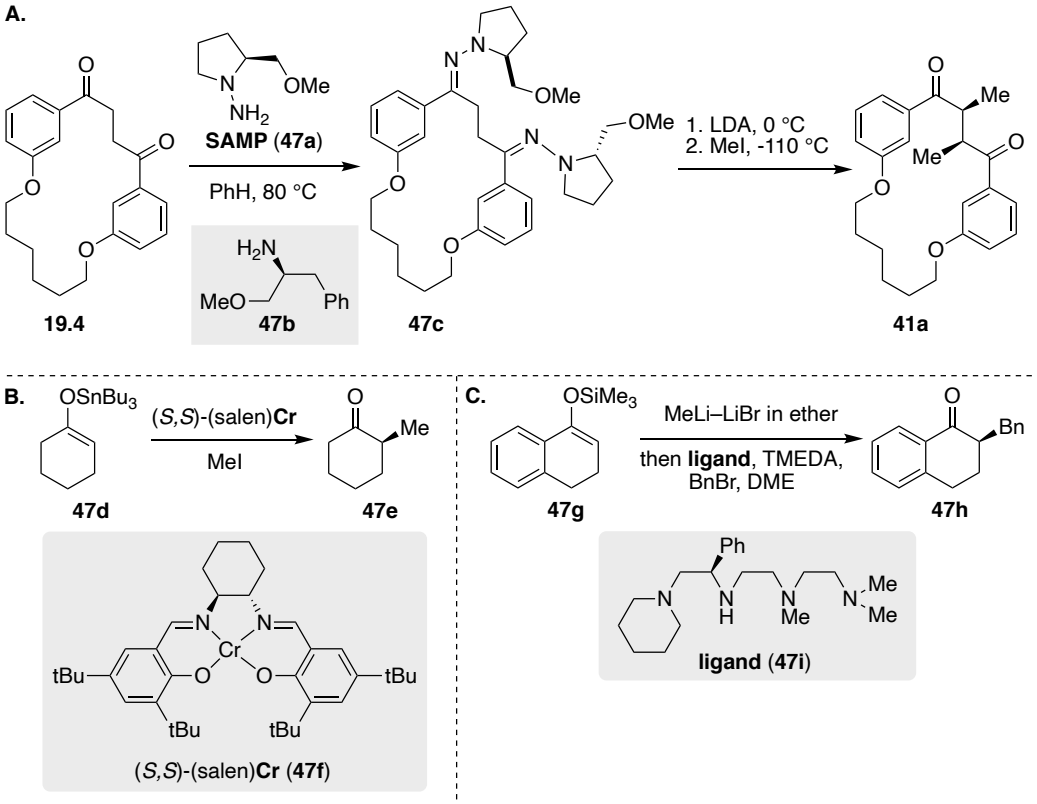

Figure 47: Enantioselective alkylation approaches for the asymmetric total synthesis of lignan-type natural products: **A.** SAMP (**47a**) hydrazone alkylation or chiral amine **47b** enolate alkylation;[75] **B.** Jacobsen's salen catalyst **47f** for asymmetric enolate alkylation;[76] and **C.** Koga's chiral amine ligand for asymmetric enolate alkylations.[77]

ployed chiral ligands to asymmetrically alkylate the α-position of 6-membered ketones (Jacobsen's salen catalyst **Figure 47B**, and Koga's chiral amine ligand **Figure 47C**).

2.4 Conclusion

Presented here is a novel approach to the formation of 1,2,3,4-tetrasubstituted cyclobutane rings and the racemic synthesis of di-*O*-methyl-endiandrin A (**23f**). This approach showcases a completely diastereoselective enolate alkylation to a macrocyclic 1,4-diketone followed by a transannular McMurry reaction to form a 1,2,3,4-tetrasubstituted cyclobutene ring. One of the obvious benefits to this approach is the ability to tune reactions throughout the synthesis to access cyclobutane rings with varying relative stereochemistry in order to access several compounds through a common intermediate. Such an approach has the potential to produce many natural products and analogs of natural products, which could all be tested for efficacy as pharmaceuticals.

References

(1) Li, J.; Gao, K.; Bian, M.; Ding, H. *Org. Chem. Front* **2020**, *7*, 136–154.

(2) Carmignani, M.; Volpe, A. R.; Delle Monache, F.; Botta, B.; Espinal, R.; De Bonnevaux, S. C.; De Luca, C.; Botta, M.; Corelli, F.; Tafi, A.; Ripanti, G.; Delle Monache, G. *J. Med. Chem.* **1999**, *42*, 3116–3125.

(3) Dembitsky, V. M. *J. Nat. Med.* **2008**, *62*, 1–33.

(4) Ryu, J.-H.; Son, H. J.; Lee, S. H.; Sohn, D. H. *Bioorg. Med. Chem. Lett.* **2002**, *12*, 649–651.

(5) Davis, R. A.; Barnes, E. C.; Longden, J.; Avery, V. M.; Healy, P. C. *Bioorganic Med. Chem.* **2009**, *17*, 1387–1392.

(6) Sergeiko, A.; Poroikov, V. V; Hanu, L. O.; Dembitsky, V. M. *Open Med. Chem. J.* **2008**, *2*, 26–37.

(7) Cipres, A.; O'malley, D. P.; Li, K.; Finlay, D.; Baran, P. S.; Vuori, K. *ACS Chem. Biol.* **2010**, *5*, 195–202.

(8) Davis, R. A.; Carroll, A. R.; Duffy, S.; Avery, V. M.; Guymer, G. P.; Forster, P. I.; Quinn, R. J. *J. Nat. Prod.* **2007**, *70*, 1118–1121.

(9) Jiao, W. H.; Hong, L. L.; Sun, J. B.; Piao, S. J.; Chen, G. D.; Deng, H.; Wang, S. P.; Yang, F.; Lin, H. W. *European J. Org. Chem.* **2017**, *2017*, 3421–3426.

(10) Piao, S.-J.; Song, Y.-L.; Jiao, W.-H.; Yang, F.; Liu, X.-F.; Chen, W.-S.; Han, B.-N.; Lin, H.-W. *Org. Lett.* **2013**, *15* , 3526–3529.

(11) Barton, L. M.; Edwards, J. T.; Johnson, E. C.; Bukowski, E. J.; Sausa, R. C.; Byrd, E. F. C.; Orlicki, J. A.; Sabatini, J. J.; Baran, P. S. *J. Am. Chem. Soc.* **2019**, *141*, 12531–12535.

(12) Wang, Z.; Miller, B.; Mabin, M.; Shahni, R.; Wang, Z. D.; Ugrinov, A.; Chu, Q. R. *Sci. Rep.* **2017**, *7*, 13704–13710.

(13) Wang, Z. D.; Elliott, Q.; Wang, Z.; Setien, R. A.; Puttkammer, J.; Ugrinov, A.; Lee, J.; Webster, D. C.; Chu, Q. R. *ACS Sustain. Chem. Eng.* **2018**, *6*, 8136–8141.

(14) Hancock, E. N.; Wiest, J. M.; Brown, M. K. *Nat. Prod. Rep.* **2019**, *36*, 1383–1393.

(15) Wang, M.; Lu, P. *Org. Chem. Front.* **2018**, *5*, 254–259.

(16) Poplata, S.; Tröster, A.; Zou, Y.-Q.; Bach, T. *Chem. Rev.* **2016**, *116*, 9748–9815.

(17) Schuster, D. I. Mechanistic Issues in [2+2]-Photocycloadditions of Cyclic Enones to Alkenes. In *CRC Handbook of Organic Photochemistry and Photobiology*; Horspool, W., Lenci, F., Eds.; CRC: Boca Raton, 2004; pp 72-1–72-24.

(18) Hu, F. L.; Mi, Y.; Zhu, C.; Abrahams, B. F.; Braunstein, P.; Lang, J. P. *Angew. Chemie - Int. Ed.* **2018**, *57*, 12696–12701.

(19) Cohen, M. D.; Schmidt, G. M. J. *J. Chem. Soc.* **1964**, 1996–2000.

(20) Iriondo-Alberdi, J.; Greaney, M. F. *European J. Org. Chem.* **2007**, No. 29, 4801–4815.

(21) Feldman, K. S.; Campbell, R. F. *J. Org. Chem.* **1995**, *60*, 1924–1925.

(22) Weathersby, S.; Dinkelmeyer, B.; Pike, R.; Huffman, S. *Tetrahedron Lett.* **2018**, *59*, 3453–3457.

(23) Mangion, I. K.; Macmillan, D. W. C. *J. Am. Chem. Soc.* **2005**, *127*, 3696–3697.

(24) Bastos Lemos Silva, S.; Beniddir, M. A.; Gallard, J. F.; Poupon, E.; Thomas, O. P.; Evanno, L. *European J. Org. Chem.* **2019**, 5515–5518.

(25) Flores-Giubi, M. E.; Durán-Peña, M. J.; Botubol-Ares, J. M.; Escobar-Montaño, F.; Zorrilla, D.; Macías-Sánchez, A. J.; Hernández-Galán, R. *J. Nat. Prod.* **2017**, *80*, 2161–2165.

(26) Maeda, H.; Hiranabe, R. ichiro; Mizuno, K. *Tetrahedron Lett.* **2006**, *47*, 7865–7869.

(27) Barra, L.; Dickschat, J. S. *European J. Org. Chem.* **2017**, *2017*, 4566–4571.

(28) Birman, V. B.; Jiang, X.-T. *Org. Lett.* **2004**, *6*, 2369–2371.

(29) Fedorova, O. A.; Saifutiarova, A. E.; Gulakova, E. N.; Guskova, E. O.; Aliyeu, T. M.; Shepel, N. E.; Fedorov, Y. V. *Photochem. Photobiol. Sci.* **2019**, *18*, 2208–2215.

(30) Jha, K. K.; Dutta, S.; Sar, S.; Sen, S.; Munshi, P. *Tetrahedron* **2018**, *74*, 7326–7334.

(31) Wei, P.; Zhang, J.-X.; Zhao, Z.; Chen, Y.; He, X.; Chen, M.; Gong, J.; H-Y Sung, H.; Williams, I. D.; Y Lam, J. W.; Zhong Tang, B. *J. Am. Chem. Soc.* **2018**, *140*, 1966–1975.

(32) Damen, J.; Neckers, D. C. *J. Am. Chem. Soc.* **1980**, *102*, 3265–3267.

(33) Pattabiraman, M.; Natarajan, A.; Kaanumalle, L. S.; Ramamurthy, V. *Org. Lett.* **2005**, *7*, 529–532.

(34) Sutyak, K. B.; Lee, W.; Zavalij, P. V.; Gutierrez, O.; Davis, J. T. *Angew. Chemie - Int. Ed.* **2018**, *57*, 17146–17150.

(35) Duchemin, N.; Skiredj, A.; Mansot, J.; Leblanc, K.; Vasseur, J. J.; Beniddir, M. A.; Evanno, L.; Poupon, E.; Smietana, M.; Arseniyadis, S. *Angew. Chemie - Int. Ed.* **2018**, *57*, 11786–11791.

(36) Campillo-Alvarado, G.; D'mello, K. P.; Swenson, D. C.; Santhana Mariappan, S. V.; Höpfl, H.; Morales-Rojas, H.; MacGillivray, L. R.; Santhana Mariappan, S. V.; Höpfl, H.; Morales-Rojas, H.; MacGillivray, L. R.; Santhana Mariappan, S. V.; Höpfl, H.; Morales-Rojas, H.; MacGillivray, L. R.; Santhana Mariappan, S. V.; Höpfl, H.; Morales-Rojas, H.; MacGillivray, L. R. *Angew. Chemie Int. Ed.* **2019**, *58*, 5413–5416.

(37) Rath, B. B.; Kole, G. K.; Vittal, J. J. *Cryst. Growth Des.* **2018**, *18*, 6221–6226.

(38) Ali Al-Mohsin, H.; AlMousa, A.; Oladepo, S. A.; Jalilov, A. S.; Fettouhi, M.; Malik Peedikakkal, A. P. *Inorg. Chem.* **2019**, *58*, 10167–10173.

(39) Dutta, B.; Sinha, C.; Mir, M. H. *Chem. Commun.* **2019**, *55*, 11049–11051.

(40) Jiang, Y.; Wang, C.; Rogers, C. R.; Kodaimati, M. S.; Weiss, E. A. *Nat. Chem.* **2019**, *11*, 1034–1040.

(41) Carrera, C.; Denisi, A.; Cativiela, C.; Urriolabeitia, E. P. *Eur. J. Inorg. Chem.* **2019**, *5*, 3481–3489.

(42) Ischay, M. A.; Ament, M. S.; Yoon, T. P. *Chem. Sci.* **2012**, *3*, 2807–2811.

(43) Ma, Z.; Wang, X.; Wang, X.; Rodrigues, R. A.; Moore, C. E.; Gao, S.; Tan, X.; Ma, Y.; Rheingold, A. L.; Baran, P. S.; Chen, C. *Science* **2014**, *346*, 219–224.

(44) Hu, J.-L.; Feng, L.-W.; Wang, L.; Xie, Z.; Tang, Y.; Li, X. *J. Am. Chem. Soc.* **2016**, *138*, 13151–13154.

(45) Yu, Y.; Fu, Y.; Zhong, F. *Green Chem* **2018**, *20*, 1743–1747.

(46) Riener, M.; Nicewicz, D. A. *Chem. Sci.* **2013**, *4*, 2625–2629.

(47) Colomer, I.; Coura Barcelos, R.; Donohoe, T. J. *Angew. Chemie - Int. Ed.* **2016**, *55*, 4748–4752.

(48) Zhu, Y.; Colomer, I.; Donohoe, T. J.; Li, R. *Chem. Commun* **2019**, *55*, 10316–10319.

(49) Bach, T.; Hehn, J. P. *Angew. Chemie - Int. Ed.* **2011**, *50*, 1000–1045.

(50) Lewis, F. D.; Quillen, S. L.; Hale, P. D.; Oxman, J. D. *J. Am. Chem. Soc.* **1988**, *110*, 1261–1267.

(51) Crimmins, M. T. *Chem. Rev.* **1988**, *88*, 1453–1473.

(52) Ahuja, S.; Raghunathan, R.; Kumarasamy, E.; Jockusch, S.; Sivaguru, J. *J. Am. Chem. Soc.* **2018**, *140*, 13185–13189.

(53) Baran, P. S.; Zografos, A. L.; O'malley, D. P. *J. Am. Chem. Soc.* **2004**, *126*, 3726–3727.

(54) Gutekunst, W. R.; Baran, P. S. *J. Org. Chem.* **2014**, *79*, 2430–2452.

(55) Ayer, W. A.; Browne, L. M. T *Can. J. Chem.* **1974**, *52*, 1352–1360.

(56) Tanino, K.; Takahashi, M.; Tomata, Y.; Tokura, H.; Uehara, T.; Narabu, T.; Miyashita, M. *Nat. Chem.* **2011**, *3*, 484–488.

(57) Wolleb, H.; Carreira, E. M. *Angew. Chemie - Int. Ed.* **2017**, *56*, 10890–10893.

(58) Sugimura, T.; Paquette, L. A. *J. Am. Chem. Soc.* **1987**, *109*, 3017–3024.

(59) Paquette, L. A.; Sugimura, T. *J. Am. Chem. Soc.* **1986**, *108*, 3841–3842.

(60) Akula, P. S.; Hong, B.-C.; Lee, G.-H. *Org. Lett.* **2018**, *20*, 7835–7839.

(61) Chapman, L. M.; Beck, J. C.; Wu, L.; Reisman, S. E. *J. Am. Chem. Soc.* **2016**, *138*, 9803–9806.

(62) Chapman, L. M.; Beck, J. C.; Lacker, C. R.; Wu, L.; Reisman, S. E. *J. Org. Chem.* **2018**, *83*, 6066–6085.

(63) Beck, J. C.; Lacker, C. R.; Chapman, L. M.; Reisman, S. E. *Chem. Sci.* **2019**, *10*, 2315–2319.

(64) Liu, R.; Zhang, M.; Wyche, T. P.; Winston-Mcpherson, G. N.; Bugni, T. S.; Tang, W. *Angew. Chemie - Int. Ed.* **2012**, *51*, 7503–7506.

(65) Panish, R. A.; Chintala, S. R.; Fox, J. M. *Angew. Chemie - Int. Ed.* **2016**, *55*, 4983–4987.

(66) Baran, P. S.; Li, K.; O'Malley, D. P.; Mitsos, C. Short, *Angew. Chemie - Int. Ed.* **2005**, *45*, 249–252.

(67) Drewes, S. E.; Hogan, C. J.; Kaye, P. T.; Roos, G. H. P. *J. Chem. Soc. PERKIN TRANS. I.* **1989**.

(68) Nandaluru, P. R.; Dongare, P.; Kraml, C. M.; Pascal Jr., R. A.; Dawe, L. N.; Thompson, D. W.; Bodwell, G. J. *Chem. Commun.* **2012**, *48*, 7747–7749.

(69) Akther, T.; Islam, M. M.; Rahman, S.; Georghiou, P. E.; Matsumoto, T.; Tanaka, J.; Redshaw, C.; Yamato, T. *Org. Biomol. Chem.* **2017**, *15*, 3519–3527.

(70) Panini, S. R.; Sexton, R. C.; Gupta, A. K.; Parish, E. J.; Chitrakorn, S.; Rudney, H. *J. Lipid Res.* **1986**, *27*, 1190–1204.

(71) Dervan, P. B.; Santilli, D. S.; Santilli, D. S. *J. Am. Chem. Soc* **1980**, *102*, 3863–3870.

(72) Sawadjoon, S.; Lundstedt, A.; Samec, J. S. M. *ACS Catal.* **2013**, *3*, 635–642.

(73) Mitra, N. K.; Meudom, R.; Corzo, H. H.; Gorden, J. D.; Merner, B. L. *J. Am. Chem. Soc.* **2016**, *138*, 3235–3240.

(74) Barnes, T. H.; Johnson, K. F.; Gorden, J. D.; Merner, B. L. *Chem. Commun.* **2020**, *56*, 8747–8749.

(75) Moinuddin, S. G. A.; Hishiyama, S.; Cho, M. H.; Davin, L. B.; Lewis, N. G. *Org. Biomol. Chem.* **2003**, *1*, 2307–2313.

(76) Kohler, M. C.; Wengryniuk, S. E.; Coltart, D. M. In *Stereoselective Synthesis of Drugs and Natural Products*; 2013; 183–213.

(77) Imai, M.; Hagihara, A.; Kawasaki, H.; Manabe, K.; Koga, K. *J. Am. Chem. Soc* **1994**, *116*, 8829–8830.

(78) Doyle, A. G.; Jacobsen, E. N. *J. Am. Chem. Soc.* **2005**, *127*, 62–63.

APPENDIX 1: CHAPTER 1 Supplementary Information

General experimental conditions

All reactions were run in flame or oven-dried (120 °C) glassware and cooled under a positive pressure of ultra high pure nitrogen or argon gas. All chemicals were used as received from commercial sources, unless otherwise stated. Anhydrous reaction solvents were purified and dried by passing HPLC grade solvents through activated columns of alumina (Glass Contour SDS). All solvents used for chromatographic separations were HPLC grade (hexanes, ethyl acetate, and dichloromethane). Chromatographic separations were performed using flash chromatography, as originally reported by Still and co-workers,[1] on silica gel 60 (particle size 43-60 μm), and all chromatography conditions have been reported as diameter × height in centimeters. Reaction progress was monitored by thin layer chromatography (TLC), on glass-backed silica gel plates (pH = 7.0). TLC plates were visualized using a handheld UV lamp (254 nm or 365 nm) and stained using an aqueous ceric ammonium molybdate (CAM) solution. Plates were dipped, wiped clean, and heated from the back. ^{1}H and ^{13}C nuclear magnetic resonance (NMR) spectra were recorded at 400 or 600 MHz, calibrated using residual undeuterated solvent as an internal reference ($CHCl_3$, δ 7.27 and 77.2 ppm), reported in parts per million relative to trimethylsilane (TMS, δ 0.00 ppm), and presented as follows: chemical shift (δ, ppm), multiplicity (s = singlet, d = doublet, dd = doublet of doublets, ddt = doublet of doublet of triplets, bs = broad singlet, m = multiplet), coupling constants (*J*, Hz), and integration. High-resolution mass spectrometric (HRMS) data were obtained using a quadrupole time-of-flight (Q-TOF) spectrometer and electrospray ionization (ESI).

Compounds not included in text

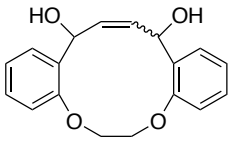

S-1

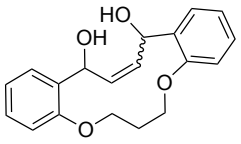

S-2

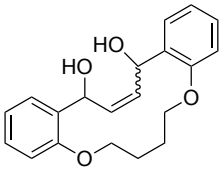

S-3

Experimental Procedures

General procedure for determining diastereoselectivity of addition of phenyl or ethyl metal reagents to *meta*-cylophanes:

Phenyl (**Table 7**) or ethyl (**Table 8**) metal reagent (2.5 equiv.) was added to a stirred solution of 1,4-diketone (1.0 equiv.) in the indicated solvent (0.1 M). Once all of the starting material was consumed

[1] Still, W.C., Kahn, M., Mitra, A. *J. Org. Chem.* **1978**, *43*, 2923-2925.

based on TLC analysis, the reaction was poured into water and diluted with 1 M HCl. The resulting mixture was extracted with dichloromethane (3 ×). The combined organic extracts were washed with a saturated solution of $NaHCO_3$ and brine, dried over $MgSO_4$, filtered, and concentrated under reduced pressure. The mixture of *syn* diol, *anti* diol, and hydroxyketone were analyzed by ^1H NMR to determine the diastereoselectivity and ratio of products formed in the addition reaction.

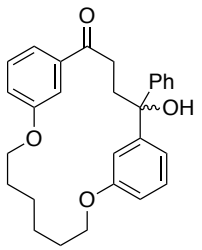

19.21

Hydroxyketone 19.21: R_f = 0.63 (2% acetone/dichloromethane); ^1H NMR (600 MHz, $CDCl_3$-*d*) δ 7.58 (ddd, *J* = 7.7, 1.7, 1.0 Hz, 1H), 7.50 – 7.45 (m, 2H), 7.38 (t, *J* = 7.9 Hz, 1H), 7.35 – 7.27 (m, 4H), 7.27 – 7.23 (m, 2H), 7.20 (t, *J* = 7.9 Hz, 1H), 7.08 (ddd, *J* = 8.1, 2.5, 1.0 Hz, 1H), 6.75 (ddd, *J* = 8.2, 2.7, 0.9 Hz, 1H), 6.73 – 6.68 (m, 1H), 4.14 – 4.06 (m, 3H), 4.06 – 3.99 (m, 2H), 3.12 (ddd, *J* = 15.8, 7.9, 6.8 Hz, 1H), 2.90 (ddd, *J* = 13.6, 7.9, 6.9 Hz, 1H), 2.69 (ddd, *J* = 13.7, 6.8, 5.6 Hz, 1H), 2.60 (ddd, *J* = 15.7, 6.9, 5.7 Hz, 1H), 1.91 – 1.76 (m, 4H), 1.71 – 1.61 (m, 2H); ^{13}C NMR (151 MHz, $CDCl_3$) δ 201.81, 159.05, 159.03, 147.85, 146.96, 138.34, 129.94, 129.53, 128.53, 127.60, 126.33, 125.98, 120.14, 118.90, 118.59, 116.48, 114.73, 113.40, 110.88, 77.99, 68.10, 66.40, 36.90, 33.09, 29.90, 28.26, 28.02, 24.73, 24.48; HRMS (APCI) calculated for $C_{28}H_{30}O_4Na$ ($[M + Na]^+$) *m/z* 453.2042, found 453.2032.

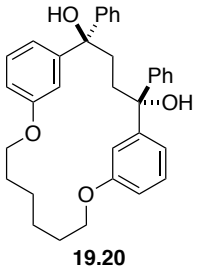

19.20

***Anti*-Diol 19.20:** R_f = 0.45 (2% acetone/dichloromethane); ^1H NMR (600 MHz, $CDCl_3$-*d*) δ 7.38 – 7.34 (m, 4H), 7.30 – 7.26 (m, 2H), 7.25 (dd, *J* = 7.5, 6.1 Hz, 4H), 7.18 (tt, *J* = 8.0, 1.4 Hz, 4H), 6.76 (ddd, *J* = 8.2, 2.5, 0.9 Hz, 2H), 6.63 – 6.59 (m, 2H), 4.01 (dt, *J* = 9.5, 4.9 Hz, 2H), 3.93 (td, *J* = 9.1, 4.2 Hz, 2H), 2.46 – 2.38 (m, 2H), 2.17 – 2.10 (m, 2H), 2.08 (s, 2H), 1.86 – 1.72 (m, 4H), 1.67 – 1.52 (m, 4H); ^{13}C NMR (151 MHz, $CDCl_3$) δ 158.94, 148.12, 147.54, 129.37, 128.39, 127.26, 126.15, 118.16, 113.70, 111.20, 77.97, 66.68, 35.81, 29.90, 28.15, 24.51; HRMS (APCI) calculated for $C_{34}H_{36}O_4Na$ ($[M + Na]^+$) *m/z* 531.2512, found 531.2545.

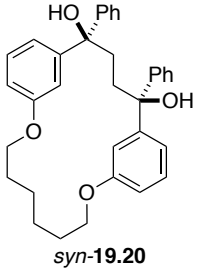

syn-**19.20**

***Syn*-Diol 22.20:** R_f = 0.38 (2% acetone/dichloromethane); ^1H NMR (600 MHz, $CDCl_3$-*d*) δ 7.35 – 7.31 (m, 4H), 7.30 – 7.27 (m, 4H), 7.25 – 7.21 (m, 2H), 7.21 – 7.18 (m, 2H), 7.13 (t, *J* = 7.9 Hz, 2H), 6.76 (ddd, *J* = 8.1, 2.6, 0.9 Hz, 2H), 6.61 – 6.58 (m, 2H), 4.14 – 4.02 (m, 4H), 3.06 (s, 2H), 2.29 – 2.20 (m, 4H), 1.82 (q, *J* = 6.0 Hz, 4H), 1.70 – 1.53 (m, 4H); ^{13}C NMR (151 MHz, $CDCl_3$) δ 158.87, 148.91, 146.38, 129.34, 128.32, 127.19, 126.56, 119.37, 113.05, 112.90, 78.11, 67.55, 36.12, 29.89, 28.27, 24.72; HRMS (ESI) calculated for $C_{34}H_{36}O_4Na$ ($[M + Na]^+$) *m/z* 531.2512, found 531.2516.

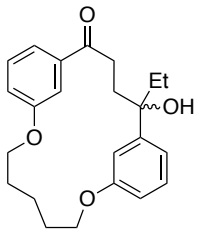

19.18

Hydroxyketone 19.18: ^{1}H NMR (600 MHz, $CDCl_3$) δ 7.49 (d, *J* = 7.6 Hz, 1H), 7.30 (dd, *J* = 17.6, 9.8 Hz, 2H), 7.09 (t, *J* = 2.2 Hz, 1H), 7.02 (d, *J* = 7.6 Hz, 2H), 6.92 (d, *J* = 7.7 Hz, 1H), 6.80 (dd, *J* = 8.1, 2.5 Hz, 1H), 4.17 – 3.99 (m, 4H), 2.78 (ddd, *J* = 16.0, 9.4, 7.0 Hz, 1H), 2.59 (ddd, *J* = 14.9, 9.2, 4.6 Hz, 1H), 2.29 (ddd, *J* = 13.9, 9.1, 7.0 Hz, 1H), 2.10 (ddd, *J* = 14.1, 9.4, 4.6 Hz, 1H), 2.03 (dd, *J* = 14.5, 7.4 Hz, 1H), 1.91 – 1.68 (m, 5H), 0.82 (t, *J* = 7.4 Hz, 3H).

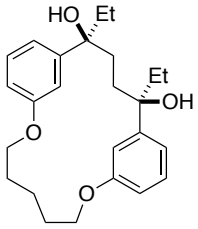

syn-**19.16**

***Syn*-diol 19.16:** ^{1}H NMR (600 MHz, $CDCl_3$) δ 7.22 – 7.18 (m, 2H), 6.85 – 6.81 (m, 4H), 6.76 – 6.73 (m, 2H), 4.10 (dt, *J* = 10.5, 6.1 Hz, 2H), 4.01 (dt, *J* = 10.6, 6.3 Hz, 2H), 2.74 (s, 2H), 1.87 (qd, *J* = 7.2, 3.7 Hz, 4H), 1.78 (pd, *J* = 7.2, 6.4, 1.6 Hz, 4H), 1.72 – 1.52 (m, 8H), 0.80 (t, *J* = 7.4 Hz, 6H).

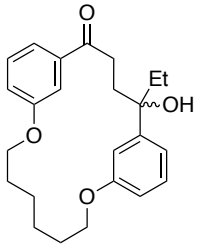

19.19

Hydroxyketone 19.19: ^{1}H NMR (600 MHz, $CDCl_3$) δ 7.54 (d, J = 7.7 Hz, 1H), 7.34 (t, J = 7.9 Hz, 1H), 7.29 (d, J = 8.1 Hz, 1H), 7.19 (t, J = 2.4 Hz, 1H), 7.05 (dt, J = 5.5, 2.9 Hz, 2H), 6.89 (dd, J = 7.7, 1.8 Hz, 1H), 6.77 (dt, J = 6.1, 3.0 Hz, 1H), 4.12 – 3.97 (m, 4H), 2.87 (ddd, J = 12.9, 8.9, 6.5 Hz, 1H), 2.51 (ddd, J = 15.7, 7.5, 5.5 Hz, 1H), 2.39 (ddd, J = 14.5, 8.8, 6.4 Hz, 1H), 2.12 (ddd, J = 13.7, 7.6, 5.5 Hz, 1H), 2.04 – 1.94 (m, 1H), 1.82 (ddp, J = 13.2, 10.5, 7.1 Hz, 4H), 1.68 – 1.53 (m, 5H), 0.78 (t, J = 7.5 Hz, 3H); ^{13}C NMR (151 MHz, $CDCl_3$) δ 201.94, 159.36, 159.06, 146.50, 138.45, 129.88, 129.60, 120.18, 118.71, 117.74, 116.33, 113.42, 111.16, 68.06, 66.53, 38.68, 36.42, 33.41, 28.27, 28.08, 24.82, 24.44, 7.80; HRMS (ESI) calculated for $C_{24}H_{30}O_4Na$ ([M+Na]$^+$) *m/z* = 405.2042, found 405.2057.

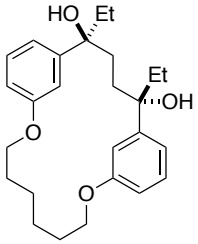

anti-**19.17**

***Anti*-diol 22.17:** ^{1}H NMR (600 MHz, $CDCl_3$) δ 7.27 – 7.24 (m, 2H), 7.13 – 7.09 (m, 2H), 6.74 (dd, J = 8.2, 2.4 Hz, 2H), 6.40 (d, J = 2.1 Hz, 2H), 4.03 (dt, J = 8.9, 4.4 Hz, 2H), 3.91 (td, J = 9.5, 3.4 Hz, 2H), 1.86 (ddt, J = 20.1, 10.1, 4.6 Hz, 2H), 1.75 (qt, J = 9.6, 3.9 Hz, 2H), 1.69 – 1.62 (m, 8H), 1.57 (d, J = 2.8 Hz, 2H), 1.47 – 1.40 (m, 2H), 0.65 (t, J = 7.4 Hz, 6H); HRMS (ESI) calculated for $C_{24}H_{28}O_4Na$ ([M+Na]$^+$) *m/z* = 403.1885, found 403.1873.

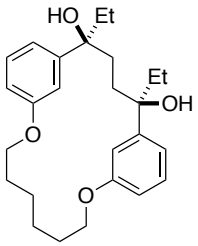

syn-**19.17**

***Syn*-diol 19.17:** ^{1}H NMR (600 MHz, $CDCl_3$) δ 7.24 – 7.19 (m, 2H), 6.89 (d, J = 7.8 Hz, 2H), 6.78 (s, 1H), 6.75 (td, J = 7.9, 2.6 Hz, 3H), 4.01 (td, J = 6.1, 2.7 Hz, 4H), 2.26 (s, 2H), 1.87 – 1.81 (m, 4H), 1.77 (q, J = 5.7 Hz, 4H), 1.69 – 1.61 (m, 4H), 1.60 – 1.49 (m, 4H), 0.78 (t, J = 7.4 Hz, 6H); HRMS (ESI) calculated for $C_{26}H_{36}O_4Na$ ([M+Na]$^+$) *m/z* = 435.2535, found 435.2507.

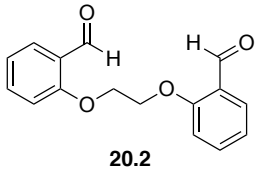

20.2

***Dialdehyde* 20.2:** Salicylaldehyde (2.6 mL, 25 mmol) was added to a stirred solutuon of 1,2-dibromoethane (1.1 mL, 13 mmol) and potassium carbonate (5.12 g, 37.1 mmol) in DMF (30 mL). The reaction was heated to 80 °C for 15 minutes and then heated to 110 °C. After 24 h, the reaction was cooled to room temperature and poured into water (75 mL). The resulting mixture was extracted with ethyl acetate (3 × 30 mL). The organic extracts were combined, washed with 1 M HCl (20 mL) and brine (20 mL), dried over $MgSO_4$, filtered, and concentrated under reduced pressure. The residue was purified by flash chromatography (18 × 6.0 cm; 20% to 40% ethyl acetate/hexane) to afford **20.2** as a white solid (1.80 g, 52%): R_f = 0.18 (20% ethyl acetate/hexane); ^{1}H NMR (400 MHz, $CDCl_3$) δ 10.45 (d, *J* = 0.8 Hz, 1H), 7.86 (dd, *J* = 7.6, 1.9 Hz, 1H), 7.58 (ddd, *J* = 8.3, 7.4, 1.8 Hz, 1H), 7.15 – 7.03 (m, 2H), 4.54 (s, 2H). ^{13}C NMR (101 MHz, $CDCl_3$) δ 189.35, 160.72, 135.94, 128.68, 125.19, 121.50, 112.70, 67.01; HRMS (ESI) calculated for $C_{16}H_{15}O_4$ ([M + H]$^+$) *m/z* 271.0971, found 271.0989.

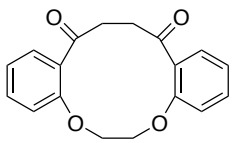

20.5

***1,4-diketone* 20.5:** Vinylmagnesium chloride (1.6 M in THF, 2.9 mL, 4.6 mmol) was added to a stirred solution of dialdehyde **20.2** (0.53 g, 1.9 mmol) in dichloromethane (20 mL). After 2.5 h, the reaction was poured into water (20 mL). The resulting mixture was extracted with dichloromethane (3 × 20 mL). The combined organic extracts were washed with 1 M HCl (20 mL), dried over $MgSO_4$, filtered, and concentrated under reduced pressure. The pale yellow residue was dissolved in dichloromethane (190 mL), stirred at room temperature, followed by the addition of the Hoveyda-Grubbs second-generation catalyst (0.0348 g, 0.0555 mmol). After 14 h, the reaction was concentrated under reduced pressure to afford **S-1**. The dark brown residue was dissolved in 1:9 methanol/dichloromethane (19 mL), and sodium borohydride (0.30 g, 7.8 mmol) was added. After 24 h, the reaction was poured into water (25 mL) and further diluted with 1 M HCl (25 mL). The layers were separated, and the aqueous phase was extracted with dichloromethane (3 × 30 mL). The combined organic extracts were washed with water (30 mL), dried over $MgSO_4$, filtered, and concentrated under reduced pressure. The dark brown residue was dissolved in dichloromethane (19 mL), stirred at room temperature, and pyridinium chlorochromate (1.4 g, 6.5 mmol) was added. After 5 h, silica gel was added and the resulting slurry was filtered through a 2.5 cm Celite pad, which was washed

with dichloromethane (5 × 20 mL) and diethyl ether (5 × 20 mL). The mother liquor was concentrated under reduced pressure to afford a brown residue, which was purified by flash chromatography (2.5 × 13 cm; 50% ethyl acetate/hexane) to give diketone **20.5** as an off-white solid (0.2959 g, 51% over 4 steps): R_f = 0.33 (40% ethyl acetate/hexane); ^{1}H NMR (400 MHz, $CDCl_3$) δ 7.60 – 7.58 (dd, *J* = 7.7, 1.8 Hz, 2H), 7.50 – 7.41 (m, 2H), 7.09 – 7.03 (m, 2H), 7.00 (d, *J* = 8.2, 0.9 Hz, 2H), 4.48 (s, 4H), 3.11 (s, 4H); ^{13}C NMR (101 MHz, $CDCl_3$) δ 202.56, 157.45, 133.65, 130.68, 129.27, 122.27, 113.74, 67.65, 40.79; HRMS (ESI) calculated for $C_{18}H_{17}O_4$ ([M + H]$^+$) *m/z* 297.1128, found 297.1107.

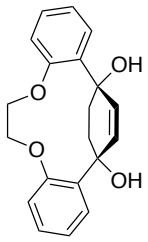

20.14

***Cyclohex-2-ene-1,4-diol* 20.14:** Vinylmagnesium chloride (1.6 M in THF, 0.31 mL, 0.50 mmol) was added to a stirred solution of 1,4-diketone **20.5** (0.30 g, 0.10 mmol) in dichloromethane (1 mL) room temperature. After 35 min., the reaction was poured into water (5 mL) and further diluted with 1 M HCl (5 mL). The resulting mixture was extracted with dichloromethane (3 × 5 mL). The combined organic extracts were washed with a saturated solution of $NaHCO_3$ (10 mL) and water (10 mL), dried over $MgSO_4$, filtered, and concentrated under reduced pressure. The pale yellow residue was dissolved in dichloromethane (2.3 mL), heated to 40 °C, and Grubbs second-generation catalyst (0.0043 g, 0.0051 mmol) was added. After 45 min., the solvent was removed under reduced pressure, and the residue was purified by flash chromatography (0.8 × 12 cm; 3% to 10% acetone/dichloromethane). The cyclohexene (formed from the *syn*-diastereomer), *anti*-allylic diol, and hydroxyketone were combined for ^{1}H NMR analysis of the diastereoselectivity.

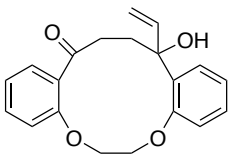

20.11

***Hydroxyketone* 20.11:** ^{1}H NMR (600 MHz, $CDCl_3$) δ 7.62 (dd, *J* = 7.7, 1.8 Hz, 1H), 7.59 (dd, *J* = 7.8, 1.7 Hz, 1H), 7.48 – 7.44 (m, 1H), 7.30 – 7.25 (m, 1H), 7.03 (dd, *J* = 7.9 Hz, 2H), 6.97 (d, *J* = 8.3 Hz, 1H), 6.95 – 6.91 (m, 1H), 6.34 (dd, *J* = 17.2, 10.6 Hz, 1H), 5.30 – 5.23 (m, 1H), 5.08 – 5.02 (m, 1H), 4.62 (ddd, *J* = 11.5, 5.1, 2.5 Hz, 1H), 4.57 – 4.46 (m, 2H), 4.37 (ddd, *J* = 10.2, 7.5, 2.5 Hz, 1H), 3.12 (td, *J* = 13.7, 4.5 Hz, 1H), 2.79 (td, *J* = 13.4, 4.6 Hz, 1H), 2.50 (td, *J* = 13.5, 3.9 Hz, 1H), 2.26 (s, 1H), 1.85 (td, *J* = 13.6, 4.0 Hz, 1H). ^{13}C NMR (151 MHz, $CDCl_3$) δ 203.66, 156.98, 155.22, 143.51, 133.33, 132.56, 130.78, 128.78, 128.55, 127.53, 121.92, 121.69, 113.95, 112.68, 111.75, 76.39, 68.27, 66.50, 40.34, 37.29; HRMS (ESI) calculated for $C_{20}H_{19}O_4Na$ ([M + Na]$^+$) *m/z* 347.1259, found 347.1449.

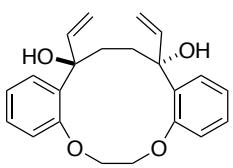

20.8

***Anti-allylic diol* 20.8:** ^{1}H NMR (600 MHz, $CDCl_3$) δ 7.67 – 7.66 (dd, *J* = 7.8, 1.8 Hz, 2H), 7.31 – 7.29 (m, 2H), 7.07 – 7.04 (m, 2H), 6.92 – 6.90 (dd, *J* = 8.1, 1.2 Hz, 2H), 6.19 – 6.15 (dd, *J* = 17.2, 10.5 Hz, 2H), 5.14 – 5.11 (dd, *J* = 17.3, 1.3 Hz, 2H), 4.90 – 4.88 (dd, *J* = 10.6, 1.3 Hz, 2H), 4.61 – 4.56 (m, 2H), 4.35 – 4.29 (m, 2H),

2.86 (s, 2H), 2.53 – 2.47 (m, 2H), 1.64 – 1.58 (m, 2H); ^{13}C NMR (151 MHz, $CDCl_3$) δ 155.34, 144.85, 132.55, 128.28, 127.44, 121.71, 113.41, 110.39, 76.86, 68.85, 36.39; HRMS (ESI) calculated for $C_{22}H_{24}O_4Na$ ([M + Na]$^+$) *m/z* 375.1573, found 375.1613.

Cyclohex-2-ene-1,4-diol **20.14:** ^{1}H NMR (600 MHz, $CDCl_3$) δ 7.83 – 7.80 (dd, *J* = 7.9, 1.8 Hz, 2H), 7.33 – 7.26 (m, 2H), 7.16 – 7.06 (m, 2H), 7.00 – 6.98 (dd, *J* = 8.1, 1.3 Hz, 2H), 5.90 (s, 2H), 4.42 – 4.21 (m, 4H), 2.58 – 2.48 (m, 2H), 2.39 (s, 2H), 2.17 – 2.03 (m, 2H); ^{13}C NMR (151 MHz, $CDCl_3$) δ 156.35, 137.33, 132.48, 128.54, 127.69, 122.55, 117.18, 71.28, 70.13, 35.76; HRMS (ESI) calculated for $C_{20}H_{20}O_4Na$ ([M + Na]$^+$) *m/z* 347.1260, found 347.1449.

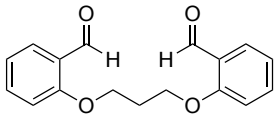

20.3

Dialdehyde **20.3:** Salicylaldehyde (1.3 mL, 12 mmol) was added to a stirred solution of 1,3-dibromopropane (0.65 mL, 6.4 mmol) and potassium carbonate (2.6 g, 19 mmol) in DMF (20 mL). The reaction was heated to 80 °C for 15 minutes and then heated to 110 °C. After 24 h, the reaction was cooled to room temperature and poured into water (70 mL). The resulting mixture was extracted with ethyl acetate (3 × 30 mL). The organic extracts were combined, washed with 1 M HCl (20 mL) and brine (20 mL), dried over $MgSO_4$, filtered, and concentrated under reduced pressure. The residue was purified by flash chromatography (18 × 5.0 cm; 20% to 30% ethyl acetate/hexane) to afford **20.3** as a white solid (1.1 g, 60%). R_f = 0.25 (20% ethyl acetate/hexane); ^{1}H NMR (400 MHz, $CDCl_3$) δ 10.50 (d, *J* = 0.8 Hz, 2H), 7.84 (dd, *J* = 7.7, 1.9 Hz, 2H), 7.56 (ddd, *J* = 8.4, 7.3, 1.9 Hz, 2H), 7.10 – 6.99 (m, 4H), 4.34 (t, *J* = 6.0 Hz, 4H), 2.44 (p, *J* = 6.0 Hz, 2H); ^{13}C NMR (101 MHz, $CDCl_3$) δ 189.46, 160.94, 136.07, 128.69, 124.84, 120.98, 112.39, 64.60, 29.10; HRMS (ESI) calculated for $C_{17}H_{16}O_4Na$ ([M + Na]$^+$) *m/z* 307.0947, found 307.0909.

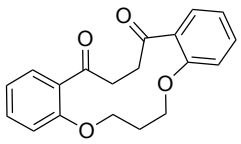

20.6

1,4-diketone **20.6:** Vinylmagnesium chloride (1.6 M in THF, 7.5 mL, 12 mmol) was added to a stirred solution of dialdehyde **20.3** (1.1 g, 3.7 mmol) in dichloromethane (30 mL). After 1 h, the reaction was poured into water (10 mL) and further diluted with 1 M HCl (10 mL). The resulting mixture was extracted with dichloromethane (3 × 30 mL). The combined organic extracts were washed with a saturated solution of $NaHCO_3$ (20 mL) and water (20 mL), dried over $MgSO_4$, filtered, and concentrated under reduced pressure. The pale yellow residue was dissolved in dichloromethane (440 mL), stirred at room temperature, followed by the addition of the Hoveyda-Grubbs second-generation catalyst (0.12 g, 0.20 mmol). After 17 h, the reaction was concentrated under reduced pressure to afford **S-2**. The dark brown residue was dissolved in 1:9 methanol/dichloromethane (30 mL), and sodium borohydride (0.46 g, 12 mmol) was added. After 4.5 h, the reaction was poured into water (20 mL) and further diluted with 1 M HCl (20 mL). The layers were

separated, and the aqueous phase extracted with dichloromethane (2 × 20 mL). The combined organic extracts were washed with water (20 mL), dried over $MgSO_4$, filtered, and concentrated under reduced pressure. The dark brown residue was then dissolved in dichloromethane (32 mL), stirred at room temperature, pyridinium chlorochromate (1.8 g, 8.4 mmol) was added. After 15 h, silica gel was added and the resulting slurry was filtered through a 2.5 cm Celite pad, which was washed with dichloromethane (5 × 10 mL) and diethyl ether (5 × 10 mL). The mother liquor was concentrated under reduced pressure to afford a brown residue, which was purified by flash chromatography (18 × 2.5 cm; 40% ethyl acetate/hexane) to give diketone **20.6** as an off-white solid (0.30 g, 36% over 4 steps): R_f = 0.22 (30% ethyl acetate/hexane); ^{1}H NMR (600 MHz, $CDCl_3$) δ 7.67 – 7.65 (dd, *J* = 7.7, 1.9 Hz, 2H), 7.48 – 7.45 (ddd, *J* = 8.8, 7.3, 1.9 Hz, 2H), 7.02 – 6.95 (m, 2H), 6.96 – 6.95 (d, *J* = 8.4 Hz, 2H), 4.32 – 4.30 (m, 4H), 3.25 (s, 4H), 2.45 – 2.42 (m, 2H); ^{13}C NMR (151 MHz, $CDCl_3$) δ 202.75, 157.54, 133.67, 130.66, 128.33, 120.87, 111.26, 68.56, 40.00, 29.13; HRMS (ESI) calculated for $C_{19}H_{18}O_4Na$ ([M + Na]$^+$) *m/z* 333.1103, found 333.1115.

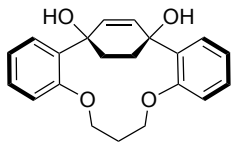

20.15

***Cyclohex-2-ene-1,4-diol* 20.15:** Vinylmagnesium chloride (1.6 M in THF, 0.54 mL, 0.86 mmol) was added to a stirred solution of 1,4-diketone **20.6** (0.054 g, 0.17 mmol) in dichloromethane (1.6 mL) at room temperature. After 40 min., the reaction was poured into water (5 mL) and further diluted with 1 M HCl (5 mL). The resulting mixture was extracted with dichloromethane (3 × 5 mL). The combined organic extracts were washed with a saturated solution of $NaHCO_3$ (10 mL) and water (10 mL), dried over $MgSO_4$, filtered, and concentrated under reduced pressure. The pale yellow residue was dissolved in dichloromethane (4.4 mL), heated to 40 °C, and Grubbs second-generation catalyst (0.0076 g, 0.0090 mmol) was added. After 45 min., the solvent was removed under reduced pressure, and the residue was purified by flash chromatography (18 × 1.3 cm; 5% acetone/dichloromethane). The cyclohexene (formed from the *syn*-diastereomer), *anti*-allylic diol, and hydroxyketone were combined for ^{1}H NMR analysis of the diastereoselectivity.

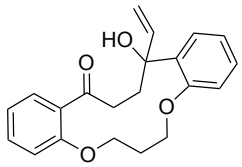

20.12

***Hydroxyketone* 20.12**: ^{1}H NMR (400 MHz, $CDCl_3$) δ 7.73 (dd, *J* = 7.7, 1.8 Hz, 1H), 7.52 (dd, *J* = 7.8, 1.8 Hz, 1H), 7.44 (ddd, *J* = 8.7, 7.3, 1.9 Hz, 1H), 7.23 (m, 1H), 7.07 – 6.91 (m, 3H), 6.86 (d, *J* = 8.2 Hz, 1H), 6.37 (dd, *J* = 17.3, 10.7 Hz, 1H), 5.41 (dd, *J* = 17.4, 1.3 Hz, 1H), 5.16 (dd, *J* = 10.7, 1.3 Hz, 1H), 4.39 – 4.33 (m, 2H), 4.26 (t, *J* = 5.1 Hz, 2H), 3.27 (s, 1H), 3.07 – 2.94 (m, 2H), 2.85 – 2.71 (m, 1H), 2.44 (dt, *J* = 8.9, 4.2 Hz, 2H), 2.12 – 1.98 (m, 1H); ^{13}C NMR (126 MHz, $CDCl_3$) δ 203.58, 158.06, 154.99, 143.43, 133.58, 132.04, 130.84, 128.35, 128.34, 127.98, 120.90, 120.77, 112.39, 111.37, 110.70, 76.70, 68.92, 67.50, 39.78, 37.41, 28.79; HRMS (ESI) calculated for $C_{21}H_{22}O_4Na$ ([M + Na]$^+$) *m/z* 361.1416, found 361.1431.

***Cyclohex-2-ene-1,4-diol* 20.15**: ^{1}H NMR (600 MHz, $CDCl_3$) δ 7.82 (d, *J* = 7.8 Hz, 2H), 7.26 – 7.18 (m, 2H), 7.04 – 6.96 (m, 2H), 6.81 (d, *J* = 8.2 Hz, 2H), 5.99 (s, 2H), 4.22 (dt, *J* = 8.2, 3.4 Hz, 2H), 4.01 (t, *J* = 10.2 Hz, 2H), 2.54 (s, 2H), 2.40 (q, *J* = 11.3, 2.8 Hz, 1H), 2.26 (td, *J* = 13.2, 11.5, 4.6 Hz, 2H), 2.10 – 1.99 (m, 3H); ^{13}C NMR (151 MHz, $CDCl_3$) δ 155.48, 134.73, 132.34, 128.34, 127.89, 120.49, 110.46, 71.38, 67.57, 36.37, 29.03; HRMS (ESI) calculated for $C_{21}H_{22}O_4Na$ ([M + Na]$^+$) *m/z* 361.1416, found 361.1420.

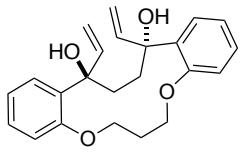

20.9

***Anti-allylic diol* 20.9**: ^{1}H NMR (600 MHz, $CDCl_3$) δ 7.58 (dd, *J* = 7.8, 1.8 Hz, 2H), 7.24 (td, *J* = 7.8, 1.8 Hz, 2H), 6.99 – 6.93 (m, 2H), 6.86 (d, *J* = 8.2 Hz, 2H), 6.26 (dd, *J* = 17.3, 10.6 Hz, 2H), 5.18 (d, *J* = 17.2 Hz, 2H), 4.94 (d, *J* = 10.6 Hz, 2H), 4.42 (dt, *J* = 9.2, 4.6 Hz, 2H), 4.23 (dt, *J* = 10.4, 4.8 Hz, 2H), 2.88 – 2.82 (m, 2H), 2.42 – 2.33 (m, 2H), 2.29 – 2.23 (m, 2H), 1.74 – 1.64 (m, 2H); ^{13}C NMR (151 MHz, $CDCl_3$) δ 154.42, 144.32, 132.28, 128.09, 127.55, 120.64, 110.90, 110.18, 68.22, 35.89, 27.97; HRMS (ESI) calculated for $C_{23}H_{26}O_4Na$ ([M + Na]$^+$) *m/z* 389.1729, found 389.1738.

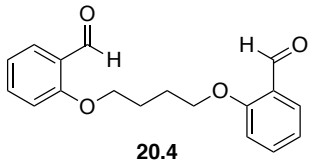

20.4

***Dialdehyde* 20.4:** Salicylaldehyde (0.85 mL, 8.1 mmol) was added to a stirred solution of 1,4-dibromobutane (0.44 mL, 4.1 mmol) and potassium carbonate (1.7 g, 19 mmol) in DMF (6.8 mL). The reaction was heated to 80°C for 15 minutes and then heated to 110°C. After 15 h, the reaction was cooled to room temperature and poured into water (115 mL). The resulting mixture was extracted with ethyl acetate (3 × 75 mL). The organic extracts were combined, washed with 1 M HCl (50 mL), dried over $MgSO_4$, filtered, and concentrated under reduced pressure. The residue was purified by flash chromatography (18 × 3.8 cm; 20% to 30% ethyl acetate/hexane) to afford dialdehyde **20.4** as a yellowish oil (0.92 g, 76%). R_f = 0.31 (20% ethyl acetate/hexane); ^{1}H NMR (400 MHz,$CDCl_3$) δ 10.50 (s, 2H), 7.84 – 7.83 (d, *J* = 7.7 Hz, 2H), 7.57 – 7.53 (m, 2H), 7.06 – 6.98 (m, 4H), 4.20 (s, 4H), 2.11 (s, 4H); ^{13}C NMR (101 MHz, $CDCl_3$) δ 189.58, 161.15, 136.00, 128.53, 124.85, 120.78, 112.36, 67.84, 25.94; HRMS (ESI) calculated for $C_{18}H_{18}O_4Na$ ([M + Na]$^+$) *m/z* 321.1103, found 321.1241.

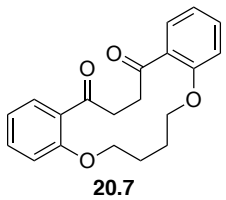

20.7

1,4-diketone* 20.7*: Vinylmagnesium chloride (1.6 M in THF, 3.4 mL, 5.4 mmol) was added to a stirred mixture of dialdehyde **20.4** (0.44 g, 1.5 mmol) in dichloromethane (18 mL). After 45 min., the reaction was poured into water (100 mL) and further diluted with 1 M HCl (50 mL). The resulting mixture was extracted with dichloromethane (3 × 20 mL). The combined organic extracts were dried over $MgSO_4$, filtered, and concentrated under reduced pressure. The pale yellow residue was dissolved in

dichloromethane (107 mL), stirred at room temperature, followed by the addition of the Grubbs second-generation catalyst (0.039 g, 0.046 mmol). The reaction was heated to 40 °C for 1.5 h, after which the reaction was concentrated under reduced pressure to afford **S-3**. The dark brown residue was dissolved in 1:9 methanol/dichloromethane (16 mL), and sodium borohydride (0.28 g, 7.5 mmol) was added. After 16 h, the reaction was poured into water (75 mL) and further diluted with 1 M HCl (20 mL). The layers were separated, and the aqueous phase was extracted with dichloromethane (3 × 30 mL). The combined organic extracts were washed with water (50 mL), dried over $MgSO_4$, filtered, and concentrated under reduced pressure. The dark brown residue was dissolved in dichloromethane (15 mL), stirred at room temperature, and pyridinium chlorochromate (0.83 g, 3.9 mmol) was added. After 27 h, silica gel was added and the resulting slurry was filtered through a 2.5 cm Celite pad, which was washed with dichloromethane (5 × 20 mL) and diethyl ether (5 × 20 mL). The mother liquor was concentrated under reduced pressure to afford a brown residue, which was purified by flash chromatography (18 × 1.0 cm; 20% ethyl acetate/hexane) to give diketone **20.7** as an off-white solid (0.30, 62% over 4 steps): R_f = 0.11 (20% ethyl acetate/hexane); ^{1}H NMR (400 MHz,) δ 7.52 – 7.50 (dd, *J* = 7.6, 1.8 Hz, 2H), 7.45 – 7.41 (m, 2H), 7.02 – 6.99 (m, 2H), 6.92 – 6.90 (d, *J* = 8.3 Hz, 2H), 4.11 (s, 3H), 3.43 (s, 4H), 2.10 – 2.08 (m, 4H); ^{13}C NMR (101 MHz, $CDCl_3$) δ 204.93, 157.49, 132.95, 130.17, 129.66, 120.78, 111.86, 67.52, 38.31, 25.99; HRMS (ESI) calculated for $C_{20}H_{21}O_4$ ([M + H]$^+$) *m/z* 325.1441, found 325.1485.

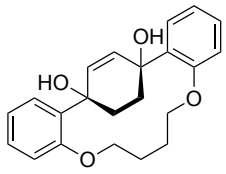

20.16

Cyclohex-2-ene-1,4-diol* 20.16*: Vinylmagnesium chloride (1.6 M in THF, 0.50 mL, 0.80 mmol) was added to a stirred mixture of 1,4-diketone **20.7** (0.047 g, 0.15 mmol) in dichloromethane (2.0 mL) at room temperature. After 40 min., the reaction was poured into water (5 mL) and further diluted with 1 M HCl (5 mL). The resulting mixture was extracted with dichloromethane (3 × 5 mL). The combined organic extracts were washed with a saturated solution of $NaHCO_3$ (10 mL) and water (10 mL), dried over $MgSO_4$, filtered, and concentrated under reduced pressure. The pale yellow residue was dissolved in dichloromethane (5.0 mL), heated to 40°C, and Grubbs second-generation catalyst (0.0092 g, 0.011 mmol) was added. After 2 h, the solvent was removed under reduced pressure, and the residue was purified by flash chromatography (18 × 1.3 cm; 5% acetone/dichloromethane). The cyclohexene (formed from the *syn*-diastereomer), *anti*-allylic diol, and hydroxyketone were combined for ^{1}H NMR analysis of the diastereoselectivity.

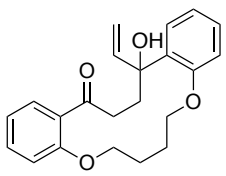

20.13

***Hydroxyketone* 20.13**: ^{1}H NMR (600 MHz, $CDCl_3$) δ 7.51 – 7.50 (dd, *J* = 7.6, 1.9 Hz, 1H), 7.40 – 7.37 (m, 1H), 7.35 – 7.33 (dd, *J* = 7.8, 1.7 Hz, 1H), 7.21 – 7.18 (m, 1H), 6.95 – 6.87 (m, 4H), 6.37 – 6.32 (dd, *J* = 17.3, 10.8 Hz, 1H), 5.50 – 5.47 (dd, *J* = 17.4, 1.5 Hz, 1H), 5.32 – 5.30 (dd, *J* = 10.8, 1.5 Hz, 1H), 4.27 – 4.24 (ddd, *J* = 9.2,

6.2, 2.8 Hz, 1H), 4.21 – 4.15 (m, 3H), 4.04 – 4.00 (td, *J* = 9.2, 1.7 Hz, 1H), 3.28 – 3.23 (td, *J* = 13.1, 12.4, 3.3 Hz, 1H), 2.74 – 2.64 (m, 2H), 2.34 – 2.29 (td, *J* = 13.5, 12.7, 3.5 Hz, 1H), 2.26 – 2.20 (qd, *J* = 9.6, 2.7 Hz, 1H), 2.15 – 2.07 (m, 2H), 2.00 – 1.95 (m, 1H); ^{13}C NMR (151 MHz, $CDCl_3$) δ 205.55, 157.92, 156.22, 141.43, 133.90, 133.08, 130.19, 129.91, 128.49, 127.61, 121.04, 120.70, 114.56, 112.62, 111.98, 67.83, 67.31, 38.21, 36.14, 26.74, 25.92; HRMS (ESI) calculated for $C_{22}H_{24}O_4Na$ ($[M + Na]^+$ *m/z* 375.1572, found 375.1542.

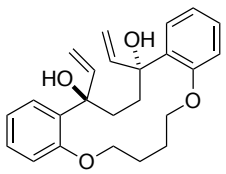

20.10

***Anti-allylic diol* 20.10**: ^{1}H NMR (600 MHz, $CDCl_3$) δ 7.33 – 7.32 (dd, *J* = 7.7, 1.7 Hz, 2H), 7.17 – 7.14 (m, 2H), 6.89 – 6.85 (m, 4H), 6.27 – 6.23 (dd, *J* = 17.3, 10.7 Hz, 2H), 5.37 – 5.34 (dd, *J* = 17.4, 1.5 Hz, 2H), 5.20 – 5.18 (dd, *J* = 10.7, 1.4 Hz, 2H), 4.19 – 4.11 (m, 4H), 3.58 (d, *J* = 3.1 Hz, 2H), 2.42 – 2.36 (m, 2H), 2.18 – 2.06 (m, 4H), 1.81 – 1.75 (m, 2H); ^{13}C NMR (151 MHz, $CDCl_3$) δ 155.92, 142.65, 134.46, 128.18, 127.13, 121.14, 113.27, 112.93, 76.68, 66.76, 35.06, 25.80; HRMS (ESI) calculated for $C_{24}H_{28}O_4Na$ ($[M + Na]^+$) *m/z* 403.1885, found 403.2010.

***Cyclohex-2-ene-1,4-diol* 20.16**: ^{1}H NMR (600 MHz, $CDCl_3$) δ 7.76 – 7.74 (dd, *J* = 7.7, 1.8 Hz, 2H), 7.30 – 7.27 (m, 2H), 7.04 – 7.01 (m, 2H), 6.86 – 6.85 (d, *J* = 6.0 Hz, 2H), 5.99 (s, 2H), 4.07 – 3.98 (m, 4H), 2.76 – 2.69 (m, 2H), 2.45 (s, 2H), 2.18 – 2.09 (m, 4H), 2.00 – 1.95 (m, 2H); ^{13}C NMR (151 MHz, $CDCl_3$) δ 155.46, 136.41, 135.27, 128.07, 125.16, 119.97, 110.87, 69.65, 67.32, 34.75, 26.23; HRMS (ESI) calculated for $C_{22}H_{24}O_4Na$ ($[M + Na]^+$) *m/z* 375.1572, found 375.1756.

General procedure for determining diastereoselectivity of Grignard addition to *ortho*-cylophanes:

Vinylmagnesium chloride (1.6 M in THF, 5.0 equiv.) was added to a stirred solution of 1,4-diketone (1.0 equiv.) in the indicated solvent (0.1 M). Once all of the starting material was consumed based on TLC analysis, the reaction was poured into water and diluted with 1 M HCl. The resulting mixture was extracted with dichloromethane (3 ×). The combined organic extracts were washed with a saturated solution of $NaHCO_3$ and water, dried over $MgSO_4$, filtered, and concentrated under reduced pressure. The resulting residues were then dissolved in dichloromethane, heated to 40 °C, and subjected to Grubbs second-generation catalyst (5 mol %). Once all of the starting material was consumed based on TLC analysis, the solvent was removed under reduced pressure. The residue was purified by flash chromatography. The mixture of cyclohex-2-ene1,4-diol (formed from *syn*-diastereomer), *anti*-allylic diol, and hydroxyketone were analyzed by ^{1}H NMR to determine the diastereoselectivity and ratio of products formed in the Grignard reaction.

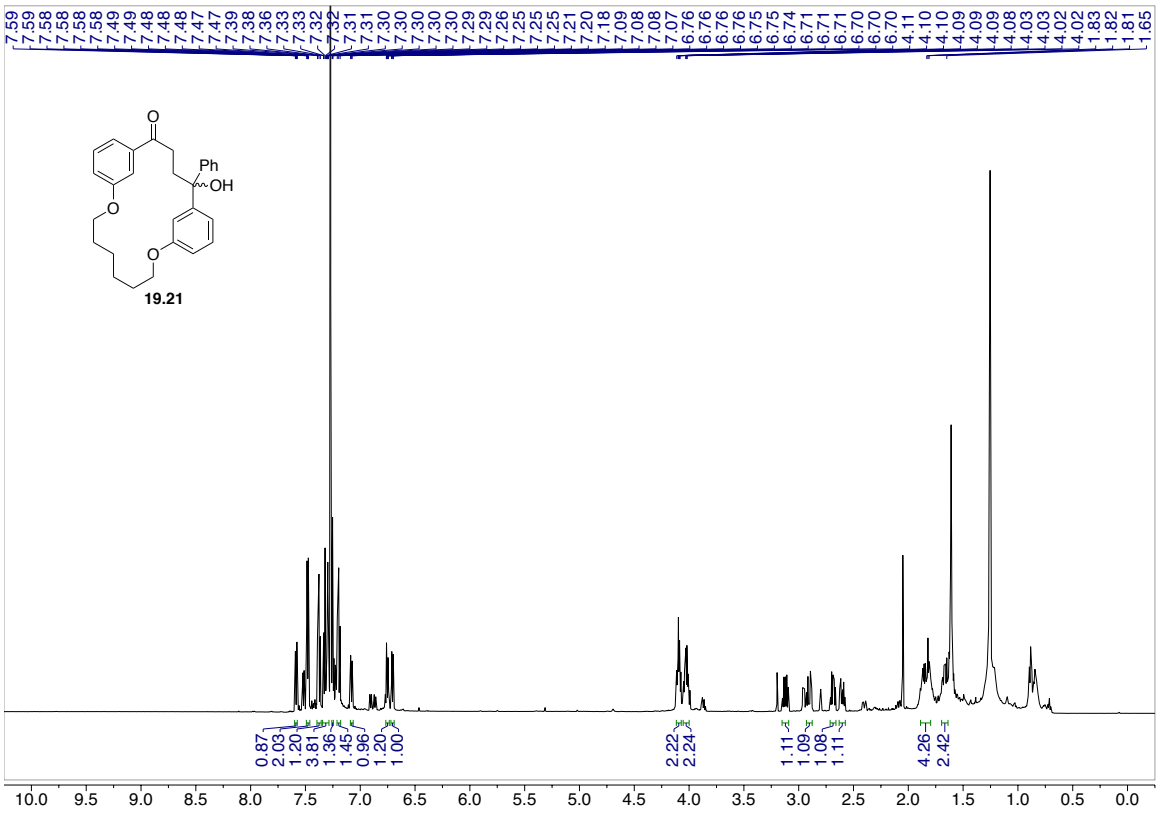
19.21

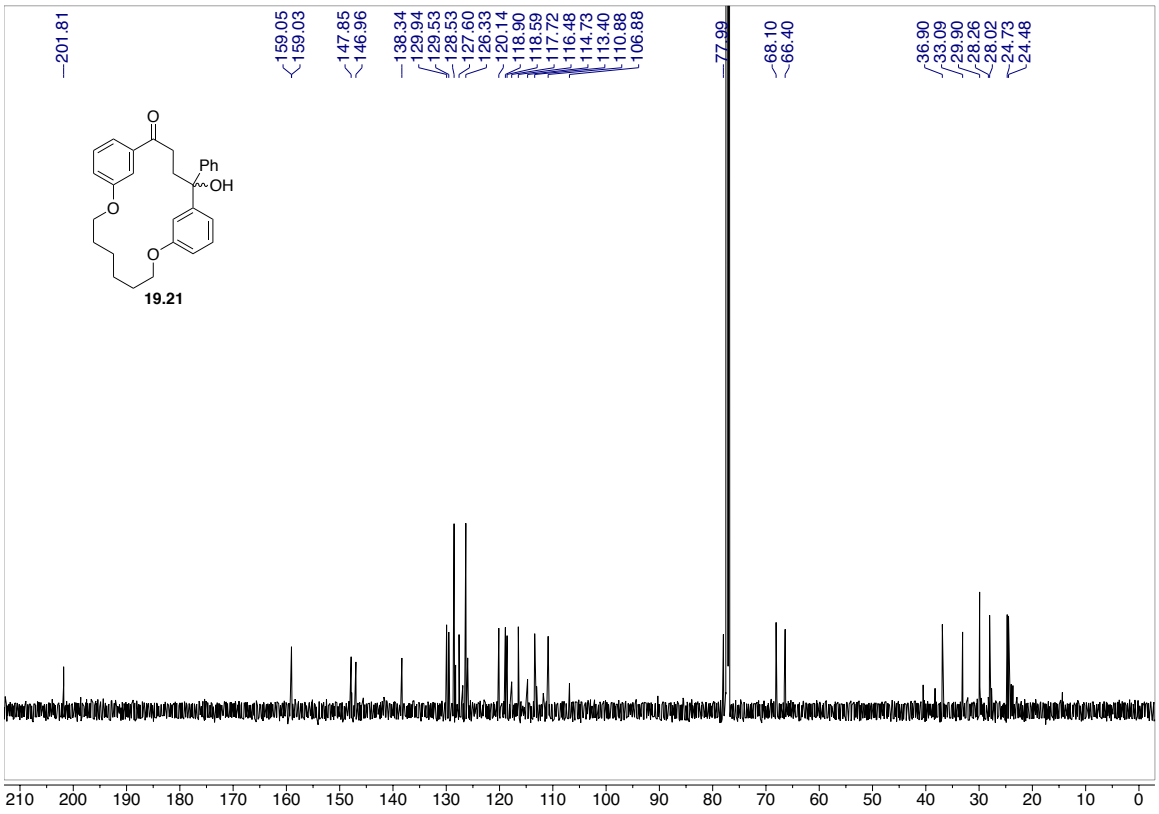
19.21

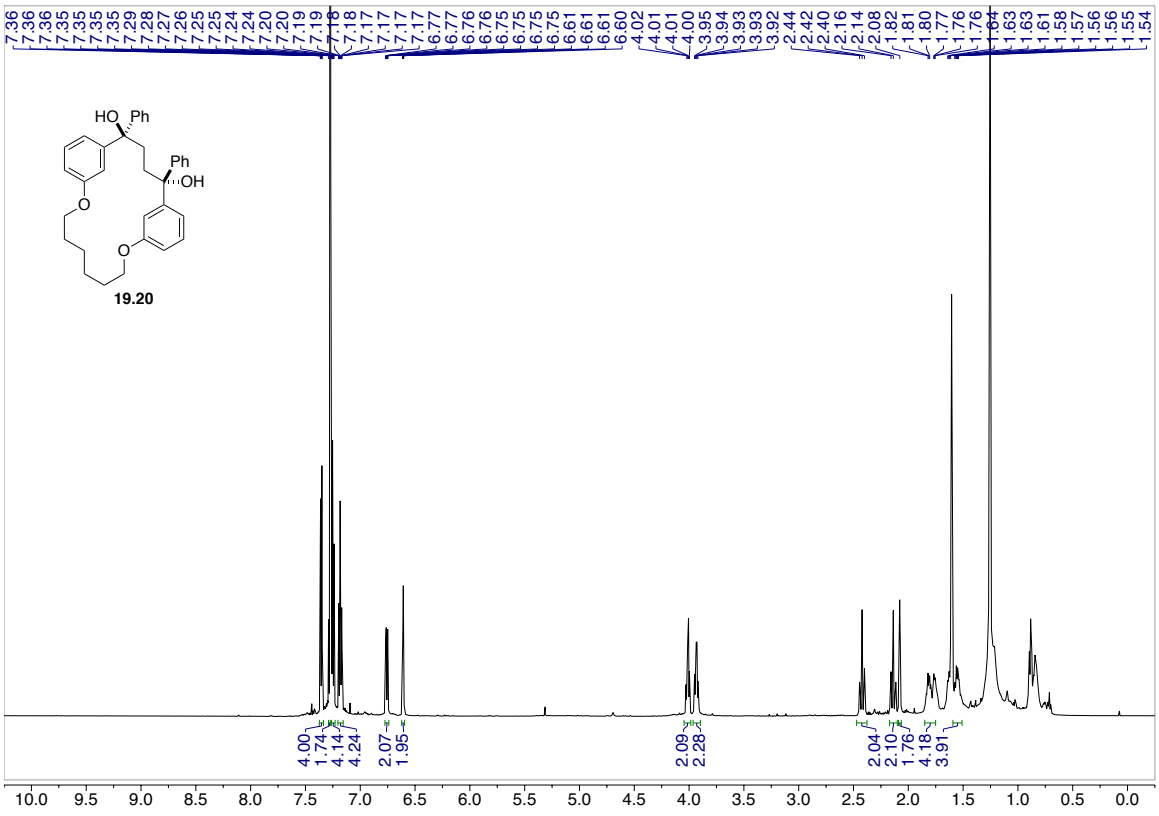
HO
Ph
Ph
OH
O
O
19.20
7.36 7.36 7.36 7.35 7.35 7.35 7.35 7.29 7.28 7.27 7.26 7.25 7.25 7.24 7.24 7.20 7.20 7.19 7.19 7.18 7.18 7.18 7.17 7.17 7.17 7.17 6.77 6.77 6.76 6.76 6.75 6.75 6.75 6.61 6.61 6.60 4.02 4.01 4.01 4.00 3.95 3.94 3.93 3.92 2.44 2.42 2.40 2.16 2.14 2.08 1.82 1.81 1.80 1.77 1.76 1.76 1.64 1.63 1.63 1.61 1.58 1.57 1.56 1.56 1.55 1.54
4.00 1.74 4.14 4.24 2.07 1.95 2.09 2.28 2.04 2.10 1.76 4.18 3.91
10.0 9.5 9.0 8.5 8.0 7.5 7.0 6.5 6.0 5.5 5.0 4.5 4.0 3.5 3.0 2.5 2.0 1.5 1.0 0.5 0.0

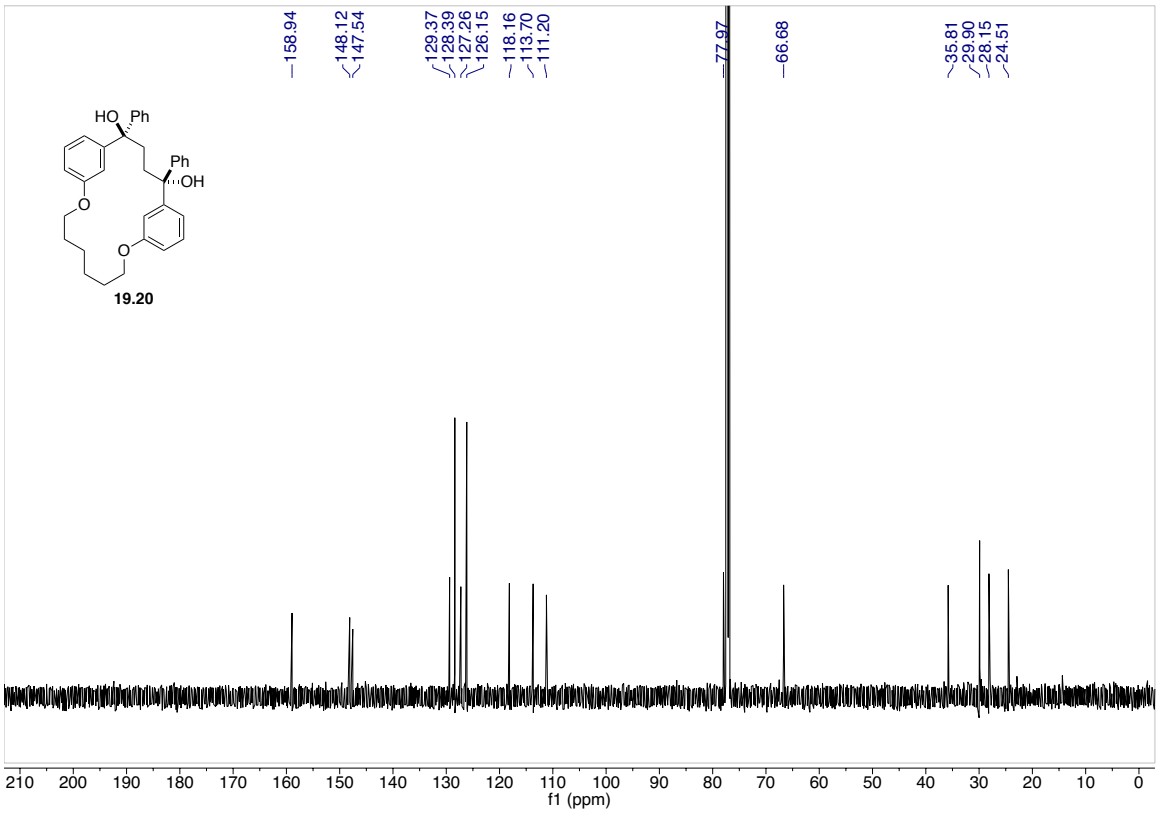
HO
Ph
Ph
OH
O
O
19.20
158.94 148.12 147.54 129.37 128.39 127.26 126.15 118.16 113.70 111.20 77.97 66.68 35.81 29.90 28.15 24.51
210 200 190 180 170 160 150 140 130 120 110 100 90 80 70 60 50 40 30 20 10 0
f1 (ppm)

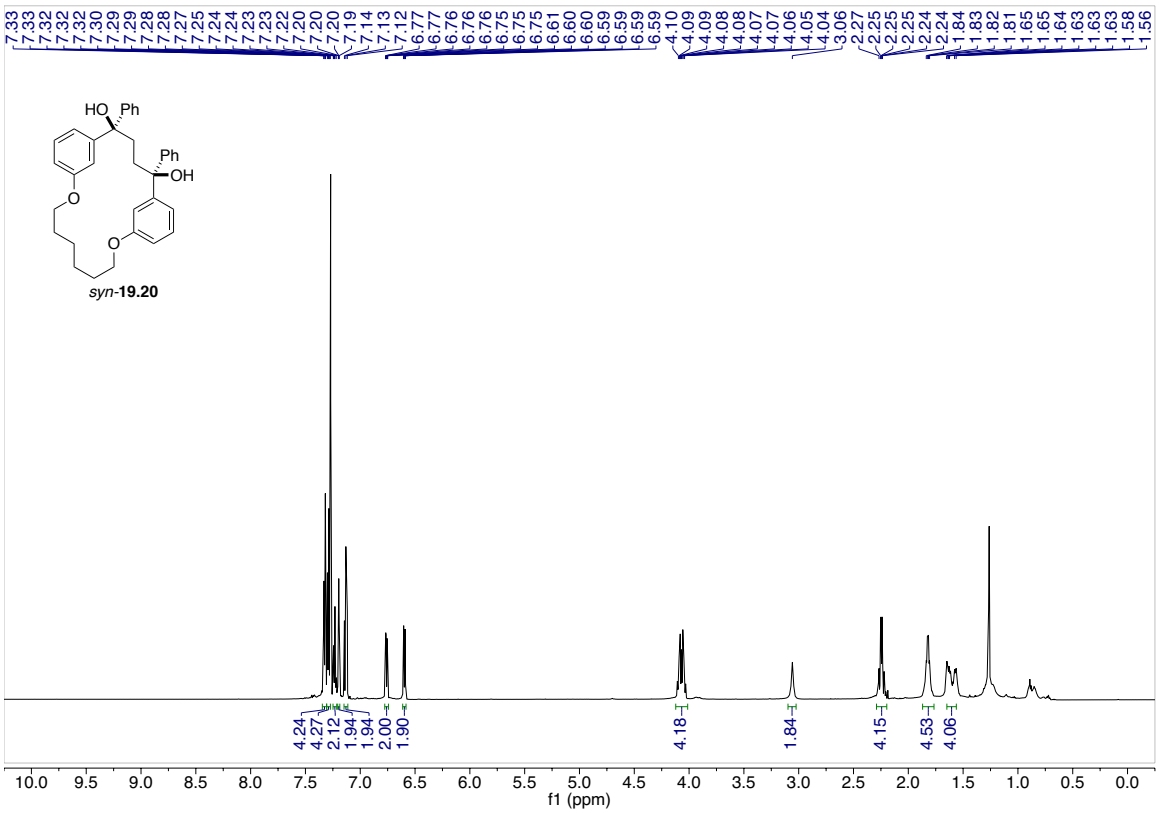
HO
Ph
Ph
OH
O
O
syn-19.20
f1 (ppm)

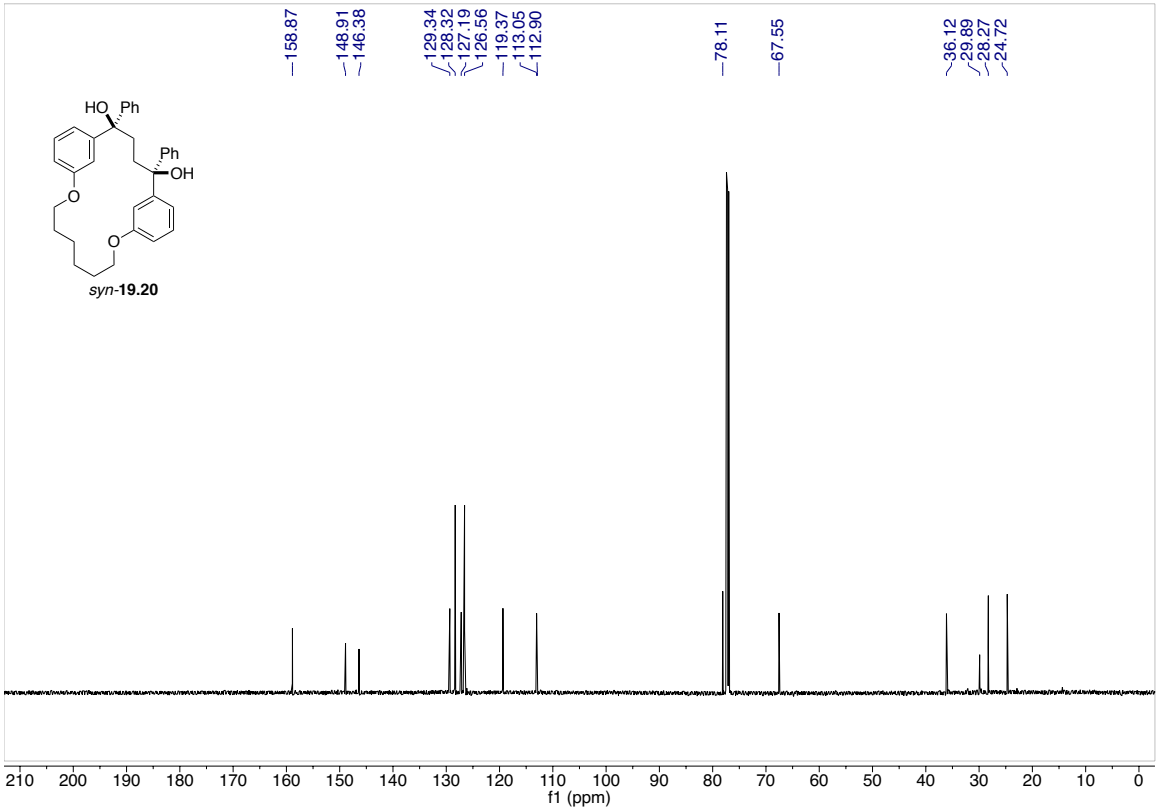
HO
Ph
Ph
OH
O
O
syn-19.20
f1 (ppm)

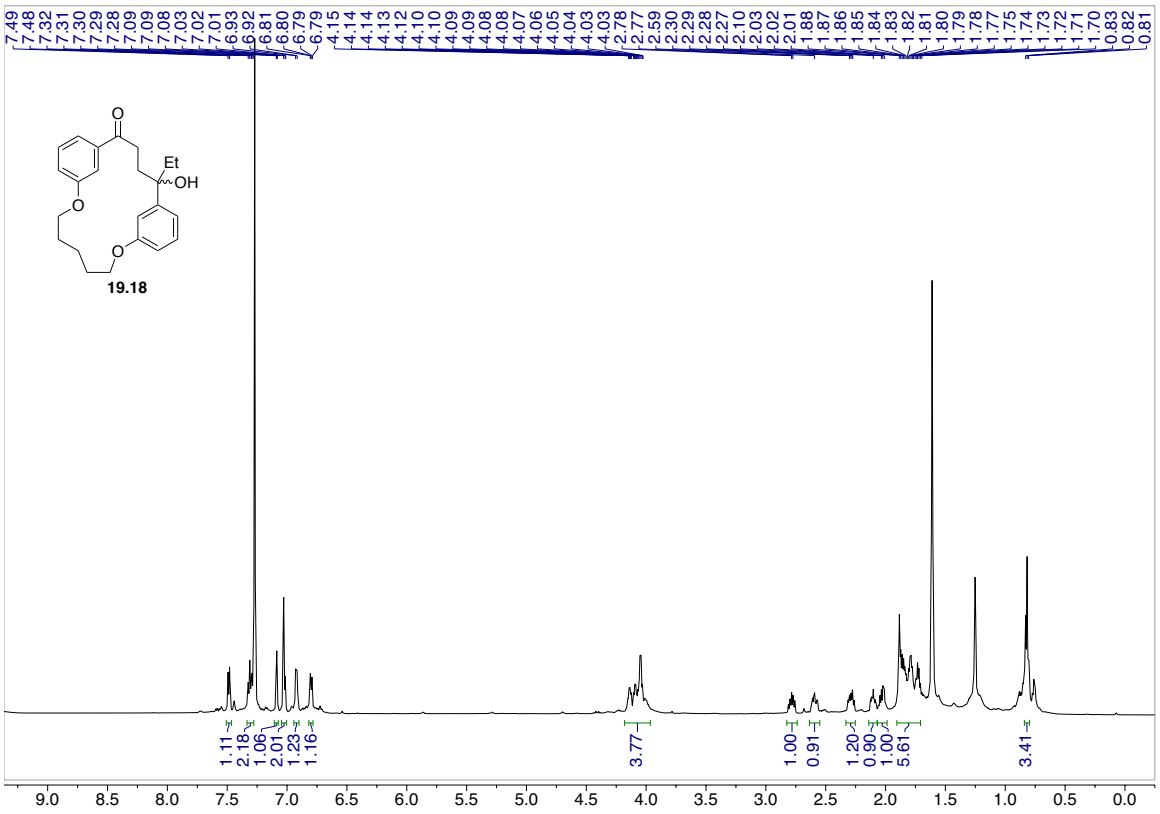
19.18

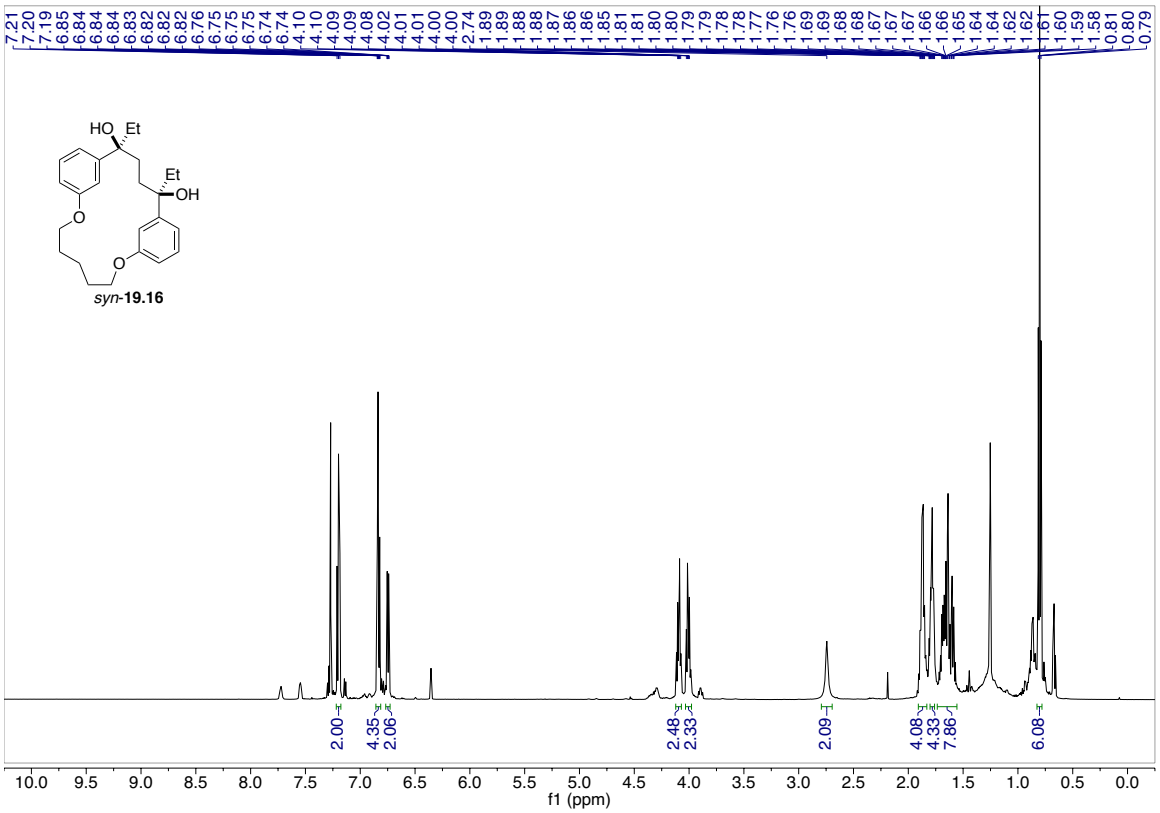
syn-19.16
f1 (ppm)

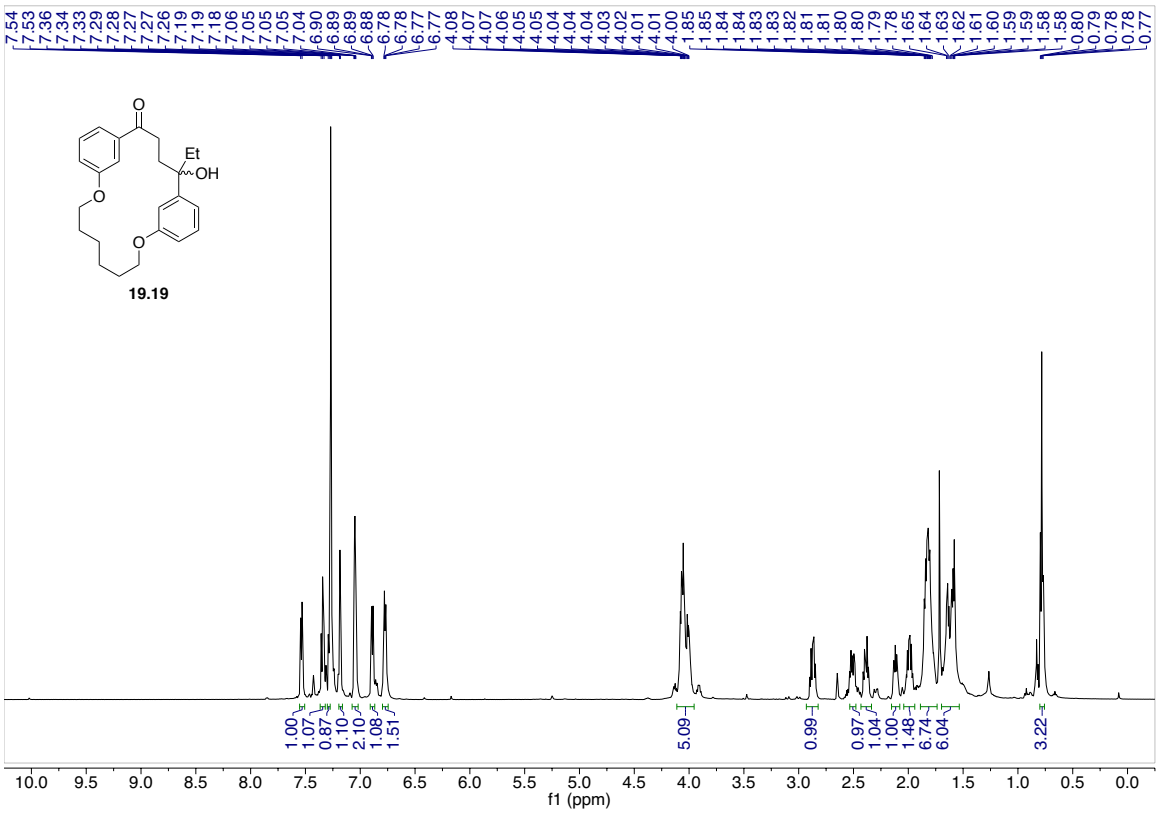
19.19
f1 (ppm)

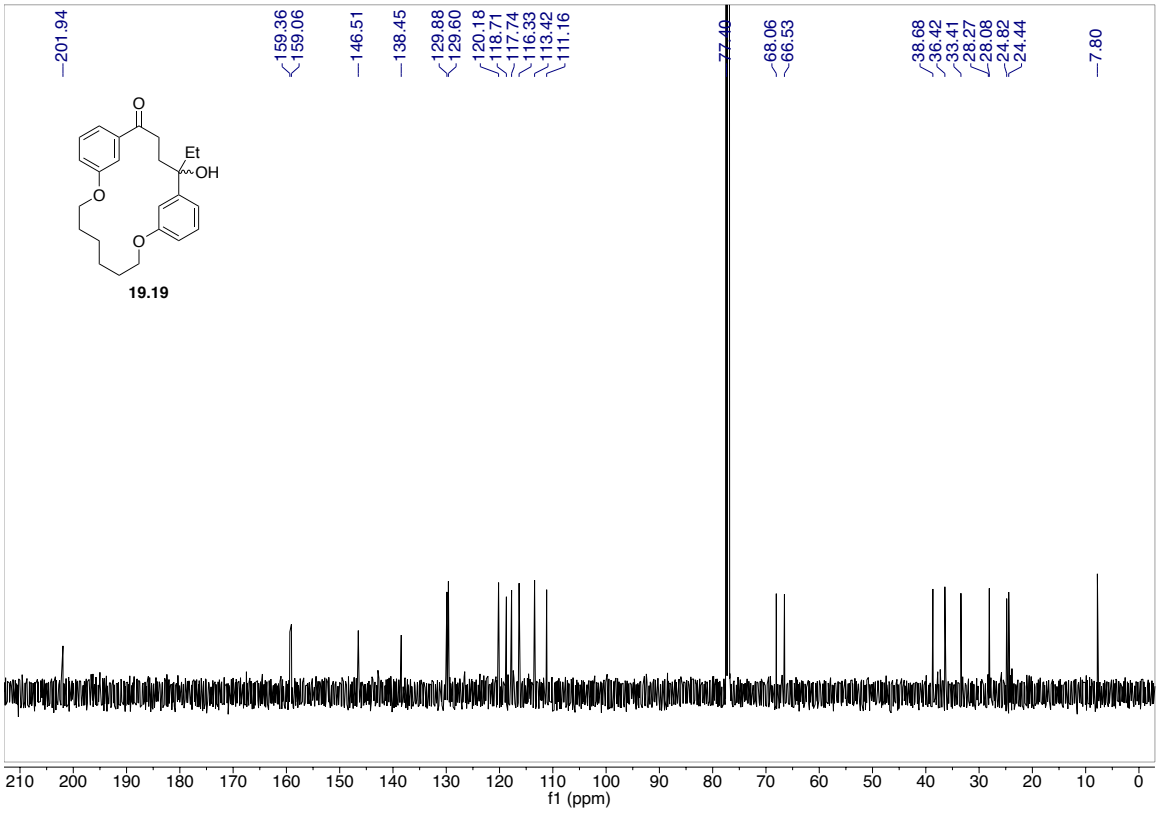
19.19
f1 (ppm)

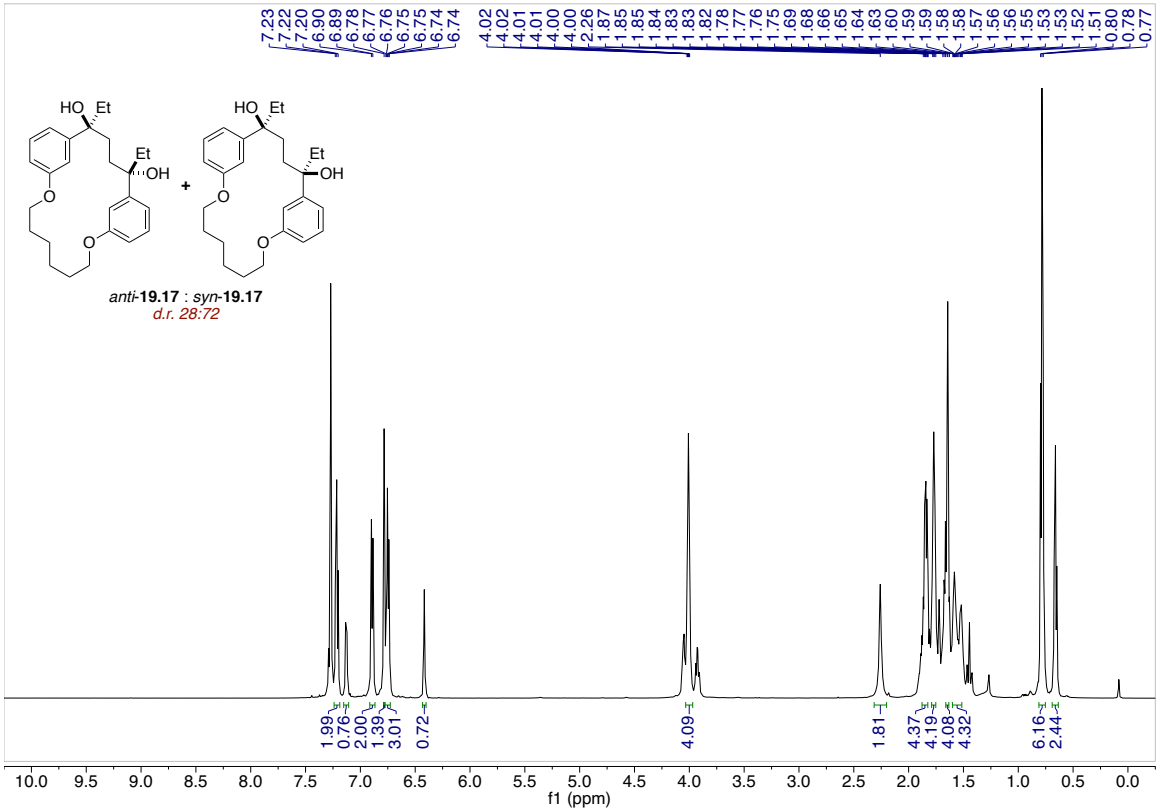
7.23 7.22 7.20 6.90 6.89 6.78 6.77 6.76 6.75 6.75 6.74 6.74
4.02 4.02 4.01 4.01 4.00 4.00 2.26 1.87 1.85 1.85 1.84 1.83 1.83 1.82 1.78 1.77 1.76 1.75 1.69 1.68 1.66 1.65 1.64 1.63 1.60 1.59 1.59 1.58 1.58 1.57 1.56 1.56 1.55 1.53 1.53 1.52 1.51 0.80 0.78 0.77
HO Et
Et
OH
O
O
+
HO Et
Et
OH
O
O
anti-19.17 : syn-19.17
d.r. 28:72
1.99 0.76 2.00 1.39 3.01 0.72 4.09 1.81 4.37 4.19 4.08 4.32 6.16 2.44
10.0 9.5 9.0 8.5 8.0 7.5 7.0 6.5 6.0 5.5 5.0 4.5 4.0 3.5 3.0 2.5 2.0 1.5 1.0 0.5 0.0
f1 (ppm)

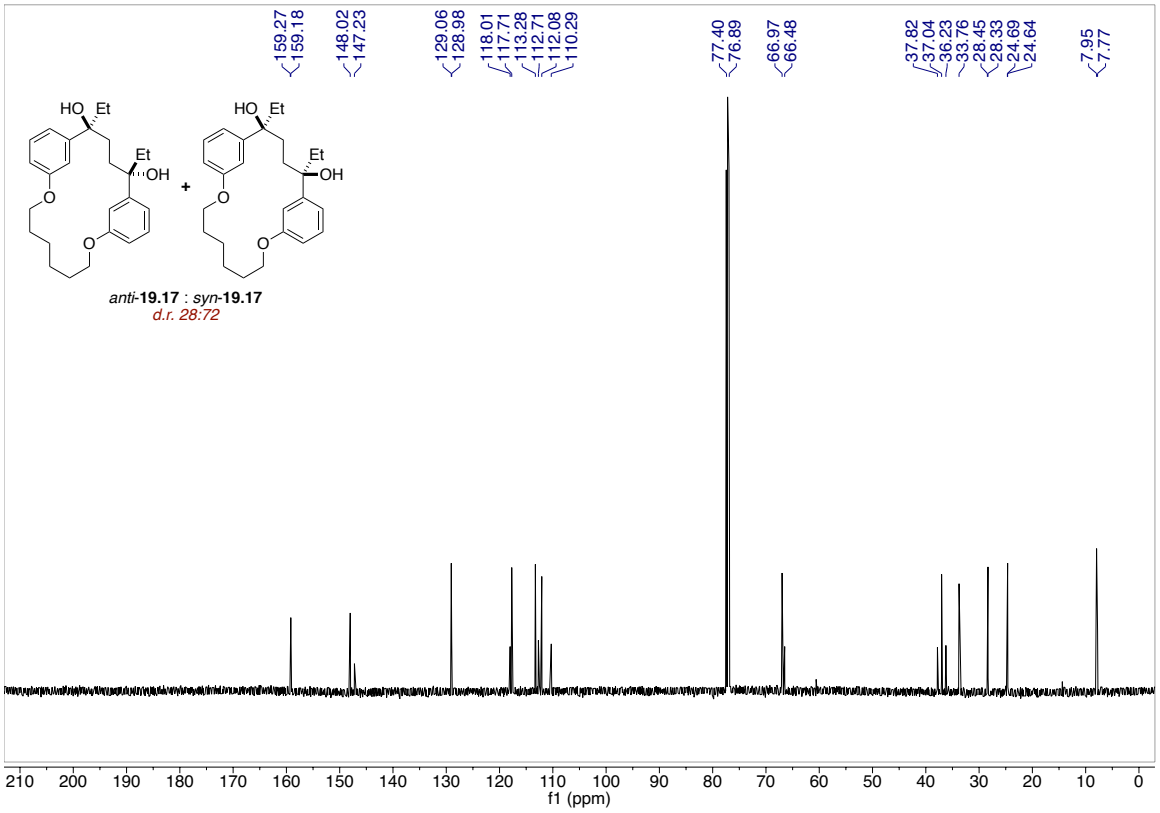
159.27 159.18 148.02 147.23 129.06 128.98 118.01 117.71 113.28 112.71 112.08 110.29 77.40 76.89 66.97 66.48 37.82 37.04 36.23 33.76 28.45 28.33 24.69 24.64 7.95 7.77
HO Et
Et
OH
O
O
+
HO Et
Et
OH
O
O
anti-19.17 : syn-19.17
d.r. 28:72
210 200 190 180 170 160 150 140 130 120 110 100 90 80 70 60 50 40 30 20 10 0
f1 (ppm)

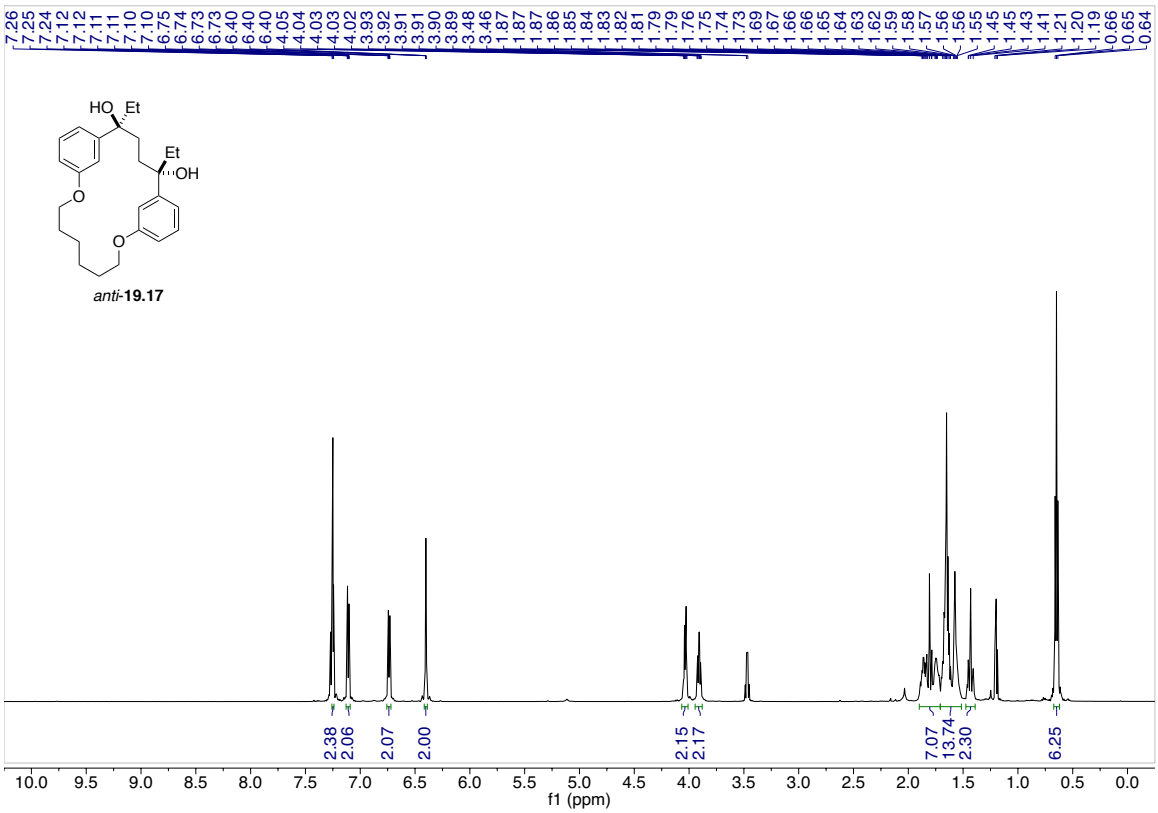
HO
Et
Et
OH
O
O
anti-19.17
7.26 7.25 7.24 7.12 7.11 7.11 7.10 7.10 6.75 6.74 6.73 6.73 6.40 6.40 6.40 4.05 4.04 4.03 4.03 4.02 3.93 3.92 3.91 3.91 3.90 3.89 3.48 3.46 1.87 1.87 1.86 1.85 1.84 1.83 1.82 1.81 1.79 1.79 1.76 1.75 1.74 1.73 1.69 1.67 1.66 1.66 1.65 1.64 1.63 1.62 1.59 1.58 1.57 1.56 1.56 1.55 1.45 1.45 1.43 1.41 1.21 1.20 1.19 0.66 0.65 0.64
2.38 2.06 2.07 2.00 2.15 2.17 7.07 13.74 2.30 6.25
10.0 9.5 9.0 8.5 8.0 7.5 7.0 6.5 6.0 5.5 5.0 4.5 4.0 3.5 3.0 2.5 2.0 1.5 1.0 0.5 0.0
f1 (ppm)

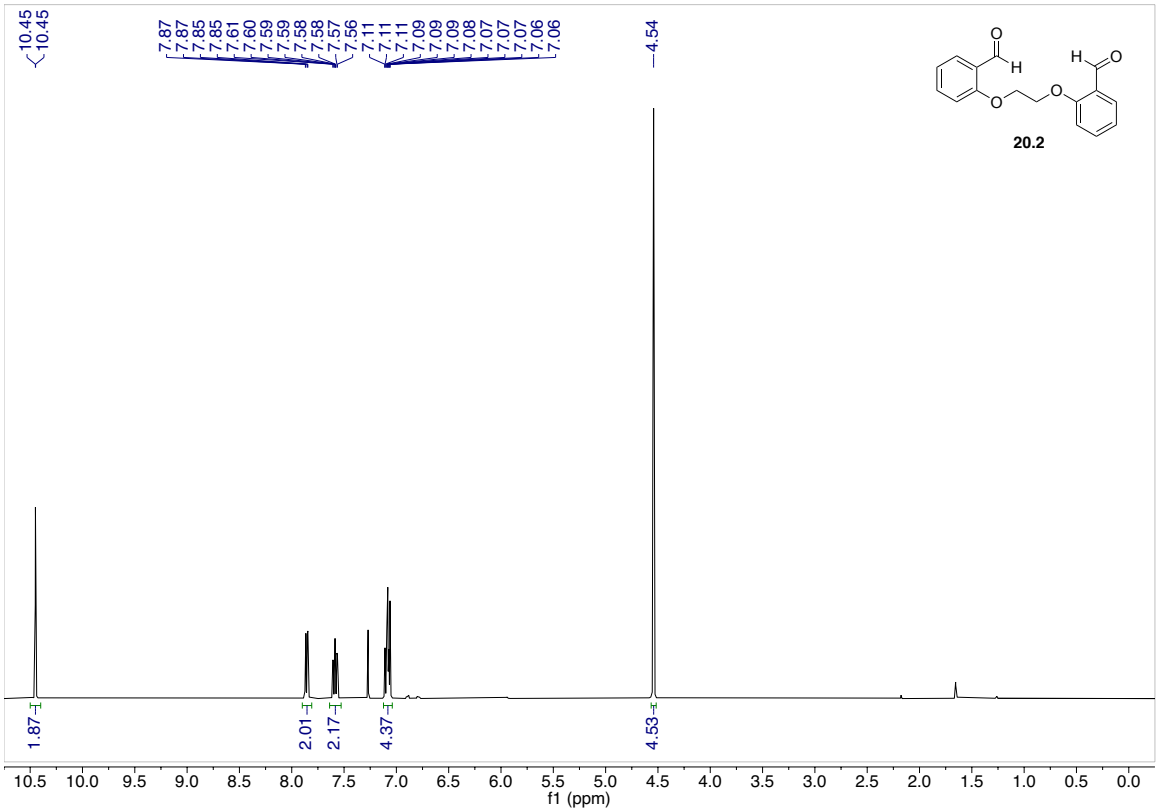
10.45
10.45
7.87
7.87
7.85
7.85
7.61
7.60
7.59
7.59
7.58
7.58
7.57
7.56
7.11
7.11
7.09
7.09
7.09
7.08
7.07
7.07
7.07
7.06
7.06
4.54
1.87
2.01
2.17
4.37
4.53
f1 (ppm)
20.2

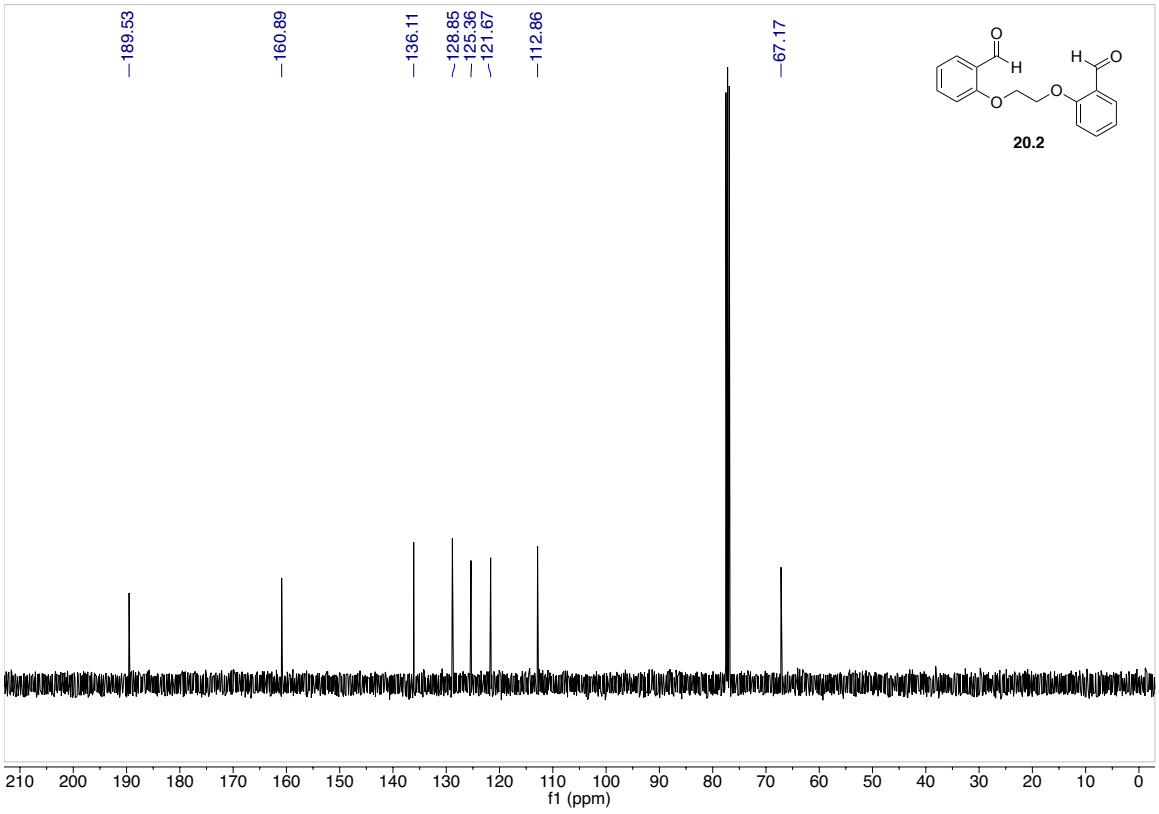
189.53
160.89
136.11
128.85
125.36
121.67
112.86
67.17
f1 (ppm)
20.2

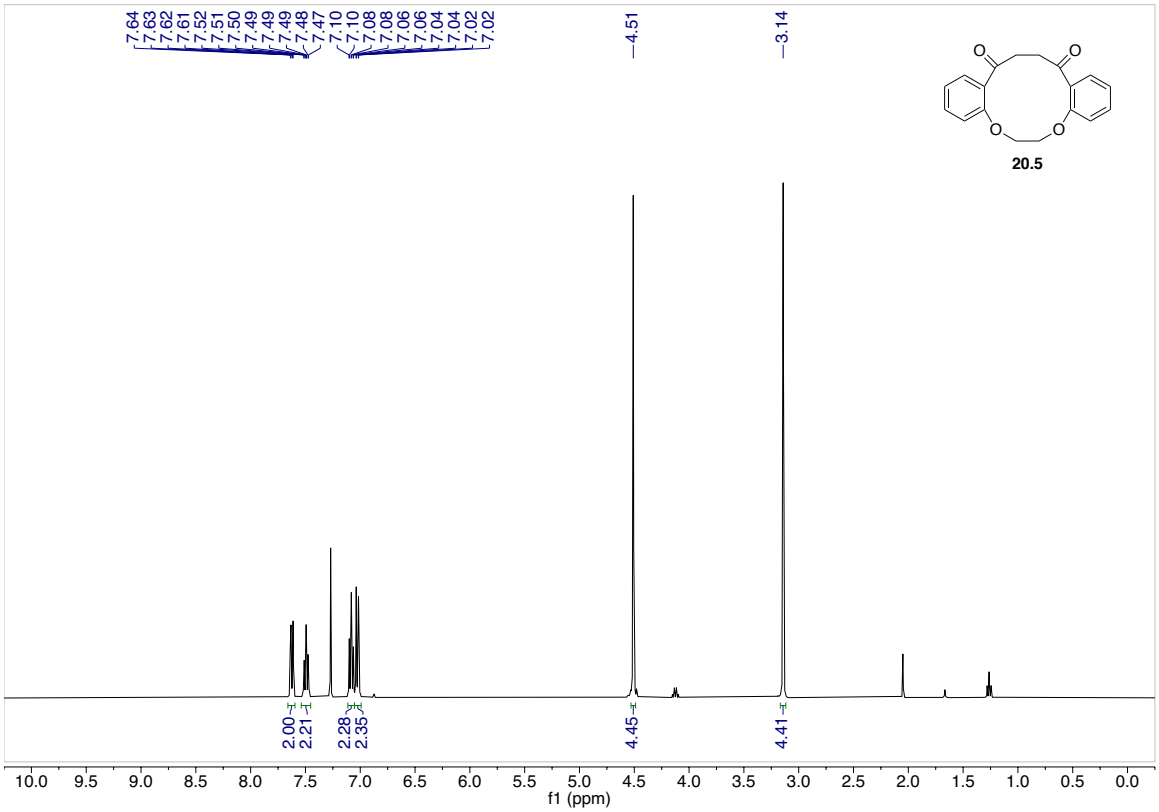
7.64
7.63
7.62
7.61
7.52
7.51
7.50
7.49
7.49
7.49
7.48
7.47
7.10
7.10
7.08
7.08
7.06
7.06
7.04
7.04
7.02
7.02
4.51
3.14
2.00
2.21
2.28
2.35
4.45
4.41
f1 (ppm)

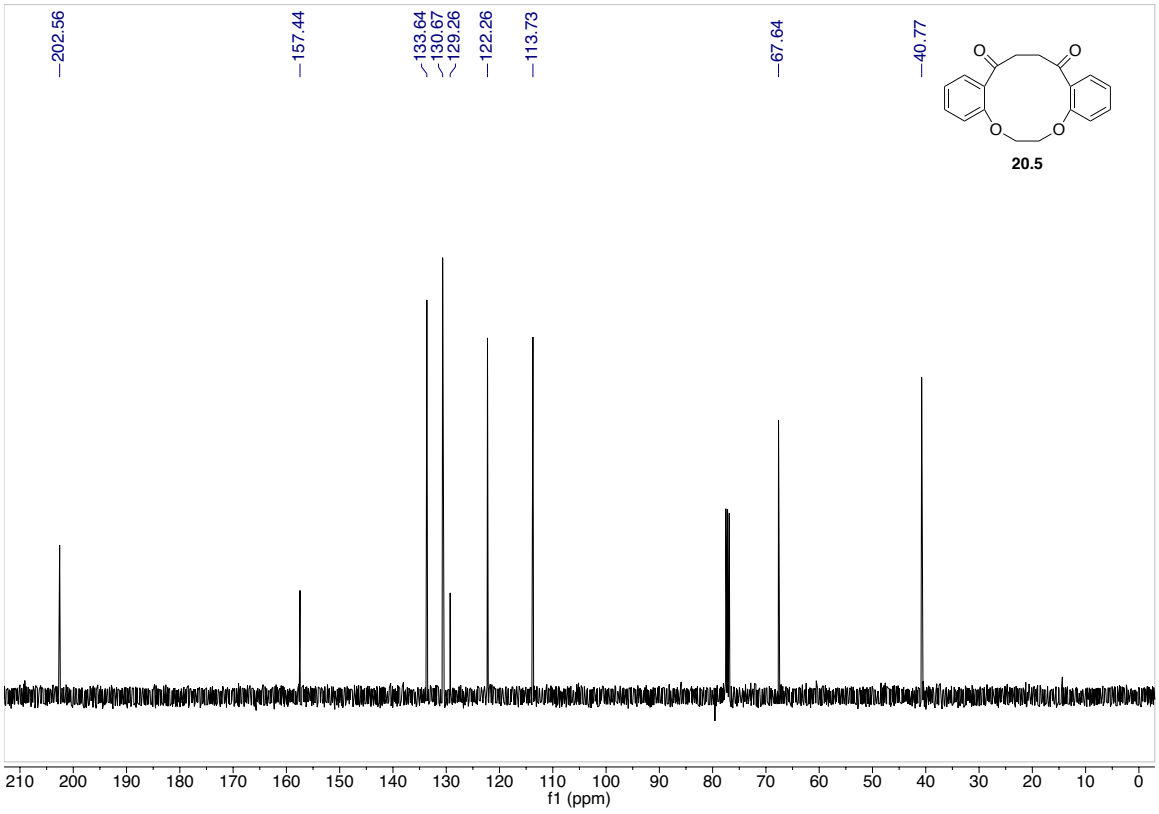
202.56
157.44
133.64
130.67
129.26
122.26
113.73
67.64
40.77
f1 (ppm)

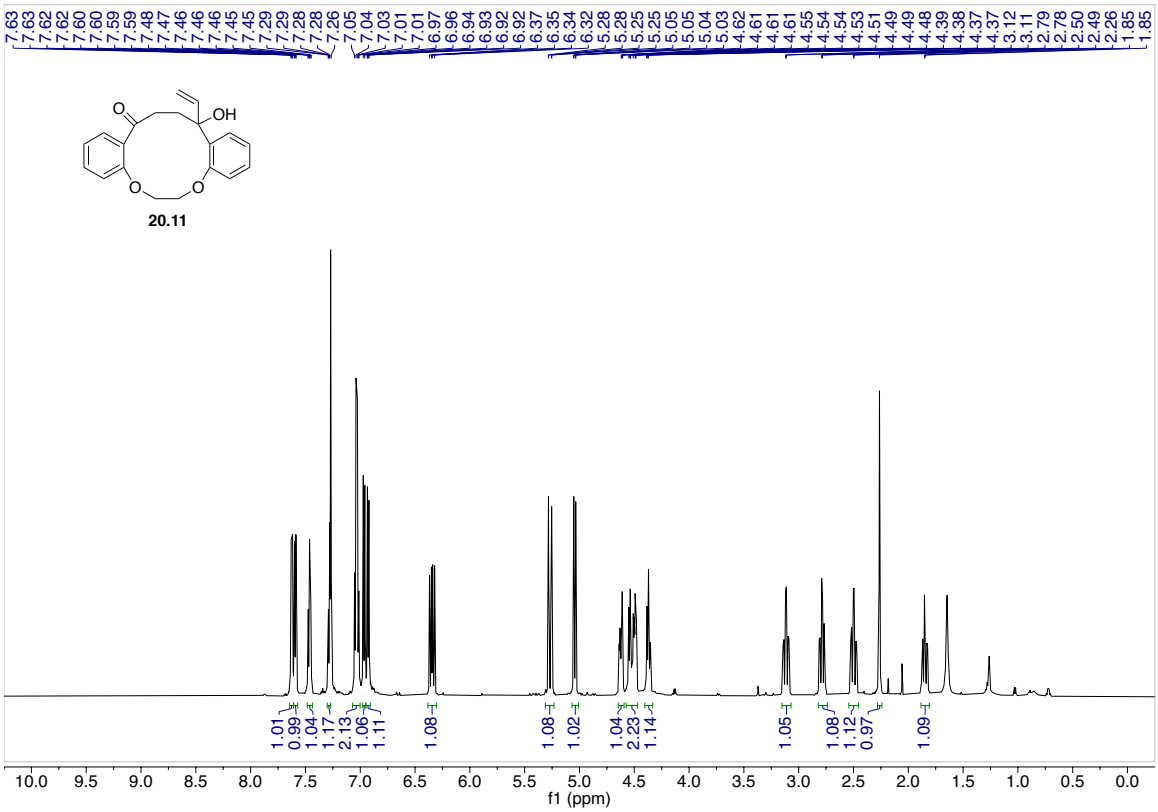
7.63 7.63 7.62 7.62 7.60 7.60 7.59 7.59 7.48 7.47 7.46 7.46 7.46 7.45 7.45 7.29 7.29 7.28 7.28 7.26 7.05 7.04 7.03 7.01 7.01 6.97 6.96 6.94 6.93 6.92 6.92 6.37 6.35 6.34 6.32 5.28 5.28 5.25 5.25 5.05 5.05 5.04 5.03 4.62 4.61 4.61 4.61 4.55 4.54 4.54 4.53 4.51 4.49 4.49 4.48 4.39 4.38 4.37 4.37 3.12 3.11 2.79 2.78 2.50 2.49 2.26 1.85 1.85
O
OH
O
O
20.11
1.01 0.99 1.04 1.17 2.13 1.06 1.11 1.08 1.08 1.02 1.04 2.23 1.14 1.05 1.08 1.12 0.97 1.09
10.0 9.5 9.0 8.5 8.0 7.5 7.0 6.5 6.0 5.5 5.0 4.5 4.0 3.5 3.0 2.5 2.0 1.5 1.0 0.5 0.0
f1 (ppm)

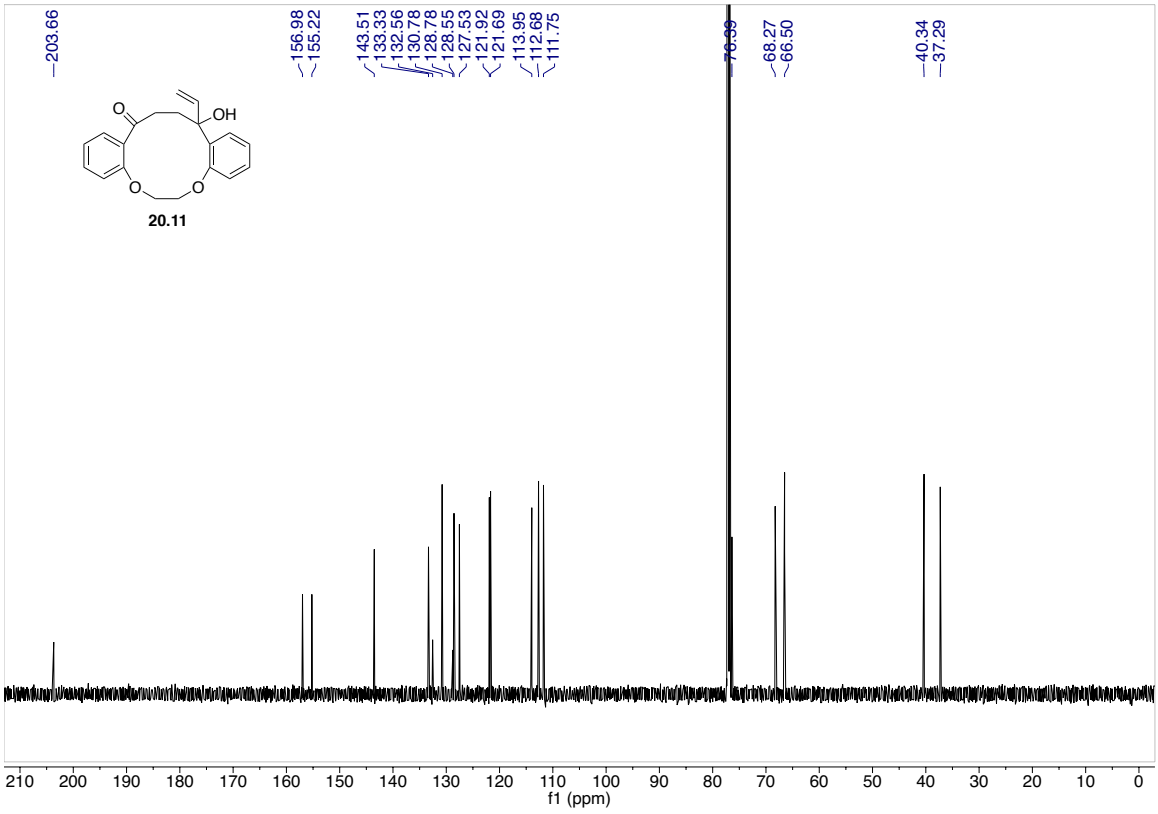
203.66
156.98 155.22 143.51 133.33 132.56 130.78 128.78 128.55 127.53 121.92 121.69 113.95 112.68 111.75
77.39
68.27 66.50
40.34 37.29
O
OH
O
O
20.11
210 200 190 180 170 160 150 140 130 120 110 100 90 80 70 60 50 40 30 20 10 0
f1 (ppm)

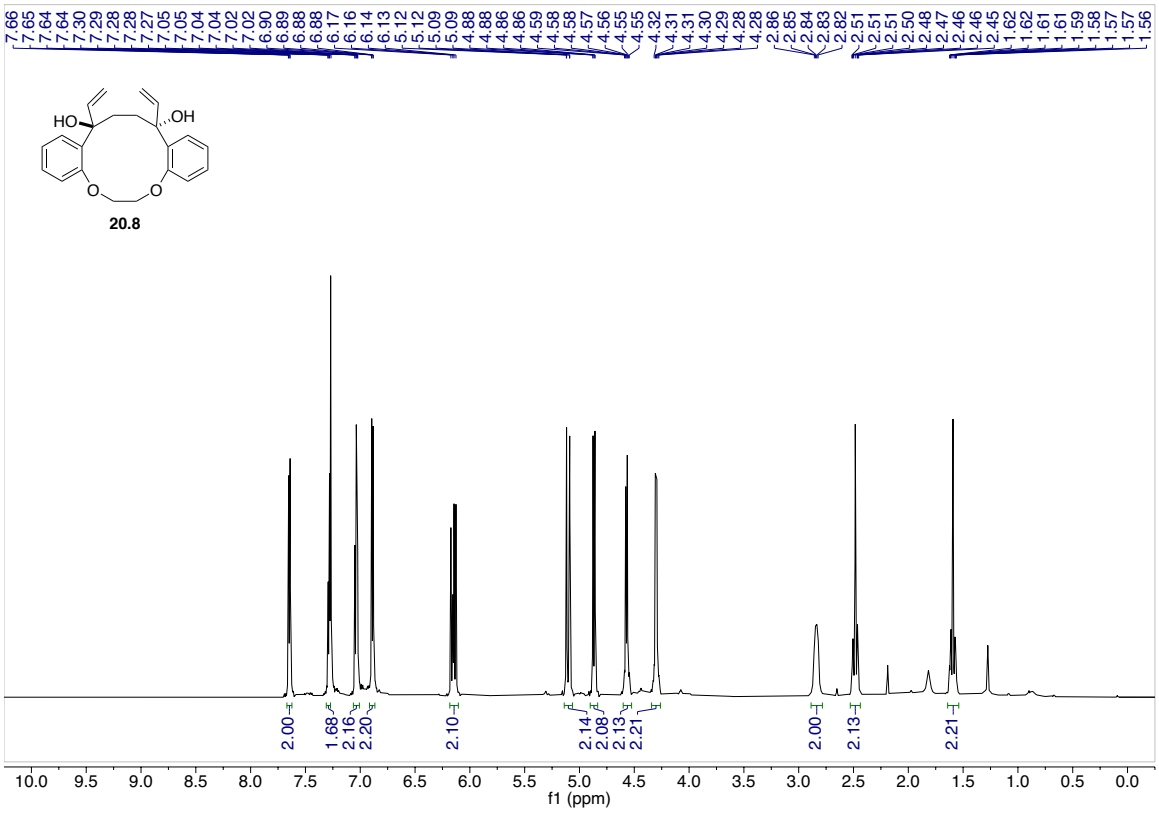
HO
OH
O
O
20.8
2.00
1.68
2.16
2.20
2.10
2.14
2.08
2.13
2.21
2.00
2.13
2.21
f1 (ppm)

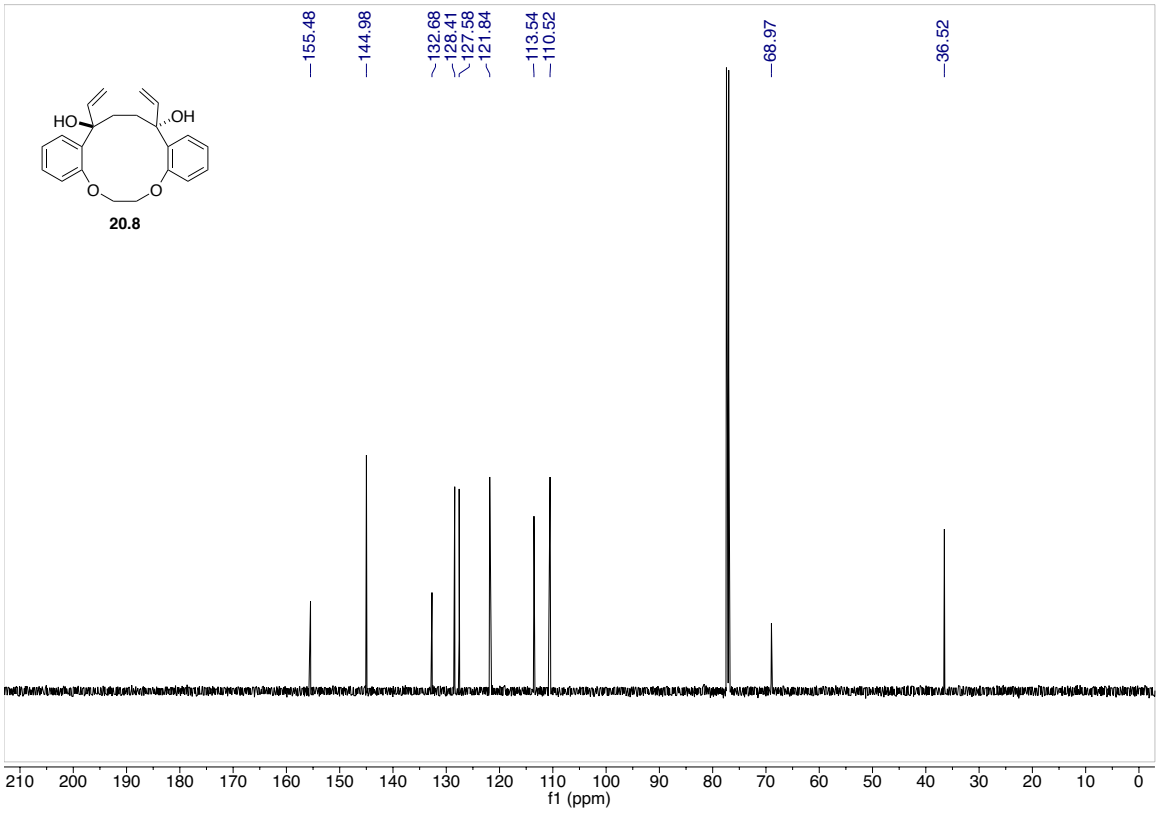
155.48
144.98
132.68
128.41
127.58
121.84
113.54
110.52
68.97
36.52
HO
OH
O
O
20.8
f1 (ppm)

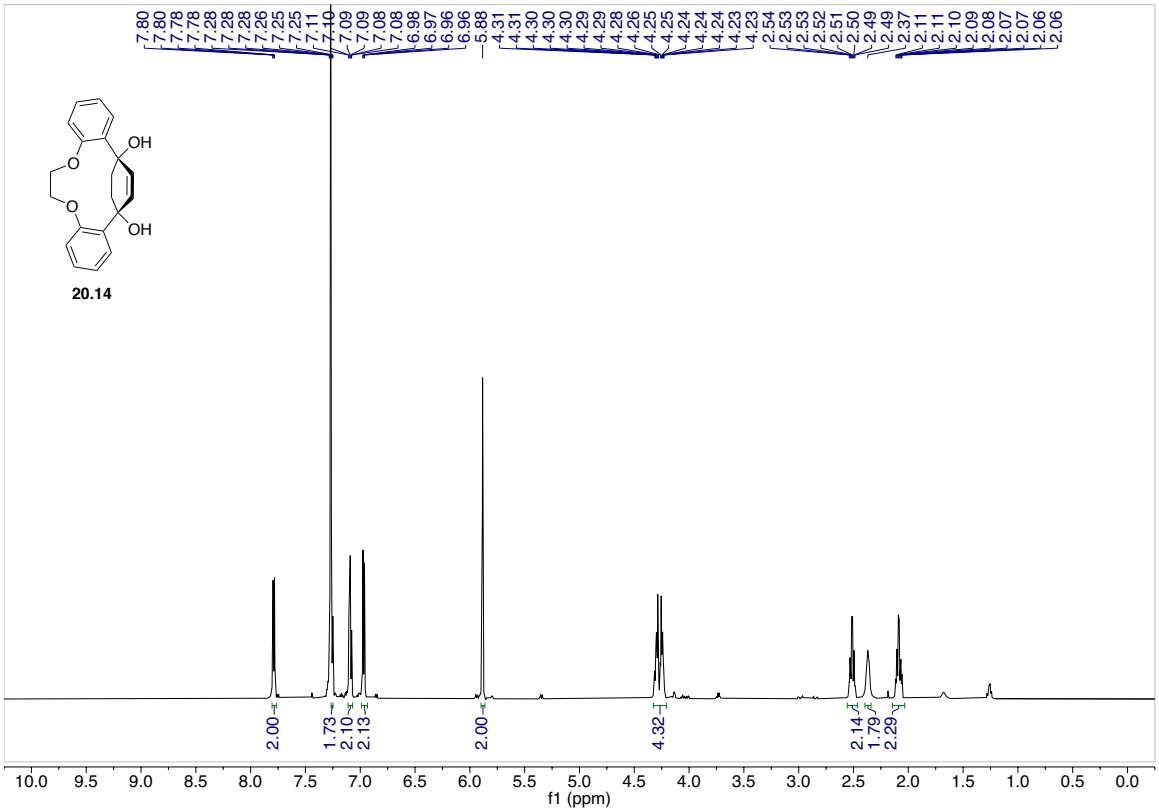
7.80
7.80
7.78
7.78
7.28
7.28
7.28
7.26
7.25
7.25
7.11
7.10
7.09
7.09
7.08
7.08
7.08
6.98
6.97
6.96
6.96
5.88
4.31
4.31
4.30
4.30
4.30
4.29
4.29
4.28
4.26
4.25
4.25
4.24
4.24
4.24
4.23
2.54
2.53
2.53
2.52
2.51
2.50
2.49
2.49
2.37
2.11
2.11
2.10
2.09
2.08
2.07
2.07
2.06
2.06
OH
O
O
OH
20.14
2.00
1.73
2.10
2.13
2.00
4.32
2.14
1.79
2.29
10.0 9.5 9.0 8.5 8.0 7.5 7.0 6.5 6.0 5.5 5.0 4.5 4.0 3.5 3.0 2.5 2.0 1.5 1.0 0.5 0.0
f1 (ppm)

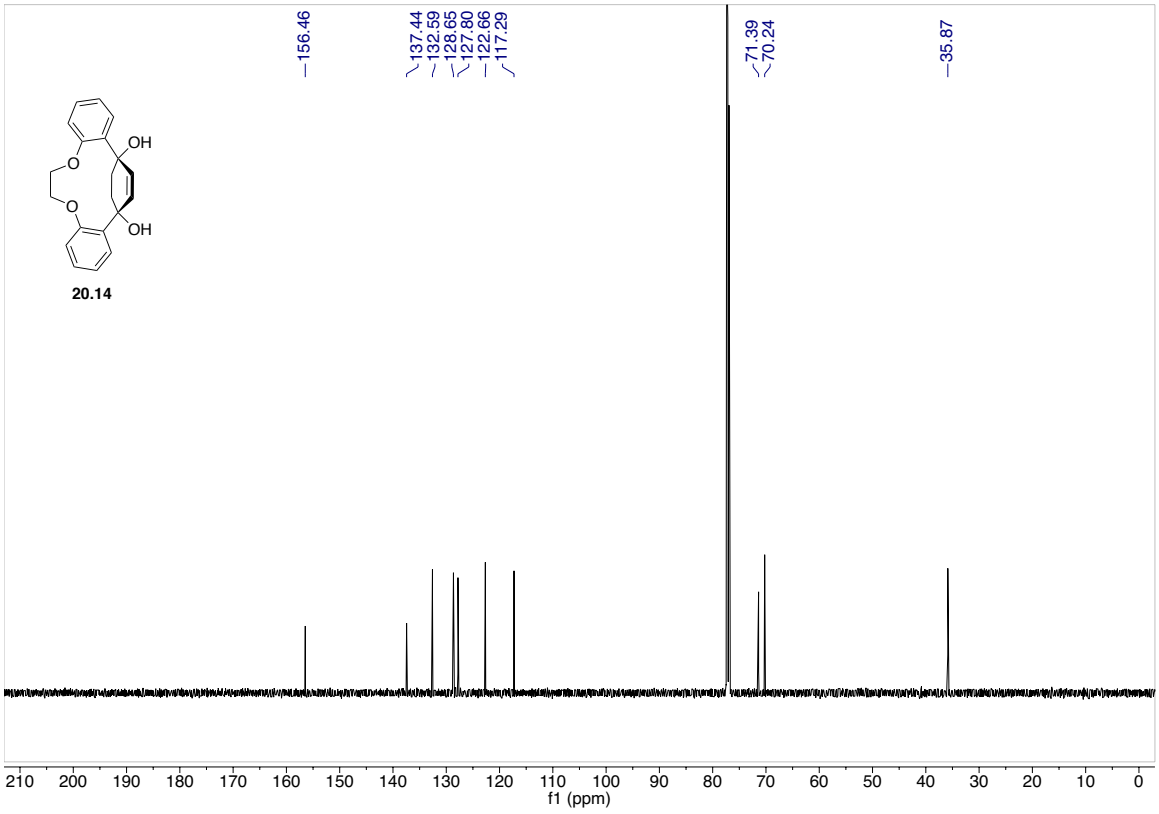
156.46
137.44
132.59
128.65
127.80
122.66
117.29
71.39
70.24
35.87
OH
O
O
OH
20.14
210 200 190 180 170 160 150 140 130 120 110 100 90 80 70 60 50 40 30 20 10 0
f1 (ppm)

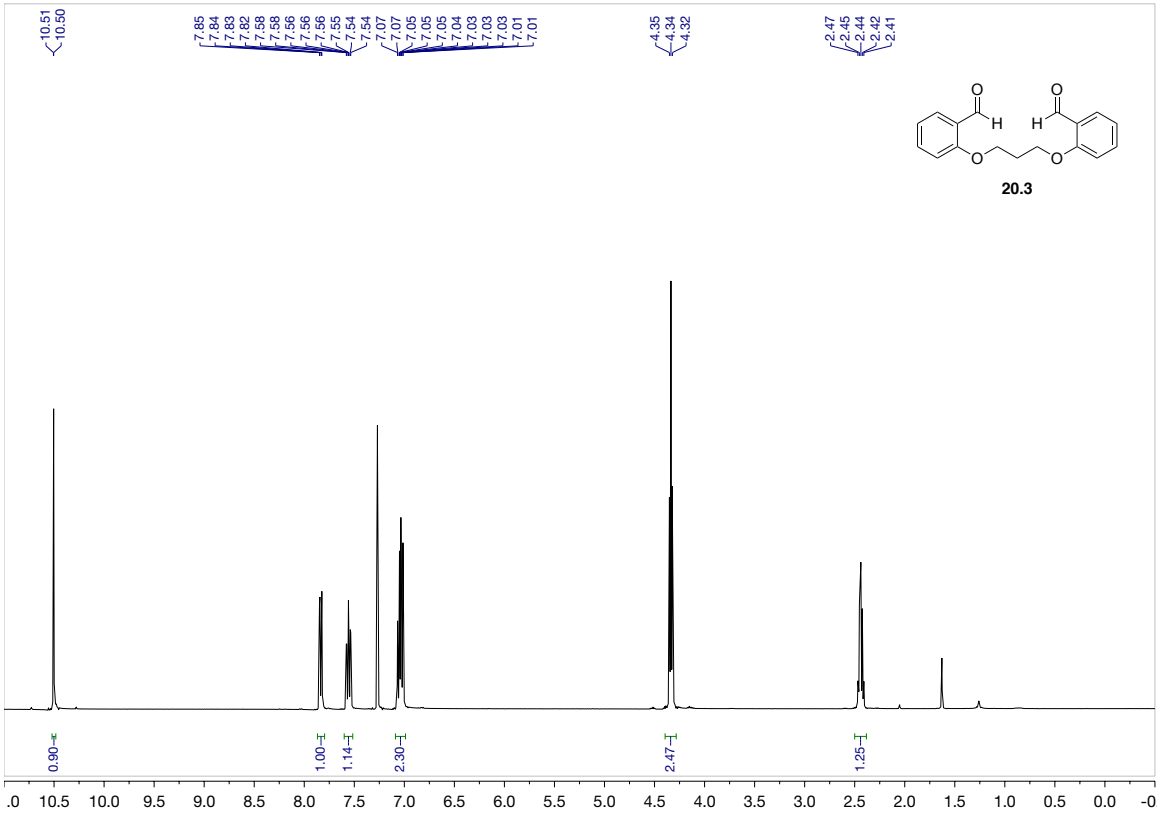
10.51
10.50
7.85
7.84
7.83
7.82
7.58
7.58
7.56
7.56
7.56
7.55
7.54
7.54
7.07
7.07
7.05
7.05
7.05
7.04
7.03
7.03
7.03
7.01
7.01
4.35
4.34
4.32
2.47
2.45
2.44
2.42
2.41
20.3
0.90
1.00
1.14
2.30
2.47
1.25

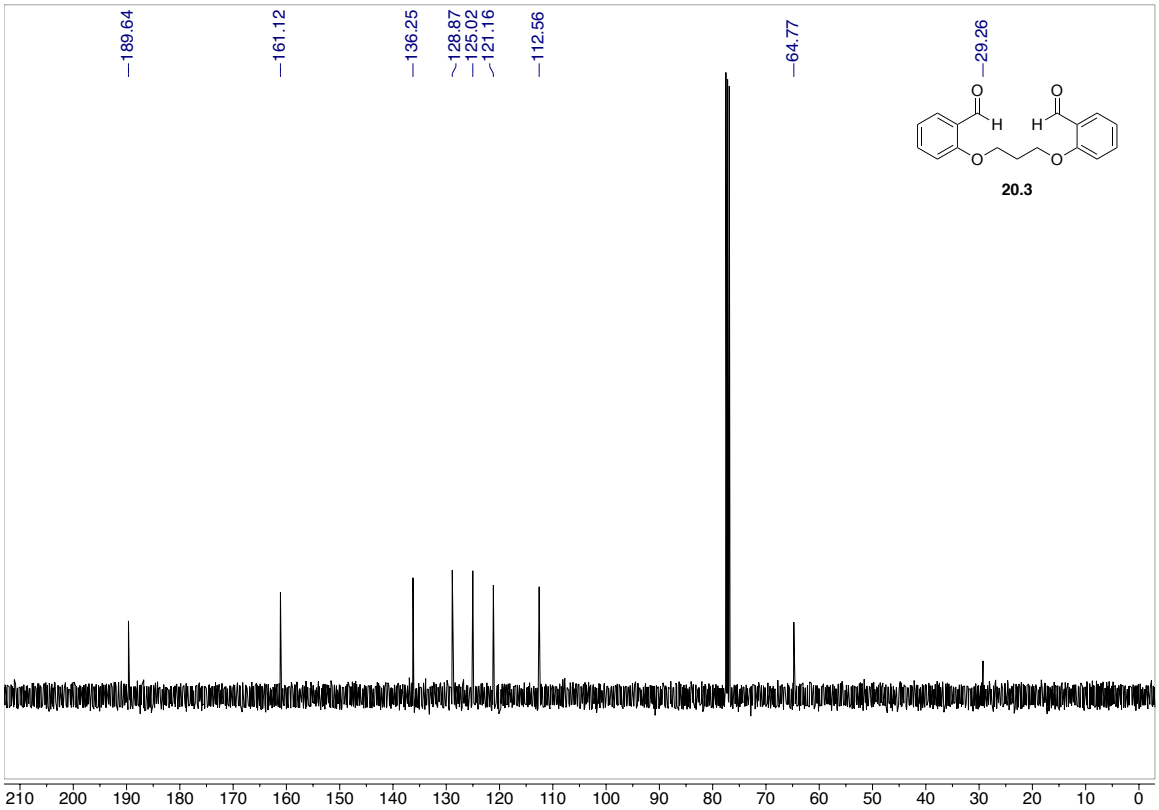
189.64
161.12
136.25
128.87
125.02
121.16
112.56
64.77
29.26
20.3

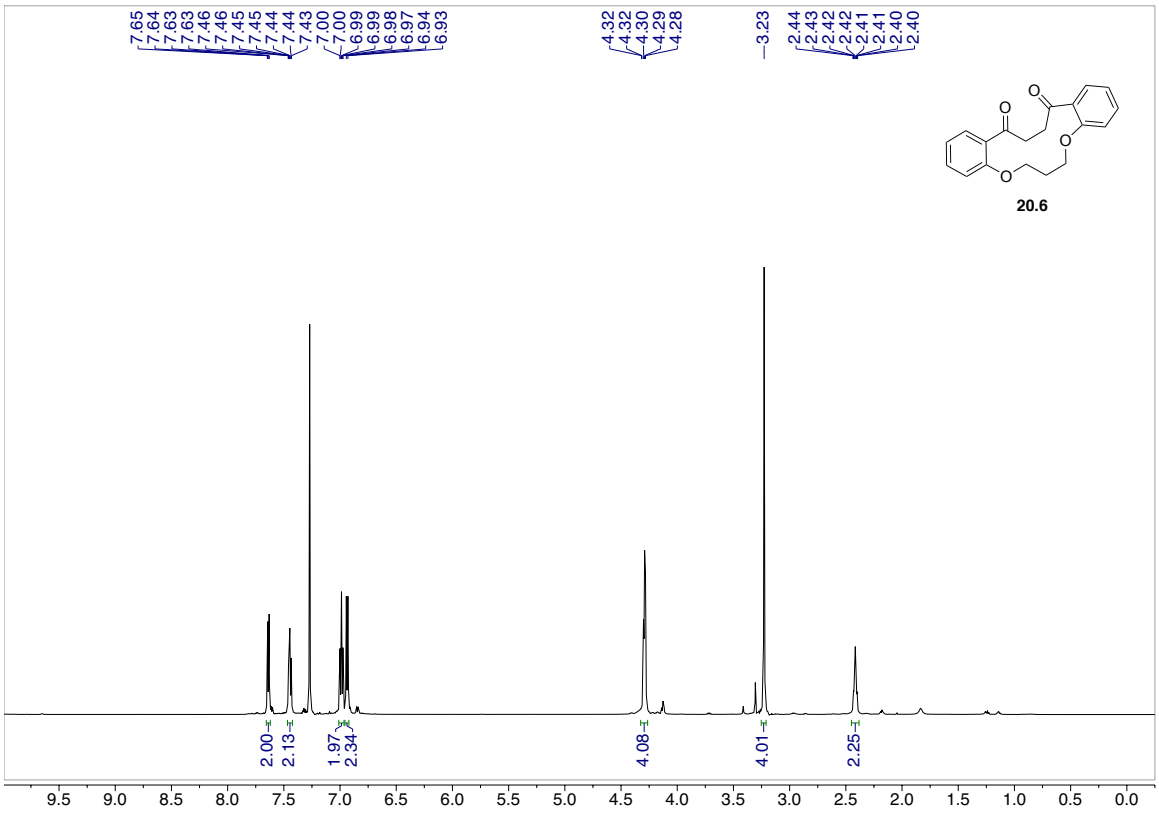
7.65
7.64
7.63
7.63
7.46
7.46
7.45
7.45
7.44
7.44
7.43
7.00
7.00
6.99
6.99
6.98
6.97
6.94
6.93
4.32
4.32
4.30
4.29
4.28
3.23
2.44
2.43
2.42
2.42
2.41
2.41
2.40
2.40
20.6
2.00
2.13
1.97
2.34
4.08
4.01
2.25
9.5 9.0 8.5 8.0 7.5 7.0 6.5 6.0 5.5 5.0 4.5 4.0 3.5 3.0 2.5 2.0 1.5 1.0 0.5 0.0

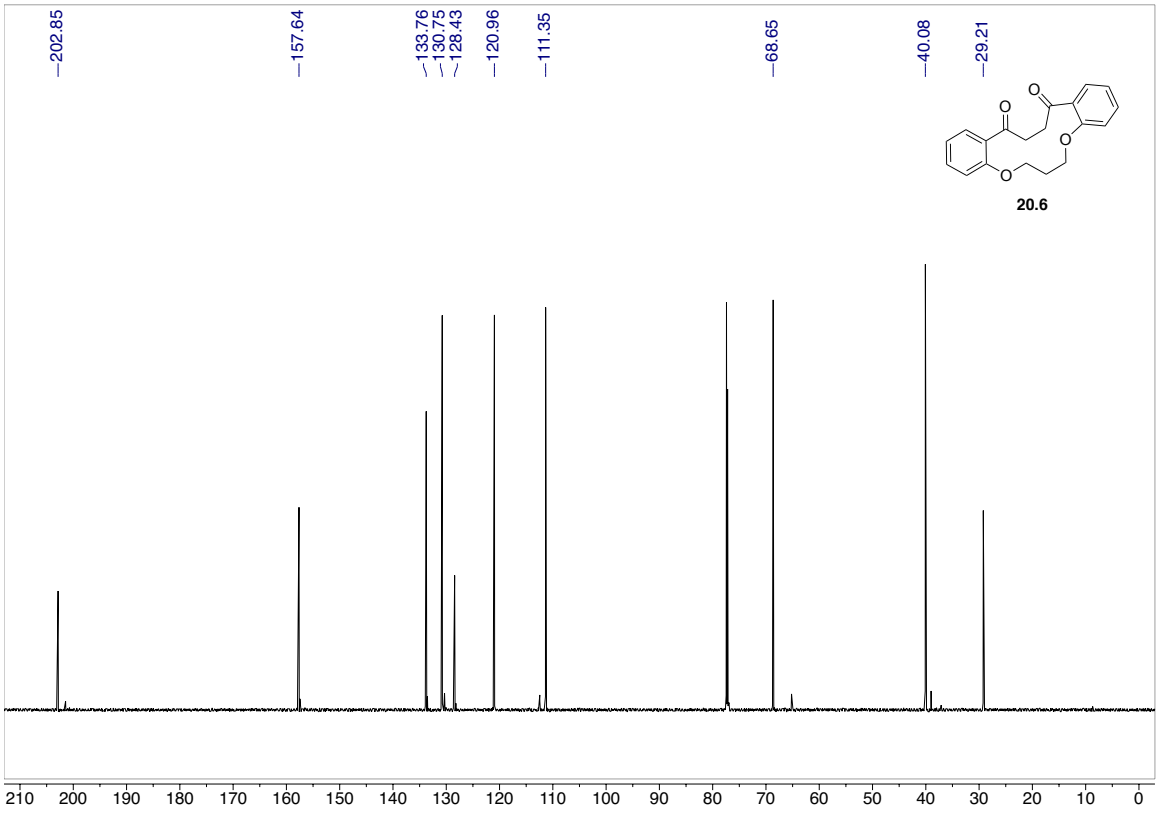
202.85
157.64
133.76
130.75
128.43
120.96
111.35
68.65
40.08
29.21
20.6
210 200 190 180 170 160 150 140 130 120 110 100 90 80 70 60 50 40 30 20 10 0

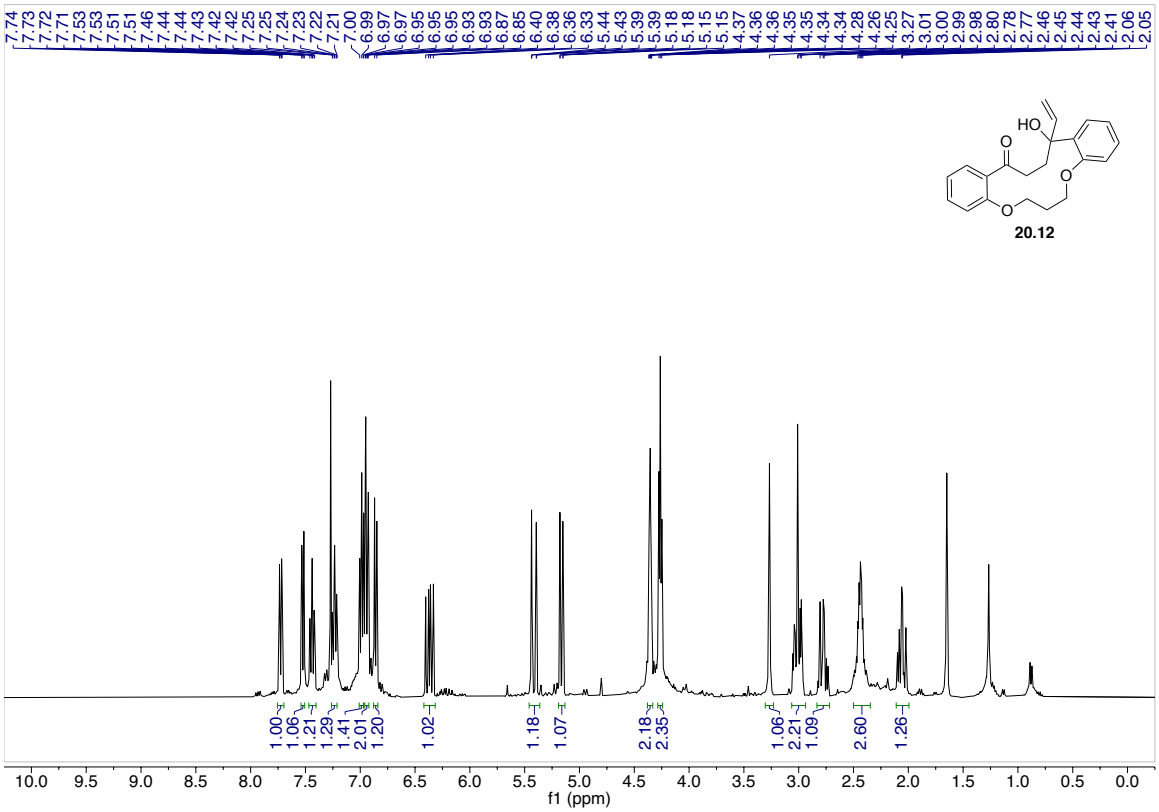
7.74 7.73 7.72 7.71 7.53 7.53 7.51 7.51 7.46 7.44 7.44 7.43 7.42 7.42 7.25 7.25 7.24 7.23 7.22 7.21 7.00 6.99 6.97 6.97 6.95 6.95 6.95 6.93 6.93 6.87 6.85 6.40 6.38 6.36 6.33 5.44 5.43 5.39 5.39 5.18 5.18 5.15 4.37 4.36 4.36 4.35 4.35 4.34 4.34 4.28 4.26 4.25 3.27 3.01 3.00 2.99 2.98 2.80 2.78 2.77 2.46 2.45 2.44 2.43 2.41 2.06 2.05
HO
O
O
O
20.12
1.00 1.06 1.21 1.29 1.41 2.01 1.20 1.02 1.18 1.07 2.18 2.35 1.06 2.21 1.09 2.60 1.26
10.0 9.5 9.0 8.5 8.0 7.5 7.0 6.5 6.0 5.5 5.0 4.5 4.0 3.5 3.0 2.5 2.0 1.5 1.0 0.5 0.0
f1 (ppm)

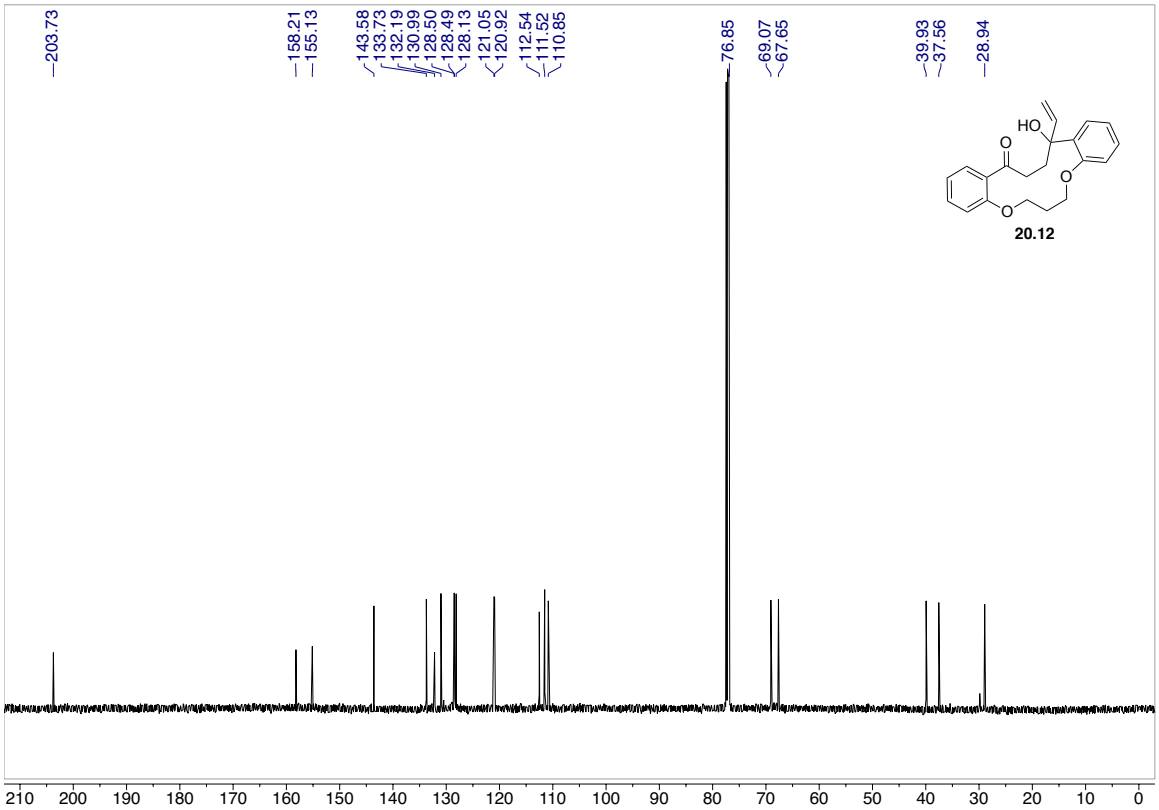
203.73
158.21 155.13
143.58 133.73 132.19 130.99 128.50 128.49 128.13 121.05 120.92 112.54 111.52 110.85
76.85
69.07 67.65
39.93 37.56
28.94
HO
O
O
O
20.12
210 200 190 180 170 160 150 140 130 120 110 100 90 80 70 60 50 40 30 20 10 0

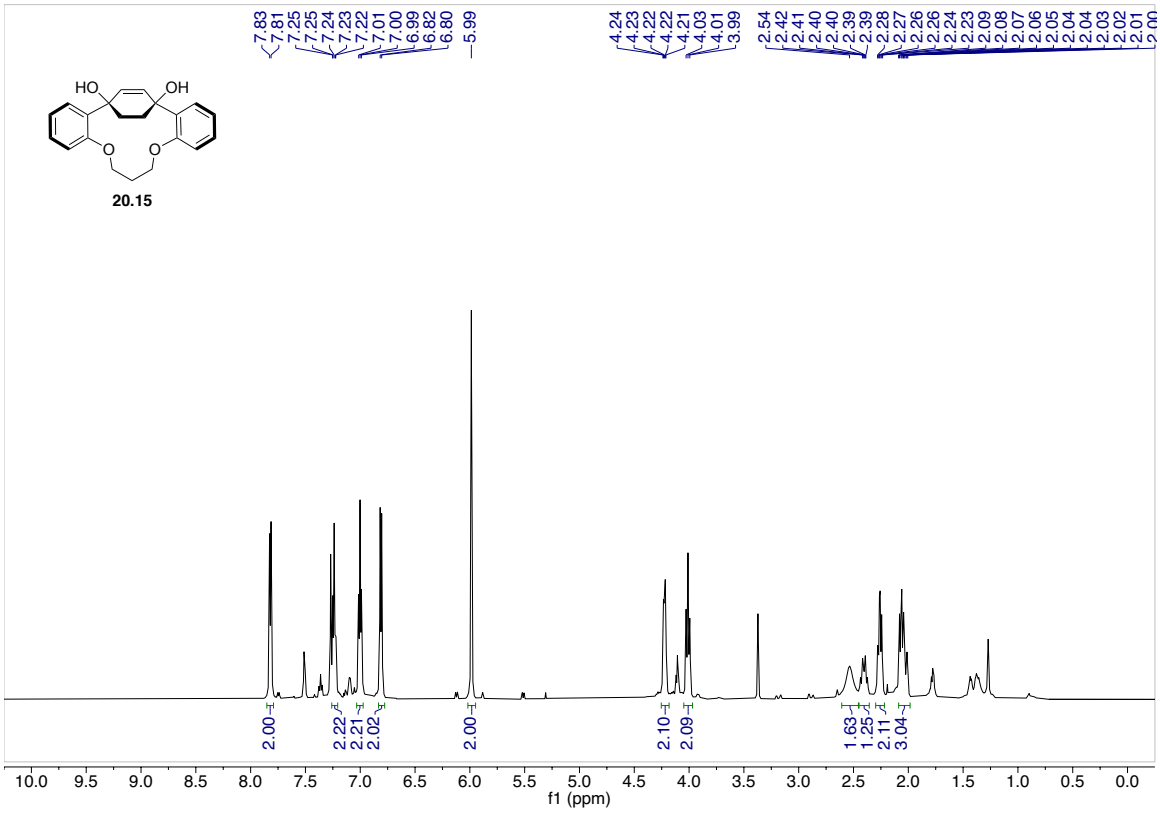
HO
OH
O
O
20.15
7.83
7.81
7.25
7.25
7.24
7.23
7.22
7.01
7.00
6.99
6.82
6.80
5.99
4.24
4.23
4.22
4.22
4.21
4.03
4.01
3.99
2.54
2.42
2.41
2.40
2.40
2.39
2.39
2.28
2.27
2.26
2.26
2.24
2.23
2.09
2.08
2.07
2.06
2.05
2.04
2.04
2.03
2.02
2.01
2.00
2.00
2.22
2.21
2.02
2.00
2.10
2.09
1.63
1.25
2.11
3.04
10.0 9.5 9.0 8.5 8.0 7.5 7.0 6.5 6.0 5.5 5.0 4.5 4.0 3.5 3.0 2.5 2.0 1.5 1.0 0.5 0.0
f1 (ppm)

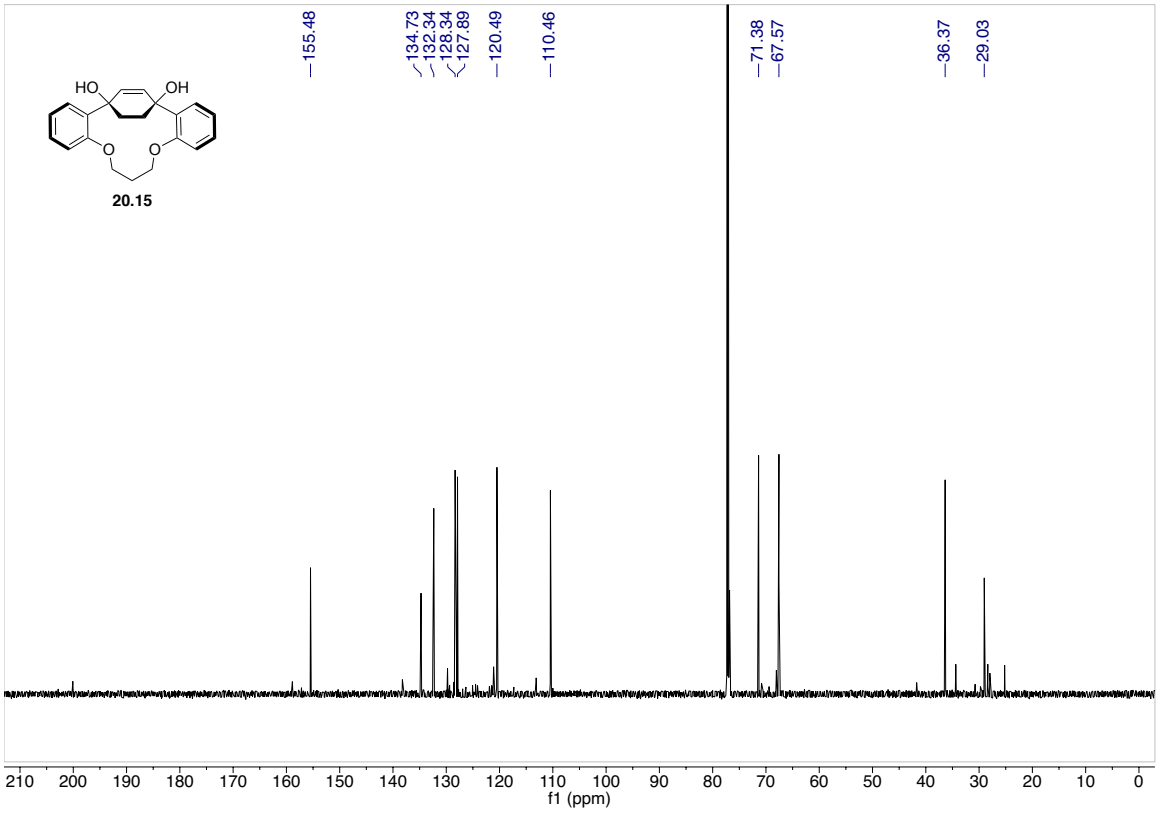
HO
OH
O
O
20.15
155.48
134.73
132.34
128.34
127.89
120.49
110.46
71.38
67.57
36.37
29.03
210 200 190 180 170 160 150 140 130 120 110 100 90 80 70 60 50 40 30 20 10 0
f1 (ppm)

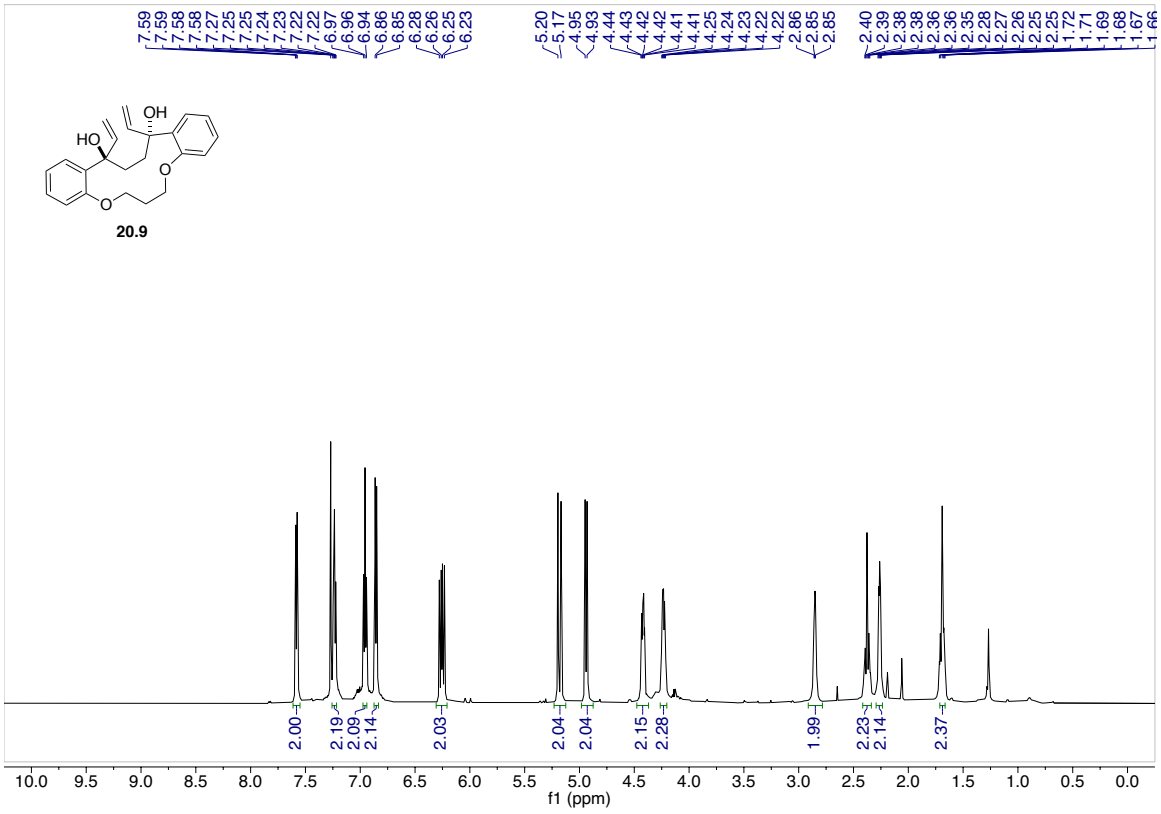
7.59
7.59
7.58
7.58
7.27
7.25
7.24
7.23
7.22
7.22
6.97
6.96
6.94
6.86
6.85
6.28
6.26
6.25
6.23
5.20
5.17
4.95
4.93
4.44
4.43
4.42
4.42
4.41
4.41
4.25
4.24
4.23
4.22
4.22
2.86
2.85
2.85
2.40
2.39
2.38
2.38
2.36
2.36
2.35
2.28
2.27
2.26
2.25
2.25
1.72
1.71
1.69
1.68
1.67
OH
HO
O
O
20.9
2.00
2.19
2.09
2.14
2.03
2.04
2.04
2.15
2.28
1.99
2.23
2.14
2.37
10.0 9.5 9.0 8.5 8.0 7.5 7.0 6.5 6.0 5.5 5.0 4.5 4.0 3.5 3.0 2.5 2.0 1.5 1.0 0.5 0.0
f1 (ppm)

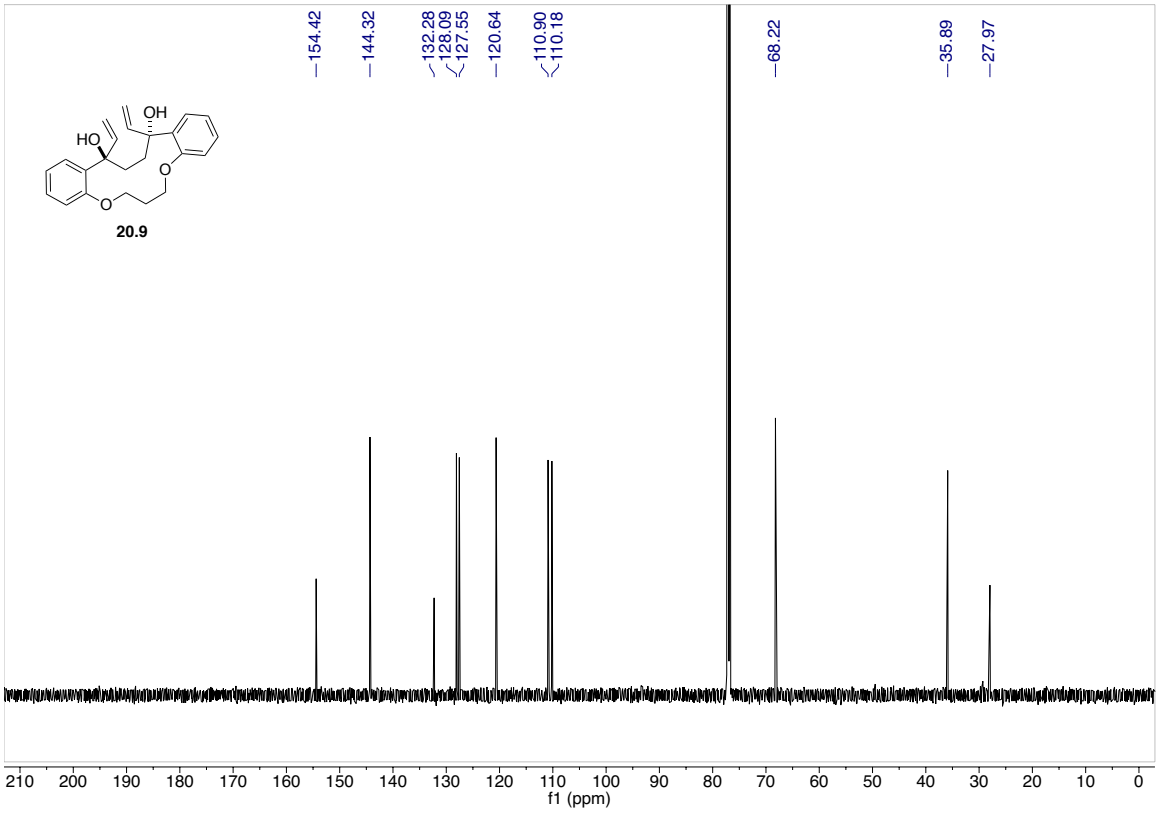
154.42
144.32
132.28
128.09
127.55
120.64
110.90
110.18
68.22
35.89
27.97
OH
HO
O
O
20.9
210 200 190 180 170 160 150 140 130 120 110 100 90 80 70 60 50 40 30 20 10 0
f1 (ppm)

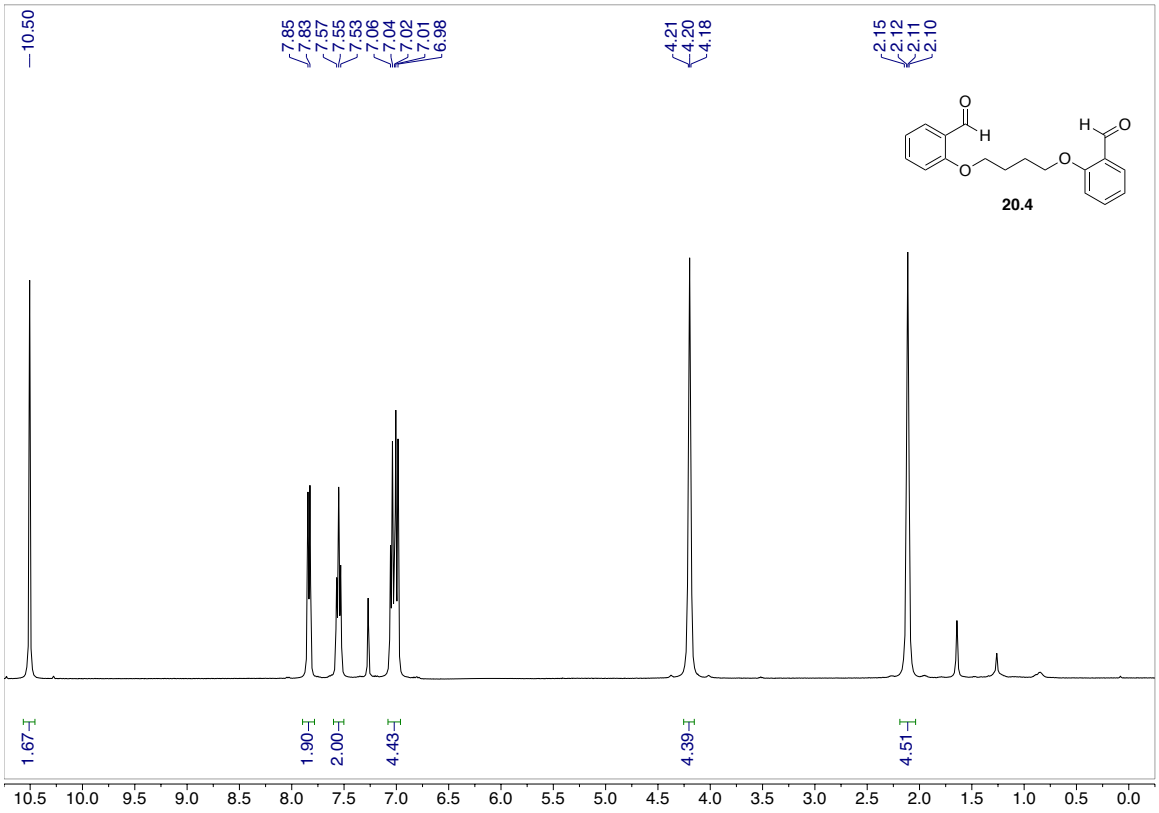
10.50
7.85
7.83
7.57
7.55
7.53
7.06
7.04
7.02
7.01
6.98
4.21
4.20
4.18
2.15
2.12
2.11
2.10
20.4
1.67
1.90
2.00
4.43
4.39
4.51
10.5 10.0 9.5 9.0 8.5 8.0 7.5 7.0 6.5 6.0 5.5 5.0 4.5 4.0 3.5 3.0 2.5 2.0 1.5 1.0 0.5 0.0

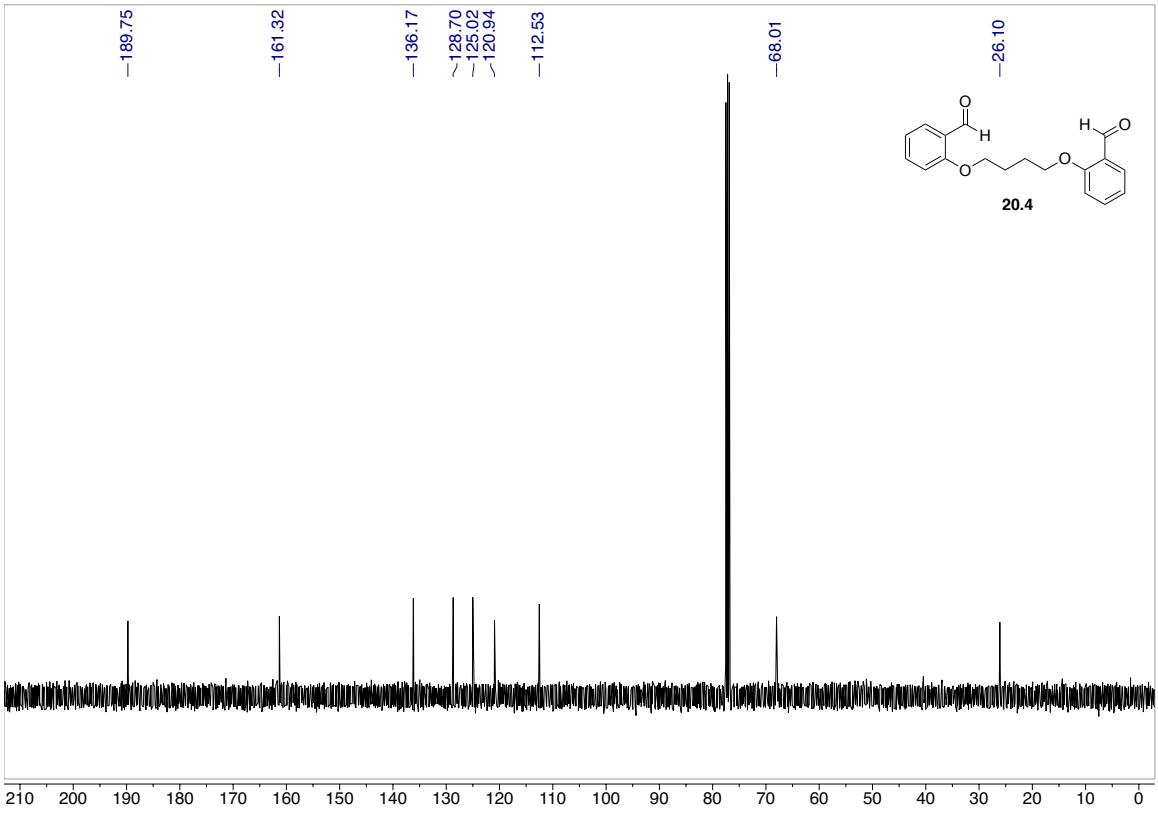
189.75
161.32
136.17
128.70
125.02
120.94
112.53
68.01
26.10
20.4
210 200 190 180 170 160 150 140 130 120 110 100 90 80 70 60 50 40 30 20 10 0

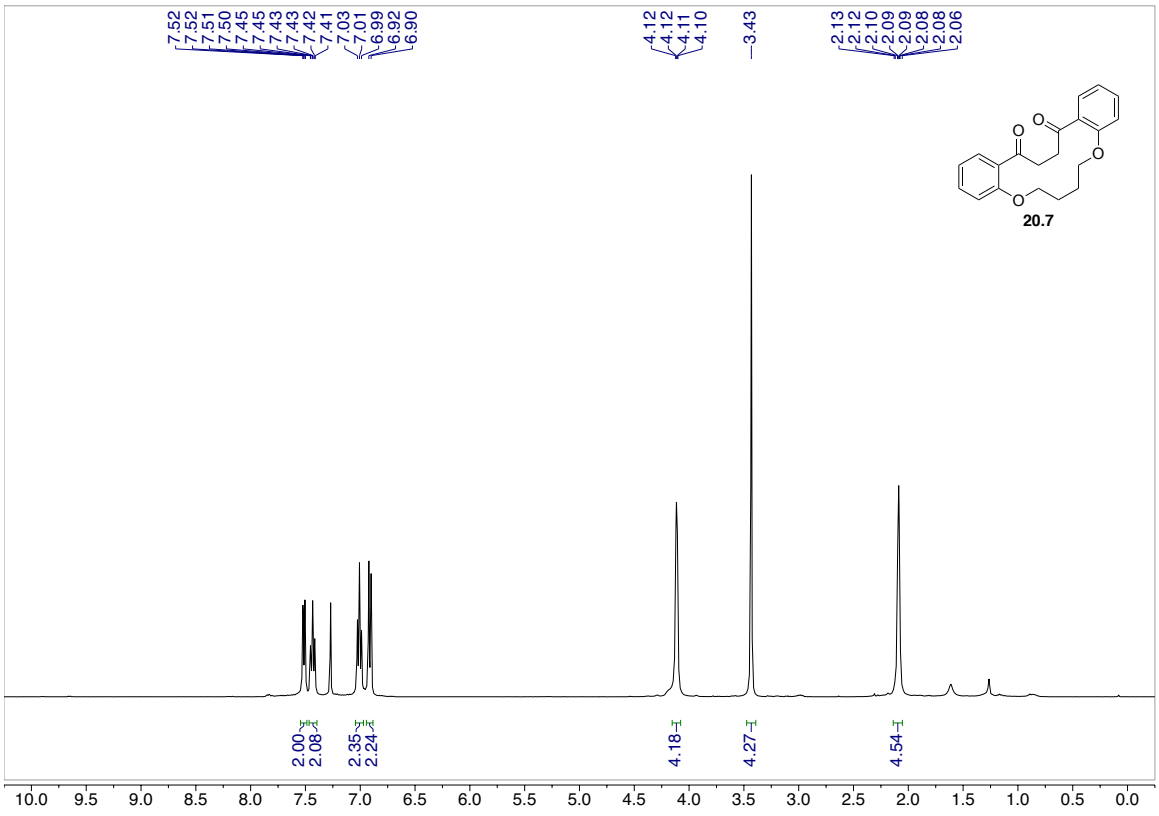
7.52
7.52
7.51
7.50
7.45
7.45
7.43
7.43
7.42
7.41
7.03
7.01
6.99
6.92
6.90
4.12
4.12
4.11
4.10
3.43
2.13
2.12
2.10
2.09
2.09
2.08
2.08
2.06
20.7
2.00
2.08
2.35
2.24
4.18
4.27
4.54
10.0 9.5 9.0 8.5 8.0 7.5 7.0 6.5 6.0 5.5 5.0 4.5 4.0 3.5 3.0 2.5 2.0 1.5 1.0 0.5 0.0

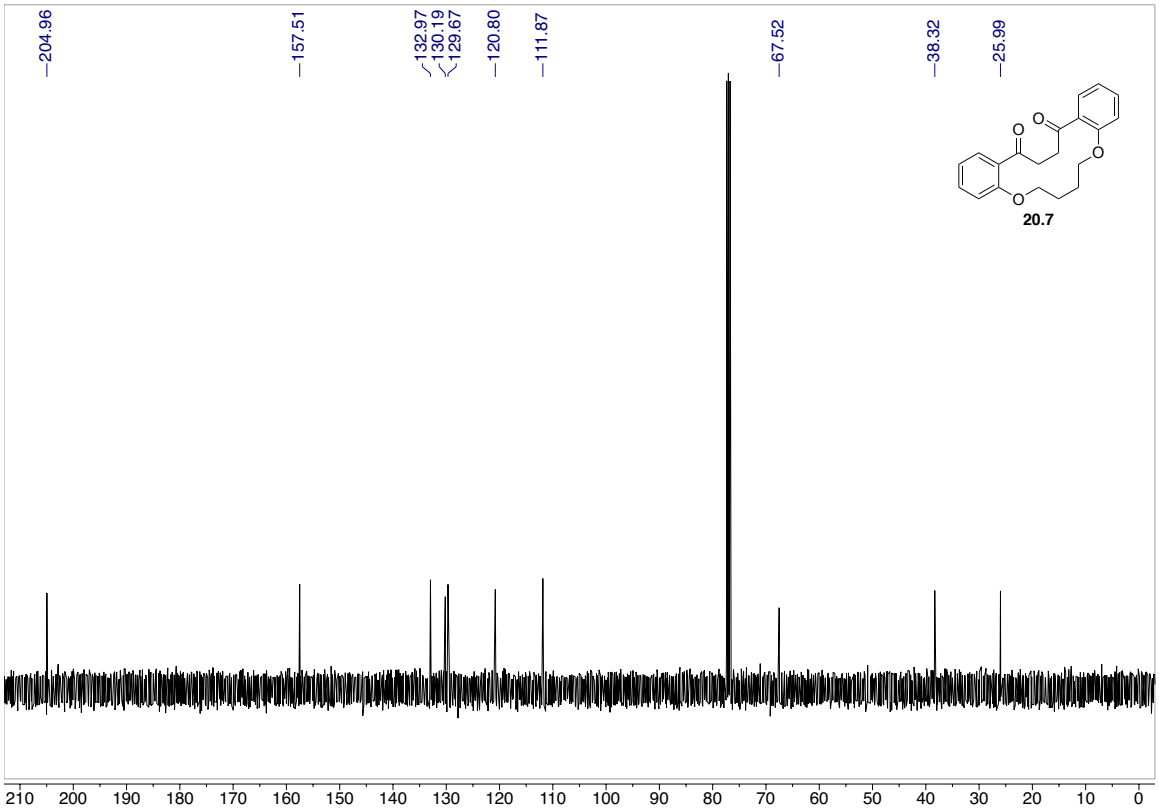
204.96
157.51
132.97
130.19
129.67
120.80
111.87
67.52
38.32
25.99
20.7
210 200 190 180 170 160 150 140 130 120 110 100 90 80 70 60 50 40 30 20 10 0

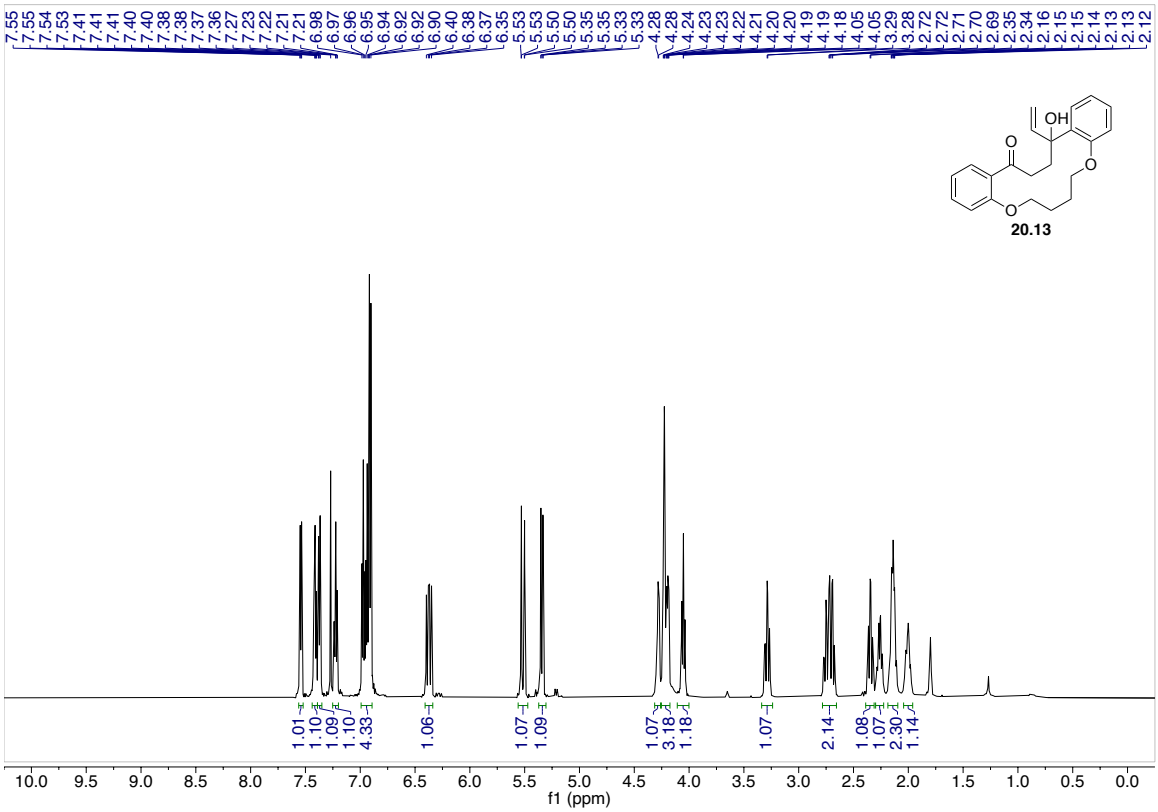
7.55 7.55 7.54 7.53 7.41 7.41 7.40 7.40 7.38 7.38 7.37 7.36 7.27 7.23 7.22 7.21 7.21 6.98 6.97 6.96 6.95 6.94 6.92 6.92 6.90 6.40 6.38 6.37 6.35 5.53 5.53 5.50 5.50 5.35 5.35 5.33 4.28 4.28 4.24 4.23 4.23 4.22 4.21 4.20 4.20 4.19 4.19 4.18 4.05 4.05 3.29 3.28 2.72 2.72 2.71 2.70 2.69 2.35 2.34 2.16 2.15 2.15 2.14 2.13 2.13 2.12
OH
O
O
O
20.13
1.01 1.10 1.09 1.10 4.33 1.06 1.07 1.09 1.07 3.18 1.18 1.07 2.14 1.08 1.07 2.30 1.14
10.0 9.5 9.0 8.5 8.0 7.5 7.0 6.5 6.0 5.5 5.0 4.5 4.0 3.5 3.0 2.5 2.0 1.5 1.0 0.5 0.0
f1 (ppm)

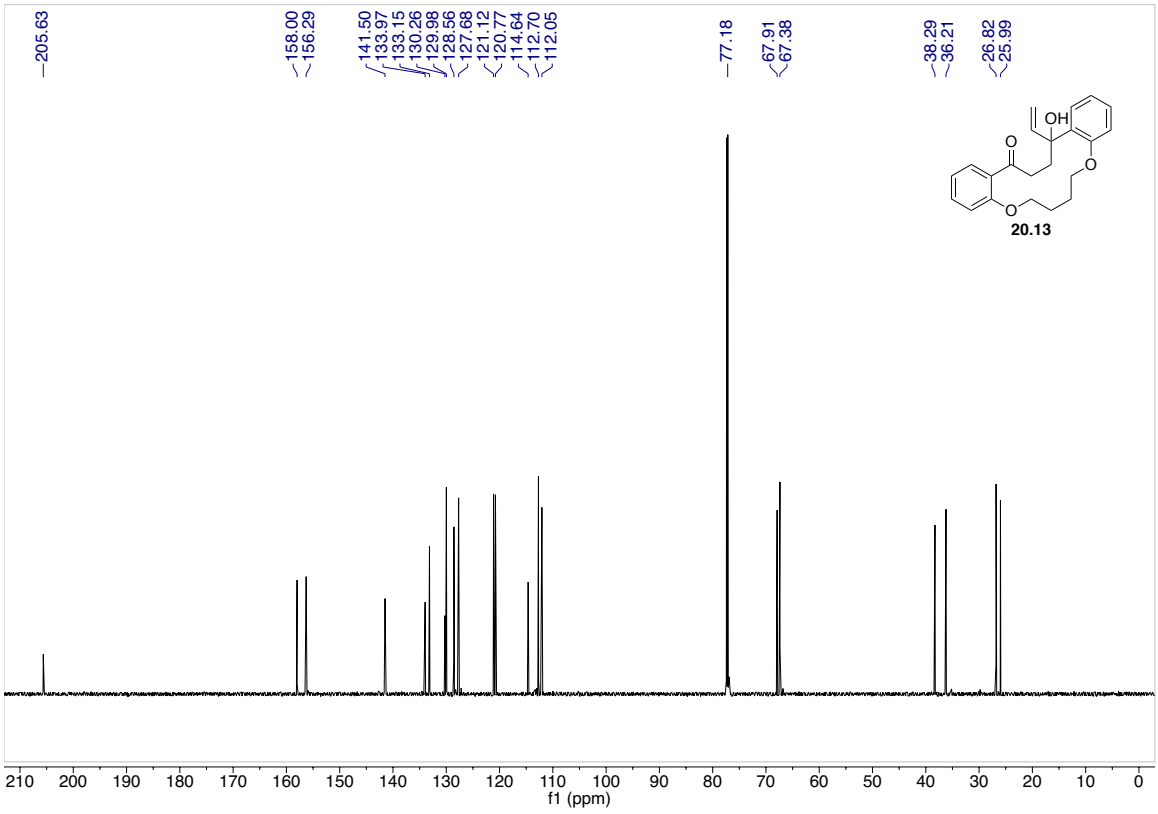
205.63
158.00 156.29 141.50 133.97 133.15 130.26 129.98 128.56 127.68 121.12 120.77 114.64 112.70 112.05 77.18 67.91 67.38 38.29 36.21 26.82 25.99
OH
O
O
O
20.13
210 200 190 180 170 160 150 140 130 120 110 100 90 80 70 60 50 40 30 20 10 0
f1 (ppm)

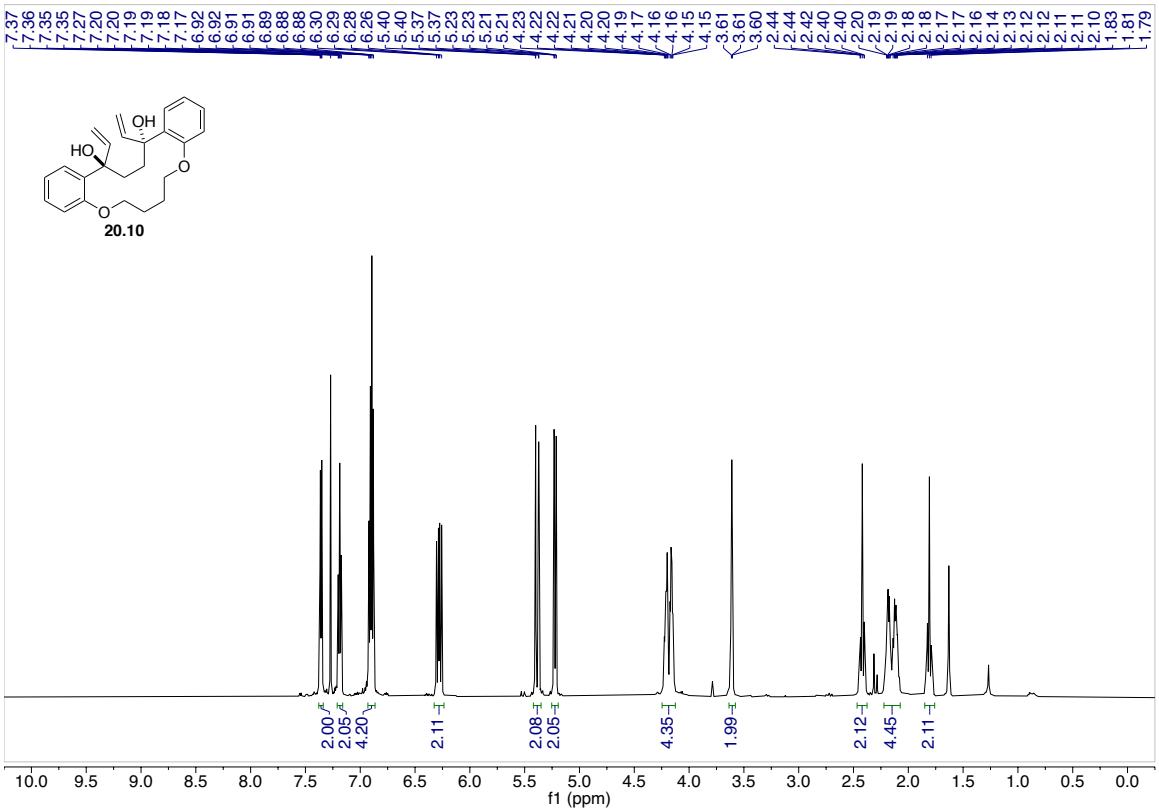
7.37 7.36 7.35 7.35 7.27 7.20 7.20 7.19 7.19 7.18 7.17 6.92 6.92 6.91 6.91 6.89 6.88 6.88 6.30 6.29 6.28 6.26 5.40 5.40 5.37 5.37 5.23 5.23 5.21 5.21 4.23 4.22 4.22 4.21 4.20 4.20 4.19 4.17 4.16 4.16 4.15 4.15 3.61 3.61 3.60 2.44 2.44 2.42 2.40 2.40 2.20 2.19 2.19 2.18 2.18 2.17 2.17 2.16 2.14 2.13 2.12 2.12 2.11 2.11 2.10 1.83 1.81 1.79
OH
HO
O
O
20.10
2.00 2.05 4.20 2.11 2.08 2.05 4.35 1.99 2.12 4.45 2.11
10.0 9.5 9.0 8.5 8.0 7.5 7.0 6.5 6.0 5.5 5.0 4.5 4.0 3.5 3.0 2.5 2.0 1.5 1.0 0.5 0.0
f1 (ppm)

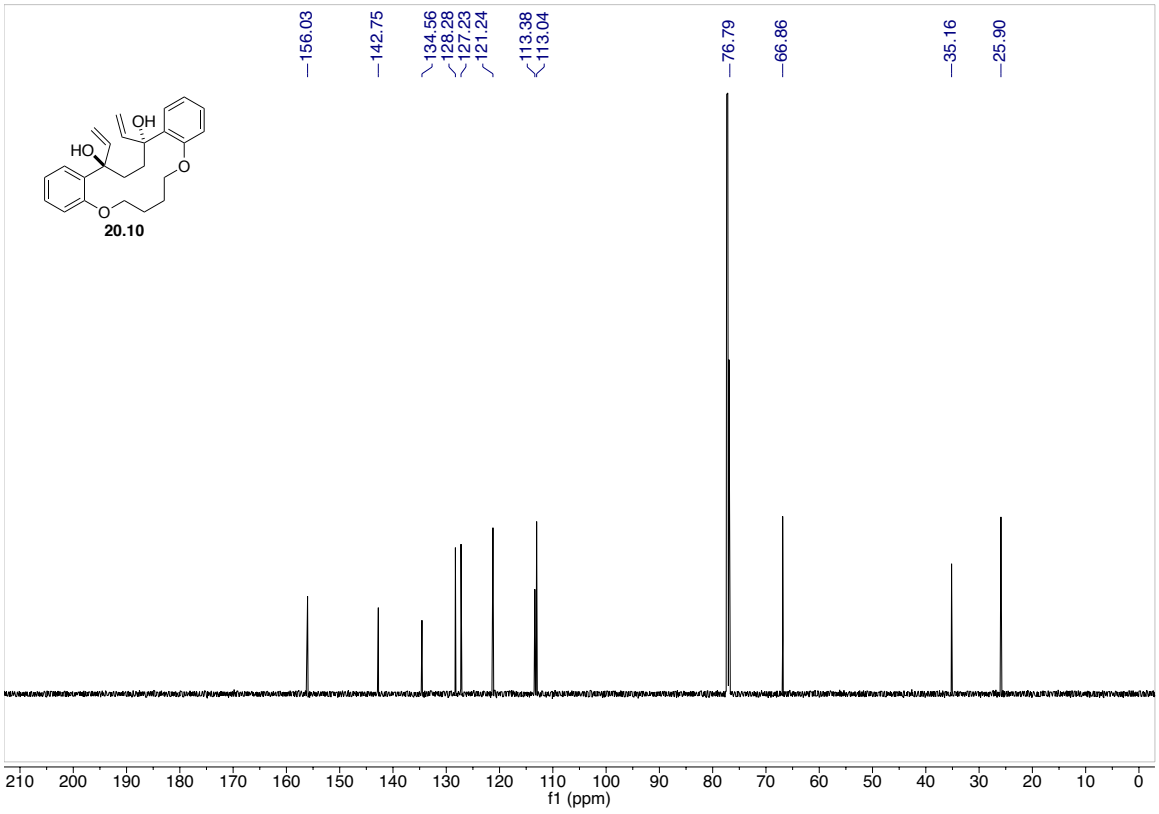
156.03 142.75 134.56 128.28 127.23 121.24 113.38 113.04 76.79 66.86 35.16 25.90
OH
HO
O
O
20.10
210 200 190 180 170 160 150 140 130 120 110 100 90 80 70 60 50 40 30 20 10 0
f1 (ppm)

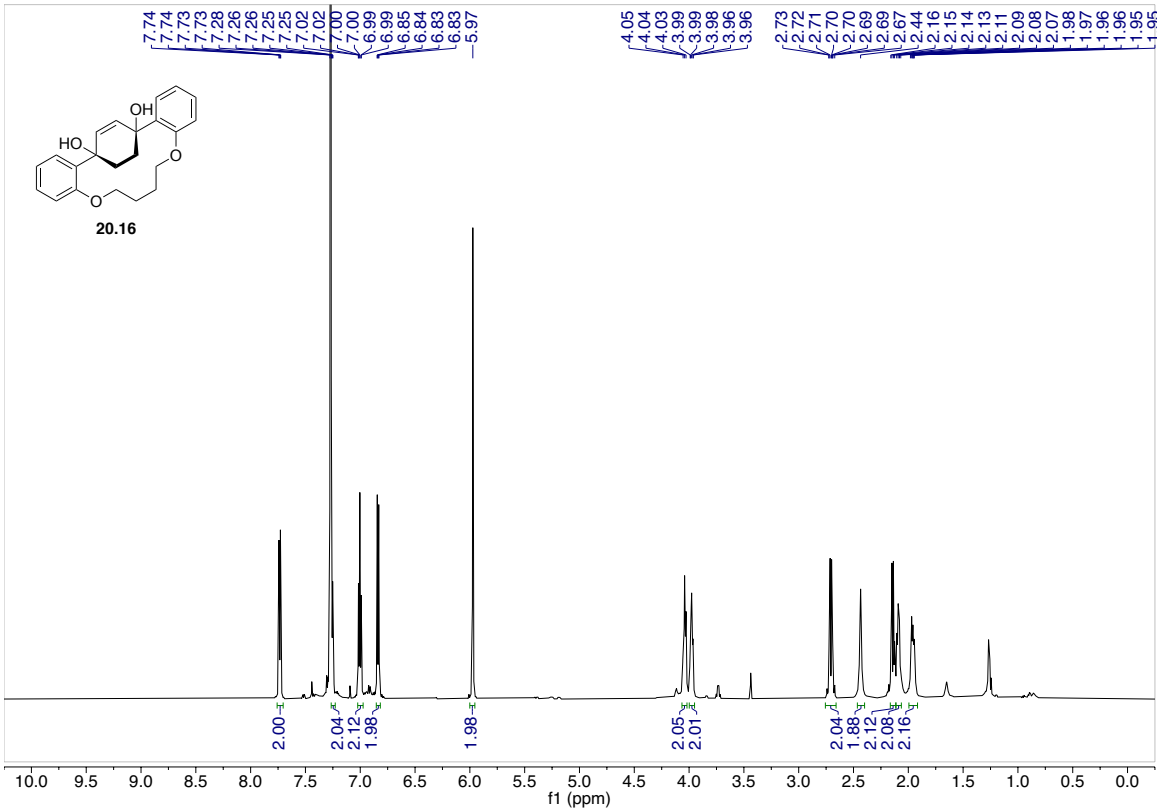
7.74
7.74
7.73
7.73
7.28
7.26
7.25
7.25
7.02
7.02
7.00
7.00
6.99
6.99
6.85
6.84
6.83
6.83
5.97
4.05
4.04
4.03
3.99
3.99
3.98
3.96
3.96
2.73
2.72
2.71
2.70
2.70
2.69
2.69
2.67
2.44
2.16
2.15
2.14
2.13
2.11
2.09
2.08
2.07
1.98
1.97
1.96
1.96
1.95
OH
HO
O
O
20.16
2.00
2.04
2.12
1.98
1.98
2.05
2.01
2.04
1.88
2.12
2.08
2.16
10.0 9.5 9.0 8.5 8.0 7.5 7.0 6.5 6.0 5.5 5.0 4.5 4.0 3.5 3.0 2.5 2.0 1.5 1.0 0.5 0.0
f1 (ppm)

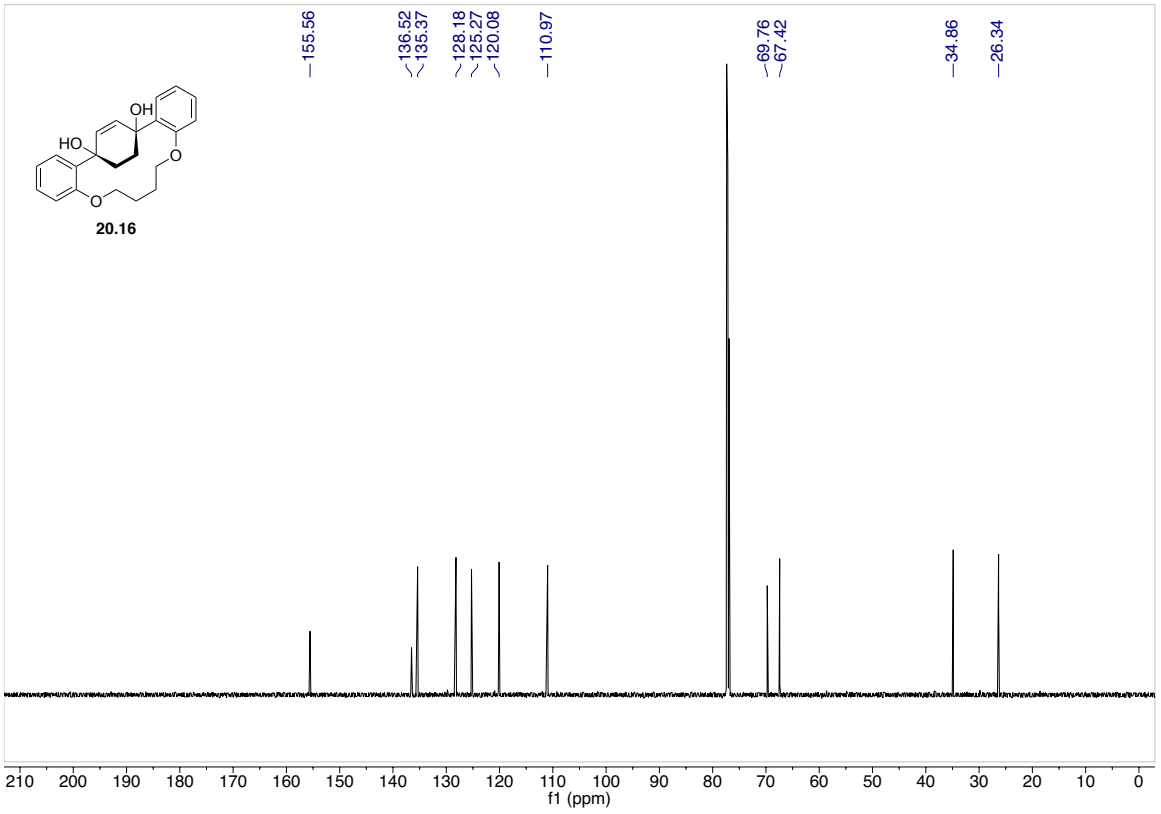
155.56
136.52
135.37
128.18
125.27
120.08
110.97
69.76
67.42
34.86
26.34
OH
HO
O
O
20.16
210 200 190 180 170 160 150 140 130 120 110 100 90 80 70 60 50 40 30 20 10 0
f1 (ppm)

APPENDIX 2: CHAPTER 2 Supplementary Information

General experimental conditions

All reactions were run in flame or oven-dried (120 °C) glassware and cooled under a positive pressure of ultra high pure nitrogen or argon gas. All chemicals were used as received from commercial sources, unless otherwise stated. Anhydrous reaction solvents were purified and dried by passing HPLC grade solvents through activated columns of alumina (Glass Contour SDS). All solvents used for chromatographic separations were HPLC grade (hexanes, ethyl acetate, and dichloromethane). Chromatographic separations were performed using flash chromatography, as originally reported by Still and co-workers,[1] on silica gel 60 (particle size 43-60 μm), and all chromatography conditions have been reported as diameter × height in centimeters. Reaction progress was monitored by thin layer chromatography (TLC), on glass-backed silica gel plates (pH = 7.0). TLC plates were visualized using a handheld UV lamp (254 nm or 365 nm) and stained using an aqueous ceric ammonium molybdate (CAM) solution. Plates were dipped, wiped clean, and heated from the back. ^{1}H and ^{13}C nuclear magnetic resonance (NMR) spectra were recorded at 400, 500, or 600 MHz, calibrated using residual undeuterated solvent as an internal reference ($CHCl_3$, δ 7.27 and 77.2 ppm), reported in parts per million relative to trimethylsilane (TMS, δ 0.00 ppm), and presented as follows: chemical shift (δ, ppm), multiplicity (s = singlet, d = doublet, dd = doublet of doublets, ddt = doublet of doublet of triplets, bs = broad singlet, m = multiplet), coupling constants (*J*, Hz), and integration. High-resolution mass spectrometric (HRMS) data were obtained using a quadrupole time-of-flight (Q-TOF) spectrometer and electrospray ionization (ESI).

Compounds not included in text

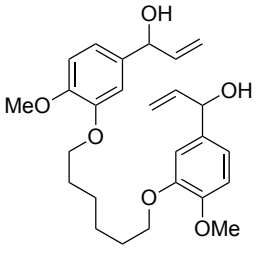

S-4

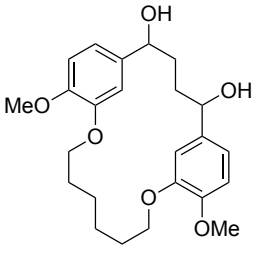

S-5

[1] Still, W.C., Kahn, M., Mitra, A. *J. Org. Chem.* **1978**, *43*, 2923-2925.

Experimental Procedures

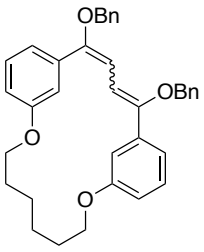

41c

1,4-bis-*O*-benzyl-1,3-dien-1,4-diol 41c: A solution of **diketone 19.4** (0.0538 g, 0.153 mmol) in THF (0.49 mL) was added to a stirring solution of LDA (0.5 M, 0.6 mL, 0.3 mmol) in THF at –78 °C. After stirring for 1 h at –78 °C, HMPA (50% v/v solution in THF, 0.10 mL, 0.3 mmol) and BnBr (0.04 mL, 0.3 mmol) was added, and the reaction slowly warmed to room temperature. After 20 h, the reaction was cooled back to –78 °C, and 1 M HCl (1 mL) was added. The aqueous phase was extracted with chloroform (3 × 3 mL). The combined organic extracts were dried over $MgSO_4$, filtered, and concentrated under reduced pressure. The residue was purified with flash chromatography (3.8 × 18 cm, hexanes to 20% ethyl acetate/hexanes) to afford **41c** as a clear oil (0.0152 g, 22%): R_f = 0.43 (10% ethyl acetate/hexanes); ^{1}H NMR (600 MHz, $CDCl_3$) δ 7.90 (d, *J* = 2.5 Hz, 1H), 7.58 (d, *J* = 7.8 Hz, 1H), 7.44 – 7.12 (m, 18H), 7.04 (d, *J* = 7.6 Hz, 1H), 7.00 (dd, *J* = 8.2, 2.3 Hz, 1H), 6.99 – 6.88 (m, 5H), 6.85 (dd, *J* = 8.3, 2.4 Hz, 1H), 6.79 (s, 1H), 5.20 (d, *J* = 10.7 Hz, 1H), 5.16 (s, 1H), 4.81 (td, *J* = 10.2, 4.5 Hz, 1H), 4.35 (d, *J* = 11.2 Hz, 1H), 4.08 (t, *J* = 6.1 Hz, 1H), 4.01 (m, 3H), 3.90 (s, 1H), 3.83 – 3.74 (m, 2H), 3.42 (dd, *J* = 16.6, 12.5 Hz, 2H), 3.32 – 3.22 (m, 2H), 2.90 (dd, *J* = 13.5, 9.6 Hz, 1H), 1.73 (dq, *J* = 10.7, 5.3, 4.3 Hz, 4H), 1.68 – 1.56 (m, 3H), 1.52 (q, *J* = 7.3 Hz, 1H), 1.40 – 1.18 (m, 6H); HRMS (ESI) calculated for $C_{36}H_{37}O_4$ ($[M+H]^+$) *m/z* = 533.2692, found 533.2679.

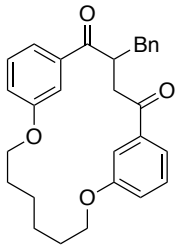

41b-Bn

2-benzyl-1,4-butanedione 41b-Bn: white solid (0.0315 g, 47%): R_f = 0.22 (10% ethyl acetate/hexanes); ^{1}H NMR (600 MHz, $CDCl_3$) δ 7.60 (d, *J* = 7.8 Hz, 1H), 7.54 – 7.44 (m, 3H), 7.42 (d, *J* = 4.9 Hz, 1H), 7.35 (t, *J* = 7.5 Hz, 2H), 7.28 (d, *J* = 8.1 Hz, 4H), 7.23 (dd, *J* = 7.9, 2.4 Hz, 1H), 7.17 (dd, *J* = 8.2, 2.4 Hz, 1H), 4.29 – 4.17 (m, 4H), 4.10 (td, *J* = 9.1, 3.9 Hz, 1H), 3.51 (dd, *J* = 13.1, 6.2 Hz, 1H), 3.42 (dd, *J* = 13.9, 8.8 Hz, 1H), 3.05 – 2.96 (m, 2H), 1.99 – 1.90 (m, 4H), 1.82 – 1.67 (m, 4H); ^{13}C NMR (126 MHz, $CDCl_3$) δ 202.07, 199.60, 159.29, 159.11, 139.19, 138.35, 137.90, 130.19, 130.08, 129.31, 128.60, 126.53, 120.62, 120.59, 118.45, 117.96, 115.65, 115.48, 67.50, 67.24, 45.73, 42.64, 37.28, 28.10, 28.04, 24.77, 24.72; HRMS (ESI) calculated for $C_{29}H_{31}O_4Na$ ($[M+H]^+$) *m/z* = 443.2222, found 443.2213.

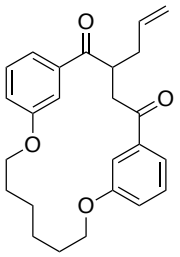

41b-Allyl

2-allyl-1,4-butanedione 41b-Allyl: A solution of **diketone 19.4** (0.032 g, 0.090 mmol) in THF (0.36 mL) was added to a stirring solution of LDA (0.4 M, 0.49 mL, 0.20 mmol) in THF at –78 °C. After stirring for 1 h at –78 °C, HMPA (50% v/v solution in THF, 0.04 mL, 0.1 mmol) and AllylBr (0.02 mL, 0.2 mmol) was added, and the reaction slowly warmed to room temperature. After 25 h, the reaction was cooled back to –78 °C, and 1 M HCl (1 mL) was added. The aqueous

phase was extracted with chloroform (4 × 1 mL). The combined organic extracts were dried over $MgSO_4$, filtered, and concentrated under reduced pressure. The residue was purified with flash chromatography (1.3 × 18 cm, hexanes to 20% ethyl acetate/hexanes) to afford **41b-Allyl** as a white solid (0.0034 g, 10%): R_f = 0.21 (20% ethyl acetate/hexanes); ^{1}H NMR (600 MHz, $CDCl_3$) δ 7.56 (d, *J* = 7.7 Hz, 1H), 7.49 (d, *J* = 7.4 Hz, 1H), 7.41 – 7.38 (m, 2H), 7.29 (m, 2H), 7.09 – 7.06 (m, 2H), 5.67 (ddt, *J* = 17.1, 10.2, 6.9 Hz, 1H), 5.03 (d, *J* = 17.1 Hz, 1H), 4.95 (d, *J* = 10.2 Hz, 1H), 4.15 – 4.10 (m, 2H), 4.03 – 3.98 (m, 2H), 3.91 (ddt, *J* = 14.2, 9.0, 5.3 Hz, 1H), 3.35 (dd, *J* = 13.1, 5.6 Hz, 1H), 2.76 (dd, *J* = 13.1, 8.6 Hz, 1H), 2.67 (dt, *J* = 15.1, 7.9 Hz, 1H), 2.29 (dt, *J* = 13.4, 6.0 Hz, 1H), 1.85 (ddd, *J* = 15.0, 10.0, 5.7 Hz, 2H), 1.82 – 1.74 (m, 2H), 1.72 – 1.64 (m, 2H), 1.63 – 1.54 (m, 2H); ^{13}C NMR (126 MHz, $CDCl_3$) δ 202.03, 199.56, 159.33, 159.26, 138.33, 137.88, 135.18, 130.26, 130.24, 120.71, 120.59, 118.33, 118.12, 117.70, 115.80, 115.77, 67.74, 67.29, 43.25, 42.46, 35.66, 28.24, 28.07, 25.02, 24.83; HRMS (ESI) calculated for $C_{25}H_{29}O_4$ ($[M+H]^+$) *m/z* = 393.2066, found 393.2081.

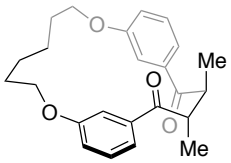

41a

(*rac*)-2,3-dimethyl-1,4-butanedione 41a: A solution of **diketone 19.4** (0.025 g, 0.070 mmol) in THF (0.28 mL) was added to a stirring solution of LDA (0.41 M, 0.61 mL, 0.25 mmol) in THF at –78 °C. After stirring for 1 h at –78 °C, HMPA (50% v/v solution in THF, 0.05 mL, 0.1 mmol) and MeI (9.9 µL, 0.16 mmol) was added, and the reaction slowly warmed to room temperature. After 4 days, the reaction was cooled back to –78 °C, and 1 M HCl (1 mL) was added. The aqueous phase was extracted with chloroform (4 × 1 mL). The combined organic extracts were dried over $MgSO_4$, filtered, and concentrated under reduced pressure. The residue was purified with flash chromatography (1.0 × 16 cm, 10% ethyl acetate/hexanes) to afford (*rac*)-2,3-dimethyl-1,4-dione **41a** as a white solid (0.0010 g, 4%): R_f = 0.53 (20% ethyl acetate/hexanes); ^{1}H NMR (600 MHz, $CDCl_3$) δ 7.50 (d, *J* = 8.0 Hz, 2H), 7.46 – 7.42 (m, 2H), 7.40 – 7.36 (m, 2H), 7.10 (dd, *J* = 8.0, 2.5 Hz, 2H), 4.16 (dt, *J* = 9.2, 4.7 Hz, 2H), 4.01 (td, *J* = 9.0, 3.9 Hz, 2H), 3.80 (qd, *J* = 5.1, 2.9 Hz, 2H), 2.00 – 1.80 (m, 4H), 1.78 – 1.65 (m, 4H), 1.02 (d, *J* = 6.3 Hz, 6H); ^{13}C NMR (151 MHz, $CDCl_3$) δ 202.39, 159.17, 138.27, 130.45, 120.36, 116.32, 115.48, 67.36, 42.13, 27.59, 24.76, 9.37; HRMS (ESI) calculated for $C_{24}H_{28}O_4Na$ ($[M+Na]^+$) *m/z* = 403.1885, found 403.1873.

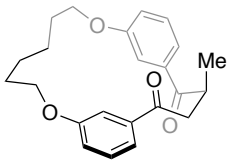

41b-Me

2-methyl-1,4-butanedione 41b-Me: white solid (0.0034 g, 13%): R_f = 0.46 (20% ethyl acetate/hexanes); ^{1}H NMR (600 MHz, $CDCl_3$) δ 7.58 (d, *J* = 7.7 Hz, 1H), 7.53 (d, *J* = 7.7 Hz, 1H), 7.41 (m, 3H), 7.35 (m, 1H), 7.10 (dd, *J* = 8.0, 2.5 Hz, 2H), 4.16 (dt, *J* = 9.3, 4.6 Hz, 2H), 4.00 (td, *J* = 9.1, 3.7 Hz, 2H), 3.89 (td, *J* = 6.5, 3.4 Hz, 1H), 3.47 (dd, *J* = 12.7, 4.4 Hz, 1H), 2.54 (dd, *J* = 12.7, 10.3 Hz, 1H), 1.95 – 1.62 (m, 8H), 1.20 (d, *J* = 6.6 Hz, 3H); ^{13}C NMR (126 MHz, $CDCl_3$) δ

202.63, 199.49, 159.38, 159.35, 137.75, 137.73, 130.40, 120.80, 120.46, 117.91, 117.74, 116.30, 115.89, 68.03, 67.53, 43.96, 38.16, 28.22, 28.02, 25.30, 25.06, 15.83; HRMS (ESI) calculated for $C_{23}H_{27}O_4$ ([M+Na]$^+$) *m/z* = 367.1909, found 367.1897.

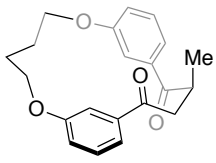

14x

Table 11, entry 1: A solution of **diketone 19.2** in THF (50 mM, 0.62 mL, 0.031 mmol) was added to a stirring solution of LDA (0.10 M, 0.68 mL, 0.068 mmol) in THF at –78 °C. After stirring for 1 h at –78 °C, HMPA (50% v/v solution in THF, 0.02 mL, 0.06 mmol) and MeI (4.4 µL, 0.071 mmol) was added, and the reaction slowly warmed to room temperature. After 24 h, the reaction was cooled back to –78 °C, and 1 M HCl (1 mL) was added. The aqueous phase was extracted with chloroform (4 × 1 mL). The combined organic extracts were dried over $MgSO_4$, filtered, and concentrated under reduced pressure. The residue was purified with flash chromatography (1.0 × 10 cm, 10% to 20% ethyl acetate/hexanes) to afford 2-methyl-1,4-dione **14x** as a white solid (0.0024 g, 23%): R_f = 0.32 (20% ethyl acetate/hexanes); ^{1}H NMR (400 MHz, $CDCl_3$) δ 7.59 – 7.50 (m, 2H), 7.47 – 7.38 (m, 2H), 7.31 (dd, *J* = 2.1 Hz, 1H), 7.24 (dd, *J* = 2.5, 1.7 Hz, 1H), 7.19 – 7.10 (m, 2H), 4.43 – 4.32 (m, 2H), 4.17 – 4.01 (m, 2H), 3.80 – 3.67 (m, 1H), 3.42 (dd, *J* = 12.1, 3.6 Hz, 1H), 2.43 (dd, *J* = 12.1, 10.5 Hz, 1H), 2.10 – 1.93 (m, 4H), 1.25 (d, *J* = 6.5 Hz, 3H); ^{13}C NMR (151 MHz, $CDCl_3$) δ 202.38, 199.41, 158.47, 137.74, 137.49, 130.43, 130.41, 121.03, 120.72, 119.71, 119.35, 115.93, 114.77, 68.46, 68.04, 43.90, 38.62, 26.18, 25.91, 14.75; HRMS (ESI) calculated for $C_{21}H_{22}O_4Na$ ([M+Na]$^+$) *m/z* =361.1416, found 361.1405.

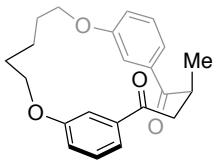

14y

Table 11, entry 2: A solution of **diketone 19.3** (0.0124 g, 0.0366 mmol) in THF (0.30 mL) was added to a stirring solution of LDA (0.1 M, 0.7 mL, 0.7 mmol) in THF at –78 °C. After stirring for 1 h at –78 °C, HMPA (50% v/v solution in THF, 0.02 mL, 0.06 mmol) and MeI (4.0 µL, 0.064 mmol) was added, and the reaction slowly warmed to room temperature. After 3 days, the reaction was cooled back to –78 °C, and 1 M HCl (1 mL) was added. The aqueous phase was extracted with chloroform (4 × 1 mL). The combined organic extracts were dried over $MgSO_4$, filtered, and concentrated under reduced pressure. The residue was purified with flash chromatography (1.0 × 10 cm, 20% ethyl acetate/hexanes) to afford 2-methyl-1,4-dione **14y** as a white solid (0.0041 g, 32%): R_f = 0.38 (20% ethyl acetate/hexanes); ^{1}H NMR (400 MHz, $CDCl_3$) δ 7.54 (ddd, *J* = 7.7, 1.7, 1.0 Hz, 1H), 7.50 (ddd, *J* = 7.7, 1.6, 1.0 Hz, 1H), 7.41 – 7.35 (m, 2H), 7.34 – 7.32 (m, 2H), 7.13 – 7.05 (m, 2H), 4.19 (ddd, *J* = 10.0, 6.1, 5.0 Hz, 2H), 4.05 (ddd, *J* = 9.4, 7.2, 5.6 Hz, 2H), 3.93 – 3.79 (m, 1H), 3.46 (dd, *J* = 13.0, 4.9 Hz, 1H), 2.56 (dd, *J* = 13.1, 9.0 Hz, 1H), 1.93 – 1.81 (m, 4H), 1.76 (q, *J* = 6.3 Hz, 2H), 1.26 (d, *J* = 6.5 Hz, 3H); ^{13}C NMR (151 MHz, CDCl3) δ 202.66, 199.64, 159.12, 158.98, 137.67, 137.62, 130.41, 130.38, 120.91, 120.55,

118.94, 118.75, 115.82, 115.17, 67.92, 67.78, 44.25, 38.56, 28.15, 27.87, 21.85, 15.79; HRMS (ESI) calculated for $C_{22}H_{24}O_4Na$ ([M+Na]$^+$) *m/z* =375.1572, found 375.1558.

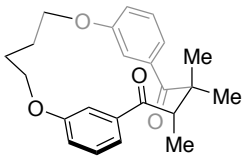

41g

Table 11, entry 4: A solution of **diketone 19.2** (0.0215 g, 0.0663 mmol) in THF (0.30 mL) was added to a stirring suspension of NaH (60% in oil, 0.0.202 g, 0.505 mmol) in THF (0.30 mL) at 0 °C. After stirring for 1.5 h at 0 °C, MeI (0.02 mL, 0.32 mmol) was added, and the reaction was allowed to warm to room temperature. After 21 h, a saturated solution of NH_4Cl (1 mL) was slowly added. The resulting mixture was extracted with ethyl acetate (3 × 1 mL). The organic extracts were dried over $MgSO_4$, filtered, and concentrated under reduced pressure. The residue was purified via flash chromatography (1.0 × 10 cm, hexanes to 15% ethyl acetate/hexanes) to afford 2,2,3-trimethyl-1,4-dione **41g** as a white solid. (0.0010 g, 4%): R_f = 0.50 (20% ethyl acetate/hexanes); ^{1}H NMR (600 MHz, $CDCl_3$) δ 7.54 (d, *J* = 7.6 Hz, 1H), 7.42 – 7.35 (m, 4H), 7.23 (d, *J* = 7.7 Hz, 1H), 7.14 (dd, *J* = 8.3, 2.4 Hz, 1H), 7.02 (dd, *J* = 8.0, 2.5 Hz, 1H), 4.36 – 4.28 (m, 3H), 4.21 – 4.11 (m, 2H), 2.16 – 1.97 (m, 4H), 1.42 (s, 3H), 1.36 (s, 3H), 1.09 (d, *J* = 6.8 Hz, 3H); ^{13}C NMR (151 MHz, $CDCl_3$) δ 203.05, 158.50, 158.41, 130.31, 130.24, 121.31, 121.10, 120.52, 116.42, 114.86, 114.54, 113.82, 109.99, 68.53, 68.52, 55.39, 51.06, 48.76, 43.44, 31.66, 26.53, 25.42, 24.75, 20.51, 19.49, 13.59; HRMS (ESI) calculated for $C_{23}H_{27}O_4$ ([M+H]$^+$) *m/z* =367.1909, found 367.1922.

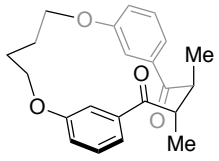

41d

(*rac*)-2,3-dimethyl-1,4-dione 41d: white solid (0.0027 g, 12%): R_f = 0.38 (20% ethyl acetate/hexanes); ^{1}H NMR (600 MHz, $CDCl_3$) δ 7.52 (d, *J* = 7.6 Hz, 2H), 7.47 – 7.43 (m, 2H), 7.31 – 7.29 (m, 2H), 7.16 (dd, *J* = 8.1, 2.5 Hz, 2H), 4.45 – 4.41 (m, 2H), 4.05 – 3.99 (m, 2H), 3.70 (q, *J* = 5.8 Hz, 2H), 2.11 – 2.01 (m, 4H), 1.02 (d, *J* = 6.4 Hz, 6H); ^{13}C NMR (151 MHz, $CDCl_3$) δ 202.02, 158.61, 138.17, 130.52, 120.78, 119.03, 114.63, 68.17, 42.14, 26.43, 8.63; HRMS (ESI) calculated for $C_{22}H_{25}O_4$ ([M+H]$^+$) *m/z* =353.1753, found 353.1779.

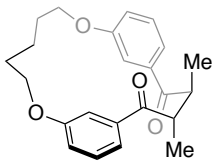

41e

Table 11, entry 5: A solution of **diketone 19.3** (0.0231 g, 0.0683 mmol) in THF (0.30 mL) was added to a stirring suspension of NaH (0.0109 g, 0.273 mmol) in THF (0.30 mL) at 0 °C. After stirring for 1 h at 0 °C, MeI (0.02 mL, 0.3 mmol) was added, and the reaction was allowed to warm to room temperature. After 20 h, a saturated solution of NH_4Cl (0.5 mL) was slowly added. The resulting mixture was extracted with ethyl acetate (3 × 1 mL). The organic extracts were dried over $MgSO_4$, filtered, and concentrated under reduced pressure. The residue was purified via automated flash chromatography (4 g silica cartridge, ethyl acetate and hexanes) to afford (*rac*)-2,3-dimethyl-1,4-dione **41e** as a white solid. (0.0250 g, 50%): R_f = 0.38 (20% ethyl

acetate/hexanes); ^{1}H NMR (600 MHz, $CDCl_3$) δ 7.52 (d, *J* = 7.7 Hz, 2H), 7.47 – 7.39 (m, 4H), 7.12 (dd, *J* = 8.3, 2.4 Hz, 2H), 4.28 – 4.22 (m, 2H), 4.02 (td, *J* = 8.2, 5.5 Hz, 2H), 3.79 (q, *J* = 5.5 Hz, 2H), 1.98 – 1.88 (m, 4H), 1.86 – 1.78 (m, 2H), 1.01 (d, *J* = 6.2 Hz, 6H); ^{13}C NMR (126 MHz, $CDCl_3$) δ 202.22, 159.31, 138.42, 130.58, 120.85, 118.22, 114.83, 67.97, 42.70, 28.51, 21.97, 9.50; HRMS (ESI) calculated for $C_{23}H_{26}O_4Na$ ([M+Na]$^+$) *m/z* =389.1729, found 389.1711.

Table 11, entry 6: A solution of **diketone 19.4** (0.2376 g, 0.6742 mmol) in THF (3.7 mL) was added to a stirring suspension of NaH (0.1543 g, 3.858 mmol) in THF (3.7 mL) at 0 °C. After stirring for 1 h at 0 °C, MeI (0.24 mL, 3.9 mmol) was added, and the reaction was allowed to warm to room temperature. After 5 h, a saturated solution of NH_4Cl (10 mL) was slowly added. The resulting mixture was extracted with ethyl acetate (3 × 10 mL). The organic extracts were combined and washed with brine (10 mL), dried over $MgSO_4$, filtered, and concentrated under reduced pressure. The residue was purified via flash chromatography (2.5 × 18 cm, hexanes to 10% ethyl acetate/hexanes) to afford (*rac*)-2,3-dimethyl-1,4-dione **41a** as a white solid. (0.1448 g, 53%) and 2-methyl-1,4-dione **41b-Me** as a white solid (0.0119 g, 5%)

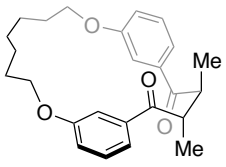

41f

Table 11, entry 7: A solution of **diketone 19.5** (0.0210 g, 0.057 mmol) in THF (0.30 mL) was added to a stirring suspension of NaH (0.0114 g, 0.285 mmol) in THF (0.30 mL) at 0 °C. After stirring for 2 h at 0 °C, MeI (0.02 mL, 0.32 mmol) was added, and the reaction was allowed to warm to room temperature. After 3 days, a saturated solution of NH_4Cl (1 mL) was slowly added. The resulting mixture was extracted with ethyl acetate (3 × 1 mL). The organic extracts were combined and dried over $MgSO_4$, filtered, and concentrated under reduced pressure. The residue was purified via flash chromatography (1.0 × 10 cm, 20% ethyl acetate/hexanes) to afford (*rac*)-2,3-dimethyl-1,4-dione **41f** as a white solid. (0.0098 g, 43%): R_f = 0.56 (20% ethyl acetate/hexanes); ^{1}H NMR (500 MHz, $CDCl_3$) δ 7.58 (d, *J* = 7.6 Hz, 2H), 7.49 (t, *J* = 7.7 Hz, 2H), 7.38 (d, *J* = 5.9 Hz, 2H), 7.20 (d, *J* = 8.2 Hz, 2H), 4.15 (p, *J* = 8.6, 7.4 Hz, 4H), 3.95 (t, *J* = 5.6 Hz, 2H), 1.93 (m, 4H), 1.62 (m, 6H), 1.29 (d, *J* = 5.4 Hz, 6H); ^{13}C NMR (126 MHz, $CDCl_3$) δ 203.86, 159.34, 138.82, 130.11, 120.78, 119.69, 113.13, 67.81, 44.04, 28.01, 27.23, 25.12, 12.84; HRMS (ESI) calculated for $C_{25}H_{30}O_4Na$ ([M+Na]$^+$) *m/z* =417.2-42, found 417.2039.

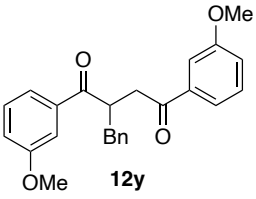

12y

2-benzyl-1,4-bis(3-methoxyphenyl)-1,4-butanedione 12y: A solution of **diketone 39a** (0.0294 g, 0.0985 mmol) in THF (1.0 mL) was added to a stirring solution of LDA (0.1 M, 2.2 mL, 0.21 mmol) in THF at –78 °C. After stirring for 1 h at –78 °C, HMPA (50% v/v solution in THF, 0.08 mL, 0.2 mmol) and BnBr (0.027 mL, 0.23 mmol) was added, and the reaction slowly warmed to room temperature. After 43 h, the reaction was cooled back to –78 °C, and 1 M

HCl (3.5 mL) was added. The aqueous phase was extracted with chloroform (3 × 4 mL). The combined organic extracts were dried over $MgSO_4$, filtered, and concentrated under reduced pressure. The residue was purified with flash chromatography (1.3 × 16 cm, 10 to 20% ethyl acetate/hexanes) to afford 2-benzyl-1,4-dione **12y** as a clear oil (0.014 g, 36%): R_f = 0.25 (20% ethyl acetate/hexanes); ^{1}H NMR (500 MHz, $CDCl_3$) δ 7.68 (dt, *J* = 7.7, 1.2 Hz, 1H), 7.54 (dd, *J* = 2.6, 1.5 Hz, 1H), 7.51 (dt, *J* = 7.7, 1.3 Hz, 1H), 7.42 (dd, *J* = 2.7, 1.5 Hz, 1H), 7.40 (t, *J* = 7.9 Hz, 1H), 7.34 (t, *J* = 7.9 Hz, 1H), 7.31 – 7.26 (m, 2H), 7.25 – 7.19 (m, 3H), 7.12 (ddd, *J* = 8.2, 2.7, 0.9 Hz, 1H), 7.09 (ddd, *J* = 8.3, 2.7, 1.0 Hz, 1H), 4.38 (tdd, *J* = 9.4, 5.7, 4.1 Hz, 1H), 3.86 (s, 3H), 3.82 (s, 3H), 3.77 – 3.65 (m, 1H), 3.16 (dd, *J* = 13.7, 5.6 Hz, 1H), 3.10 (dd, *J* = 18.0, 4.0 Hz, 1H), 2.73 (dd, *J* = 13.7, 9.0 Hz, 1H); ^{13}C NMR (126 MHz, $CDCl_3$) δ 202.62, 198.44, 160.06, 159.92, 138.84, 138.13, 138.04, 129.82, 129.69, 129.21, 128.81, 126.83, 121.28, 121.00, 120.01, 119.83, 112.90, 112.29, 55.60, 55.59, 43.76, 40.63, 38.42.

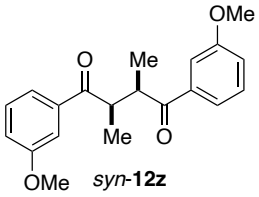

syn-**12z**

***syn*-2,3-dimethyl-1,4-bis(3-methoxyphenyl)-1,4-butanedione 12z:** A solution of **diketone 39a** (0.0260 g, 0.0871 mmol) in THF (0.40 mL) was added to a stirring suspension of NaH (60% in oil, 0.0149 g, 0.373 mmol) in THF (0.20 mL) at 0 °C. After stirring for 1 h at 0 °C, MeI (0.02 mL, 0.3 mmol) was added. After 5.5 h at 0 °C, a saturated solution of NH_4Cl (0.5 mL) was slowly added. The resulting mixture was extracted with ethyl acetate (3 × 1 mL). The organic extracts were combined and washed with water (1 mL) and brine (1 mL), dried over $MgSO_4$, filtered, and concentrated under reduced pressure. The residue was purified via flash chromatography (1.0 × 10 cm, hexanes to 30% ethyl acetate/hexanes) to afford *syn*-2,3-dimethyl-1,4-dione **12z** as a colorless oil (0.0022 g, 8%): R_f = 0.39 (30% ethyl acetate/hexanes) and *anti*-2,3-dimethyl-1,4-dione **12z** as a colorless oil (0.0054 g, 19%): R_f = 0.33 (30% ethyl acetate/hexanes); ^{1}H NMR (600 MHz, $CDCl_3$) δ 7.66 (d, *J* = 7.9 Hz, 2H), 7.58 – 7.55 (m, 2H), 7.42 (t, *J* = 8.1 Hz, 2H), 7.18 – 7.14 (m, 2H), 4.07 – 3.98 (m, 2H), 3.89 (s, 6H), 1.14 (d, *J* = 5.4 Hz, 6H); ^{13}C NMR (126 MHz, $CDCl_3$) δ 203.71, 160.21, 138.46, 129.94, 121.29, 120.08, 112.81, 55.68, 43.72, 17.69.

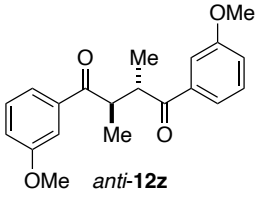

anti-**12z**

***anti*-2,3-dimethyl-1,4-bis(3-methoxyphenyl)-1,4-butanedione 12z:** ^{1}H NMR (600 MHz, $CDCl_3$) δ 7.64 – 7.59 (m, 2H), 7.49 – 7.46 (m, 2H), 7.41 – 7.36 (m, 2H), 7.11 (dd, *J* = 8.5, 2.6 Hz, 2H), 3.94 (dd, *J* = 4.8, 2.4 Hz, 1H), 3.85 (s, 6H), 1.32 – 1.26 (m, 6H) ; ^{13}C NMR (126 MHz, $CDCl_3$) δ 204.25, 160.06, 137.69, 129.78, 121.29, 119.82, 112.80, 55.60, 44.03, 15.73.

Table 13, entry 2: A solution of **diketone 19.4** (0.02 g, 0.06 mmol) in THF (0.3 mL) was added to a stirring solution of LiHMDS (0.0397 g, 0.237 mmol) in THF (0.6 mL) at –78 °C. HMPA (0.10 mL, 0.57 mmol) and MeI (0.035 mL, 0.57 mmol) were then added sequentially. After 1 h the reaction was allowed to slowly warm to room temperature. After 4 h the reaction was cooled back to 0 °C, and a saturated solution of NH_4Cl (0.9 mL) was slowly added. The resulting mixture was extracted with ethyl acetate (3 × 1 mL). The organic extracts were combined and washed with water (2 mL) and brine (2 mL), dried over $MgSO_4$, filtered, and concentrated under reduced pressure. The residue was purified via flash chromatography (1.0 × 10 cm, hexanes to 20% ethyl acetate/hexanes) to afford (*rac*)-2,3-dimethyl-1,4-dione **41a** as a white solid (0.0051 g, 24%) and 2-methyl-1,4-dione **41b-Me** as a white solid (0.0034 g, 16%).

Table 13, entry 3: A solution of **diketone 19.4** (0.0267 g, 0.0758 mmol) in THF (0.3 mL) and MeI (0.014 mL, 0.23 mmol) were added sequentially to a stirring solution of LiHMDS (0.0370 g, 0.221 mmol) in THF (0.3 mL) at –78 °C. The reaction was then allowed to slowly warm to room temperature. After 21 h, a saturated solution of NH_4Cl (1 mL) was slowly added. The resulting mixture was extracted with ethyl acetate (3 × 1 mL). The organic extracts were combined and washed with water (1 mL) and brine (1 mL), dried over $MgSO_4$, filtered, and concentrated under reduced pressure. The residue was purified via flash chromatography (1.0 × 18 cm, hexanes to 10% ethyl acetate/hexanes) to afford (*rac*)-2,3-dimethyl-1,4-dione **41a** as a white solid (0.0045 g, 16%) and 2-methyl-1,4-dione **41b-Me** as a white solid (0.0053 g, 19%).

Table 13, entry 4: A solution of **diketone 19.4** (0.0508 g, 0.144 mmol) in THF (0.9 mL) was added to a stirring suspension of NaH (0.0299 g, 0.748 mmol) in THF (0.5 mL) at –20 °C. After stirring for 1 h at –20 °C, MeI (0.05 mL, 0.8 mmol) was added. The reaction was kept between –20 and 0 °C for 15 h then allowed to slowly warm to room temperature. After 6 h at room temperature, a saturated solution of NH_4Cl (1.5 mL) was slowly added. The resulting mixture was extracted with ethyl acetate (3 × 2 mL). The organic extracts were combined and dried over $MgSO_4$, filtered, and concentrated under reduced pressure. The residue was purified via flash chromatography (1.3 × 20 cm, hexanes to 30% ethyl acetate/hexanes) to afford an inseparable mixture of (*rac*)-2,3-dimethyl-1,4-dione **41a** and (*rac*)-2,2,3-trimethyl-1,4-dione **41h** as a white solid (0.0100 g, 5.6:1 *vic:tri* by NMR, 15% and 3%, respectively).

Table 13, entry 5: A solution of **diketone 19.4** (0.0616 g, 0.175 mmol) in THF (1.0 mL) was added to a stirring suspension of NaH (0.0305 g, 0.763 mmol) in THF (0.5 mL) at 0 °C. After stirring for 1 h at 0 °C, MeI (0.045 mL, 0.72 mmol) was added. After 6 h at 0 °C, a saturated solution of NH_4Cl (2 mL) was slowly added. The resulting mixture was extracted with ethyl

acetate (3 × 2 mL). The organic extracts were combined and dried over $MgSO_4$, filtered, and concentrated under reduced pressure. The residue was purified via flash chromatography (1.3 × 18 cm, hexanes to 30% ethyl acetate/hexanes) to afford an inseparable mixture of (*rac*)-2,3-dimethyl-1,4-dione **41a** and (*rac*)-2,2,3-trimethyl-1,4-dione **41h** as a white solid (0.0321 g, 12:1 *vic:tri* by NMR, 45% and 4%, respectively).

Table 13, entry 7: A solution of **diketone 19.4** (0.0157 g, 0.0445 mmol) in 1,4-dioxane (0.2 mL) and MeI (0.02 mL, 0.32 mmol) were added sequentially to a stirring suspension of NaH (0.014 g, 0.35 mmol) in 1,4-dioxane (0.5 mL) at room temperature. After 5 h, the reaction was cooled to 0 °C and a saturated solution of NH_4Cl (1 mL) was slowly added. The resulting mixture was extracted with ethyl acetate (3 × 1 mL). The organic extracts were combined and washed with water (3 mL) and brine (3 mL), dried over $MgSO_4$, filtered, and concentrated under reduced pressure. The residue was purified via automated flash chromatography (4 g silica, hexanes to 80% ethyl acetate/hexanes) to afford an inseparable mixture of (*rac*)-2,3-dimethyl-1,4-dione **41a** and 2,2,3-trimethyl-1,4-dione **41h** as a white solid (0.0024 g, 2.5:1 *vic:tri* by NMR, 10% and 4%, respectively).

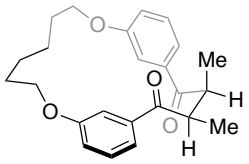

X.X

Table 13, entry 8: A solution of **diketone 19.4** (0.0174 g, 0.0494 mmol) in DMF (0.3 mL) and MeI (0.02 mL, 0.3 mmol) were added sequentially to a stirring suspension of NaH (0.0218 g, 0.545 mmol) in DMF (0.5 mL) at 0 °C. After stirring for 1 h at 0 °C, the reaction was allowed to warm to room temperature. After 5 h, the reaction was cooled back to 0 °C and a saturated solution of NH_4Cl (1 mL) was slowly added. The resulting mixture was extracted with ethyl acetate (3 × 1 mL). The organic extracts were combined and washed with water (2 mL) and brine (3 mL), dried over $MgSO_4$, filtered, and concentrated under reduced pressure. The residue was purified via automated flash chromatography (4 g silica cartridge, hexanes to 80% ethyl acetate/hexanes) to afford *syn*-2,3-dimethyl-1,4-dione **42a** as a white solid (0.0009 g, 5%): R_f = 0.45 (20% ethyl acetate/hexanes); ^{1}H NMR (600 MHz, $CDCl_3$) δ 7.51 – 7.44 (m, 2H), 7.40 (t, J = 8.3 Hz, 2H), 7.10 – 6.99 (m, 4H), 4.13 – 4.07 (m, 2H), 3.96 (ddd, J = 9.6, 7.0, 3.8 Hz, 2H), 3.78 – 3.71 (m, 2H), 1.89 – 1.75 (m, 8H), 1.26 (d, J = 6.1 Hz, 6H); ^{13}C NMR (126 MHz, $CDCl_3$) δ 201.66, 159.31, 138.77, 130.03, 120.02, 117.46, 116.60, 67.29, 43.95, 28.07, 24.66, 13.88.

Table 13, entry 9: A solution of **diketone 19.4** (0.0053 g, 0.015 mmol) in diethyl ether (1.0 mL) and MeI (0.02 mL, 0.3 mmol) were added sequentially to a stirring suspension of NaH (0.0194 g, 0.485 mmol) in diethyl ether (0.4 mL) at 0 °C. After stirring for 30 min at 0 °C, the reaction was allowed to warm to room temperature. After 4 h, the reaction was cooled back to 0 °C and a saturated solution of NH_4Cl (1 mL) was slowly added. The resulting mixture was extracted with

ethyl acetate (3 × 1 mL). The organic extracts were combined and washed with water (2 mL) and brine (2 mL), dried over $MgSO_4$, filtered, and concentrated under reduced pressure. The residue was purified via automated flash chromatography (4 g silica cartridge, hexanes to 80% ethyl acetate/hexanes), but only starting material (51%) was recovered.

Table 13, entry 10: A solution of **diketone 19.4** (0.02 g, 0.06 mmol) in THF (0.3 mL), HMPA (0.10 mL, 0.57 mmol), and MeI (0.035 mL, 0.57 mmol) were added sequentially to a stirring solution of NaHMDS (0.0447 g, 0.239 mmol) in THF (0.3 mL) at –78 °C. After 4.5 h, a saturated solution of NH_4Cl (1 mL) was slowly added. The resulting mixture was extracted with ethyl acetate (3 × 1 mL). The organic extracts were combined and washed with water (2 mL) and brine (2 mL), dried over $MgSO_4$, filtered, and concentrated under reduced pressure. The residue was purified via automated flash chromatography (4 g silica cartridge, hexanes to 80% ethyl acetate/hexanes) to afford (*rac*)-2,3-dimethyl-1,4-dione **41a** as a white solid (0.0046 g, 21%, 24% brsm) and 2-methyl-1,4-dione **41b-Me** as a white solid (0.0020 g, 10%, 11% brsm).

Table 13, entry 11: A solution of **diketone 19.4** (0.0213 g, 0.0604 mmol) in THF (0.2 mL), HMPA (0.1 mL, 0.6 mmol), and MeI (0.04 mL, 0.6 mmol) were added sequentially to a stirring solution of NaHMDS (0.0459 g, 0.245 mmol) in THF (1 mL) at –78 °C and the reaction was allowed to slowly warm to room temperature. After 4.5 h, the reaction was cooled to 0 °C and a saturated solution of NH_4Cl (1 mL) was slowly added. The resulting mixture was extracted with ethyl acetate (3 × 1 mL). The organic extracts were combined and washed with water (2 mL) and brine (2 mL), dried over $MgSO_4$, filtered, and concentrated under reduced pressure. The residue was purified via automated flash chromatography (4 g silica cartridge, hexanes to 80% ethyl acetate/hexanes) to afford an inseparable mixture of (*rac*)-2,3-dimethyl-1,4-dione **41a** and 2,2,3-trimethyl-1,4-dione **41h** as a white solid (0.0072 g, 60:1 *vic:tri* by NMR, 31%).

Table 13, entry 12: A solution of **diketone 19.4** (0.0118 g, 0.0335 mmol) in THF (0.21 mL) was added to a stirring solution of NaHMDS (0.0397 g, 0.212 mmol) in THF (1 mL) at –78 °C. After stirring for 1 h at –78 °C, MeI (14.2 µL, 0.228 mmol) was added, and the reaction was allowed to slowly warm to room temperature. After 18 h, the reaction was cooled to –78 °C, and 1 M HCl (1 mL) was slowly added. The resulting mixture was extracted with chloroform (5 × 1 mL). The organic extracts were combined and dried over $MgSO_4$, filtered, and concentrated under reduced pressure. The residue was purified via flash chromatography (1.0 × 20 cm, hexanes to 20% ethyl acetate/hexanes) to afford an inseparable mixture of (*rac*)-2,3-dimethyl-1,4-dione **41a** and 2,2,3-trimethyl-1,4-dione **41h** as a white solid (0.0054 g, 12:1 *vic:tri* by NMR, 39% and 3%, respectively) and 2-methyl-1,4-dione **41b-Me** as a white solid (0.0016 g, 13%).

Table 13, entry 13: A solution of **diketone 19.4** (0.0202 g, 0.0573 mmol) in THF (0.4 mL) was added to a stirring solution of NaHMDS (0.0368 g, 0.197 mmol) in THF (1 mL) at –78 °C and then warmed to 0 °C. After stirring for 2 h at 0 °C, the reaction was again cooled to –78 °C and MeI (14.2 µL, 0.228 mmol) was added. After 2 h at -78 °C, the reaction was allowed to slowly warm to room temperature. After 18 h, the reaction was again cooled to –78 °C, and 1 M HCl (1 mL) was slowly added. The resulting mixture was extracted with chloroform (4 × 1 mL). The organic extracts were combined and dried over $MgSO_4$, filtered, and concentrated under reduced pressure. The residue was purified via flash chromatography (1.0 × 20 cm, hexanes to 15% ethyl acetate/hexanes) to afford an inseparable mixture of (*rac*)-2,3-dimethyl-1,4-dione **41a** and 2,2,3-trimethyl-1,4-dione **41h** as a white solid (0.0027 g, 22:1 *vic:tri* by NMR, 22% and 0.5%, respectively) and 2-methyl-1,4-dione **41b-Me** as a white solid (0.0019 g, 9%).

Table 13, entry 14: A solution of **diketone 19.4** (0.0202 g, 0.0573 mmol) in THF (0.4 mL) and MeI (14.0 µL, 0.225 mmol) were added sequentially to a stirring solution of NaHMDS (0.0439 g, 0.235 mmol) in THF (1 mL) at –78 °C. After stirring for 3 h at –78 °C, the reaction was allowed to slowly warm to room temperature. After 18 h, the reaction was again cooled to –78 °C, and 1 M HCl (1 mL) was slowly added. The resulting mixture was extracted with chloroform (4 × 1 mL). The organic extracts were combined and dried over $MgSO_4$, filtered, and concentrated under reduced pressure. The residue was purified via flash chromatography (1.0 × 20 cm, hexanes to 15% ethyl acetate/hexanes) to afford an inseparable mixture of (*rac*)-2,3-dimethyl-1,4-dione **41a** and 2,2,3-trimethyl-1,4-dione **41h** as a white solid (0.0045 g, 24:1 *vic:tri* by NMR, 20% and 1%, respectively) and 2-methyl-1,4-dione **41b-Me** as a white solid (0.0014 g, 7%).

Table 13, entry 15: A solution of **diketone 19.4** (0.02 g, 0.06 mmol) in THF (0.3 mL), HMPA (0.10 mL, 0.57 mmol), and MeI (0.04 mL, 0.6 mmol) were added sequentially to a stirring solution of KHMDS (0.0450 g, 0.226 mmol) in THF (0.3 mL) at –78 °C. After 1 h at –78 °C, a saturated solution of NH_4Cl (1 mL) was slowly added. The resulting mixture was extracted with ethyl acetate (3 × 1 mL). The organic extracts were combined and washed with water (2 mL) and brine (2 mL), dried over $MgSO_4$, filtered, and concentrated under reduced pressure. The residue was purified via automated flash chromatography (4 g silica cartridge, hexanes to 80% ethyl acetate/hexanes) to afford (*rac*)-2,3-dimethyl-1,4-dione **41a** as a white solid (0.0065 g, 30%) and an inseparable mixture of 2-methyl-1,4-dione **41b-Me** and *syn*-2,3-dimethyl-1,4-dione **42a** as a white solid (0.0010 g, 6:1 *mono:vic* by NMR, 4%).

Table 13, entry 16: A solution of **diketone 19.4** (0.0178 g, 0.0505 mmol) in THF (0.35 mL) and MeI (14 µL, 0.23 mmol) were added sequentially to a stirring solution of KHMDS (0.0386 g, 0.194 mmol) in THF (0.3 mL) at –78 °C. After 5.5 h at –78 °C, a saturated solution of NH_4Cl (1 mL) was

slowly added. The resulting mixture was extracted with ethyl acetate (3 × 1 mL). The organic extracts were combined and washed with water (2 mL) and brine (2 mL), dried over $MgSO_4$, filtered, and concentrated under reduced pressure. The residue was purified via automated flash chromatography (4 g silica cartridge, hexanes to 80% ethyl acetate/hexanes) to afford (*rac*)-2,3-dimethyl-1,4-dione **41a** as a white solid (0.0071 g, 37%).

Table 13, entry 17: A solution of **diketone 19.4** (0.1629 g, 0.4622 mmol) in THF (1.7 mL) and MeI (0.14 mL, 2.2 mmol) were added sequentially to a stirring solution of KHMDS (0.4513 g, 2.262 mmol) in THF (2.0 mL) at –78 °C and then allowed to slowly warm to room temperature. After 2 h, the reaction was cooled back to 0 °C, and a saturated solution of NH_4Cl (5 mL) was slowly added. The resulting mixture was extracted with ethyl acetate (3 × 10 mL). The organic extracts were combined and washed with water (10 mL) and brine (20 mL), dried over $MgSO_4$, filtered, and concentrated under reduced pressure. The residue was purified via flash chromatography (1.3 × 20 cm, hexanes to 20% ethyl acetate/hexanes) to afford an inseparable mixture of (*rac*)-2,3-dimethyl-1,4-dione **41a** and 2,2,3-trimethyl-1,4-dione **41h** as a white solid (0.0446 g, 46:1 *vic:tri* by NMR, 25%) and an inseparable mixture of 2-methyl-1,4-dione **41b-Me** and *syn*-2,3-dimethyl-1,4-dione **42a** as a white solid (0.0158 g, 2:1 *mono:vic* by NMR, 6% and 3%, respectively).

Table 14, entry 1: MeLi (1.5 M, 0.14 mL, 0.21 mmol) was added to a stirring suspension of CuI (0.0208 g, 0.109 mmol) in THF (0.3 mL) at –40 °C. After 5 min, the reaction was warmed to room temperature for 10 min then cooled to –78 °C. A solution of (*Z*)-2-ene-1,4-dione **14w** (0.0138 g, 0.0394 mmol) in THF (0.3 mL) was slowly added. After 1 h at –78 °C, a saturated solution of NH_4Cl (1 mL) was slowly added. The resulting mixture was extracted with ethyl acetate (3 × 1 mL). The organic extracts were combined and washed with water (2 mL) and brine (2 mL), dried over $MgSO_4$, filtered, and concentrated under reduced pressure. The residue was purified via flash chromatography (1.0 × 10 cm, hexanes to 30% ethyl acetate/hexanes), but only starting material (19%) was recovered.

Table 14, entry 2: MeMgBr (3 M, 0.04 mL, 0.1 mmol) was added to a stirring suspension of CuI (0.0250 g, 0.131 mmol) in THF (0.6 mL) at 0 °C. After 30 min, a solution of (*Z*)-2-ene-1,4-dione **14w** (0.0163 g, 0.0465 mmol) in THF (0.26 mL) was slowly added. After 3 h at 0 °C, a saturated solution of NH_4Cl (1 mL) was slowly added. The resulting mixture was extracted with ethyl acetate (3 × 1 mL). The organic extracts were combined and washed with water (2 mL) and brine (2 mL), dried over $MgSO_4$, filtered, and concentrated under reduced pressure. The residue was purified via flash chromatography (1.0 × 10 cm, hexanes to 30% ethyl acetate/hexanes) to afford 2-methyl-1,4-dione **41b-Me** as a white solid (0.0024 g, 14%).

Table 14, entry 3: HMPA (0.015 mL, 0.0862 mmol) was added to a stirring suspension of CuI (0.0117 g, 0.0614 mmol) in THF (0.1 mL) and cooled to –30 °C. After 30 min, MeMgBr (3 M, 0.04 mL, 0.1 mmol) was added. After 40 min at –30 °C, the reaction was cooled to –78 °C and a solution of (*Z*)-2-ene-1,4-dione **14w** (0.0187 g, 0.0534 mmol) in THF (0.2 mL) was slowly added. After 5 h at –78 °C, the reaction was allowed to slowly warm to room temperature. After 4 days, the reaction was cooled to 0 °C, and a saturated solution of NH_4Cl (0.5 mL) was slowly added and the reaction mixture diluted with water (0.5 mL). The resulting mixture was extracted with ethyl acetate (3 × 1 mL). The organic extracts were combined and washed with water (1 mL) and brine (1 mL), dried over $MgSO_4$, filtered, and concentrated under reduced pressure. The residue was purified via flash chromatography (1.0 × 10 cm, hexanes to 30% ethyl acetate/hexanes), but only starting material (21%) was recovered.

Table 14, entry 4: HMPA (0.02 mL, 0.1 mmol) was added to a stirring suspension of CuBr•SMe_2 (0.0120 g, 0.058 mmol) in THF (0.1 mL) and cooled to –30 °C. After 30 min, MeMgBr (3 M, 0.04 mL, 0.1 mmol) was added. After 40 min at –30 °C, the reaction was cooled to –78 °C and a solution of (*Z*)-2-ene-1,4-dione **14w** (0.020 g, 0.057 mmol) in THF (0.3 mL) was slowly added. After 40 min, a saturated solution of NH_4Cl (1 mL) was slowly added. The resulting mixture was extracted with ethyl acetate (3 × 1 mL). The organic extracts were combined and washed with water (2 mL) and brine (2 mL), dried over $MgSO_4$, filtered, and concentrated under reduced pressure. The residue was purified via automated flash chromatography (4 g silica cartridge, hexanes to 80% ethyl acetate/hexanes), but only starting material (8%) was recovered.

Table 14, entry 5: MeMgBr (3 M, 0.09 mL, 0.3 mmol) was added to a stirring suspension of CuBr•SMe_2 (0.0025 g, 0.012 mmol) in THF (0.6 mL) at –78 °C. After 1 h, HMPA (0.03 mL, 0.2 mmol) was added. After 30 min at –78 °C, a solution of (*Z*)-2-ene-1,4-dione **14w** (0.0247 g, 0.0705 mmol) in THF (0.2 mL) and TMSCl (0.03 mL, 0.2 mmol) were added simultaneously. After 3.5 h, the reaction was allowed to warm to 0 °C over a 2 h period, after which a 3:1 solution of sat. NH_4Cl and sat. $NaHCO_3$ (1 mL) was slowly added. The resulting mixture was stirred until it became a deep blue, then it was extracted with ethyl acetate (3 × 1 mL). The organic extracts were combined and washed with water (1 mL) and brine (1 mL), dried over $MgSO_4$, filtered, and concentrated under reduced pressure. The residue was purified via automated flash chromatography (4 g silica cartridge, hexanes to 80% ethyl acetate/hexanes) to afford 2-methyl-1,4-dione **41b-Me** as a white solid (0.0052 g, 20%).

Table 14, entry 6: MeMgBr (3 M, 0.035 mL, 0.11 mmol) was added to a stirring suspension of CuBr•SMe_2 (0.0231 g, 0.112 mmol) in THF (0.4 mL) at 0 °C. After 20 min, the reaction was

cooled to –78 °C, and BF_3•OEt_2 (0.01 mL, 0.08 mmol) was slowly added followed by a solution of (*Z*)-2-ene-1,4-dione **14w** (0.0163 g, 0.0465 mmol) in THF (0.26 mL). The reaction was allowed to warm to room temperature. After 20 h, a saturated solution of NH_4Cl (1 mL) was slowly added. The resulting mixture was extracted with ethyl acetate (3 × 1 mL). The organic extracts were combined and washed with water (2 mL) and brine (2 mL), dried over $MgSO_4$, filtered, and concentrated under reduced pressure. The residue was purified via flash chromatography (1.0 × 10 cm, hexanes to 40% ethyl acetate/hexanes), but only starting material (27%) was recovered.

Table 14, entry 7: MeMgBr (3 M, 0.03 mL, 0.09 mmol) was added to a stirring suspension of CuI (0.0139 g, 0.0730 mmol) in THF (0.3 mL) at 0 °C. After 30 min, a solution of (*Z*)-2-ene-1,4-dione **14u** (0.0194 g, 0.0602 mmol) in THF (0.5 mL). After 4 h, the reaction was allowed to warm to room temperature. After 19 h, the reaction was cooled back to 0 °C and a saturated solution of NH_4Cl (0.5 mL) was slowly added and the reaction mixture diluted with water (0.5 mL). The resulting mixture was extracted with ethyl acetate (3 × 1 mL). The organic extracts were combined and washed with water (1 mL) and brine (1 mL), dried over $MgSO_4$, filtered, and concentrated under reduced pressure. The residue was purified via automated flash chromatography (4 g silica cartridge, hexanes to 80% ethyl acetate/hexanes), to afford an inseparble mixture of 2-methyl-1,4-dione **41b-Me** and starting material as a white solid (0.0017 g, 1.2:1 *S.M.:mono* by NMR, 4% 2-methyl-1,4-dione).

Table 14, entry 8: HMPA (0.02 mL, 0.1 mmol) was added to a stirring suspension of CuBr•SMe_2 (0.0134 g, 0.0652 mmol) in THF (0.1 mL) and the reaction cooled to –30 °C. After 30 min, MeMgBr (3 M, 0.04 mL, 0.1 mmol)was added. After another 30 min at –30 °C, the reaction was cooled to –78 °C. After 1 h at -78 °C, a solution of (*Z*)-2-ene-1,4-dione **14u** (0.0231 g, 0.0717 mmol) in THF (0.2 mL) was slowly added. After 2 h, a saturated solution of NH_4Cl (0.5 mL) was slowly added and the reaction mixture diluted with water (1 mL). The resulting mixture was extracted with ethyl acetate (3 × 1 mL). The organic extracts were combined and washed with water (1 mL) and brine (1 mL), dried over $MgSO_4$, filtered, and concentrated under reduced pressure. The residue was purified via automated flash chromatography (4 g silica cartridge, hexanes to 80% ethyl acetate/hexanes), but only starting material (9%) was recovered.

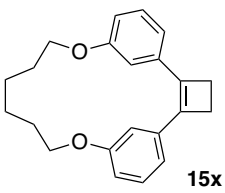

15x

Table 15, entry 1: Titanium(IV) chloride (0.04 mL, 0.4 mmol) was added to a slurry of zinc powder (0.0546 g, 0.835 mmol) in THF (1 mL) at 0 °C. After dissipation of the resulting yellow gas, the solution was heated to 68 °C. After 50 min., pyridine (0.10 mL, 1.2 mmol) was added, and 10 min. later diketone **19.4** (0.0189 g, 0.0536 mmol) as a solution in THF (2 mL) was added. The reaction was heated at 68 °C for 21 h, and then poured into chloroform (3 mL),

filtered through Celite, and concentrated under reduced pressure. The residue was purified via flash chromatography (hexanes to 5% ethyl acetate/hexanes) to afford **15x** as a white solid (0.0039 g, 23%): R_f = 0.63 (20% ethyl acetate/hexanes); ^{1}H NMR (500 MHz, $CDCl_3$) δ 7.48 (s, 2H), 7.29 (d, *J* = 8.8 Hz, 2H), 6.85 (m, 4H), 4.03 (td, *J* = 6.1, 2.4 Hz, 4H), 2.78 (d, *J* = 2.5 Hz, 4H), 1.79 – 1.71 (m, 4H), 1.58 – 1.50 (m, 4H); ^{13}C NMR (126 MHz, $CDCl_3$) δ 159.04, 139.26, 137.37, 129.78, 119.17, 115.19, 113.88, 68.48, 28.54, 26.96, 24.42; HRMS (ESI) calculated for $C_{22}H_{25}O_2$ ($[M+H]^+$) *m/z* = 321.1855, found 321.1853.

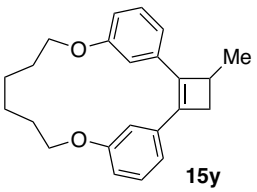

15y

Table 15, entry 2: Titanium(IV) chloride (0.04 mL, 0.4 mmol) was added to a slurry of zinc powder (0.1018 g, 1.557 mmol) in THF (1 mL) at 0 °C. After dissipation of the resulting yellow gas, the solution was heated to 68 °C. After 3 h, pyridine (0.06 mL, 0.7 mmol) was added, and 10 min. later 2-methyl-1,4-dione **41b-Me** (0.0173 g, 0.0472 mmol) as a solution in THF (2 mL) was added. The reaction was heated at 68 °C for 23 h, and then poured into chloroform (3 mL), filtered through Celite, and concentrated under reduced pressure. The residue was purified via flash chromatography (hexanes to 20% ethyl acetate/hexanes) to afford **15y** as a white solid (0.0158 g, 52%): R_f = 0.73 (20% ethyl acetate/hexanes); ^{1}H NMR (500 MHz, $CDCl_3$) δ 7.48 (s, 1H), 7.43 (s, 1H), 7.32 – 7.24 (m, 1H), 6.84 (m, 5H), 4.15 – 4.04 (m, 2H), 4.03 – 3.90 (m, 2H), 3.20 (t, *J* = 6.4 Hz, 1H), 2.88 (ddd, *J* = 13.1, 4.8, 2.4 Hz, 1H), 2.36 (d, *J* = 13.3 Hz, 1H), 1.74 (tt, *J* = 12.5, 6.5 Hz, 4H), 1.61 – 1.47 (m, 4H), 1.29 (dd, *J* = 7.1, 2.4 Hz, 3H); ^{13}C NMR (126 MHz, $CDCl_3$) δ 159.14, 158.97, 144.22, 137.28, 137.23, 136.53, 129.75, 119.28, 119.13, 115.39, 114.87, 114.71, 113.87, 68.55, 68.20, 35.37, 34.48, 28.53, 28.51, 24.43, 24.39, 18.59; HRMS (ESI) calculated for $C_{23}H_{27}O_4$ ($[M+H]^+$) *m/z* = 367.1909, found 367.1906.

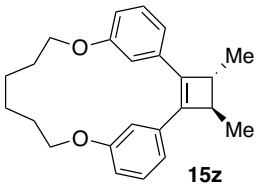

15z

Table 15, entry 3: Titanium(IV) chloride (0.03 mL, 0.3 mmol) was added to a slurry of zinc powder (0.0392 g, 0.600 mmol) in THF (1 mL) at 0 °C. After dissipation of the resulting yellow gas, the solution was heated to 68 °C. After 1.5 h, pyridine (0.10 mL, 1.2 mmol) was added, and 15 min. later (*rac*)-2,3-dimethyl-1,4-dione **41a** (0.0189 g, 0.0497 mmol) as a solution in THF (2 mL) was added. The reaction was heated at 68 °C for 19 h, and then poured into chloroform (3 mL), filtered through Celite, and concentrated under reduced pressure. The residue was purified via flash chromatography (hexanes to 5% ethyl acetate/hexanes) to afford **15z** as a white solid (0.0173 g, 81%): R_f = 0.71 (10% ethyl acetate/hexanes); ^{1}H NMR (400 MHz, $CDCl_3$) δ 7.44 (s, 2H), 7.30 (d, *J* = 7.8 Hz, 2H), 6.86 – 6.74 (m, 4H), 4.13 (dt, *J* = 10.6, 5.6 Hz, 2H), 3.93 (td, *J* = 10.1, 9.3, 6.1 Hz, 2H), 2.69 (q, *J* = 6.9 Hz, 2H), 1.82 – 1.63 (m, 4H), 1.61 – 1.44 (m, 4H), 1.25 (d, *J* = 6.9 Hz, 6H); ^{13}C NMR (151 MHz, $CDCl_3$) δ 158.99, 141.71, 136.04, 129.69,

119.28, 114.89, 114.59, 68.20, 42.57, 28.46, 24.34, 16.97; HRMS (ESI) calculated for $C_{24}H_{29}O_4$ ($[M+H]^+$) *m/z* =349.2168, found 349.2153.

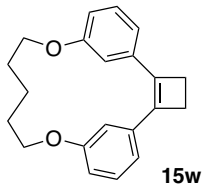

15w

Table 15, entry 4: Titanium(IV) chloride (0.05 mL, 0.5 mmol) was added to a slurry of zinc powder (0.0430 g, 0.658 mmol) in THF (1 mL) at 0 °C. After dissipation of the resulting yellow gas, the solution was heated to 68 °C. After 3 h, pyridine (0.06 mL, 0.7 mmol) was added, and 10 min. later diketone **19.3** (0.0155 g, 0.0458 mmol) as a solution in THF (2 mL) was added. The reaction was heated at 68 °C for 22 h, and then poured into chloroform (3 mL), filtered through Celite, and concentrated under reduced pressure. The residue was purified via flash chromatography (hexanes to 20% ethyl acetate/hexanes) to afford **15w** as a white solid (0.0140 g, 56%): R_f = 0.60 (20% ethyl acetate/hexanes); ^{1}H NMR (500 MHz, $CDCl_3$) δ 7.42 (s, 2H), 7.30 (dd, *J* = 8.1, 2.3 Hz, 2H), 6.89 (d, *J* = 7.6 Hz, 2H), 6.83 (d, *J* = 8.4 Hz, 2H), 4.12 (td, *J* = 7.1, 2.3 Hz, 4H), 2.77 (d, *J* = 2.6 Hz, 4H), 1.83 (m, 4H), 1.43 (tt, *J* = 6.9, 4.2 Hz, 2H); ^{13}C NMR (126 MHz, $CDCl_3$) δ 158.48, 138.98, 137.43, 130.14, 119.39, 117.70, 109.95, 67.13, 27.77, 26.98, 20.93.

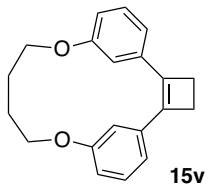

15v

Table 15, entry 5: Titanium(IV) chloride (0.05 mL, 0.5 mmol) was added to a slurry of zinc powder (0.0541 g, 0.827 mmol) in THF (1 mL) at 0 °C. After dissipation of the resulting yellow gas, the solution was heated to 68 °C. After 3 h, pyridine (0.06 mL, 0.7 mmol) was added, and 10 min. later diketone **19.2** (0.0151 g, 0.0466 mmol) as a solution in THF (2 mL) was added. The reaction was heated at 68 °C for 22 h, and then poured into chloroform (3 mL), filtered through Celite, and concentrated under reduced pressure. The residue was purified via flash chromatography (hexanes to 20% ethyl acetate/hexanes) to afford **15v** as a white solid (0.0136 g, 39%): R_f = 0.62 (20% ethyl acetate/hexanes); ^{1}H NMR (400 MHz, $CDCl_3$) δ 7.41 (q, *J* = 2.2 Hz, 2H), 7.32 (td, *J* = 7.9, 2.8 Hz, 2H), 6.95 – 6.88 (m, 3H), 4.14 – 4.03 (m, 4H), 2.80 (d, *J* = 2.6 Hz, 3H), 1.70 (qd, *J* = 4.1, 2.7, 2.1 Hz, 4H); ^{13}C NMR (126 MHz, $CDCl_3$) δ 156.62, 139.28, 137.12, 130.21, 119.98, 118.62, 114.86, 68.88, 26.83, 23.08.

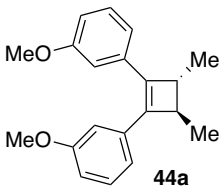

44a

Cyclobutene 44a: A solution of boron tribromide (1 M in dichloromethane, 0.9 mL, 0.9 mmol) was added dropwise over 5 min. to a stirred solution of **15z** (0.03 g, 0.09 mmol) in dichloromethane (9 mL). After 1.5 h, the reaction was added carefully to ice water (30 mL). The organic layers were separated, and the aqueous phase extracted with dichloromethane (3 × 5 mL). The organic extracts were combined and washed with sat. $NaHCO_3$ (15 mL) and brine (20 mL), dried over $MgSO_4$, filtered, and concentrated under reduced pressure. The residue was dissolved in DMF (1.7 mL) followed by the addition of NaH (0.0213 g, 0.533 mmol), TBAI (0.0014

g, 0.0038 mmol), and MeI (0.02 mL, 0.3 mmol) at 0 °C. The reaction was allowed to slowly warm to room temperature. After 24 h, MeOH (2 mL) was slowly added. The resulting mixture was slowly poured into water (2 mL) and extracted with chloroform (3 × 2 mL). The organic extracts were combined and washed with 1 M HCl (2 × 5 mL) and brine (5 mL), dried over $MgSO_4$, and concentrated under reduced pressure. The residue was purified via flash chromatography (1.0 × 10 cm, 10-30% ethyl acetate/hexanes) to afford **44a** as a white solid (0.0153 g, 60% over 2 steps): R_f = 0.79 (50% ethyl acetate/hexanes); ^{1}H NMR (600 MHz, $CDCl_3$) δ 7.28 – 7.23 (m, 2H), 7.09 (d, *J* = 7.6 Hz, 2H), 7.03 (d, *J* = 2.3 Hz, 2H), 6.81 (dd, *J* = 8.2, 2.6 Hz, 2H), 3.78 (s, 6H), 2.67 (q, *J* = 7.0 Hz, 2H), 1.23 (d, *J* = 6.8 Hz, 6H); ^{13}C NMR (151 MHz, $CDCl_3$) δ 159.59, 141.62, 136.26, 129.48, 119.49, 113.37, 111.93, 55.36, 42.62, 16.96.

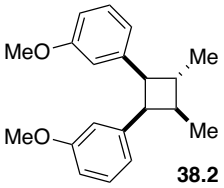

38.2

***syn/anti/anti/syn*-cyclobutane 38.2:** 10% Pd/C (0.0196 g, 0.0184 mmol) was added to a stirred solution of **15z** (0.060 g, 0.17 mmol) in a 10:1 mixture of methanol/ethyl acetate (19 mL) under an atmosphere (balloon) of hydrogen. After 2.5 h, the reaction was filtered through a pad of Celite, washed with methanol (10 mL) and chloroform (10 mL), and concentrated under reduced pressure. The residue was then dissolved in dichloromethane (17 mL), and a solution of boron tribromide (1 M in dichloromethane, 1.7 mL, 1.7 mmol) was added dropwise over 5 min. at 0 °C. After 1.5 h, the reaction was added carefully to ice water (10 mL). The organic layers were separated and the aqueous phase extracted with dichloromethane (3 × 20 mL). The organic extracts were combined and washed with sat. $NaHCO_3$ (20 mL) and water (20 mL), dried over $MgSO_4$, filtered, and concentrated under reduced pressure. The residue was dissolved in DMF (1.7 mL). NaH (0.0262 g, 0.655), TBAI (0.0020 g, 0.0054 mmol), and MeI (43 µL, 0.69 mmol) were added sequentially at 0 °C. The reaction was then allowed to slowly warm to room temperature. After 17 h, methanol (2 mL) and water (2 mL) were added slowly. The resulting mixture was extracted with dichloromethane (3 × 2 mL). The organic extracts were combined and washed with 1 M HCl (2 × 2 mL), dried over $MgSO_4$, and concentrated under reduced pressure. The residue was purified via flash chromatography (1.3 × 18 cm, hexanes to 50% dichloromethane/hexanes) to afford **38.2** as a white solid (0.0357 g, 70% over 3 steps): R_f = 0.35 (50% dichloromethane/hexanes); ^{1}H NMR (600 MHz, $CDCl_3$) δ 7.12 – 7.06 (m, 1H), 7.04 – 6.97 (m, 1H), 6.64 – 6.48 (m, 7H), 3.96 (t, *J* = 9.0 Hz, 1H), 3.68 (s, 3H), 3.64 – 3.55 (m, 4H), 2.71 – 2.60 (m, 1H), 2.39 (m, 1H), 1.33 (d, *J* = 6.4 Hz, 3H), 0.72 (d, *J* = 7.0 Hz, 3H); ^{13}C NMR (151 MHz, $CDCl_3$) δ 159.53, 158.88, 143.88, 141.09, 129.03, 128.36, 123.11, 119.55, 115.85, 112.89, 111.29, 110.65, 55.22, 55.11, 48.10, 41.89, 39.60, 20.54, 14.77; HRMS (ESI) calculated for $C_{20}H_{25}O_2$ ($[M+H]^+$) *m/z* =297.1855, found 297.1766.

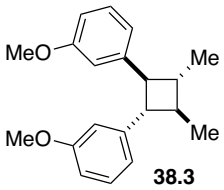

38.3

***all trans*-cyclobutane 38.3:** Potassium *tert*-butoxide (0.0704 g, 0.609 mmol) was added to a stirred solution of **38.2** (0.030 g, 0.10 mmol) in dimethyl sulfoxide (2.5 mL) and heated to 110°C. After 1.5 h, the reaction mixture was poured into ice water (10 mL) extracted with dichloromethane (3 × 3 mL), ethyl acetate (3 × 3 mL), and a 3:1 solution of chloroform:isopropanol (4 × 3 mL). The organic extracts were combined and dried over $MgSO_4$, filtered, and concentrated under reduced pressure to afford **38.3** as a colorless oil (0.0253 g, 84%): R_f = 0.30 (50% dichloromethane/hexanes); ^{1}H NMR (600 MHz, $CDCl_3$) δ 7.21 (m, 2H), 6.82 (d, *J* = 7.3 Hz, 1H), 6.78 (m, 1H), 6.74 (dd, *J* = 8.2, 2.7 Hz, 1H), 3.79 (s, 3H), 2.93 – 2.87 (m, 1H), 1.89 (q, *J* = 5.1 Hz, 1H), 1.24 – 1.16 (m, 3H); ^{13}C NMR (151 MHz, $CDCl_3$) δ 159.61, 145.37, 129.27, 119.31, 112.81, 111.02, 55.14, 52.66, 43.02, 18.96; HRMS (ESI) calculated for $C_{20}H_{25}O_2$ ($[M+H]^+$) *m/z* =297.1855, found 297.1863.

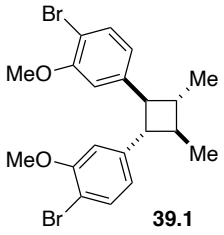

39.1

***all trans* bis-(4-bromo-3-methoxyphenyl)-dimethylcyclobutane 39.1:** A solution of Br_2 in dichloromethane (0.08 M, 3.2 mL, 0.256 mmol) was added to a stirring solution of **38.3** (0.0158 g, 0.0533 mmol) in dichloromethane (1 mL) at room temperature. After 25 min., the reaction mixture was carefully poured into ice water (10 mL) and a 5% solution of $Na_2S_2O_5$ (5 mL) was added. The resulting mixture was extracted with dichloromethane (3 × 5 mL). The organic extracts were combined and washed with brine (10 mL), dried over $MgSO_4$, filtered, and concentrated under reduced pressure to afford **39.1** as a white solid (0.0240 g, 99%): R_f = 0.52 (50% dichloromethane/hexanes); ^{1}H NMR (600 MHz, $CDCl_3$) δ 7.38 (d, *J* = 8.7 Hz, 2H), 7.08 (d, *J* = 3.1 Hz, 2H), 6.62 (dd, *J* = 8.7, 3.1 Hz, 2H), 3.83 (s, 6H), 3.55 – 3.44 (m, 2H), 1.92 – 1.81 (m, 2H), 1.24 (d, *J* = 5.2 Hz, 6H).

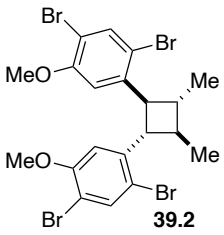

39.2

***all trans* bis-(2,4-dibromo-5-methoxyphenyl)-dimethylcyclobutane 39.2:** Br_2 (0.0207 g, 0.130 mmol) was added to a stirring solution of **38.3** (0.0022 g, 0.0074 mmol) in glacial acetic acid (0.1 mL) at 0 °C. The reaction was then allowed to warm to room temperature. After 3.5 h, a 5% solution of $Na_2S_2O_5$ (0.5 mL) was slowly added and then diluted with water (1 mL). The resulting mixture was extracted with dichloromethane (3 × 1 mL). The organic extracts were combined and washed with water (1 mL), brine (1 mL), sat. $NaHCO_3$ (1 mL), and water (1 mL) again, dried over $MgSO_4$, filtered, and concentrated under reduced pressure to afford **39.2** as a white solid (0.0045 g, 100%): R_f = 0.58 (50% dichloromethane/hexanes); **¹**H NMR (600 MHz, $CDCl_3$) δ 7.65 (s, 2H), 7.00 (s, 2H), 3.96 (s, 6H), 3.48 **–** 3.44 (m, 2H), 1.86 (d, *J* = 6.5 Hz, 2H), 1.25 (d, *J* = 5.4 Hz, 6H).

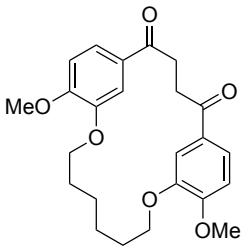

40.3

1,4-diketone 40.3: 1,6-Dibromohexane (1.1 mL, 7.2 mmol) was added to a stirred solution of isovanillin (2.06 g, 13.6 mmol), K_2CO_3 (4.16 g, 30.1 mmol), and TBAI (0.076 g, 0.21 mmol) in DMF (27 mL) at room temperature. The reaction was heated at 80 °C for 20 h, cooled to room temperature, followed by the addition of water (30 mL) and 1 M HCl (30 mL). The resulting mixture was extracted with ethyl acetate (3 × 30 mL). The organic extracts were combined and washed with 1 M HCl (2 × 30 mL) and brine (30 mL), dried over $MgSO_4$, filtered and concentrated under reduced pressure. The yellow oil was dissolved in dichloromethane (100 mL) and vinylmagnesium bromide (0.7 M in THF, 42 mL, 29 mmol) was added. After 1 h, the reaction was poured into water (100 mL) and further diluted with 1 M HCl (100 mL). The resulting mixture was extracted with dichloromethane (3 × 100 mL). The combined organic extracts were washed with a saturated solution $NaHCO_3$ (100 mL) and brine (100 mL), dried over $MgSO_4$, filtered and concentrated under reduced pressure. The residue was purified by flash chromatography (18 × 5.0 cm, 50% to 70% ethyl acetate/hexanes) to afford allylic diol **S-4** as a colorless oil that was dissolved in dichloromethane (345 mL). Hoveyda-Grubbs second-generation catalyst (0.0520 g, 0.0830 mmol) was added, and the reaction was heated at 40 °C for 2 h, and then concentrated under reduced pressure. The dark brown residue was dissolved in 1:7 methanol/dichloromethane (36.5 mL), and sodium borohydride (0.525 g, 13.9 mmol) was added. After 3 h, the reaction poured into ice cold water (35 mL) and further diluted with 1 M HCl (35 mL). The layers were separated and the aqueous phase was extracted with dichloromethane (3 × 30 mL). The combined organic extracts were washed with water (40 mL), dried over $MgSO_4$, filtered and concentrated under reduced pressure. The residue was purified by flash chromatography (15 × 3.5 cm, 80% ethyl acetate/hexanes) to afford macrocyclic 1,4-diol **S-5** as a pale yellow oil, which was dissolved in dichloromethane (15 mL), followed by the sequential addition of $NaHCO_3$ (0.556 g, 6.61 mmol) and Dess-Martin periodinane (1.70 g, 4.00 mmol). After 3 h, the reaction was poured into water (20 mL). The layers were separated and the aqueous phase was extracted with dichloromethane (3 × 15 mL). The combined organic extracts were washed with water (20 mL), dried over $MgSO_4$, filtered and concentrated under reduced pressure to afford 1,4-diketone **40.3** as a white solid (0.4048 g, 15% from isovanillin): R_f = 0.41 (60% ethyl acetate/hexanes); ^{1}H NMR (600 MHz, $CDCl_3$) δ 7.57 (dd, *J* = 8.5, 2.3 Hz, 2H), 7.44 (d, *J* = 2.5 Hz, 2H), 6.89 (d, *J* = 8.5 Hz, 2H), 4.20 (t, *J* = 7.0 Hz, 4H), 3.91 (s, 6H), 3.32 (s, 4H), 1.72 (q, *J* = 6.8 Hz, 4H), 1.49 (d, *J* = 6.6 Hz, 4H); ^{13}C NMR (151 MHz, $CDCl_3$) δ 198.83, 154.33, 147.38, 129.57, 123.00, 114.36, 111.29, 68.37, 56.21, 34.57, 28.07, 24.45; HRMS (ESI) calculated for $C_{24}H_{28}O_6Na$ ($[M+Na]^+$) *m/z* = calculated 435.1784, found 435.1790.

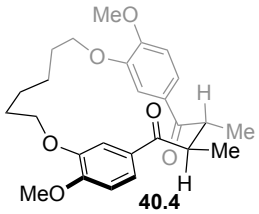

40.4

(*rac*)-2,3-Dimethyl-1,4-Dione 40.4: A solution of diketone **40.3** (0.0907 g, 0.220 mmol) in THF (2 mL) was added to a stirring suspension of NaH (0.0940 g, 2.35 mmol) in THF (1 mL) at 0 °C. After stirring for 1.5 h at 0 °C, MeI (0.062 mL, 1.0 mmol) was added, and the reaction was allowed to warm to room temperature. After 22 h, a saturated solution of NH_4Cl (3 mL) was slowly added. The resulting mixture was extracted with ethyl acetate (3 × 3 mL). The organic extracts were dried over $MgSO_4$, filtered, and concentrated under reduced pressure. The residue was purified via automated flash chromatography (12 g silica cartridge, hexanes to 80% ethyl acetate/hexanes) to afford (*rac*)-2,3-dimethyl-1,4-dione **40.4** as a white solid. (0.0557 g, 57%): R_f = 0.38 (50% ethyl acetate/hexanes); ^{1}H NMR (600 MHz, $CDCl_3$) δ 7.50 (dd, *J* = 8.4, 1.8 Hz, 2H), 7.27 (d, *J* = 1.8 Hz, 2H), 6.85 (d, *J* = 8.4 Hz, 2H), 4.15 (t, *J* = 6.2 Hz, 4H), 3.90 (s, 6H), 3.82–3.74 (m, 2H), 1.68–1.56 (m, 4H), 1.52–1.44 (m, 2H), 1.44–1.37 (m, 2H), 1.27 (d, *J* = 6.0 Hz, 6H); ^{13}C NMR (151 MHz, $CDCl_3$) δ 203.54, 153.92, 146.68, 129.85, 122.90, 113.10, 110.35, 67.97, 55.88, 43.88, 26.90, 23.61, 15.00; HRMS (ESI) calculated for $C_{26}H_{33}O_6$ ([M+H$^+$) *m/z* = 441.2277, found 441.2284.

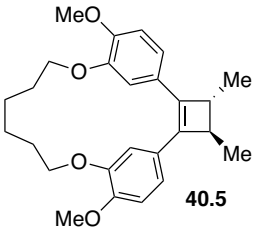

40.5

Cyclobutene 40.5: Titanium(IV) chloride (0.08 mL, 0.7 mmol) was added to a slurry of zinc powder (0.1061 g, 1.623 mmol) in THF (4 mL) at 0 °C. After dissipation of the resulting yellow gas, the solution was heated to 68 °C. After 50 min., pyridine (0.15 mL, 1.9 mmol) was added, and 10 min. later (*rac*)-2,3-dimethyl-1,4-dione **40.4** (0.0519 g, 0.118 mmol) as a solution in THF (8 mL) was added. The reaction was heated at 68 °C for 8 h, and then poured into chloroform (12 mL), filtered through Celite, and concentrated under reduced pressure. The residue was purified via flash chromatography (1.3 × 16 cm, 20–60% ethyl acetate/hexanes) to afford **40.5** as a white solid (0.0447 g, 93%): R_f = 0.30 (40% ethyl acetate/hexanes); ^{1}H NMR (600 MHz, $CDCl_3$) δ 7.36 (d, *J* = 1.7 Hz, 2H), 6.88 (d, *J* = 8.3 Hz, 2H), 6.80 (dd, *J* = 8.2, 1.7 Hz, 2H), 4.20 (dt, *J* = 11.8, 6.1 Hz, 2H), 4.01 (dt, *J* = 12.0, 6.1 Hz, 2H), 3.88 (s, 6H), 2.60 (q, *J* = 6.6 Hz, 2H), 1.78–1.68 (m, 4H), 1.60–1.49 (m, 8H), 1.21 (d, *J* = 6.7 Hz, 6H); ^{13}C NMR (101 MHz, $CDCl_3$) δ 150.02, 148.01, 139.52, 128.45, 120.40, 114.24, 111.99, 69.00, 56.10, 42.61, 28.84, 23.75, 17.12; HRMS (ESI) calculated for $C_{26}H_{33}O_4$ ([M+H]$^+$) *m/z* = calculated 409.2379, found 409.2371.

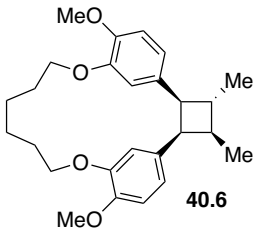

40.6

Macrocyclic cyclobutane 40.6: 10% Pd/C (0.0138 g, 0.0130 mmol) was added to a stirred solution of **40.5** (0.0447 g, 0.109 mmol) in a 10:1 mixture of methanol/ethyl acetate (11 mL) under an atmosphere (balloon) of hydrogen. After 2 h, the reaction was filtered through a pad of Celite, washed with methanol (10 mL) and chloroform (10 mL), and concentrated

under reduced pressure. This material was used on without further purification (0.034 g, 75%): R_f = 0.36 (dichloromethane); ^{1}H NMR (600 MHz, $CDCl_3$) δ 6.65 (dd, *J* = 8.3, 5.5 Hz, 2H), 6.59 (s, 1H), 6.56–6.52 (m, 1H), 6.51–6.49 (m, 1H), 6.43 (d, *J* = 8.3 Hz, 1H), 4.19–4.06 (m, 2H), 3.88 (t, *J* = 9.0 Hz, 1H), 3.82 (t, *J* = 7.3 Hz, 2H), 3.78 (d, *J* = 4.1 Hz, 6H), 3.58 (t, *J* = 9.8 Hz, 1H), 2.58–2.51 (m, 1H), 2.38 (q, *J* = 8.6 Hz, 1H), 1.79–1.49 (m, 8H), 1.32 (d, *J* = 6.5 Hz, 3H), 0.73 (d, *J* = 7.0 Hz, 3H); ^{13}C NMR (151 MHz, $CDCl_3$) δ 147.29, 147.26, 146.49, 146.43, 134.75, 131.97, 123.25, 119.92, 116.13, 113.01, 111.70, 110.51, 68.64, 68.16, 55.95, 55.70, 47.50, 47.42, 42.43, 39.39, 27.64, 27.51, 23.58, 23.29, 20.83, 14.90; HRMS (ESI) calculated for $C_{26}H_{35}O_4$ ([M+H]$^+$) *m/z* = calculated 411.2535, found 411.2526.

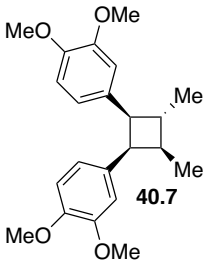

40.7

***syn/anti/anti/syn*-cyclobutane 40.7**: A solution of boron tribromide (1 M in dichloromethane, 0.85 mL, 0.85 mmol) was added dropwise over 5 min. to a stirred solution of **40.6** (0.0339 g, 0.826 mmol) in dichloromethane (8.5 mL). After 1.5 h, the reaction was added carefully to ice water (10 mL). The organic layers were separated and the aqueous phase extracted with dichloromethane (3 × 10 mL). The organic extracts were combined and dried over $MgSO_4$, filtered, and concentrated under reduced pressure. The residue (0.0309 g, 0.103 mmol) was dissolved in DMF (2.0 mL) followed by the sequential addition of NaH (0.0360 g, 0.825 mmol), TBAI (0.0035 g, 0.0095 mmol), and MeI (0.05 mL, 0.8 mmol) at 0 °C. The reaction was allowed to slowly warm to room temperature. After 16 h, methanol (2 mL) was added and the mixture poured into water (2 mL). The resulting mixture was extracted with dichloromethane (3 × 2 mL). The organic extracts were combined and washed with 1 M HCl (2 × 5 mL) and brine (5 mL), dried over $MgSO_4$, and concentrated under reduced pressure. The residue was purified via flash chromatography (1.0 × 10 cm, 20–60% ethyl acetate/hexanes) to afford **40.7** as a white solid (0.0075 g, 25% over 2 steps): R_f = 0.40 (50% ethyl acetate/hexanes); ^{1}H NMR (600 MHz, $CDCl_3$) δ 6.71 (d, *J* = 8.2 Hz, 1H), 6.62 (d, *J* = 8.2 Hz, 1H), 6.59 (d, *J* = 8.1 Hz, 1H), 6.51 (dd, *J* = 8.2, 1.8 Hz, 1H), 6.44 (d, *J* = 1.7 Hz, 1H), 6.42 (s, 1H), 3.89 (dd, *J* = 11.0, 6.9 Hz, 1H), 3.84 (dd, *J* = 11.1, 6.7 Hz, 1H), 3.80 (s, 3H), 3.78 (s, 3H), 3.66 (s, 3H), 3.58 (s, 3H), 2.63 – 2.51 (m, 1H), 2.43 – 2.29 (m, 1H), 1.32 (d, *J* = 6.4 Hz, 3H), 0.71 (d, *J* = 7.0 Hz, 3H). ^{13}C NMR (151 MHz, $CDCl_3$) δ 148.76, 147.82, 146.85, 135.03, 132.13, 122.77, 118.70, 113.88, 111.01, 110.92, 110.36, 56.05, 55.88, 55.79, 55.74, 47.76, 47.47, 42.16, 39.52, 20.59, 14.89; HRMS (ESI) calculated for $C_{22}H_{29}O_4$ ([M+H]$^+$) *m/z* =357.2066, found 357.1926.

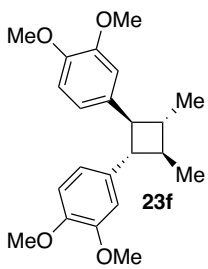

23f

Di-*O*-methylendiandrin A (23f): Potassium *tert*-butoxide (0.0035 g, 0.030 mmol) was added to a stirred solution of **40.7** (0.0016 g, 0.0045 mmol) in dimethyl sulfoxide (0.10 mL) and heated to 100°C. After 2.5 h, the reaction mixture was poured into ice water (2 mL) extracted with ethyl acetate (3 × 1

mL) and dichloromethane (3 × 1 mL). The combined organic extracts were dried over $MgSO_4$, filtered, and concentrated under reduced pressure to afford **23f** as a colorless oil (0.0009 g, 55%): R_f = 0.30 (30% ethyl acetate/hexanes); ^{1}H NMR (500 MHz, $CDCl_3$) δ 6.81 (d, *J* = 8.2 Hz, 2H), 6.77 (dd, *J* = 8.2, 1.8 Hz, 2H), 6.71 (d, *J* = 1.7 Hz, 2H), 3.85 (s, 6H), 3.84 (s, 6H), 2.79 (dd, *J* = 5.7, 3.3 Hz, 2H), 1.90 – 1.81 (m, *J* = 9.0, 3.7 Hz, 2H), 1.20 (d, *J* = 5.9 Hz, 6H); ^{13}C NMR (126 MHz, $CDCl_3$) δ 149.00, 147.60, 136.65, 118.74, 111.36, 110.40, 56.12, 56.01, 53.20, 43.12, 19.10; HRMS (ESI) $C_{22}H_{28}O_4Na$ ($[M+Na]^+$) *m/z*=379.1885, found 379.1895.

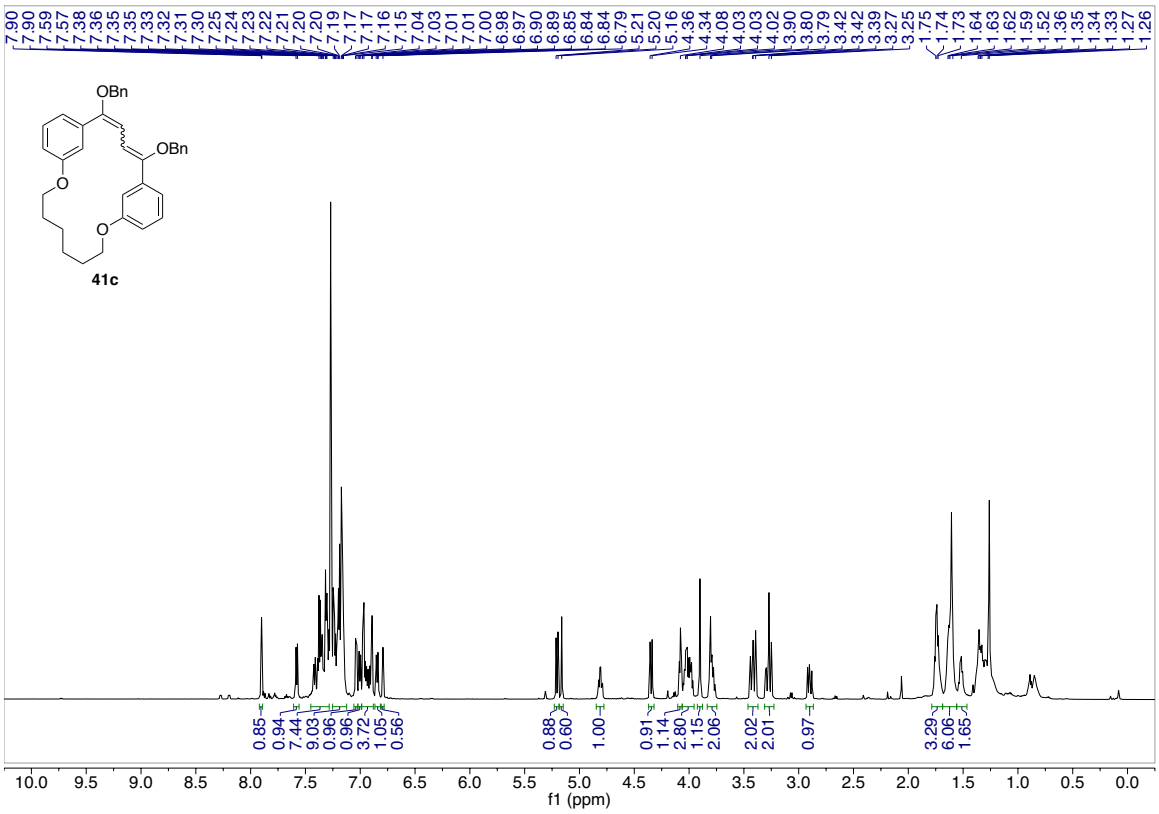
OBn
OBn
O
O
41c
7.90 7.90 7.59 7.57 7.38 7.36 7.35 7.35 7.33 7.32 7.31 7.30 7.25 7.24 7.23 7.22 7.21 7.20 7.20 7.19 7.17 7.17 7.16 7.15 7.04 7.03 7.01 7.01 7.00 6.98 6.97 6.90 6.89 6.85 6.84 6.84 6.79 5.21 5.20 5.16 4.36 4.34 4.08 4.03 4.03 4.02 3.90 3.80 3.79 3.42 3.42 3.39 3.27 3.25 1.75 1.74 1.73 1.64 1.63 1.62 1.59 1.52 1.36 1.35 1.34 1.33 1.27 1.26
0.85 0.94 7.44 9.03 0.96 0.96 3.72 1.05 0.56 0.88 0.60 1.00 0.91 1.14 2.80 1.15 2.06 2.02 2.01 0.97 3.29 6.06 1.65
10.0 9.5 9.0 8.5 8.0 7.5 7.0 6.5 6.0 5.5 5.0 4.5 4.0 3.5 3.0 2.5 2.0 1.5 1.0 0.5 0.0
f1 (ppm)

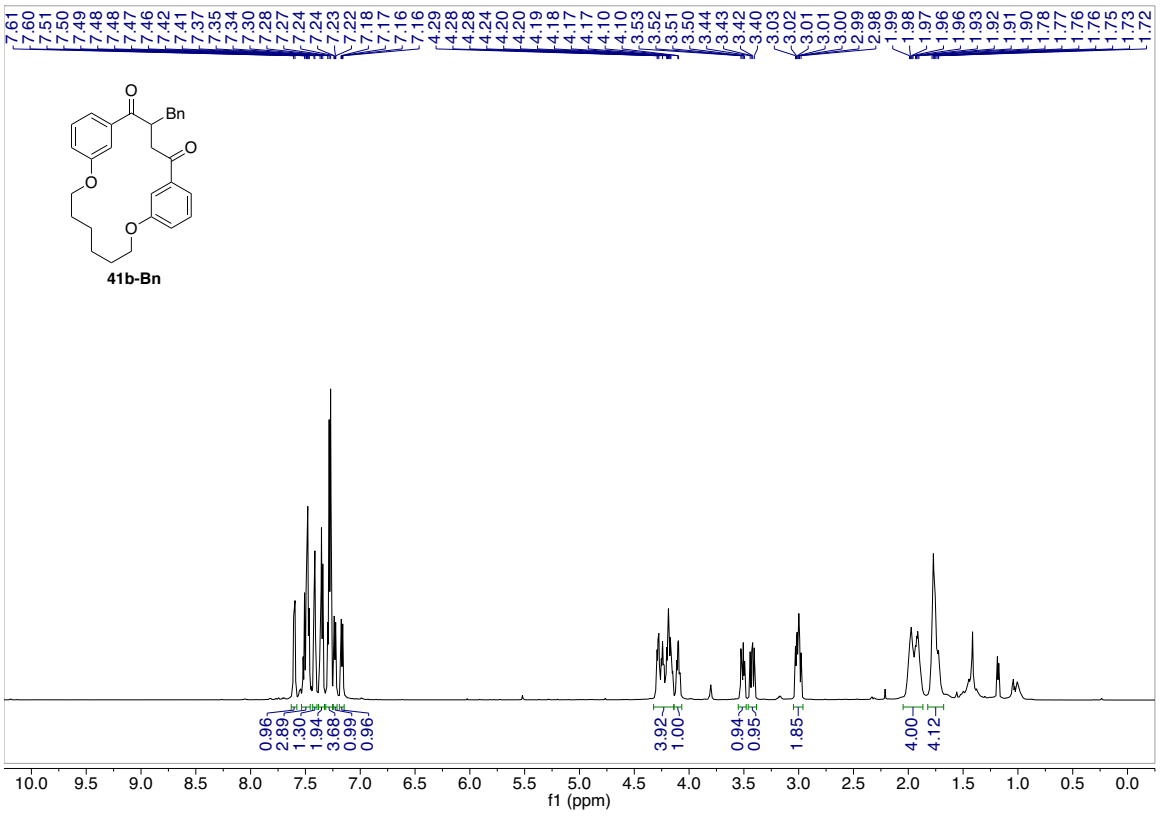
41b-Bn
f1 (ppm)

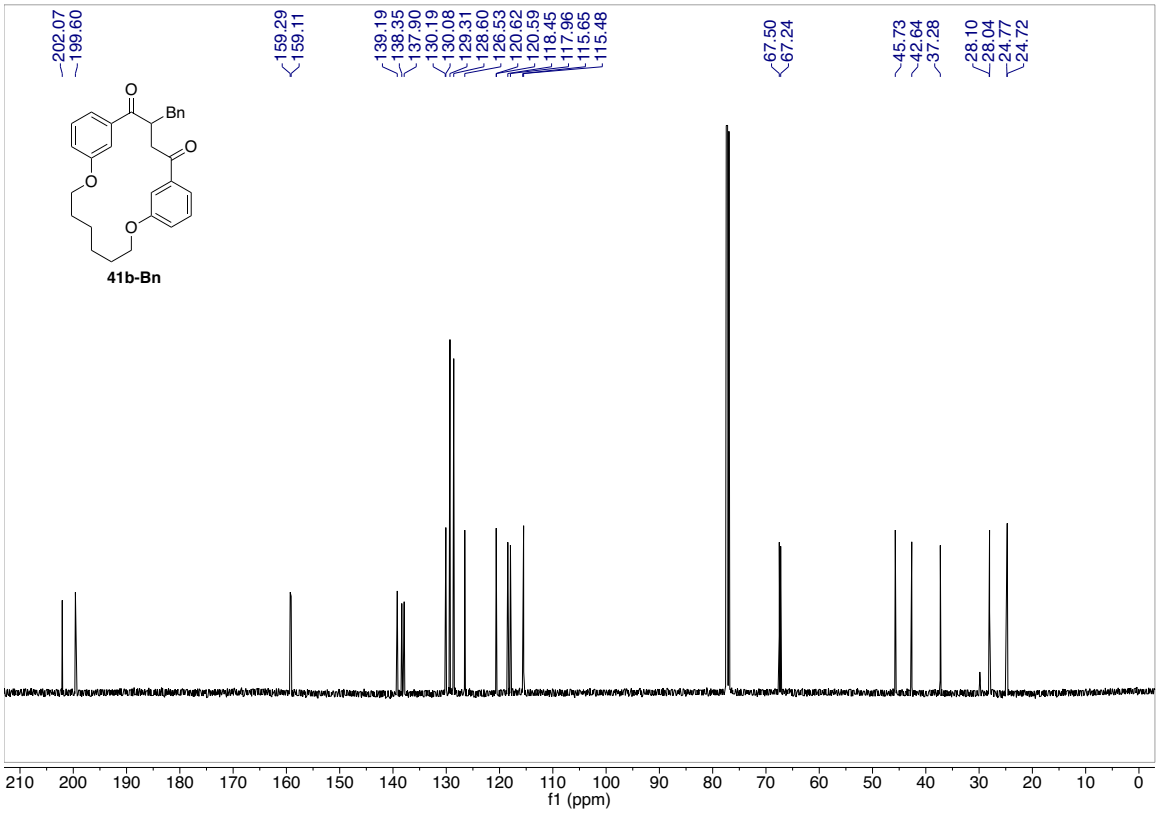
41b-Bn
f1 (ppm)

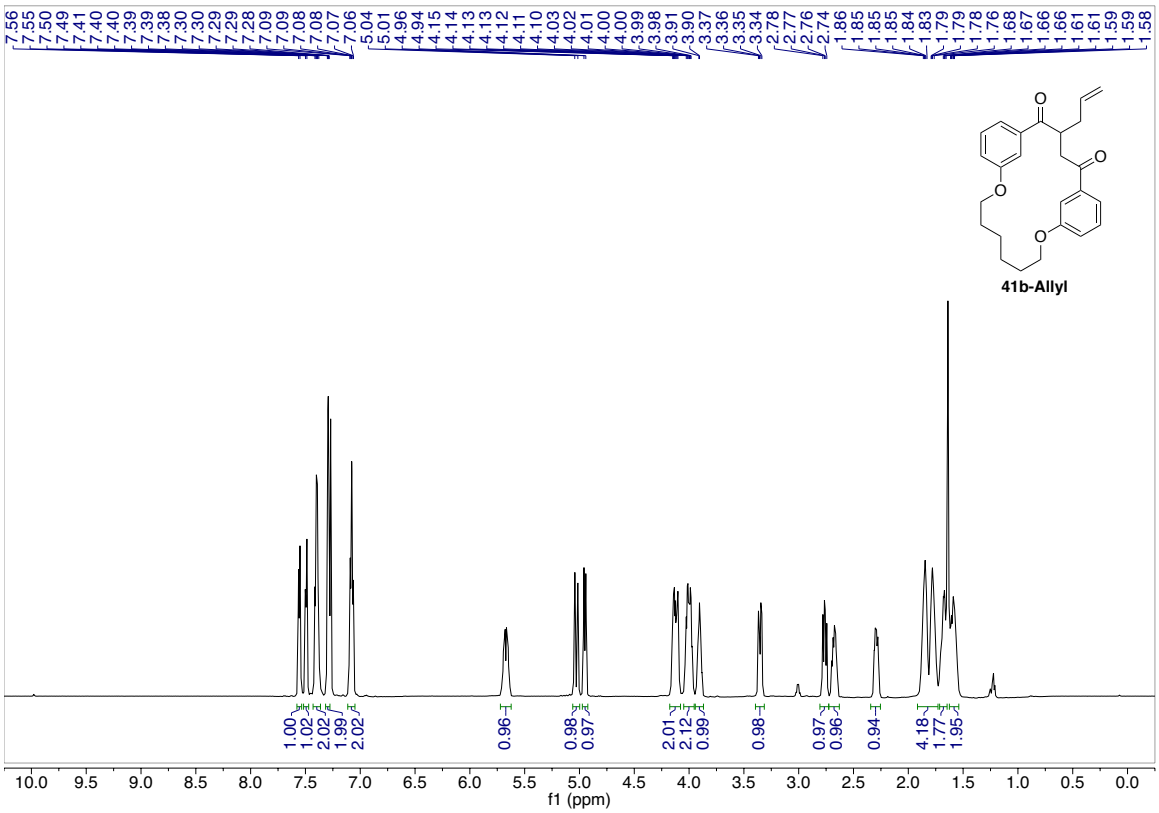
7.56 7.55 7.50 7.49 7.41 7.40 7.40 7.39 7.39 7.38 7.30 7.30 7.29 7.29 7.28 7.09 7.09 7.08 7.08 7.07 7.06 5.04 5.01 4.96 4.94 4.15 4.14 4.13 4.13 4.12 4.11 4.10 4.03 4.02 4.01 4.00 4.00 3.99 3.98 3.91 3.90 3.37 3.36 3.35 3.34 2.78 2.77 2.76 2.74 1.86 1.85 1.85 1.85 1.84 1.83 1.79 1.79 1.78 1.76 1.68 1.67 1.66 1.66 1.61 1.61 1.59 1.59 1.58
41b-Allyl
1.00 1.02 2.02 1.99 2.02 0.96 0.98 0.97 2.01 2.12 0.99 0.98 0.97 0.96 0.94 4.18 1.77 1.95
f1 (ppm)

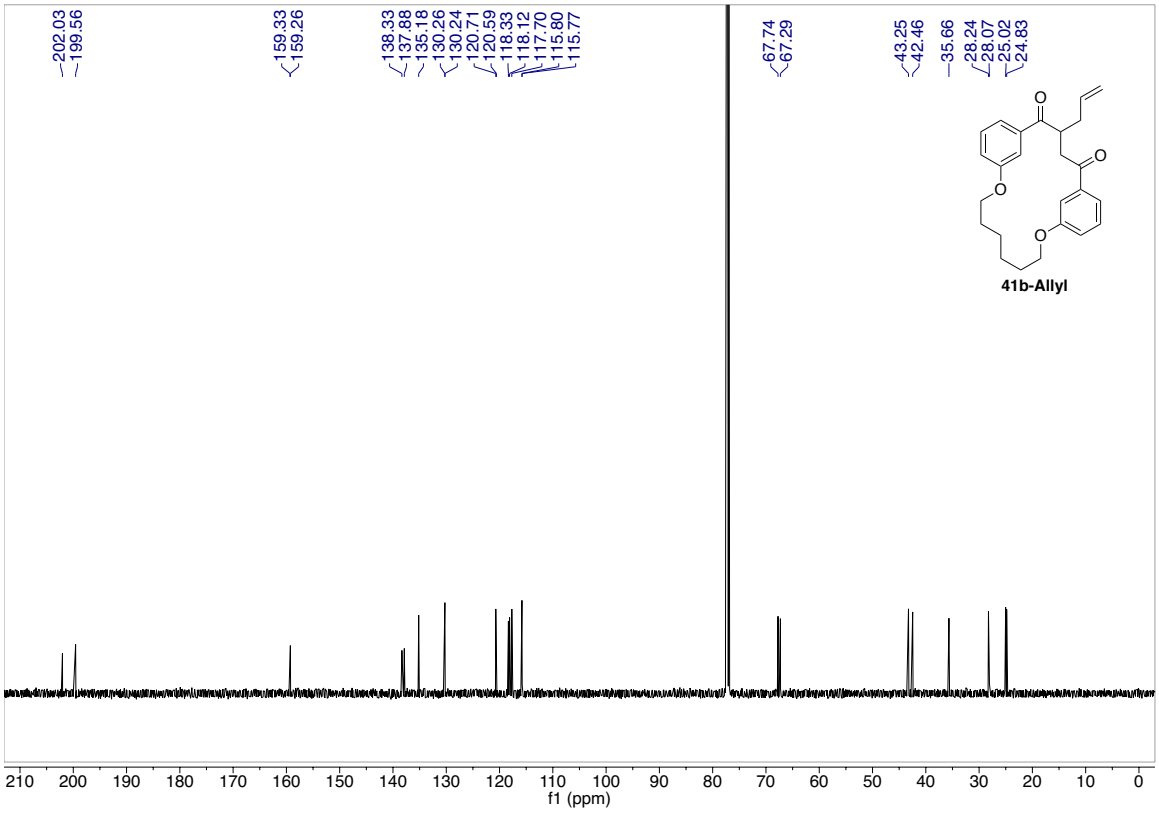
202.03 199.56 159.33 159.26 138.33 137.88 135.18 130.26 130.24 120.71 120.59 118.33 118.12 117.70 115.80 115.77 67.74 67.29 43.25 42.46 35.66 28.24 28.07 25.02 24.83
41b-Allyl
f1 (ppm)

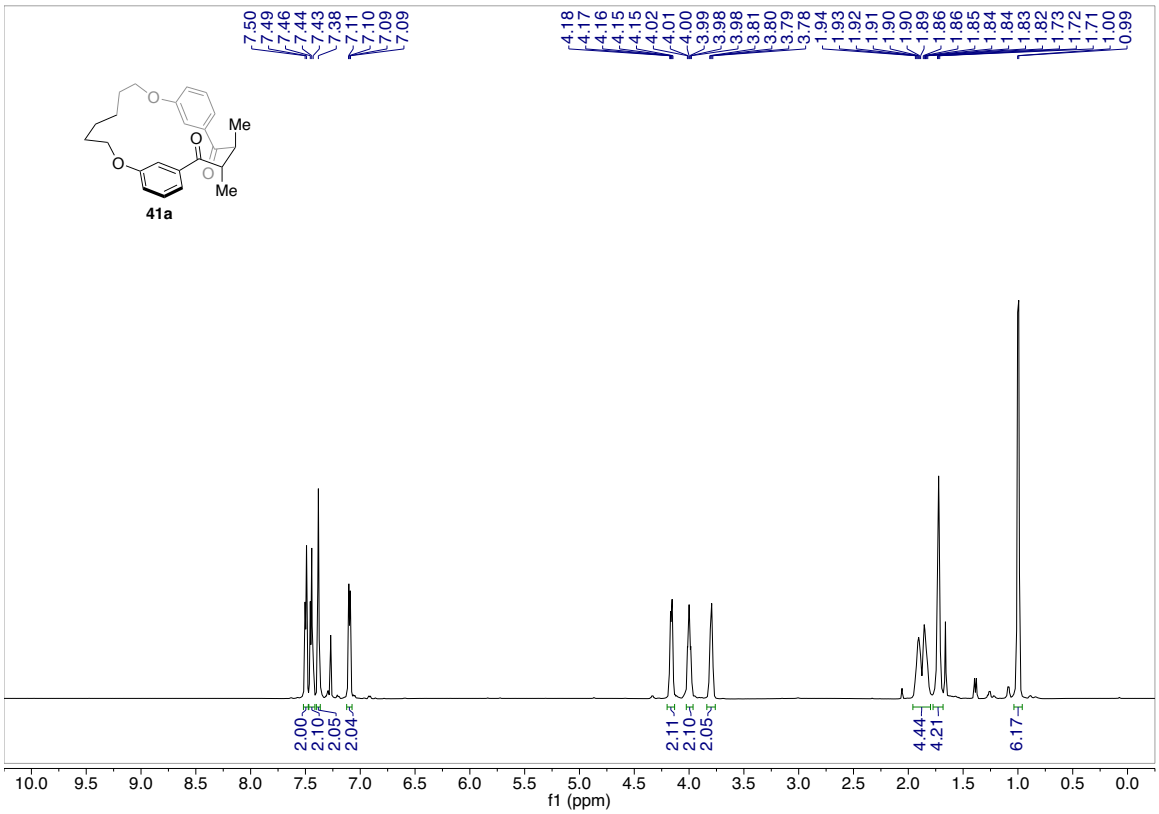
7.50
7.49
7.46
7.44
7.43
7.38
7.11
7.10
7.09
7.09
4.18
4.17
4.16
4.15
4.15
4.02
4.01
4.00
3.99
3.98
3.98
3.81
3.80
3.79
3.78
1.94
1.93
1.92
1.91
1.90
1.90
1.89
1.86
1.86
1.85
1.84
1.84
1.83
1.82
1.73
1.72
1.71
1.00
0.99
Me
Me
41a
2.00
2.10
2.05
2.04
2.11
2.10
2.05
4.44
4.21
6.17
f1 (ppm)

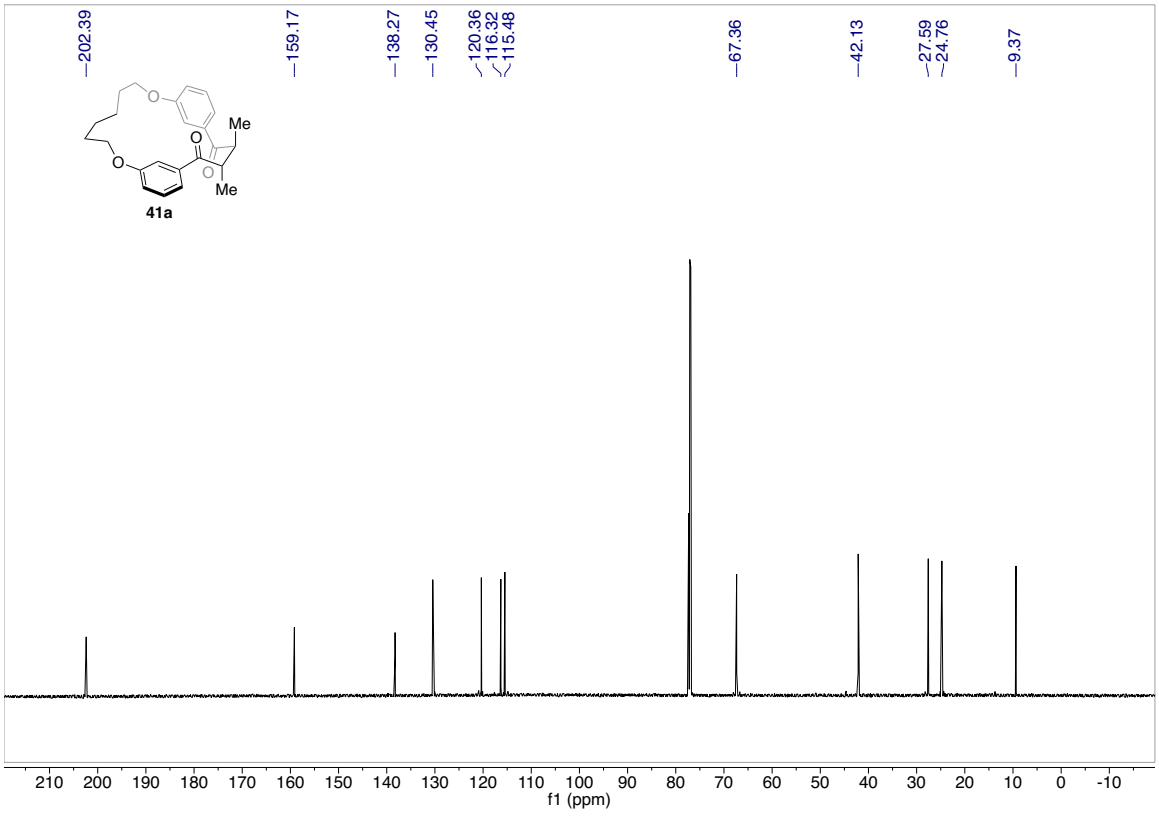
202.39
159.17
138.27
130.45
120.36
116.32
115.48
67.36
42.13
27.59
24.76
9.37
Me
Me
41a
f1 (ppm)

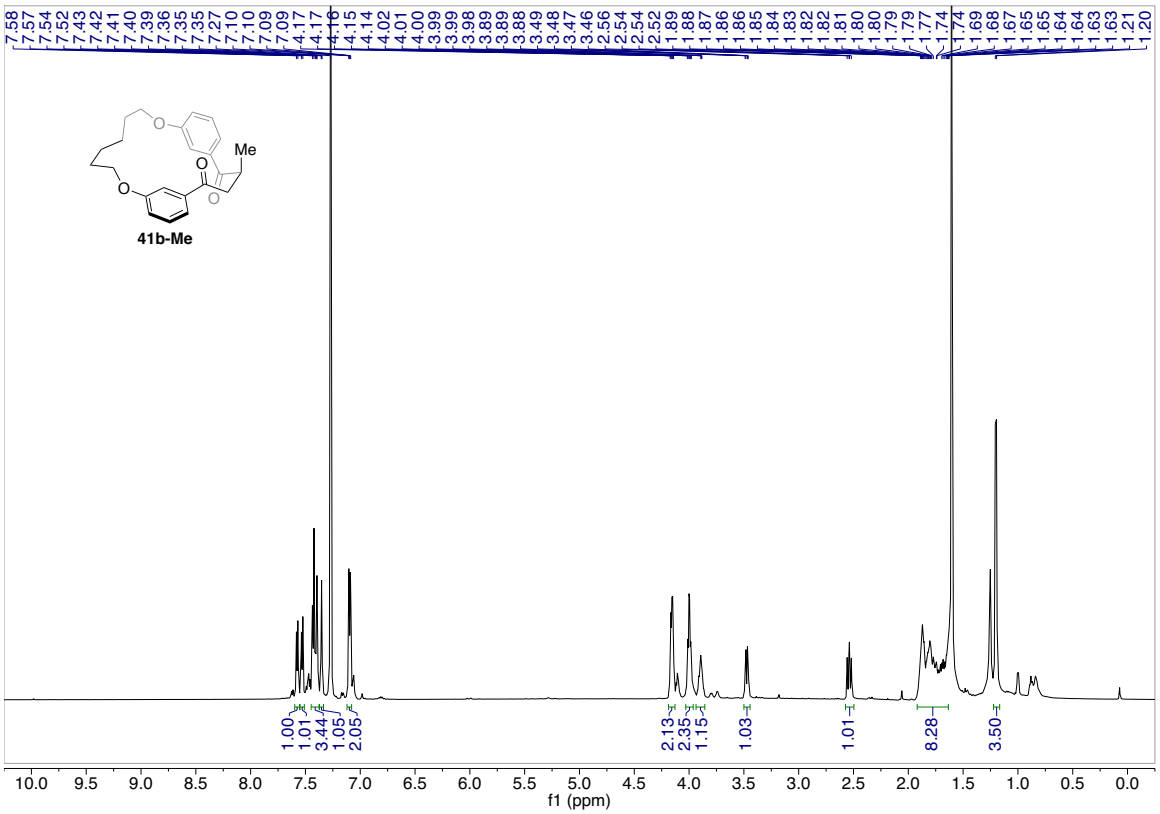
41b-Me
f1 (ppm)

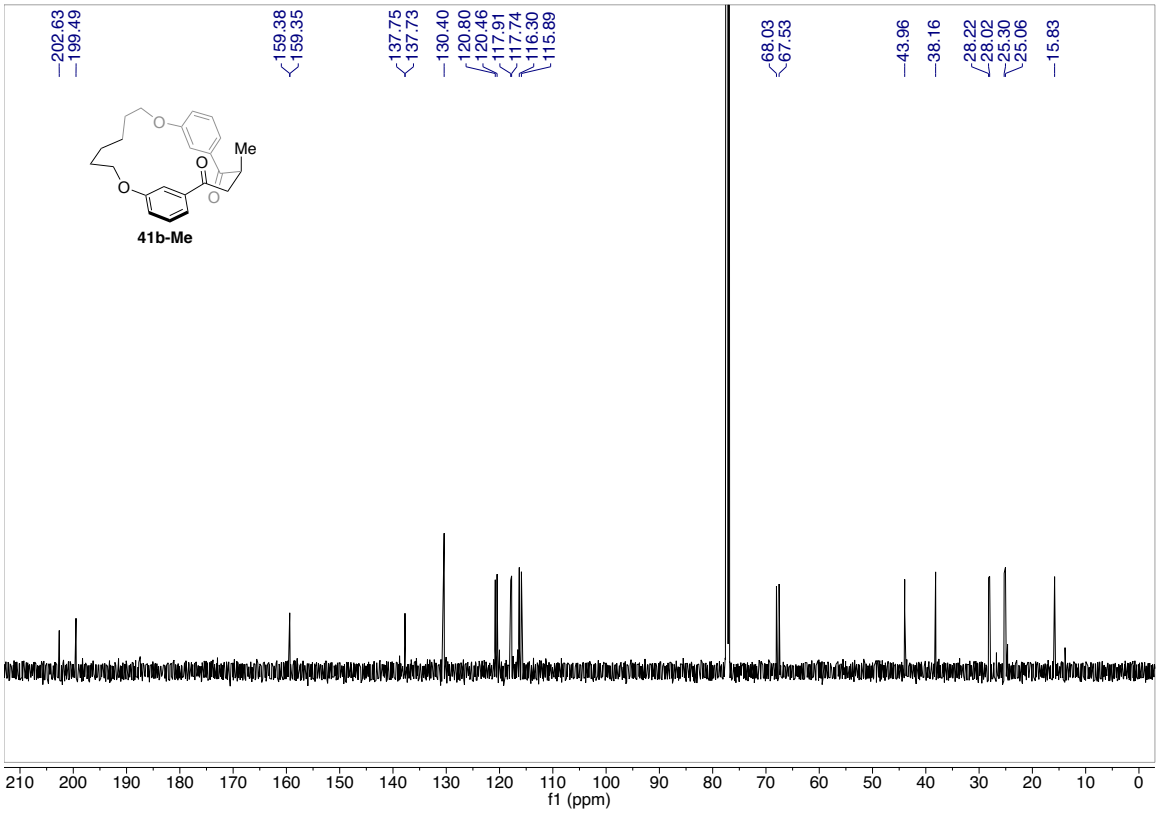
41b-Me
f1 (ppm)

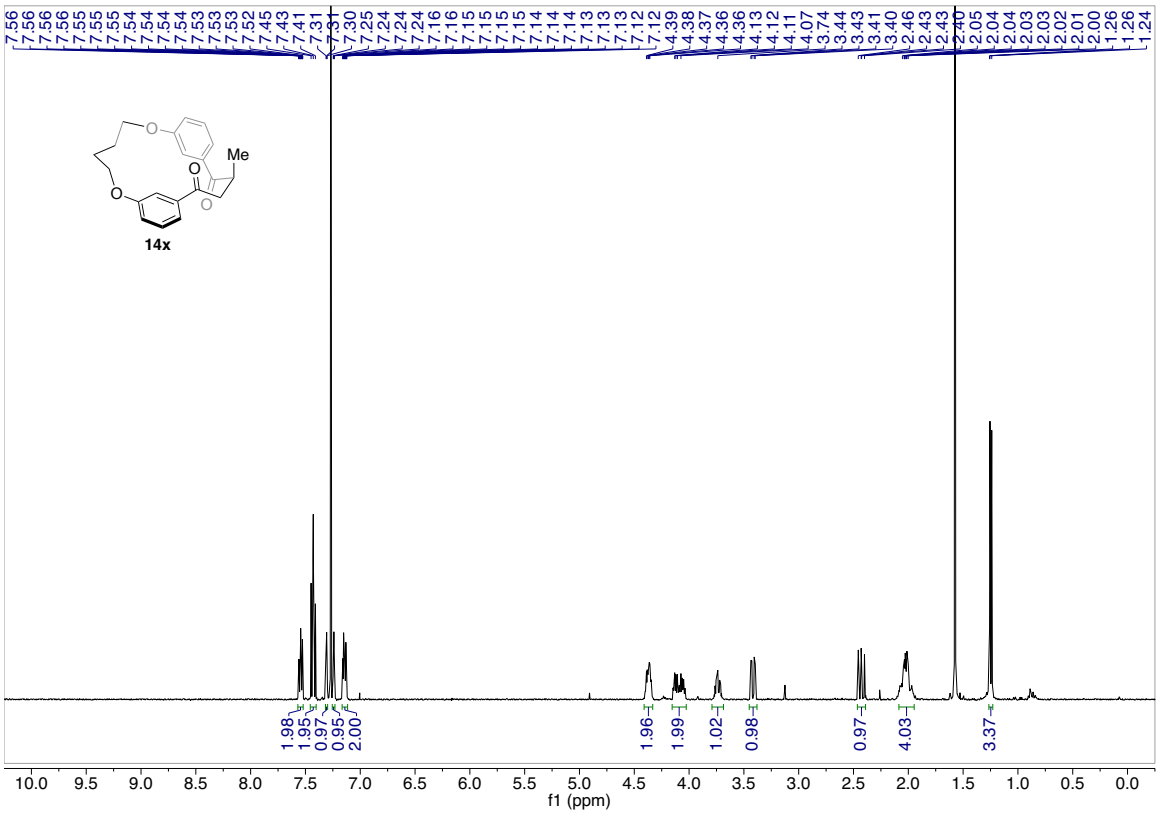
14x
f1 (ppm)

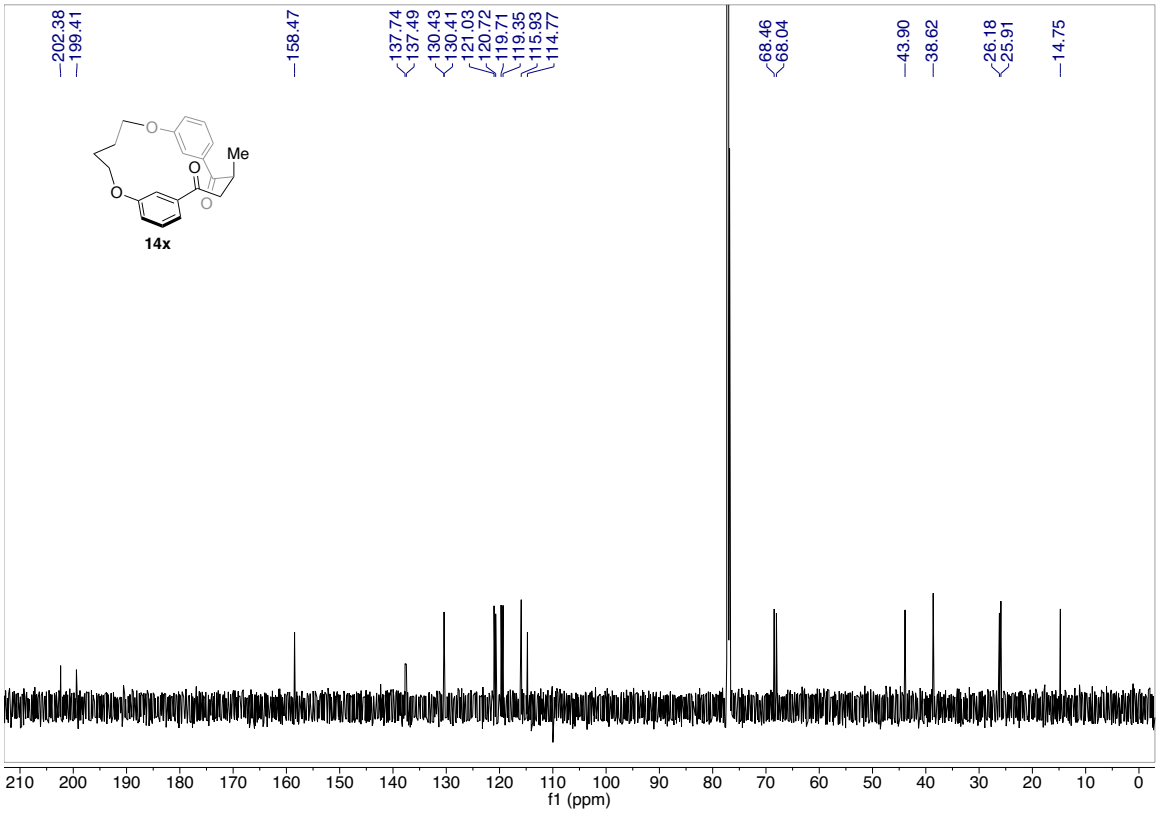
14x
f1 (ppm)

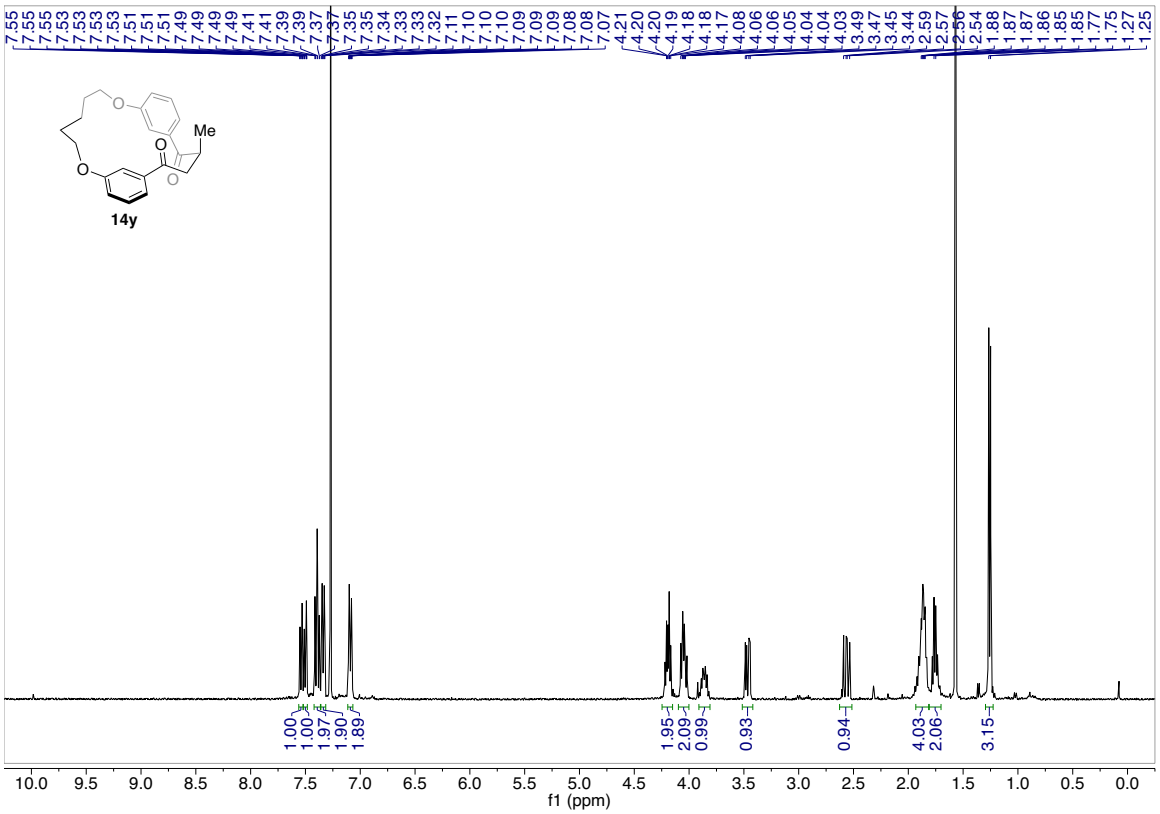
14y
f1 (ppm)

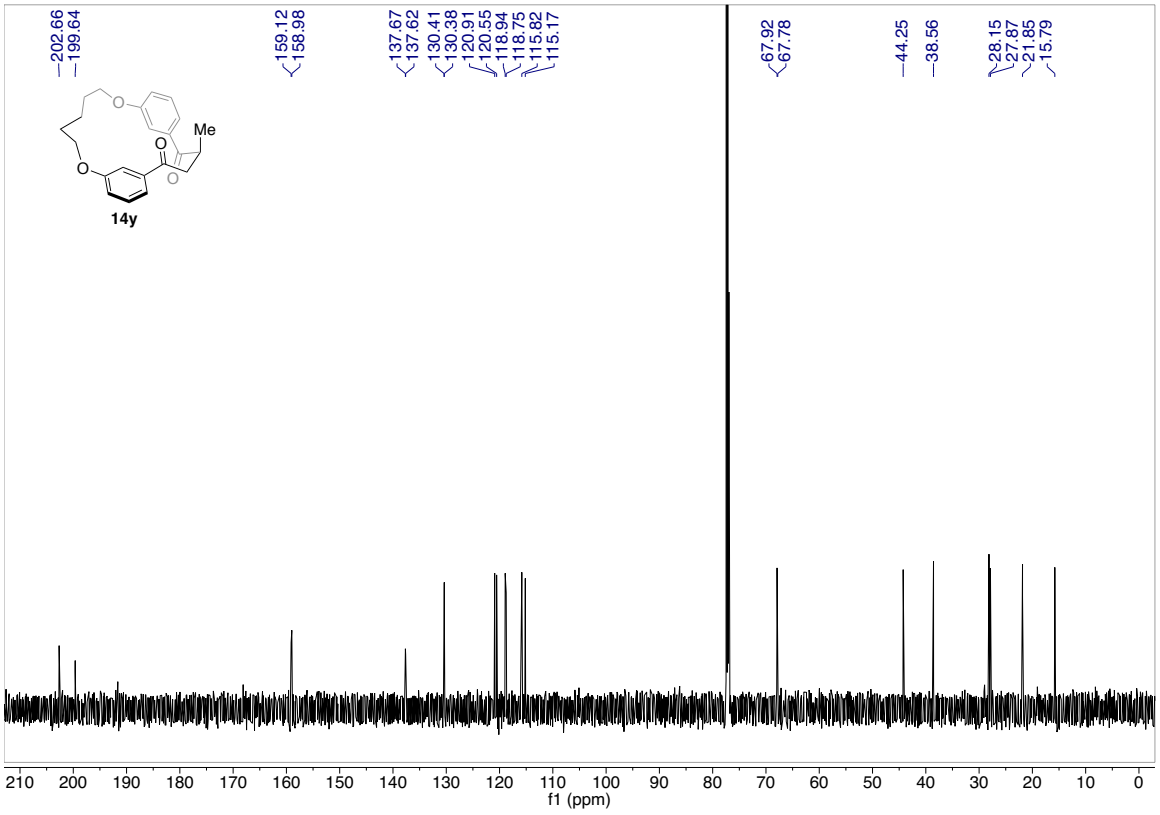
14y
f1 (ppm)

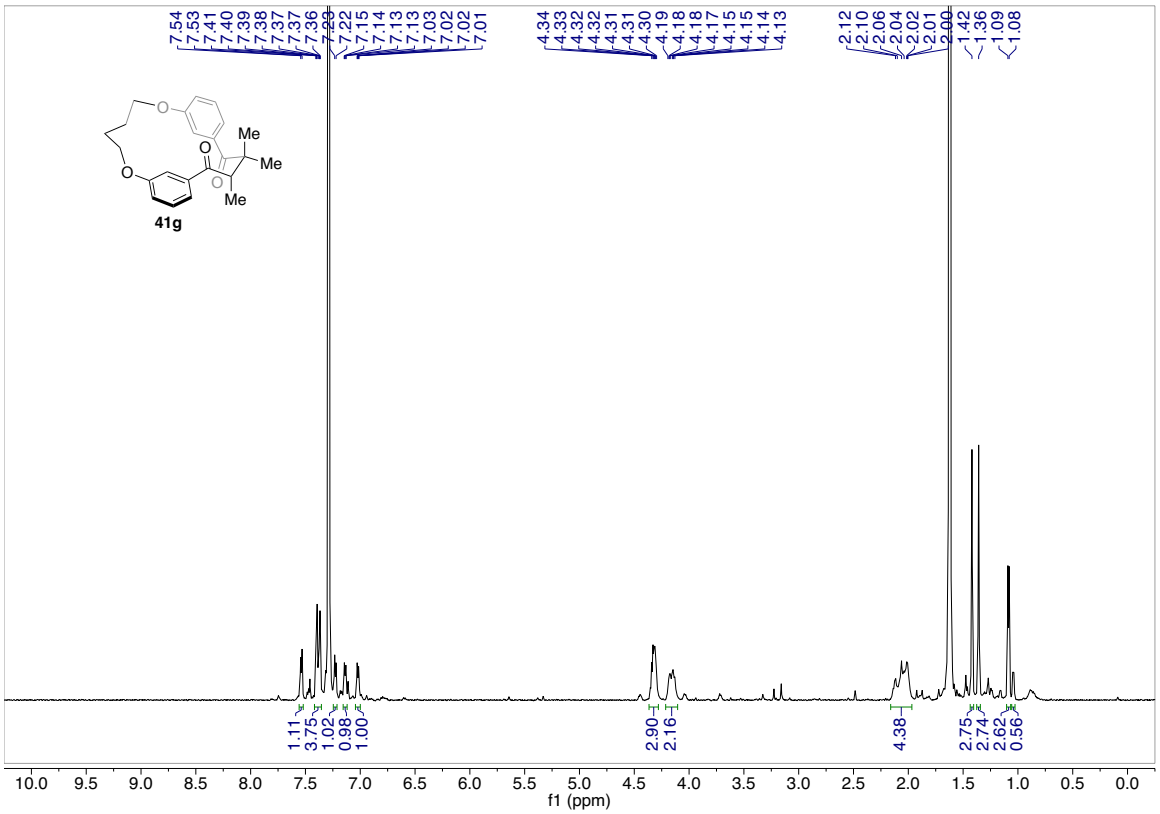
7.54
7.53
7.41
7.40
7.39
7.38
7.37
7.37
7.36
7.29
7.22
7.15
7.14
7.13
7.13
7.03
7.02
7.02
7.01
4.34
4.33
4.32
4.32
4.31
4.31
4.30
4.19
4.18
4.18
4.17
4.15
4.15
4.14
4.13
2.12
2.10
2.06
2.04
2.02
2.01
2.00
1.42
1.36
1.09
1.08
Me
Me
Me
O
O
O
41g
1.11
3.75
1.02
0.98
1.00
2.90
2.16
4.38
2.75
2.74
2.62
0.56
10.0 9.5 9.0 8.5 8.0 7.5 7.0 6.5 6.0 5.5 5.0 4.5 4.0 3.5 3.0 2.5 2.0 1.5 1.0 0.5 0.0
f1 (ppm)

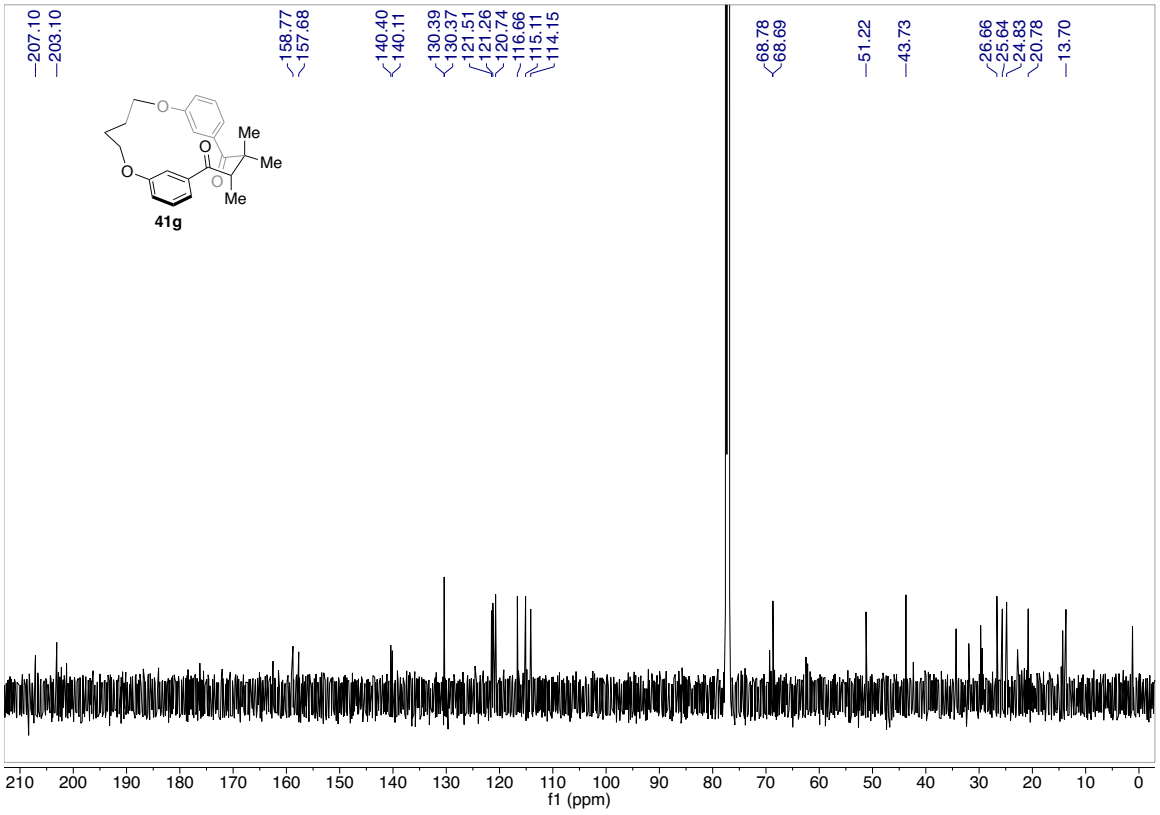
207.10
203.10
158.77
157.68
140.40
140.11
130.39
130.37
121.51
121.26
120.74
116.66
115.11
114.15
68.78
68.69
51.22
43.73
26.66
25.64
24.83
20.78
13.70
Me
Me
Me
O
O
O
41g
210 200 190 180 170 160 150 140 130 120 110 100 90 80 70 60 50 40 30 20 10 0
f1 (ppm)

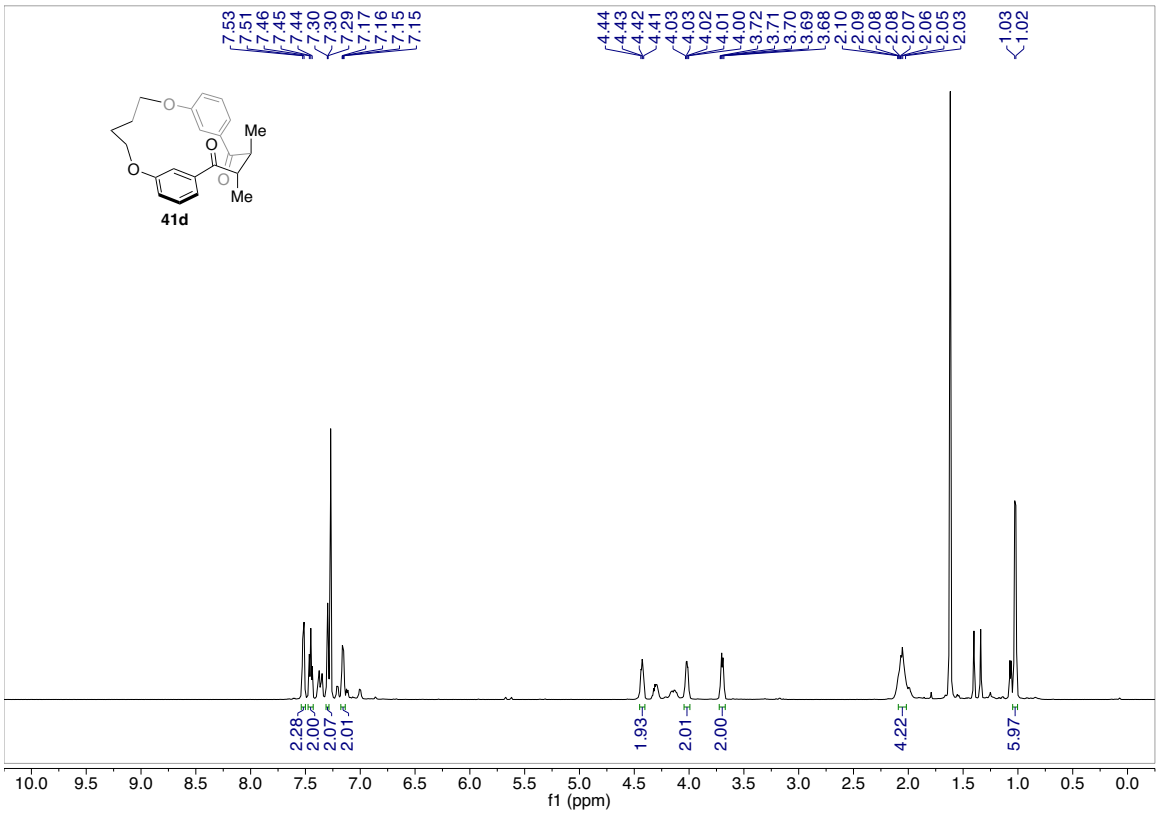
7.53
7.51
7.46
7.45
7.44
7.30
7.30
7.29
7.17
7.16
7.15
7.15
4.44
4.43
4.42
4.41
4.03
4.03
4.02
4.01
4.00
3.72
3.71
3.70
3.69
3.68
2.10
2.09
2.08
2.08
2.07
2.06
2.05
2.03
1.03
1.02
Me
O
O
O
Me
41d
2.28
2.00
2.07
2.01
1.93
2.01
2.00
4.22
5.97
10.0 9.5 9.0 8.5 8.0 7.5 7.0 6.5 6.0 5.5 5.0 4.5 4.0 3.5 3.0 2.5 2.0 1.5 1.0 0.5 0.0
f1 (ppm)

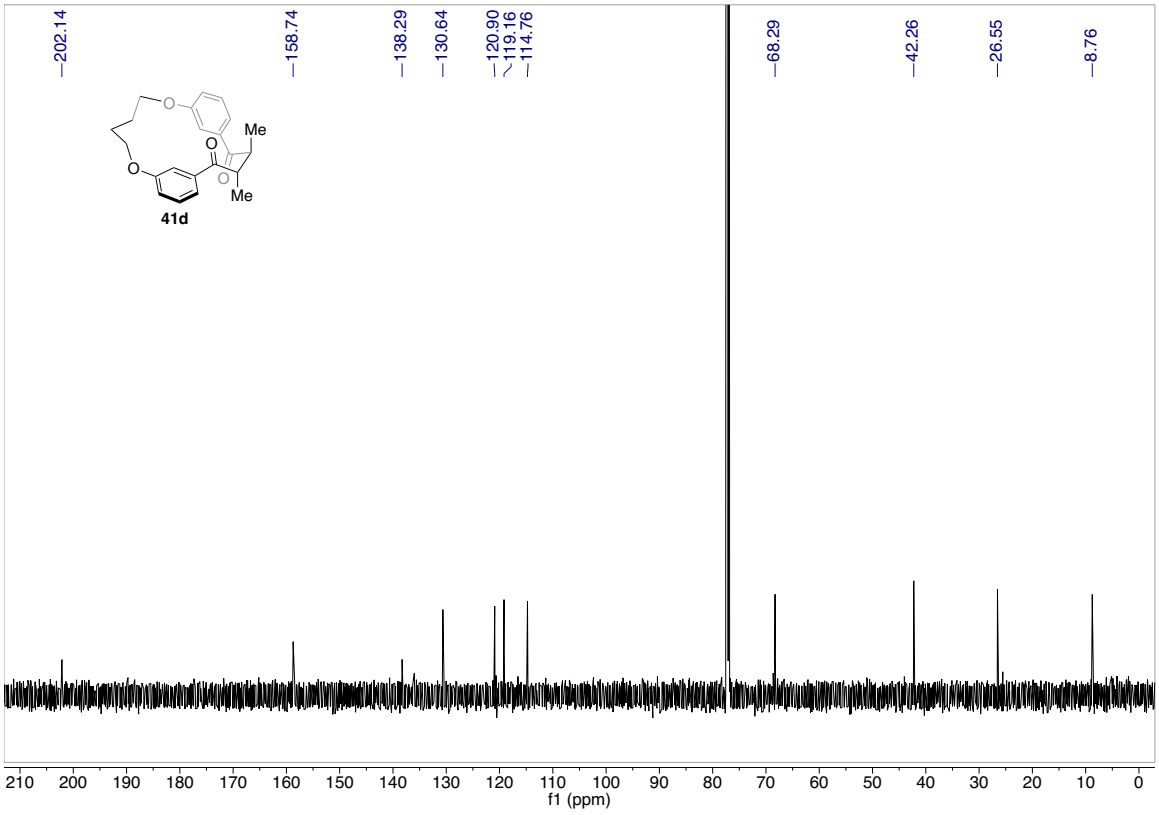
202.14
158.74
138.29
130.64
120.90
119.16
114.76
68.29
42.26
26.55
8.76
Me
O
O
O
Me
41d
210 200 190 180 170 160 150 140 130 120 110 100 90 80 70 60 50 40 30 20 10 0
f1 (ppm)

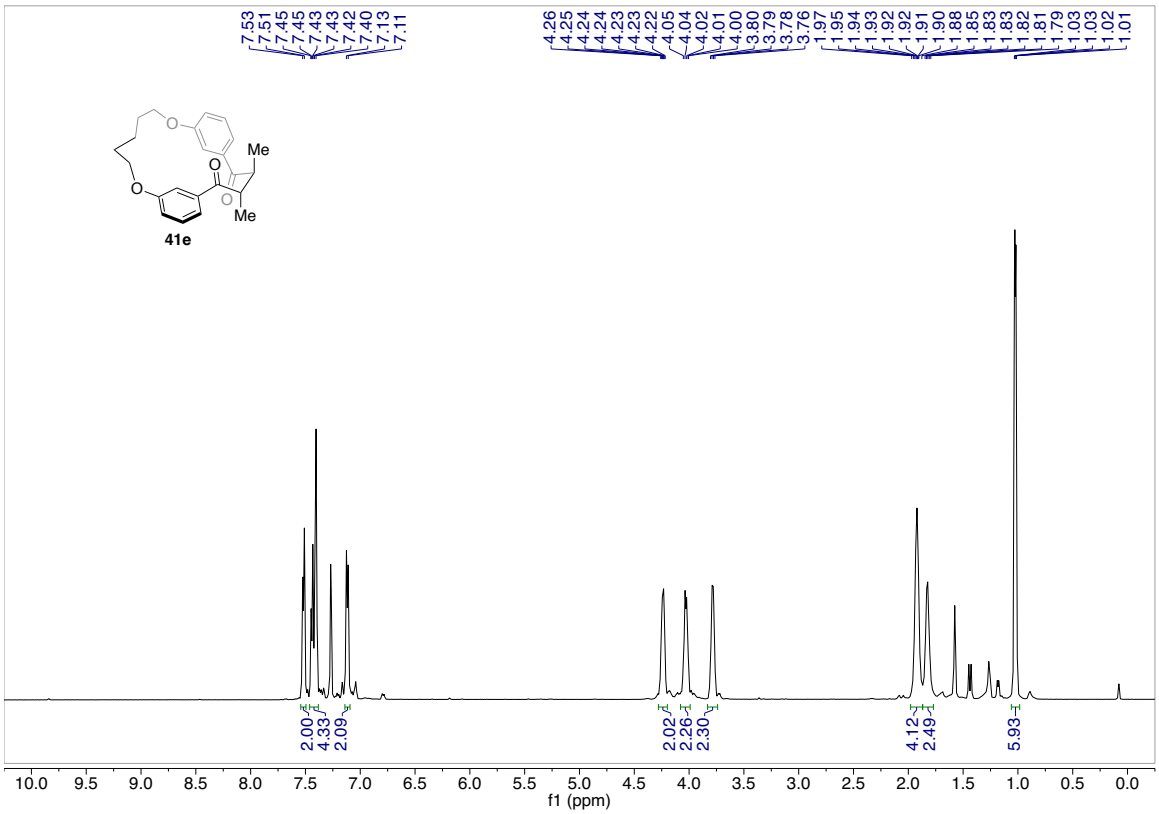
7.53
7.51
7.45
7.45
7.43
7.43
7.42
7.40
7.13
7.11
4.26
4.25
4.24
4.24
4.23
4.23
4.22
4.05
4.04
4.02
4.01
4.00
3.80
3.79
3.78
3.76
1.97
1.95
1.94
1.93
1.92
1.92
1.91
1.90
1.88
1.85
1.83
1.83
1.82
1.81
1.79
1.03
1.02
1.01
Me
Me
41e
2.00
4.33
2.09
2.02
2.26
2.30
4.12
2.49
5.93
f1 (ppm)

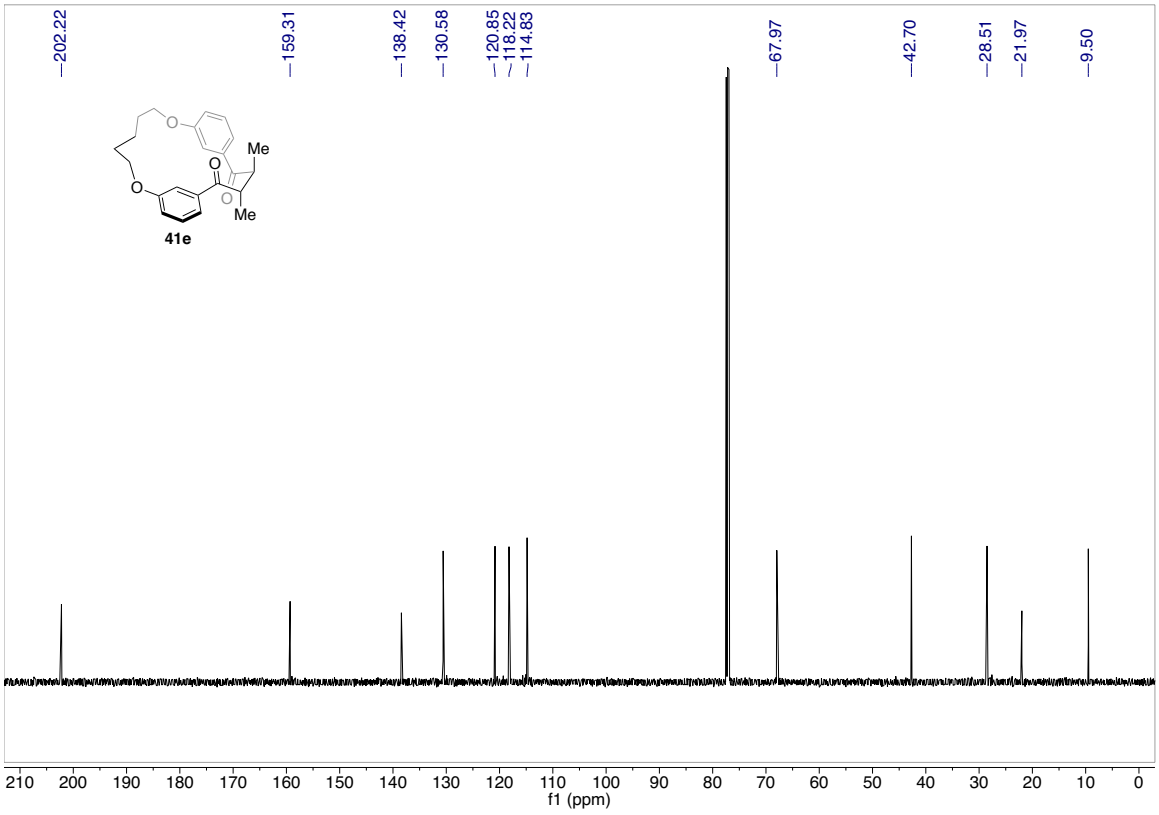
202.22
159.31
138.42
130.58
120.85
118.22
114.83
67.97
42.70
28.51
21.97
9.50
Me
Me
41e
f1 (ppm)

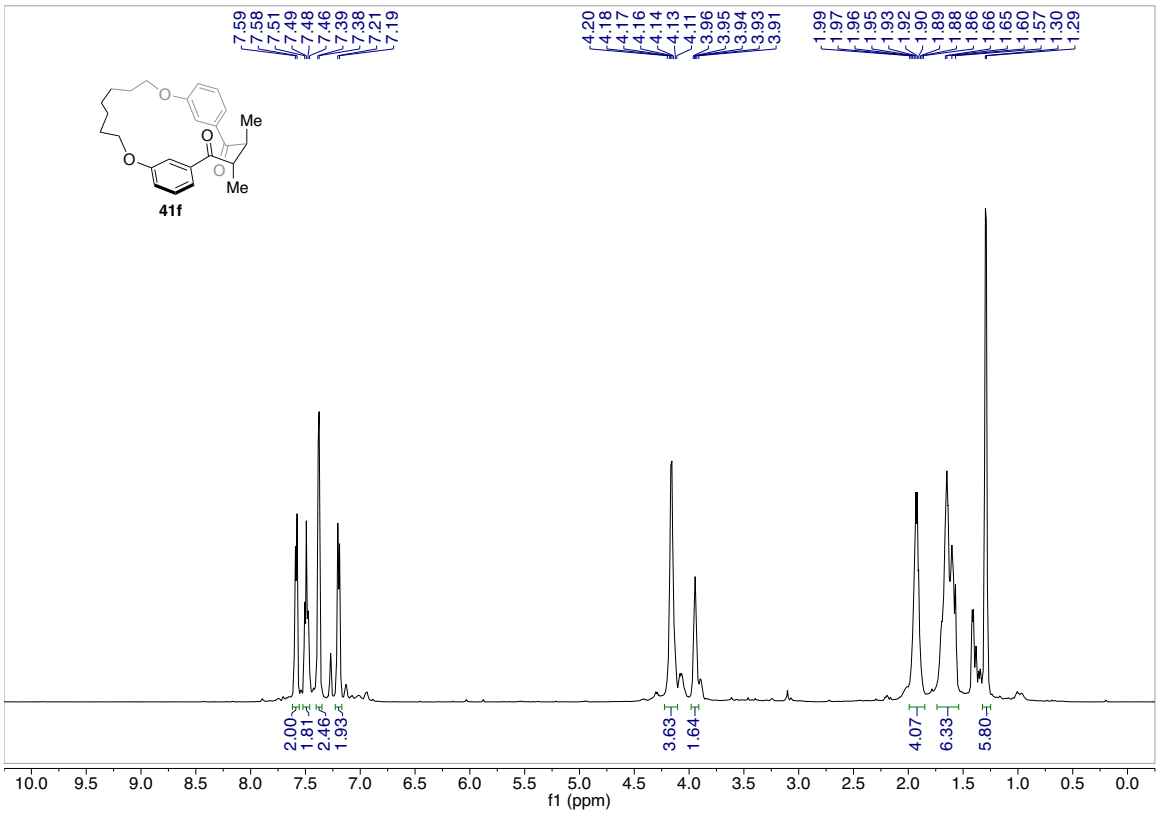
7.59
7.58
7.51
7.49
7.48
7.46
7.39
7.38
7.21
7.19
4.20
4.18
4.17
4.16
4.14
4.13
4.11
3.96
3.95
3.94
3.93
3.91
1.99
1.97
1.96
1.95
1.93
1.92
1.90
1.89
1.88
1.86
1.66
1.65
1.60
1.57
1.30
1.29
Me
O
O
O
Me
41f
2.00
1.81
2.46
1.93
3.63
1.64
4.07
6.33
5.80
10.0 9.5 9.0 8.5 8.0 7.5 7.0 6.5 6.0 5.5 5.0 4.5 4.0 3.5 3.0 2.5 2.0 1.5 1.0 0.5 0.0
f1 (ppm)

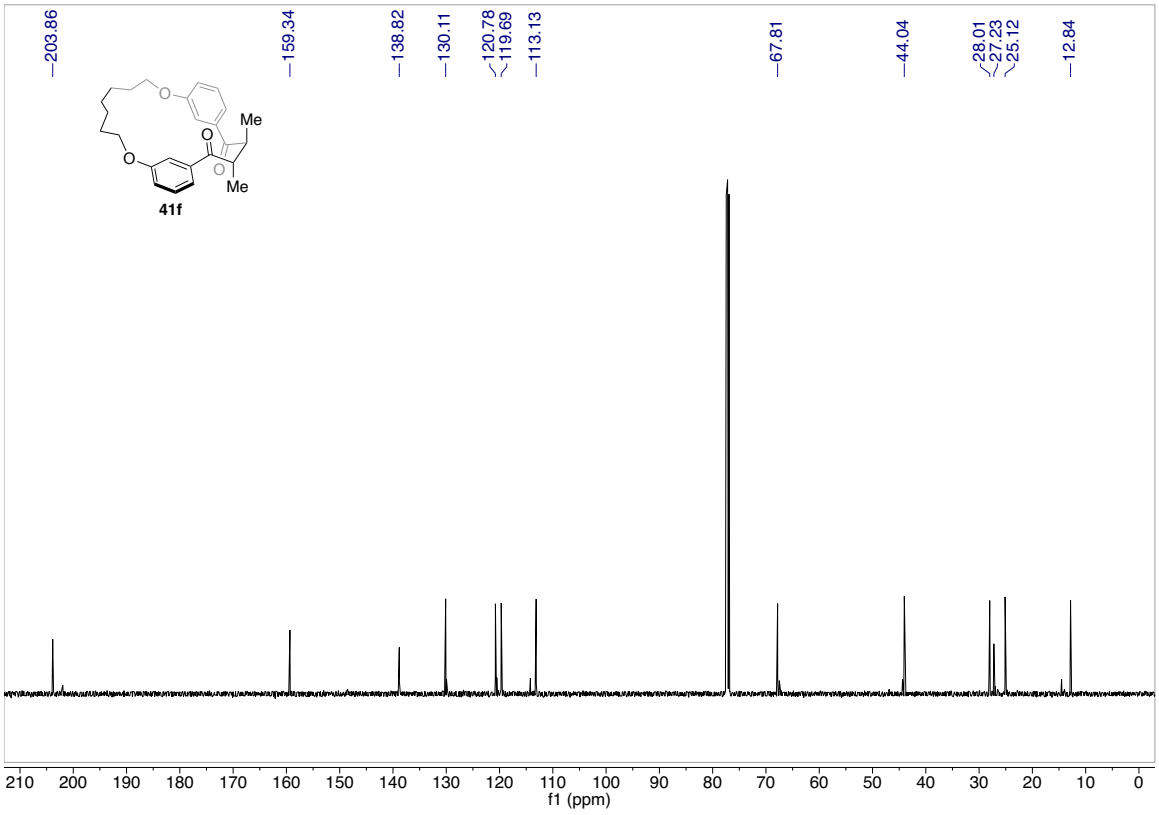
203.86
159.34
138.82
130.11
120.78
119.69
113.13
67.81
44.04
28.01
27.23
25.12
12.84
Me
O
O
O
Me
41f
210 200 190 180 170 160 150 140 130 120 110 100 90 80 70 60 50 40 30 20 10 0
f1 (ppm)

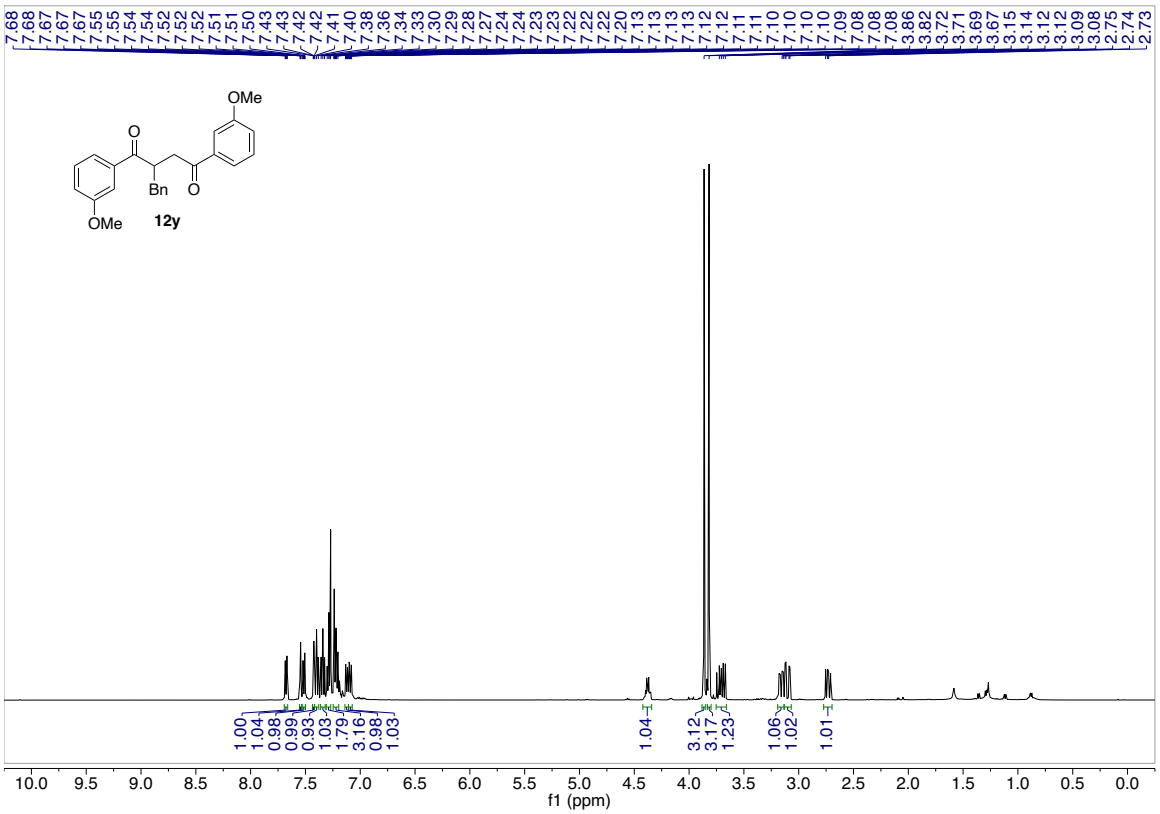
OMe
O
Bn
O
OMe
12y
f1 (ppm)

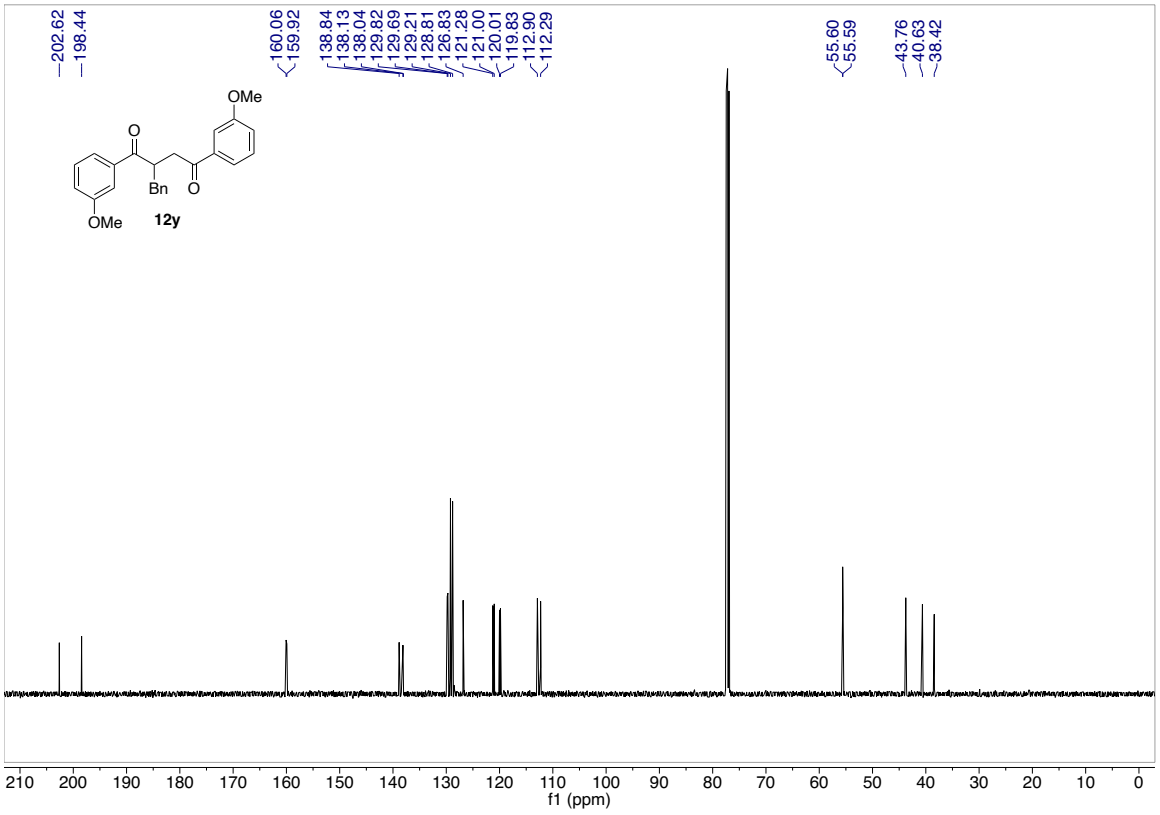
OMe
O
Bn
O
OMe
12y
f1 (ppm)

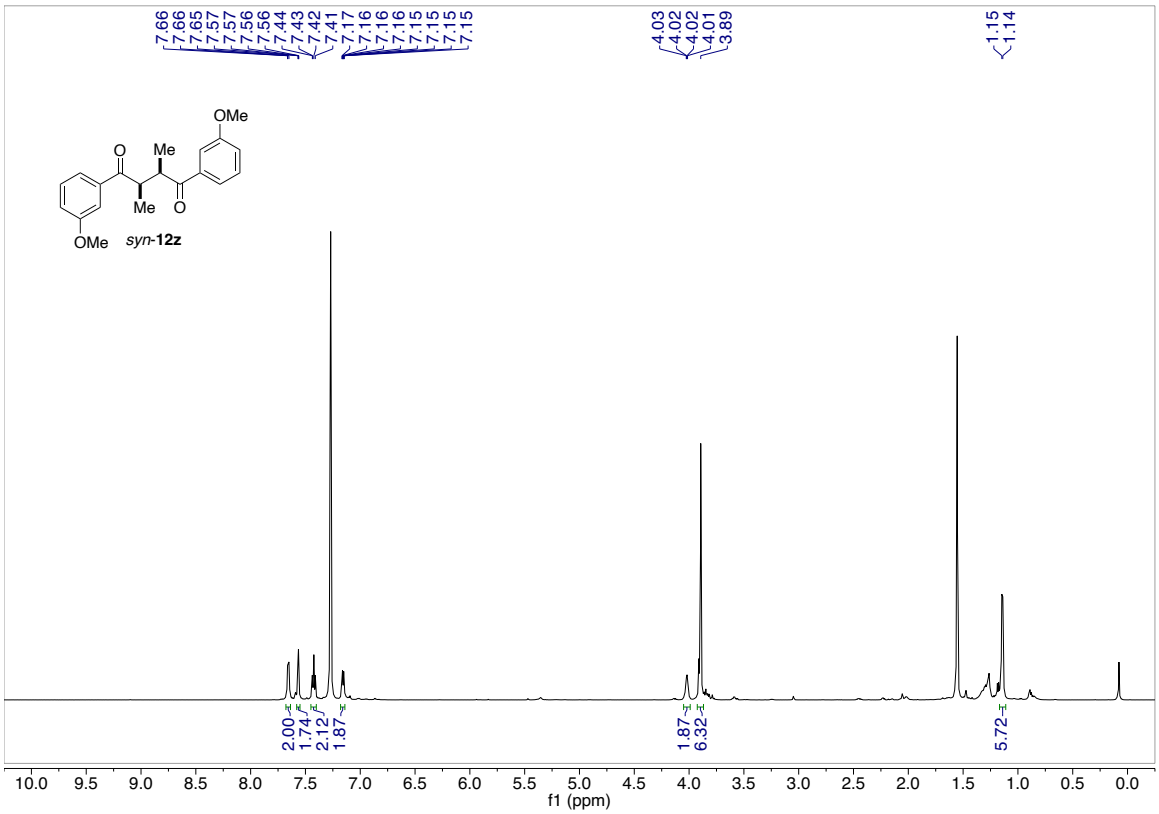
7.66
7.66
7.65
7.57
7.57
7.56
7.56
7.44
7.43
7.42
7.41
7.17
7.16
7.16
7.16
7.15
7.15
7.15
7.15
4.03
4.02
4.02
4.01
3.89
1.15
1.14
OMe
O
Me
Me
O
OMe
syn-12z
2.00
1.74
2.12
1.87
1.87
6.32
5.72
10.0 9.5 9.0 8.5 8.0 7.5 7.0 6.5 6.0 5.5 5.0 4.5 4.0 3.5 3.0 2.5 2.0 1.5 1.0 0.5 0.0
f1 (ppm)

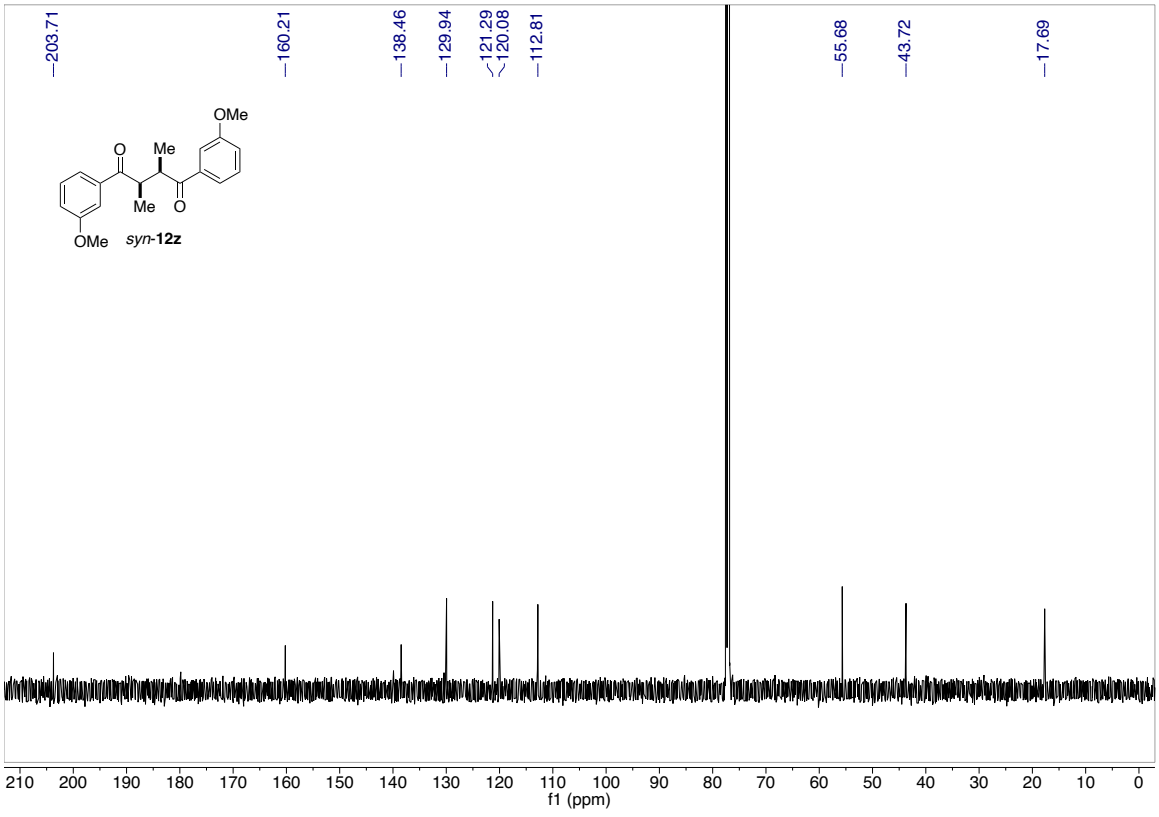
203.71
160.21
138.46
129.94
121.29
120.08
112.81
55.68
43.72
17.69
OMe
O
Me
Me
O
OMe
syn-12z
210 200 190 180 170 160 150 140 130 120 110 100 90 80 70 60 50 40 30 20 10 0
f1 (ppm)

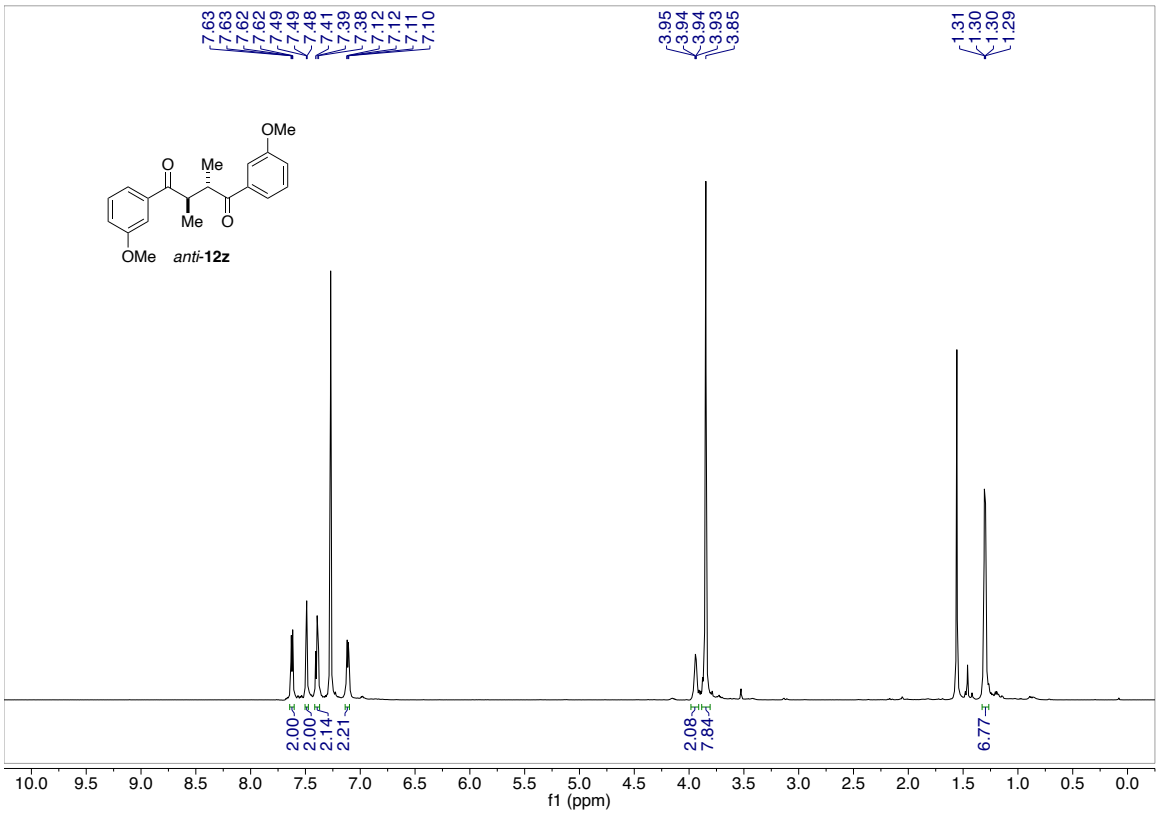
7.63
7.63
7.62
7.62
7.49
7.49
7.48
7.41
7.39
7.38
7.12
7.12
7.11
7.10
3.95
3.94
3.94
3.93
3.85
1.31
1.30
1.30
1.29
OMe
O
Me
Me
O
OMe
anti-12z
2.00
2.00
2.14
2.21
2.08
7.84
6.77
10.0 9.5 9.0 8.5 8.0 7.5 7.0 6.5 6.0 5.5 5.0 4.5 4.0 3.5 3.0 2.5 2.0 1.5 1.0 0.5 0.0
f1 (ppm)

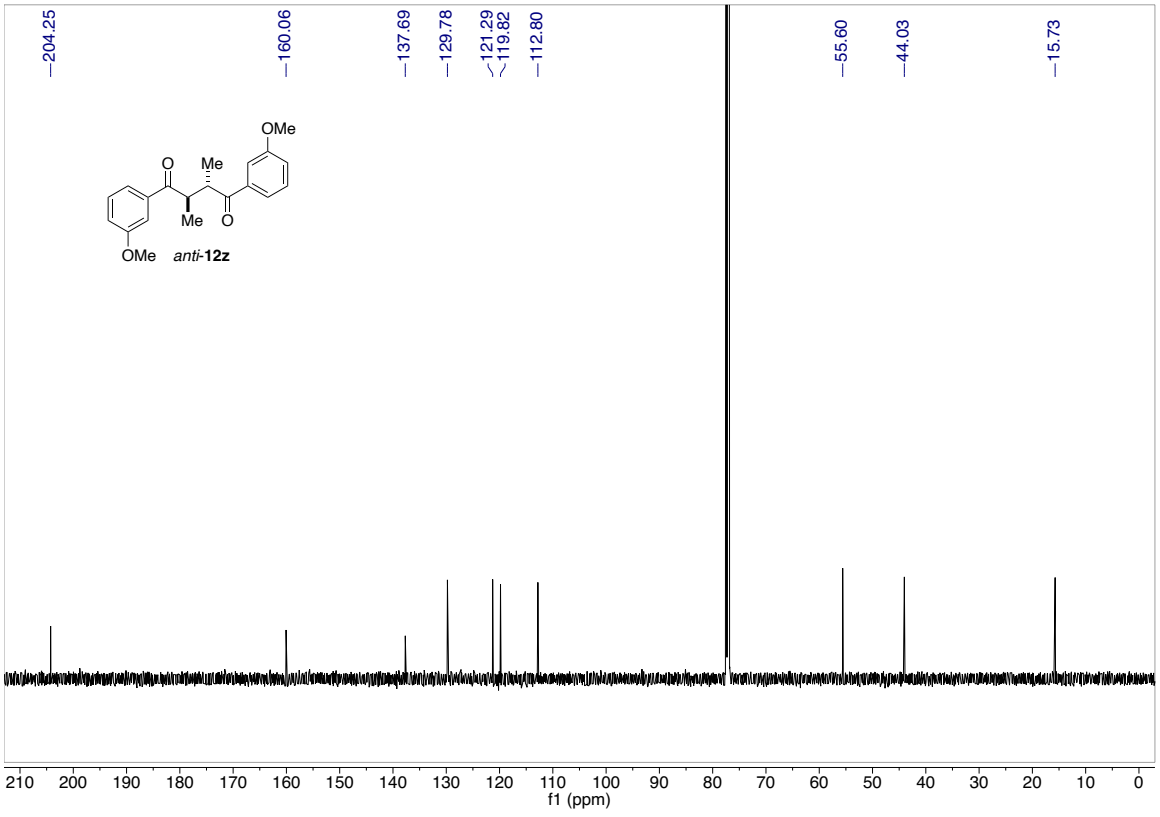
204.25
160.06
137.69
129.78
121.29
119.82
112.80
55.60
44.03
15.73
OMe
O
Me
Me
O
OMe
anti-12z
210 200 190 180 170 160 150 140 130 120 110 100 90 80 70 60 50 40 30 20 10 0
f1 (ppm)

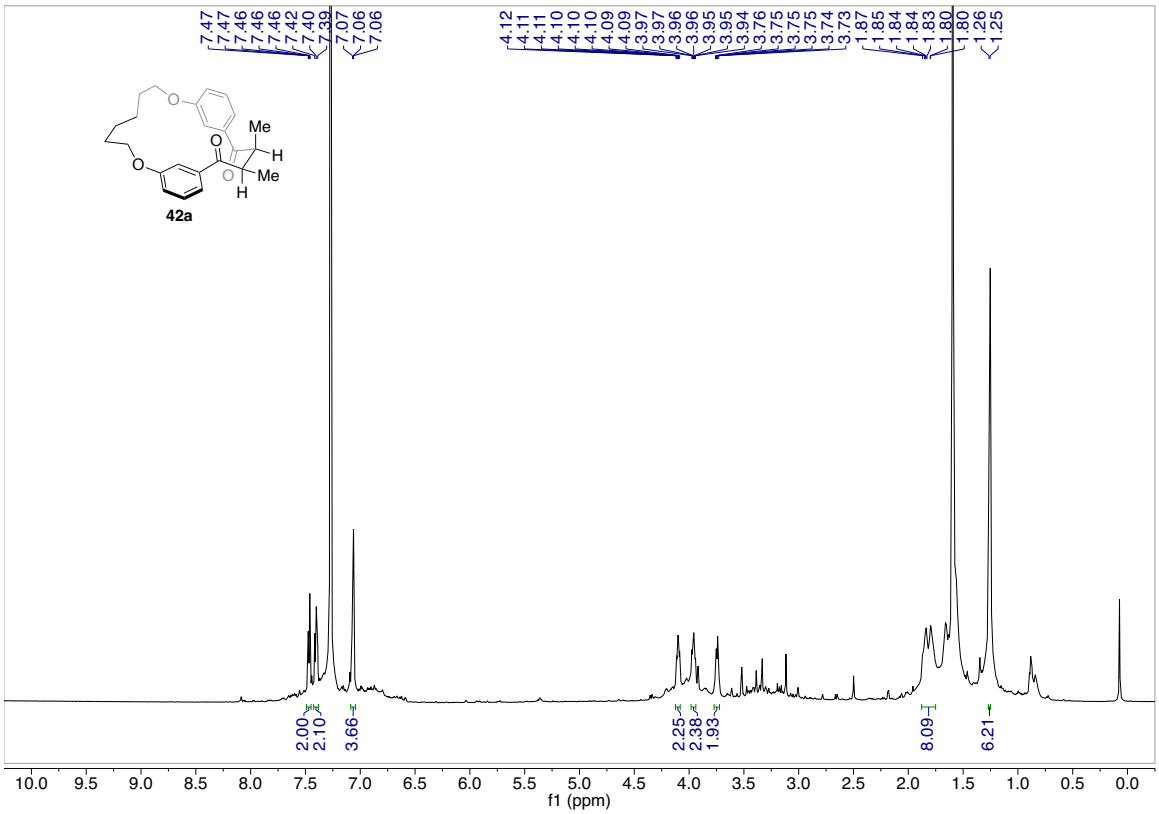
7.47
7.47
7.46
7.46
7.46
7.42
7.40
7.39
7.07
7.06
7.06
4.12
4.11
4.11
4.10
4.10
4.10
4.09
4.09
3.97
3.97
3.96
3.96
3.95
3.95
3.94
3.76
3.75
3.75
3.74
3.73
1.87
1.85
1.84
1.84
1.83
1.80
1.80
1.26
1.25
Me
H
Me
H
42a
2.00
2.10
3.66
2.25
2.38
1.93
8.09
6.21
10.0 9.5 9.0 8.5 8.0 7.5 7.0 6.5 6.0 5.5 5.0 4.5 4.0 3.5 3.0 2.5 2.0 1.5 1.0 0.5 0.0
f1 (ppm)

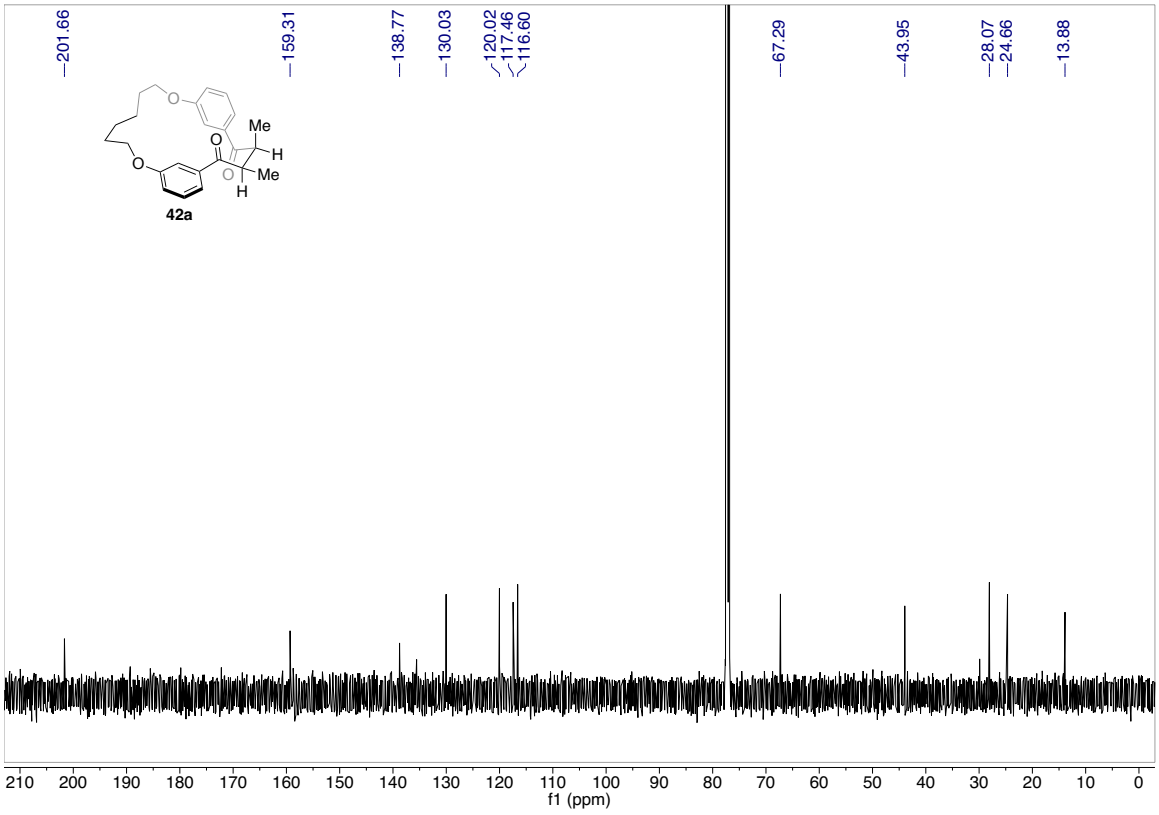
201.66
159.31
138.77
130.03
120.02
117.46
116.60
67.29
43.95
28.07
24.66
13.88
Me
H
Me
H
42a
210 200 190 180 170 160 150 140 130 120 110 100 90 80 70 60 50 40 30 20 10 0
f1 (ppm)

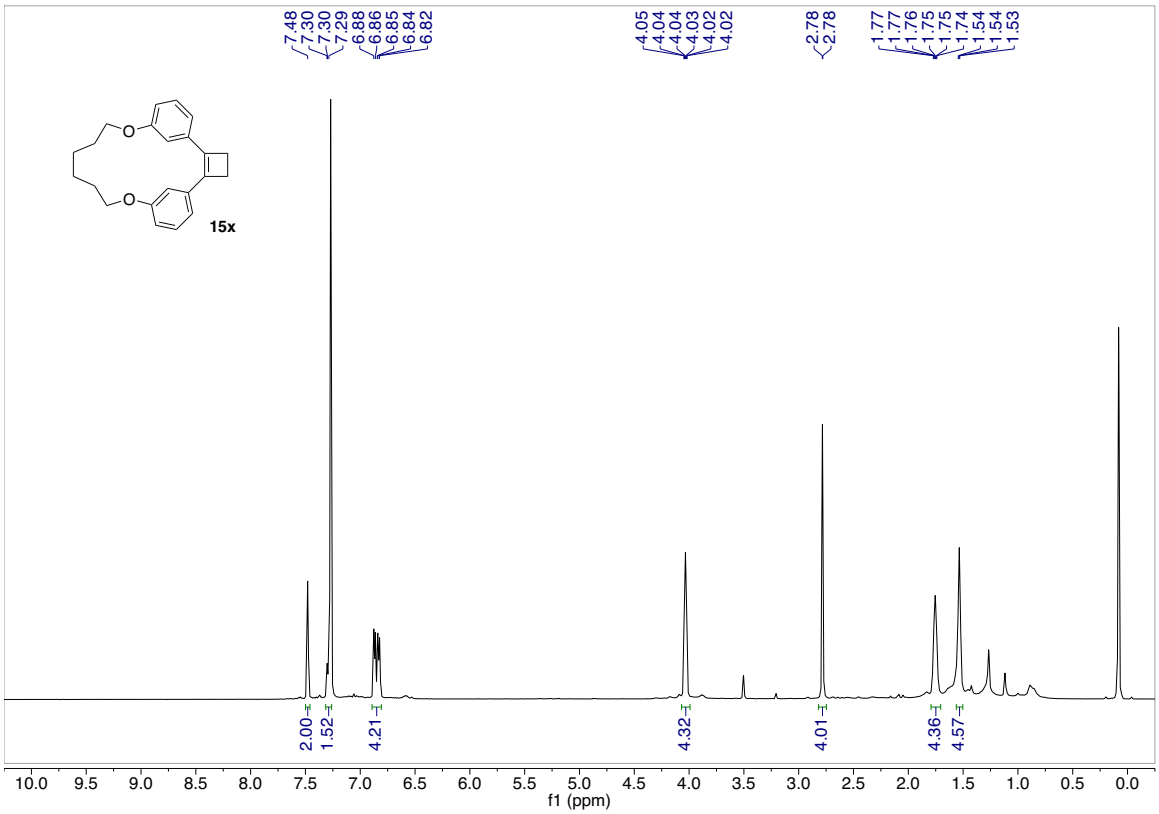
7.48
7.30
7.30
7.29
6.88
6.86
6.85
6.84
6.82
4.05
4.04
4.04
4.03
4.02
4.02
2.78
2.78
1.77
1.77
1.76
1.75
1.75
1.74
1.54
1.54
1.53
15x
2.00
1.52
4.21
4.32
4.01
4.36
4.57
10.0 9.5 9.0 8.5 8.0 7.5 7.0 6.5 6.0 5.5 5.0 4.5 4.0 3.5 3.0 2.5 2.0 1.5 1.0 0.5 0.0
f1 (ppm)

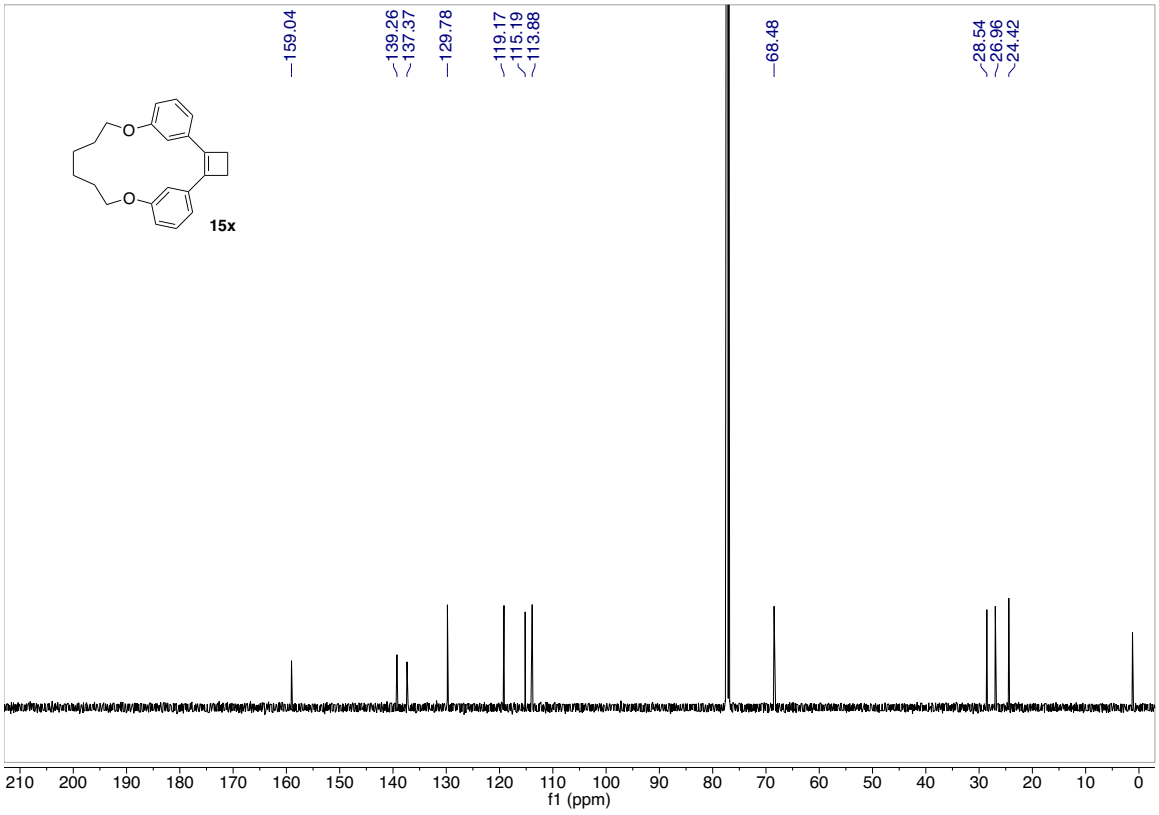
159.04
139.26
137.37
129.78
119.17
115.19
113.88
68.48
28.54
26.96
24.42
15x
210 200 190 180 170 160 150 140 130 120 110 100 90 80 70 60 50 40 30 20 10 0
f1 (ppm)

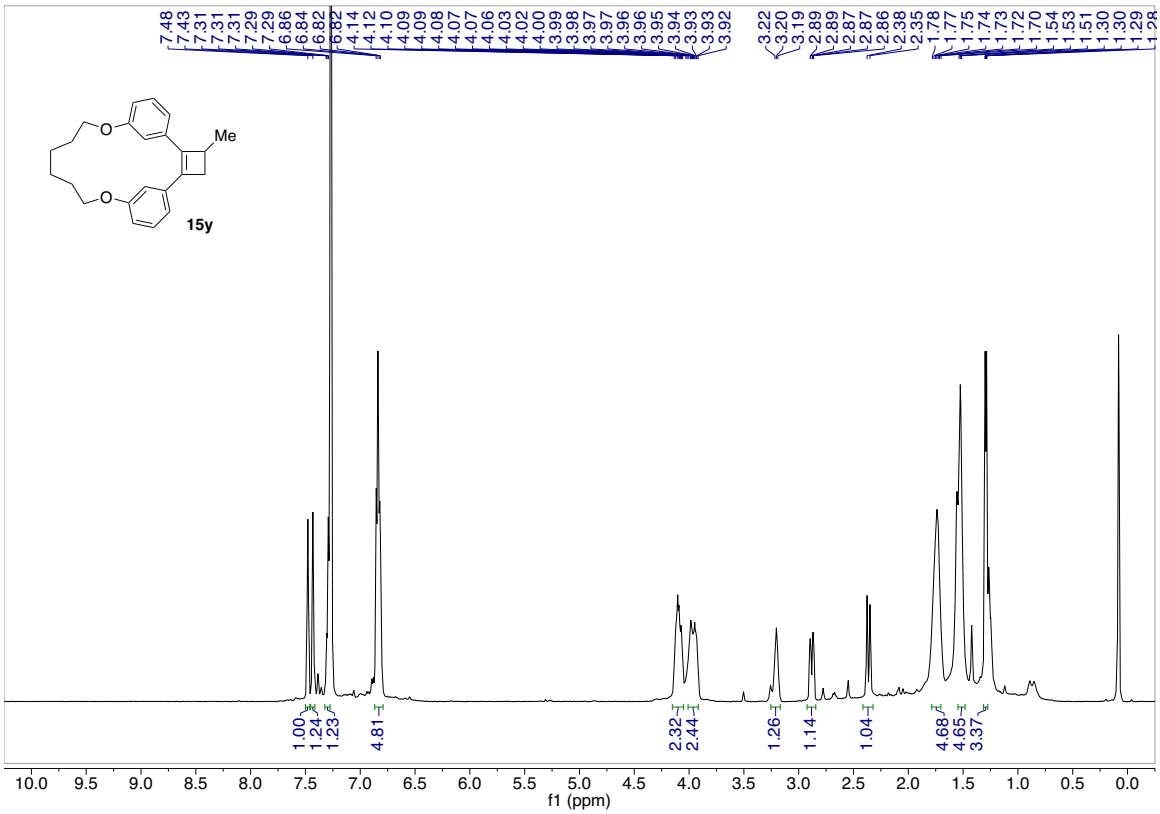
7.48
7.43
7.31
7.31
7.31
7.29
7.29
6.86
6.84
6.82
6.82
4.14
4.12
4.10
4.09
4.09
4.08
4.07
4.07
4.06
4.03
4.02
4.00
4.00
3.99
3.98
3.97
3.97
3.96
3.96
3.95
3.94
3.93
3.93
3.92
3.22
3.20
3.19
2.89
2.89
2.87
2.87
2.86
2.38
2.35
1.78
1.77
1.75
1.74
1.73
1.72
1.70
1.54
1.53
1.51
1.30
1.30
1.29
1.28
O
O
Me
15y
1.00
1.24
1.23
4.81
2.32
2.44
1.26
1.14
1.04
4.68
4.65
3.37
10.0 9.5 9.0 8.5 8.0 7.5 7.0 6.5 6.0 5.5 5.0 4.5 4.0 3.5 3.0 2.5 2.0 1.5 1.0 0.5 0.0
f1 (ppm)

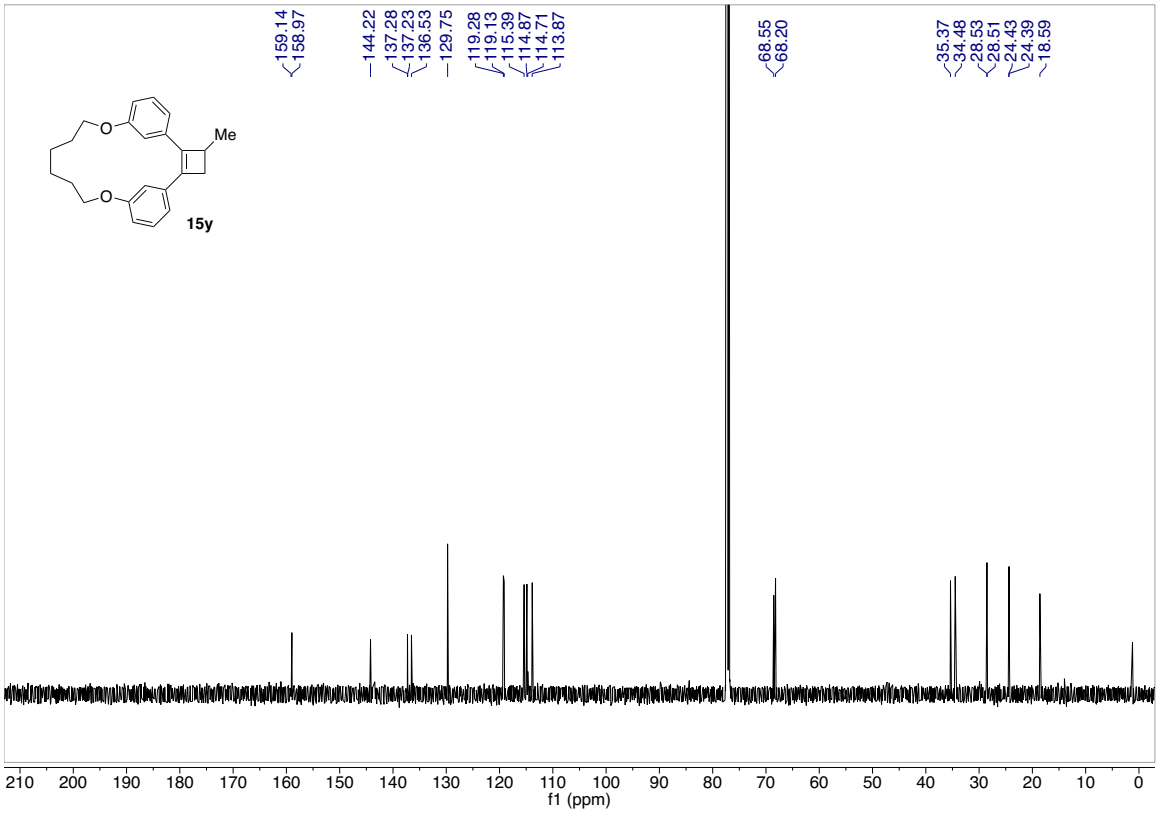
159.14
158.97
144.22
137.28
137.23
136.53
129.75
119.28
119.13
115.39
114.87
114.71
113.87
68.55
68.20
35.37
34.48
28.53
28.51
24.43
24.39
18.59
O
O
Me
15y
210 200 190 180 170 160 150 140 130 120 110 100 90 80 70 60 50 40 30 20 10 0
f1 (ppm)

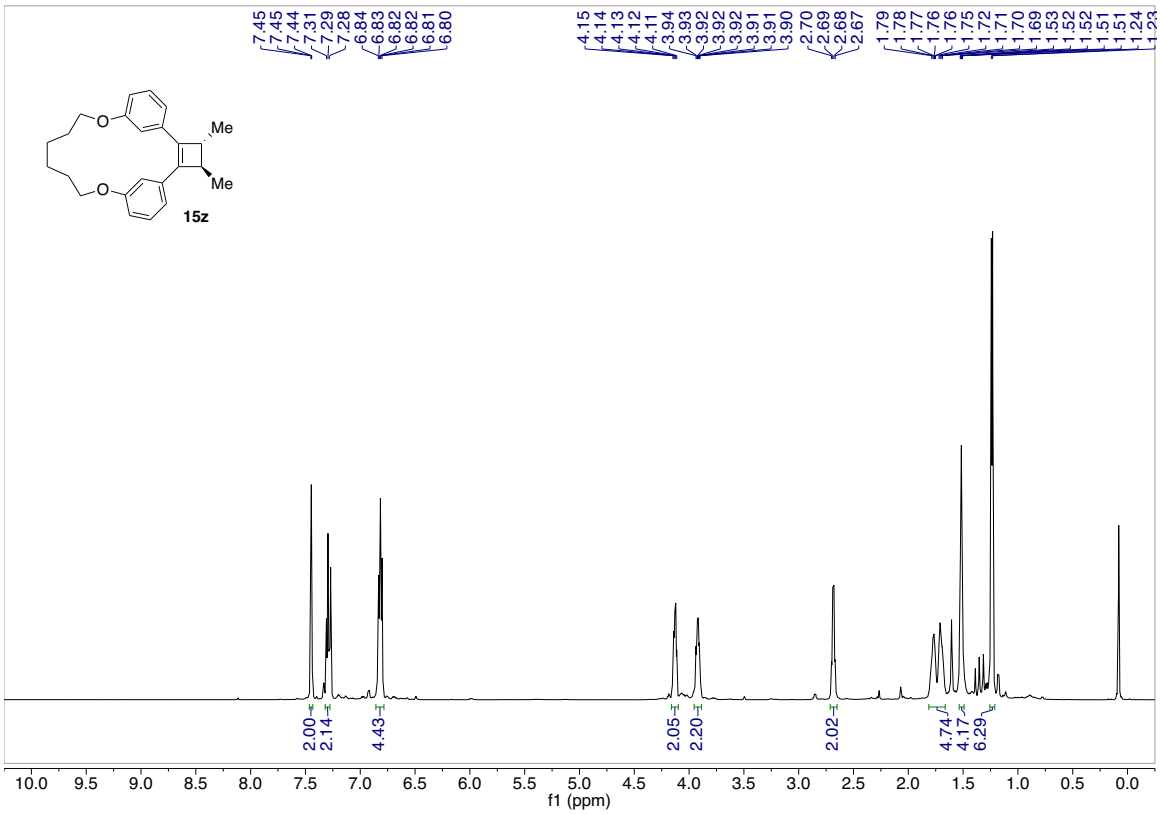
7.45
7.45
7.44
7.31
7.29
7.28
6.84
6.83
6.82
6.82
6.81
6.80
4.15
4.14
4.13
4.12
4.11
3.94
3.93
3.92
3.92
3.92
3.91
3.91
3.90
2.70
2.69
2.68
2.67
1.79
1.78
1.77
1.77
1.76
1.76
1.75
1.72
1.71
1.70
1.69
1.53
1.52
1.52
1.51
1.51
1.24
Me
Me
O
O
15z
2.00
2.14
4.43
2.05
2.20
2.02
4.74
4.17
6.29
10.0 9.5 9.0 8.5 8.0 7.5 7.0 6.5 6.0 5.5 5.0 4.5 4.0 3.5 3.0 2.5 2.0 1.5 1.0 0.5 0.0
f1 (ppm)

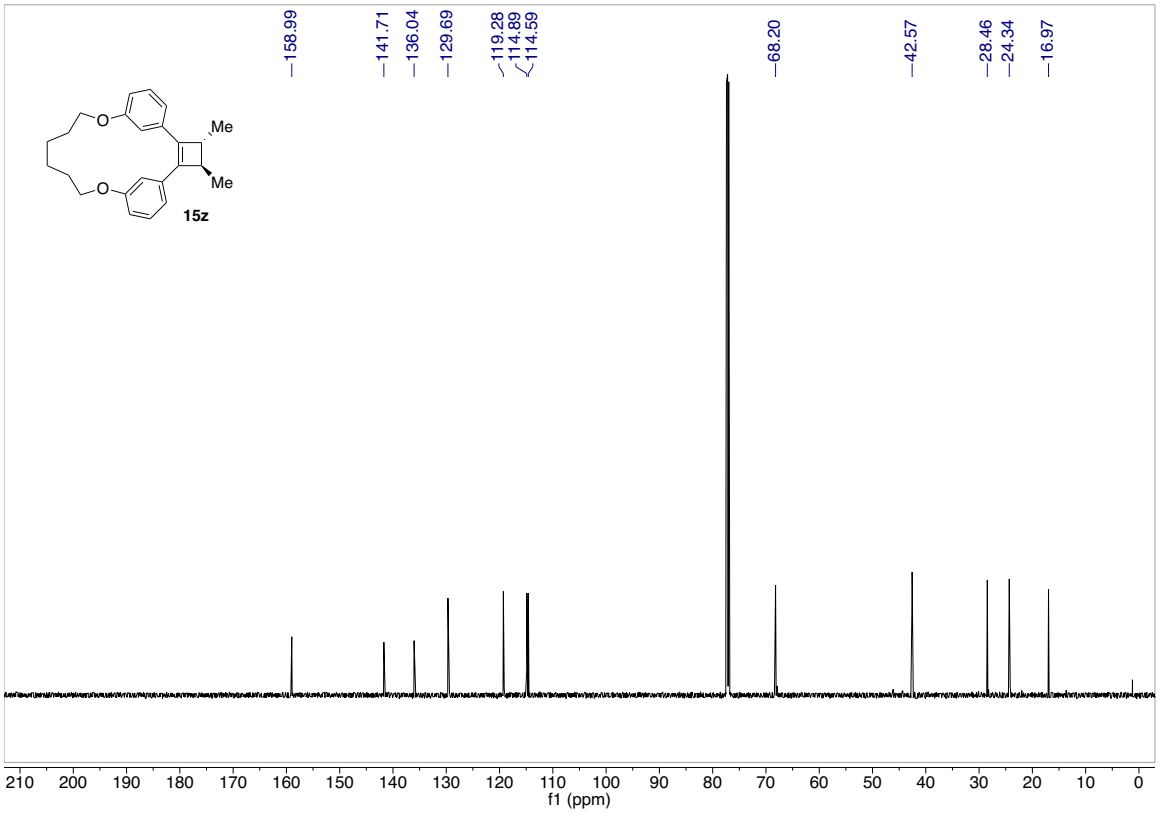
158.99
141.71
136.04
129.69
119.28
114.89
114.59
68.20
42.57
28.46
24.34
16.97
Me
Me
O
O
15z
210 200 190 180 170 160 150 140 130 120 110 100 90 80 70 60 50 40 30 20 10 0
f1 (ppm)

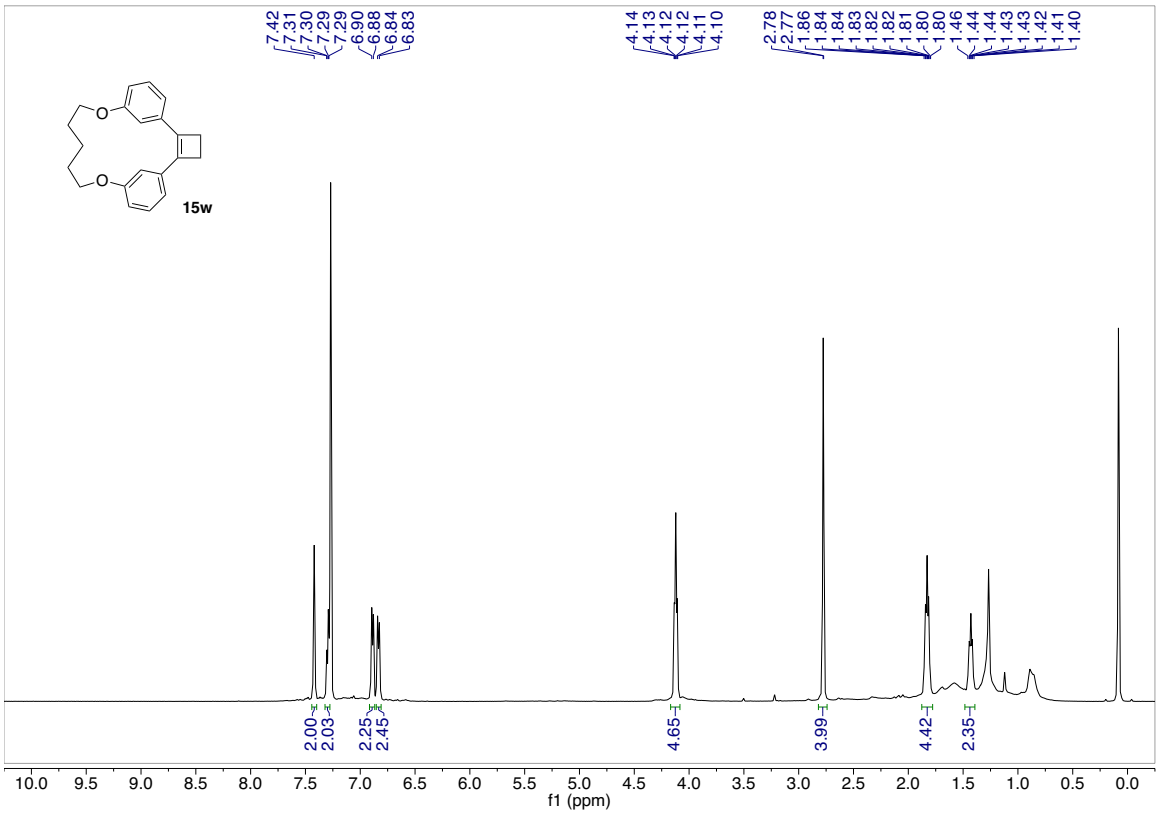
7.42
7.31
7.30
7.29
7.29
6.90
6.88
6.84
6.83
4.14
4.13
4.12
4.12
4.11
4.10
2.78
2.77
1.86
1.84
1.84
1.83
1.82
1.82
1.81
1.80
1.80
1.46
1.44
1.44
1.43
1.43
1.42
1.41
1.40
15w
2.00
2.03
2.25
2.45
4.65
3.99
4.42
2.35
f1 (ppm)

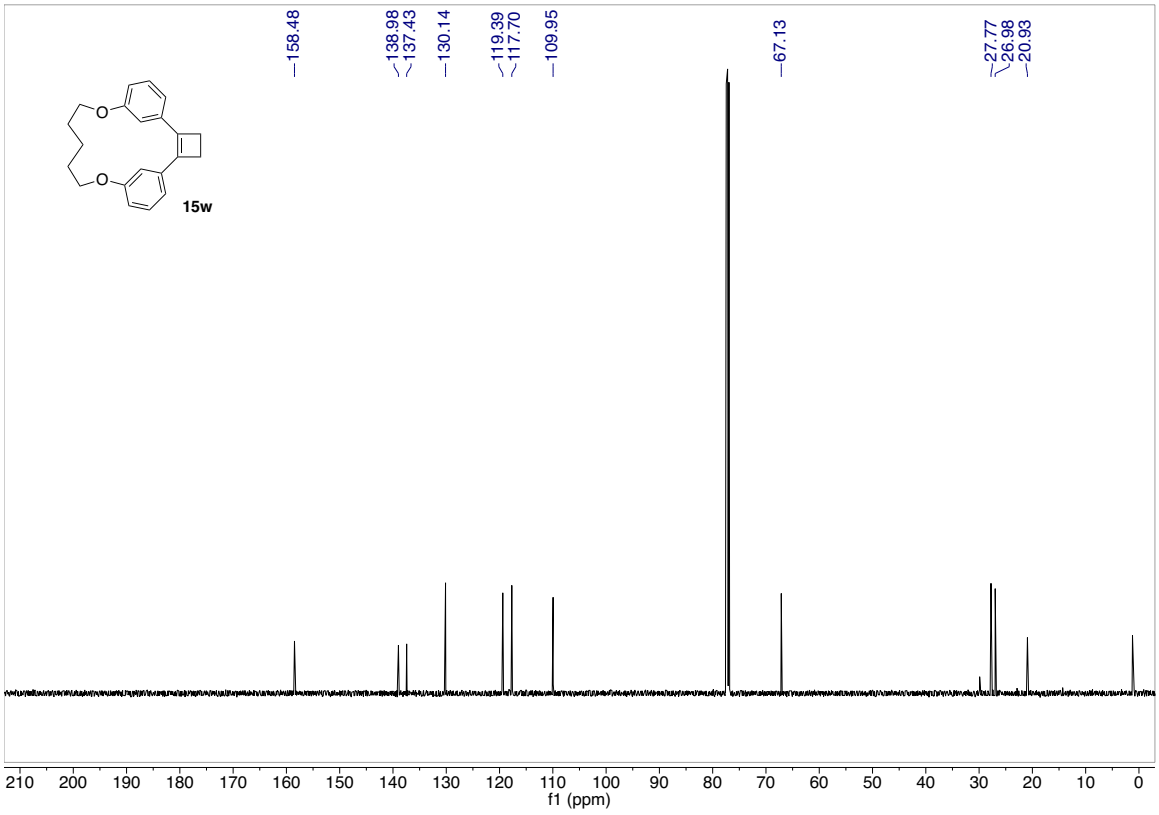
158.48
138.98
137.43
130.14
119.39
117.70
109.95
67.13
27.77
26.98
20.93
15w
f1 (ppm)

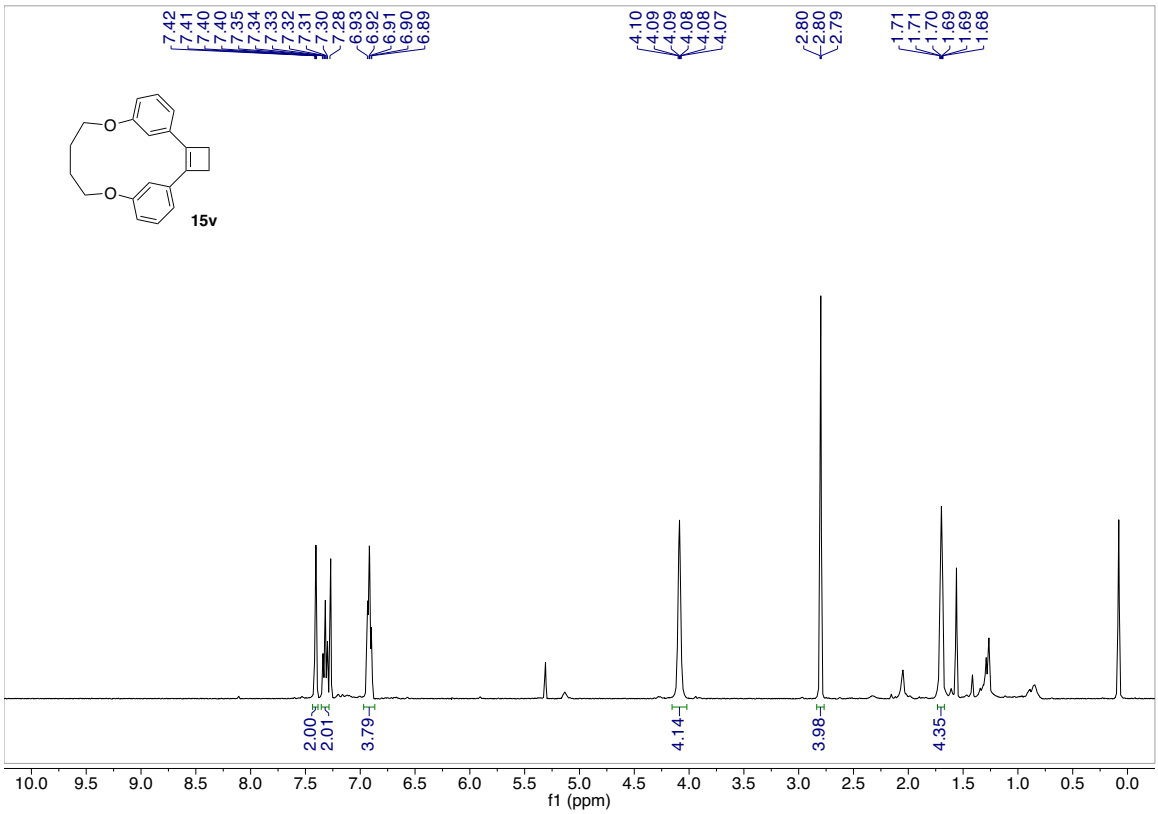
7.42
7.41
7.40
7.40
7.35
7.34
7.33
7.32
7.31
7.30
7.28
6.93
6.92
6.91
6.90
6.89
4.10
4.09
4.09
4.08
4.08
4.07
2.80
2.80
2.79
1.71
1.71
1.70
1.69
1.69
1.68
15v
2.00
2.01
3.79
4.14
3.98
4.35
f1 (ppm)

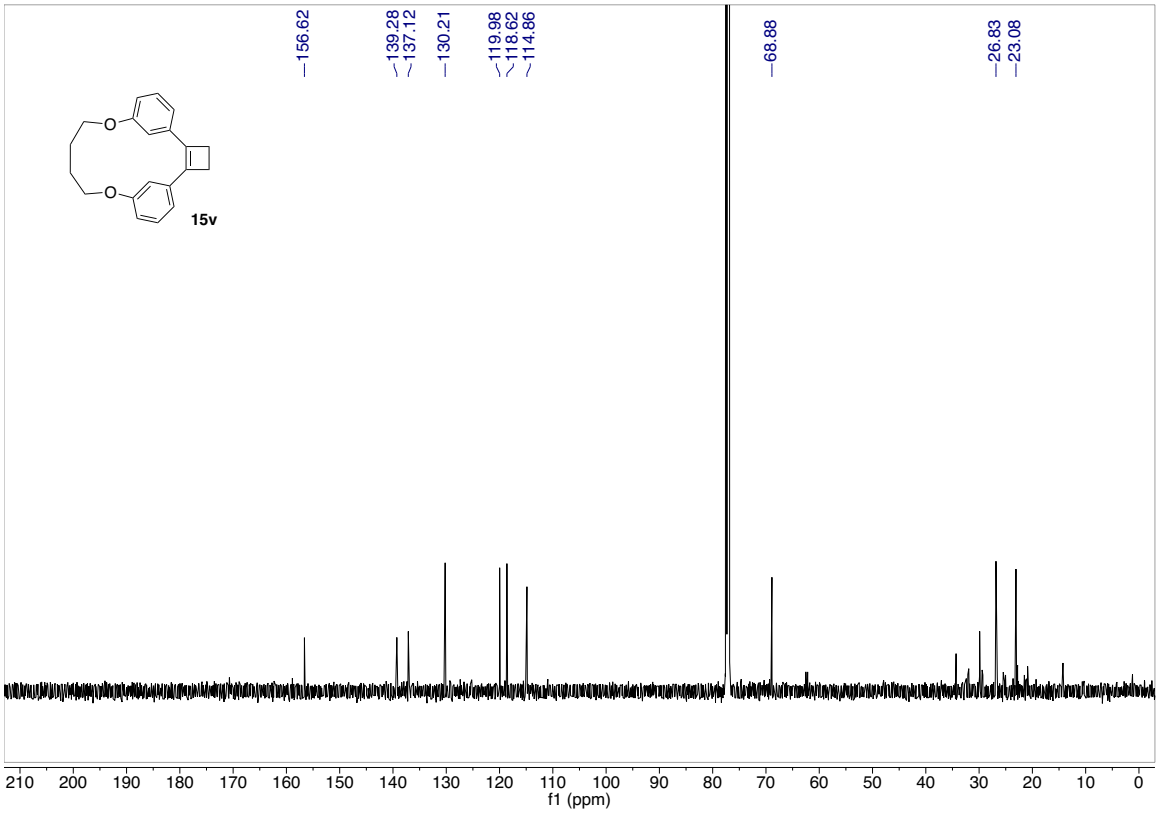
156.62
139.28
137.12
130.21
119.98
118.62
114.86
68.88
26.83
23.08
15v
f1 (ppm)

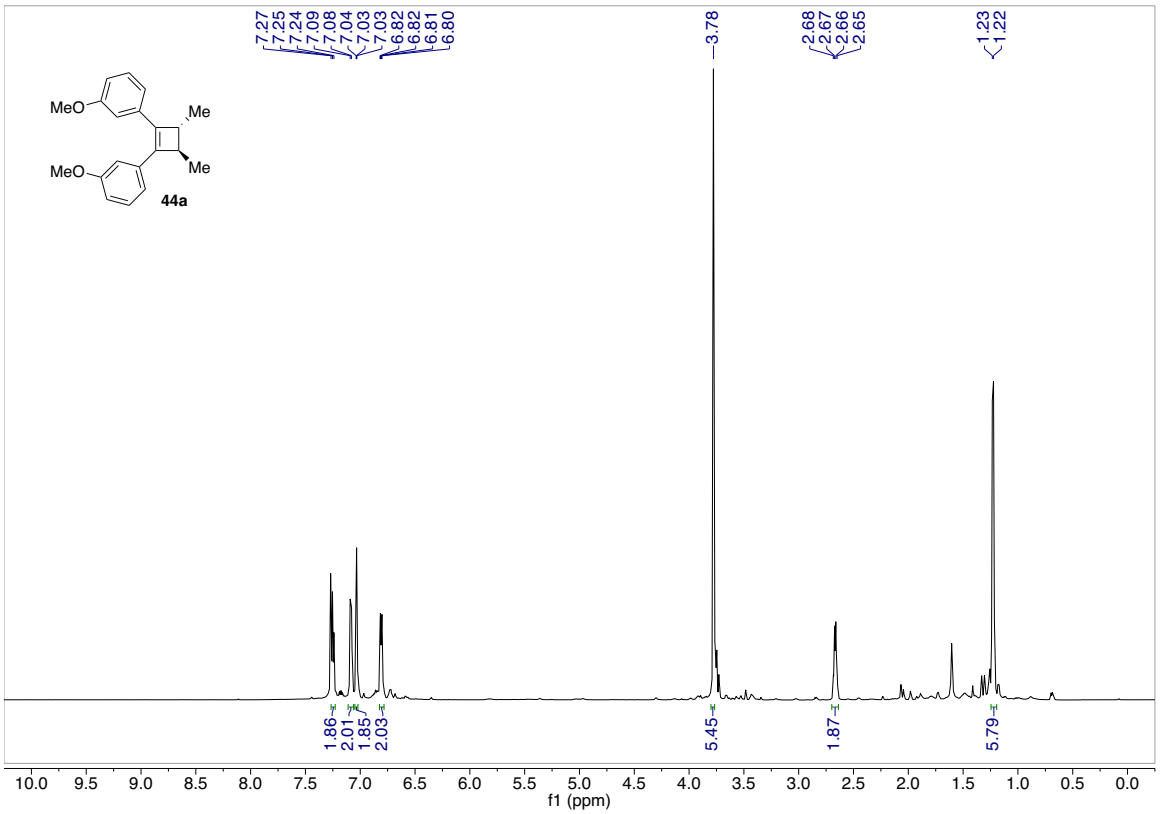
7.27
7.25
7.24
7.09
7.08
7.04
7.03
7.03
6.82
6.82
6.81
6.80
3.78
2.68
2.67
2.66
2.65
1.23
1.22
MeO
Me
MeO
Me
44a
1.86
2.01
1.85
2.03
5.45
1.87
5.79
10.0 9.5 9.0 8.5 8.0 7.5 7.0 6.5 6.0 5.5 5.0 4.5 4.0 3.5 3.0 2.5 2.0 1.5 1.0 0.5 0.0
f1 (ppm)

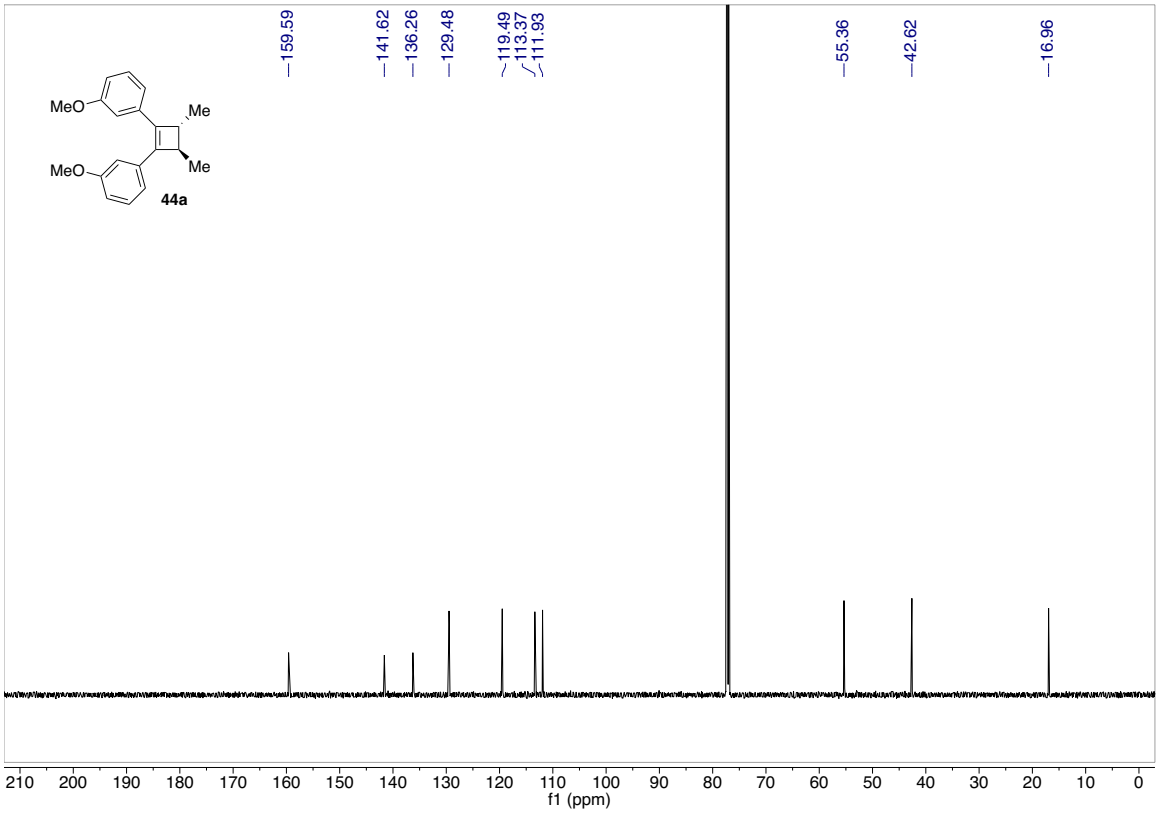
159.59
141.62
136.26
129.48
119.49
113.37
111.93
55.36
42.62
16.96
MeO
Me
MeO
Me
44a
210 200 190 180 170 160 150 140 130 120 110 100 90 80 70 60 50 40 30 20 10 0
f1 (ppm)

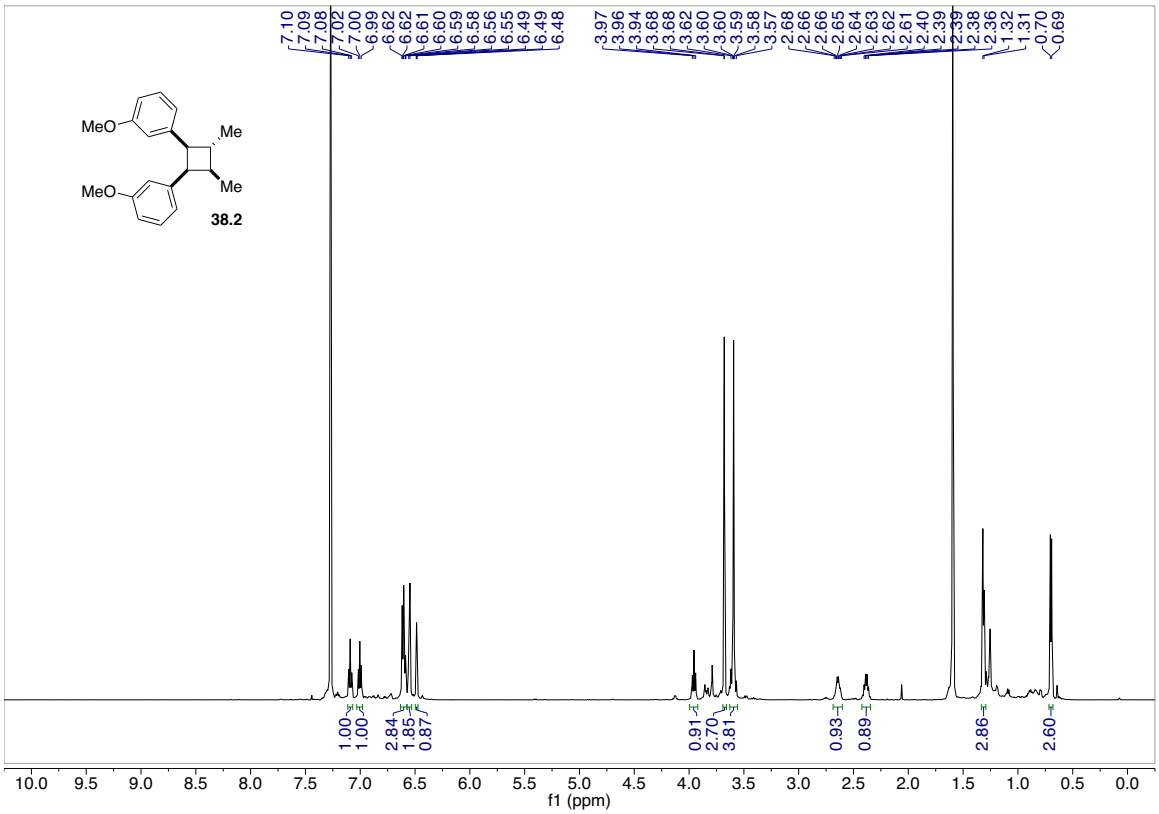
MeO
Me
MeO
Me
38.2
7.10
7.09
7.08
7.02
7.00
6.99
6.62
6.62
6.61
6.60
6.59
6.58
6.56
6.55
6.49
6.49
6.48
3.97
3.96
3.94
3.68
3.62
3.60
3.60
3.59
3.58
3.57
2.68
2.66
2.66
2.65
2.64
2.63
2.62
2.61
2.40
2.39
2.39
2.38
2.36
1.32
1.31
0.70
0.69
1.00
1.00
2.84
1.85
0.87
0.91
2.70
3.81
0.93
0.89
2.86
2.60
10.0 9.5 9.0 8.5 8.0 7.5 7.0 6.5 6.0 5.5 5.0 4.5 4.0 3.5 3.0 2.5 2.0 1.5 1.0 0.5 0.0
f1 (ppm)

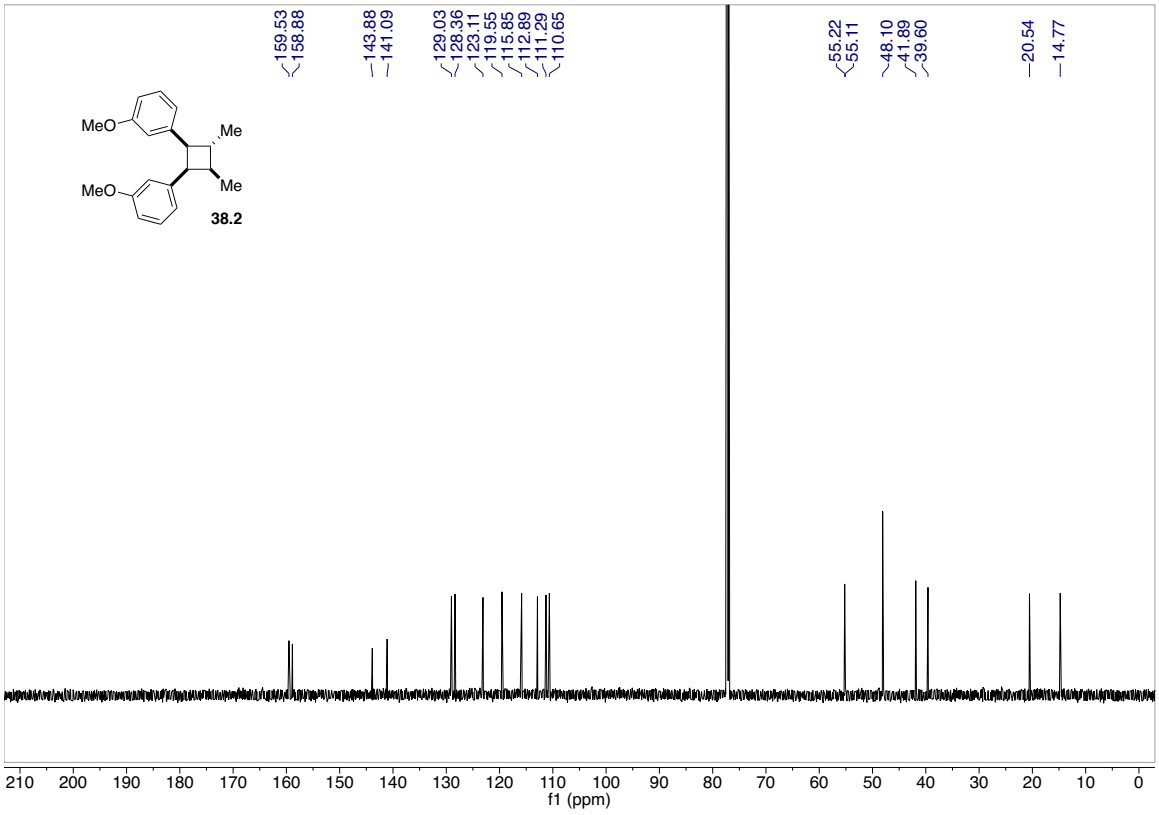
MeO
Me
MeO
Me
38.2
159.53
158.88
143.88
141.09
129.03
128.36
123.11
119.55
115.85
112.89
111.29
110.65
55.22
55.11
48.10
41.89
39.60
20.54
14.77
210 200 190 180 170 160 150 140 130 120 110 100 90 80 70 60 50 40 30 20 10 0
f1 (ppm)

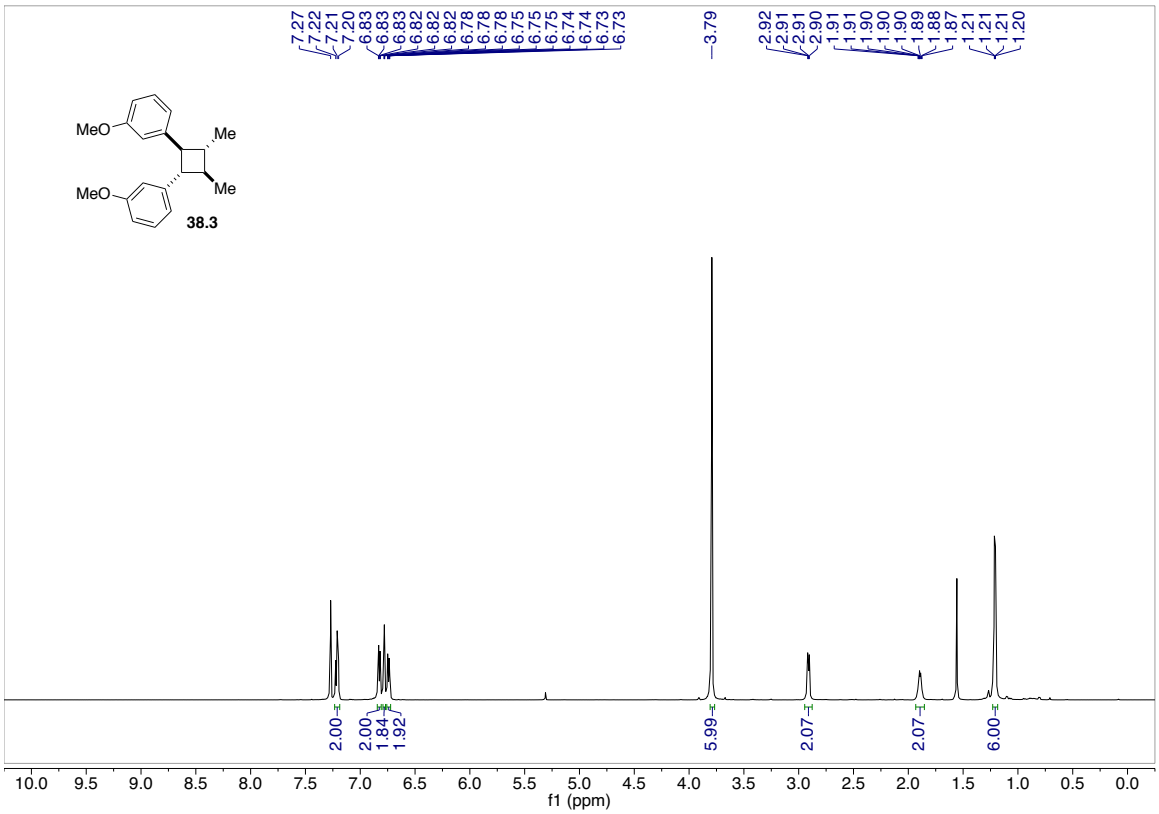
7.27
7.22
7.21
7.20
6.83
6.83
6.83
6.82
6.82
6.82
6.78
6.78
6.78
6.75
6.75
6.75
6.74
6.74
6.73
6.73
3.79
2.92
2.91
2.91
2.90
1.91
1.91
1.90
1.90
1.90
1.89
1.88
1.87
1.21
1.21
1.21
1.20
MeO
Me
MeO
Me
38.3
2.00
2.00
1.84
1.92
5.99
2.07
2.07
6.00
10.0 9.5 9.0 8.5 8.0 7.5 7.0 6.5 6.0 5.5 5.0 4.5 4.0 3.5 3.0 2.5 2.0 1.5 1.0 0.5 0.0
f1 (ppm)

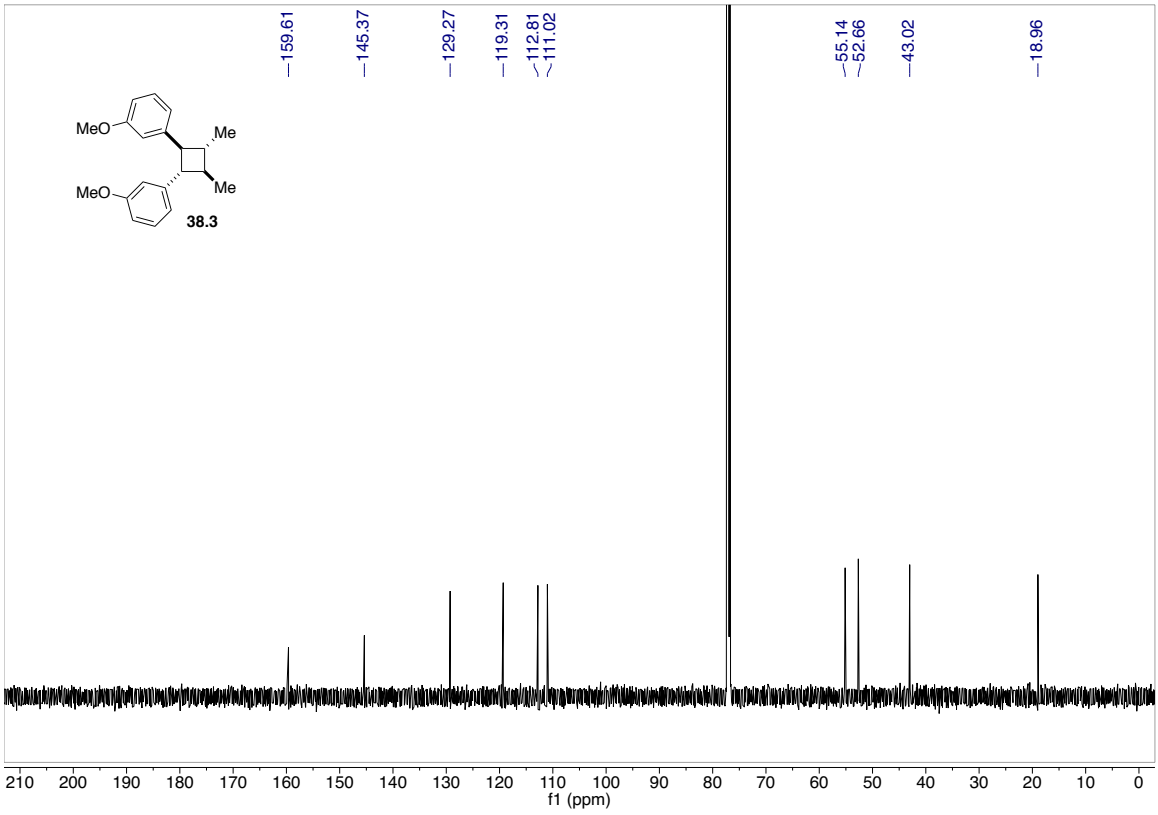
159.61
145.37
129.27
119.31
112.81
111.02
55.14
52.66
43.02
18.96
MeO
Me
MeO
Me
38.3
210 200 190 180 170 160 150 140 130 120 110 100 90 80 70 60 50 40 30 20 10 0
f1 (ppm)

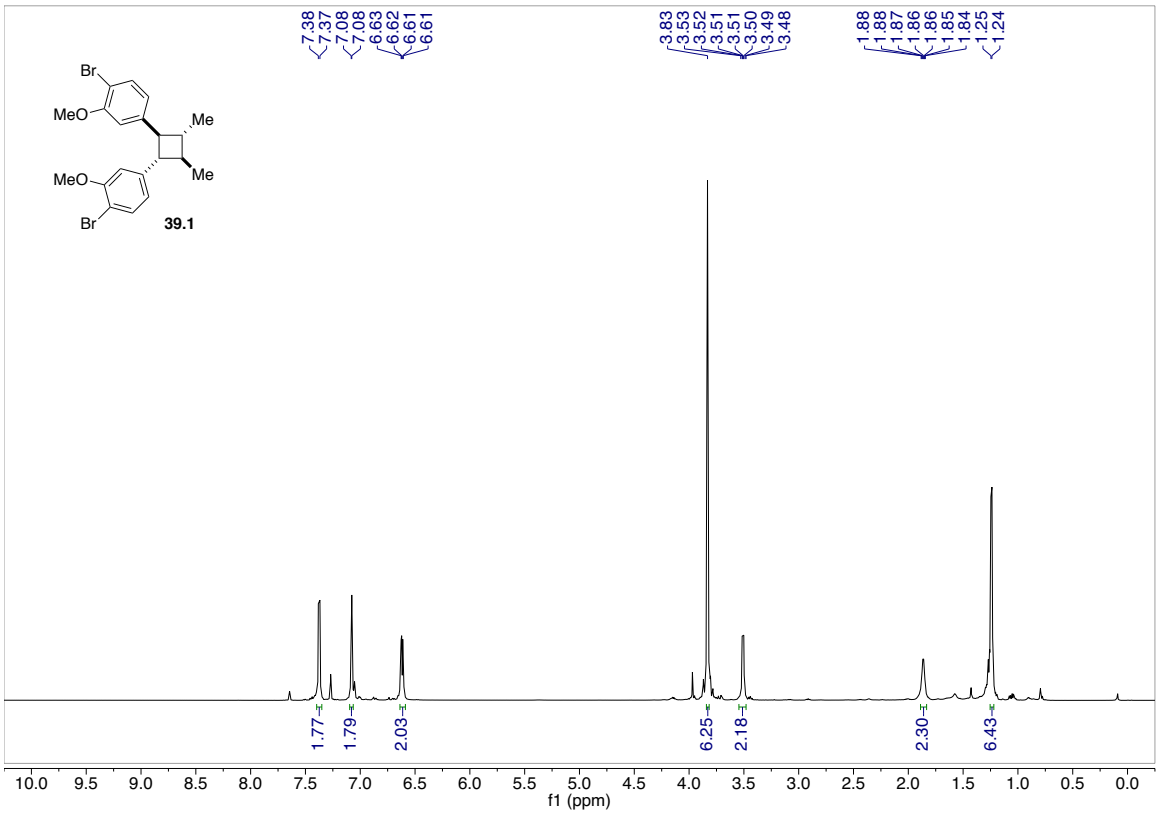
7.38
7.37
7.08
7.08
6.63
6.62
6.61
6.61
3.83
3.53
3.52
3.51
3.51
3.50
3.49
3.48
1.88
1.88
1.87
1.86
1.86
1.85
1.84
1.25
1.24
Br
MeO
Me
Me
MeO
Br
39.1
1.77
1.79
2.03
6.25
2.18
2.30
6.43
10.0 9.5 9.0 8.5 8.0 7.5 7.0 6.5 6.0 5.5 5.0 4.5 4.0 3.5 3.0 2.5 2.0 1.5 1.0 0.5 0.0
f1 (ppm)

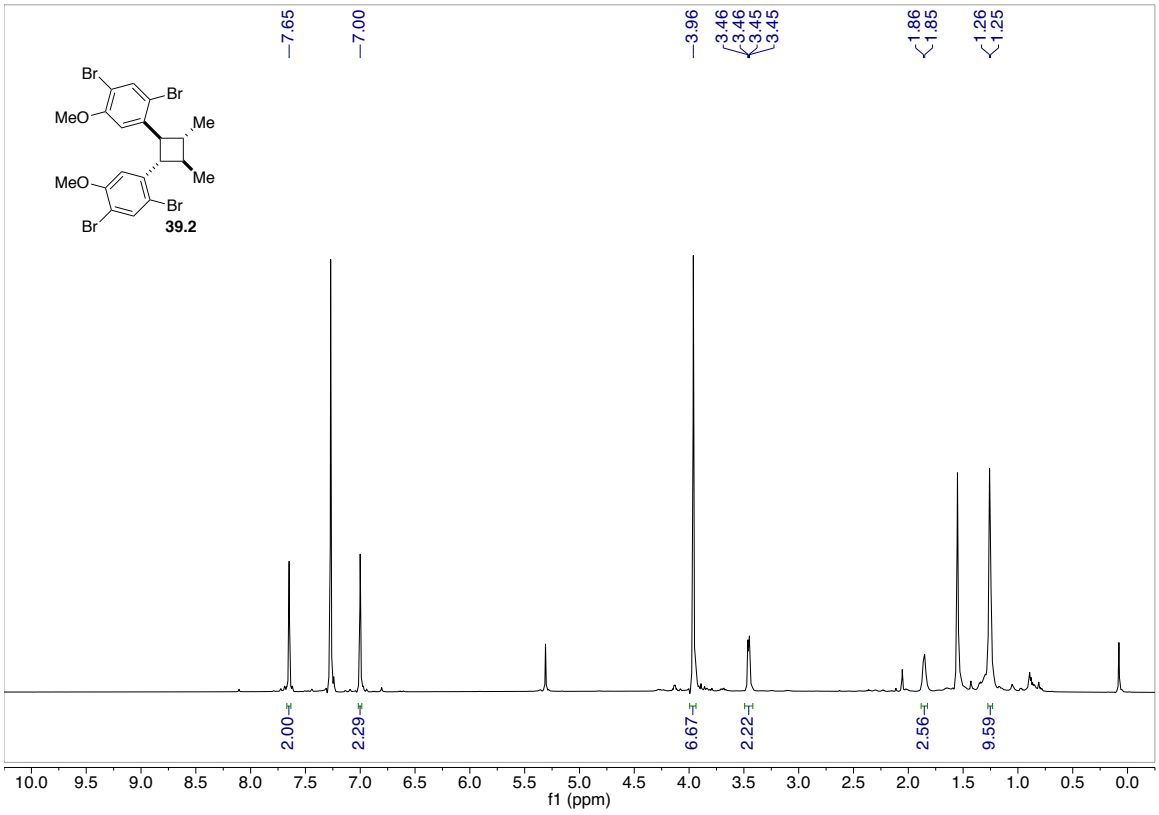
7.65
7.00
3.96
3.46
3.46
3.45
3.45
1.86
1.85
1.26
1.25
Br
Br
MeO
Me
Me
MeO
Br
Br
39.2
2.00
2.29
6.67
2.22
2.56
9.59
10.0 9.5 9.0 8.5 8.0 7.5 7.0 6.5 6.0 5.5 5.0 4.5 4.0 3.5 3.0 2.5 2.0 1.5 1.0 0.5 0.0
f1 (ppm)

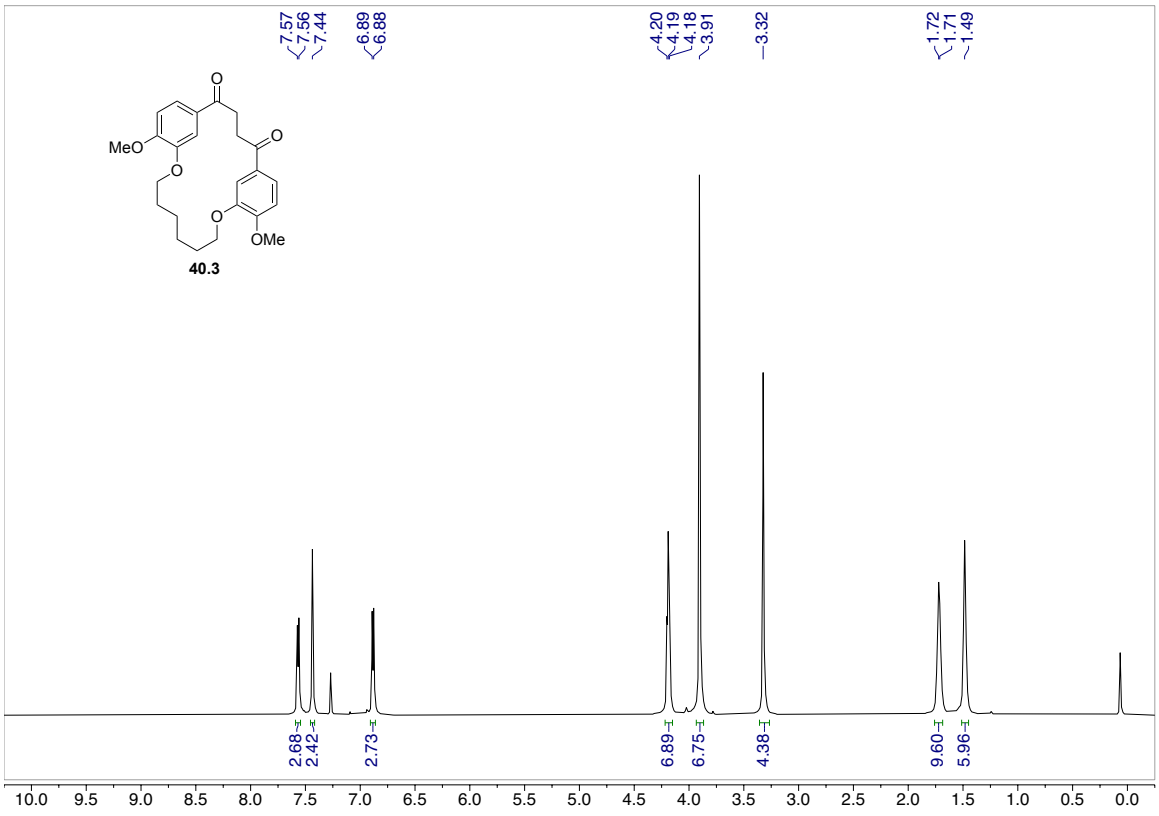
7.57
7.56
7.44
6.89
6.88
4.20
4.19
4.18
3.91
3.32
1.72
1.71
1.49
MeO
O
O
O
O
OMe
40.3
2.68
2.42
2.73
6.89
6.75
4.38
9.60
5.96
10.0 9.5 9.0 8.5 8.0 7.5 7.0 6.5 6.0 5.5 5.0 4.5 4.0 3.5 3.0 2.5 2.0 1.5 1.0 0.5 0.0

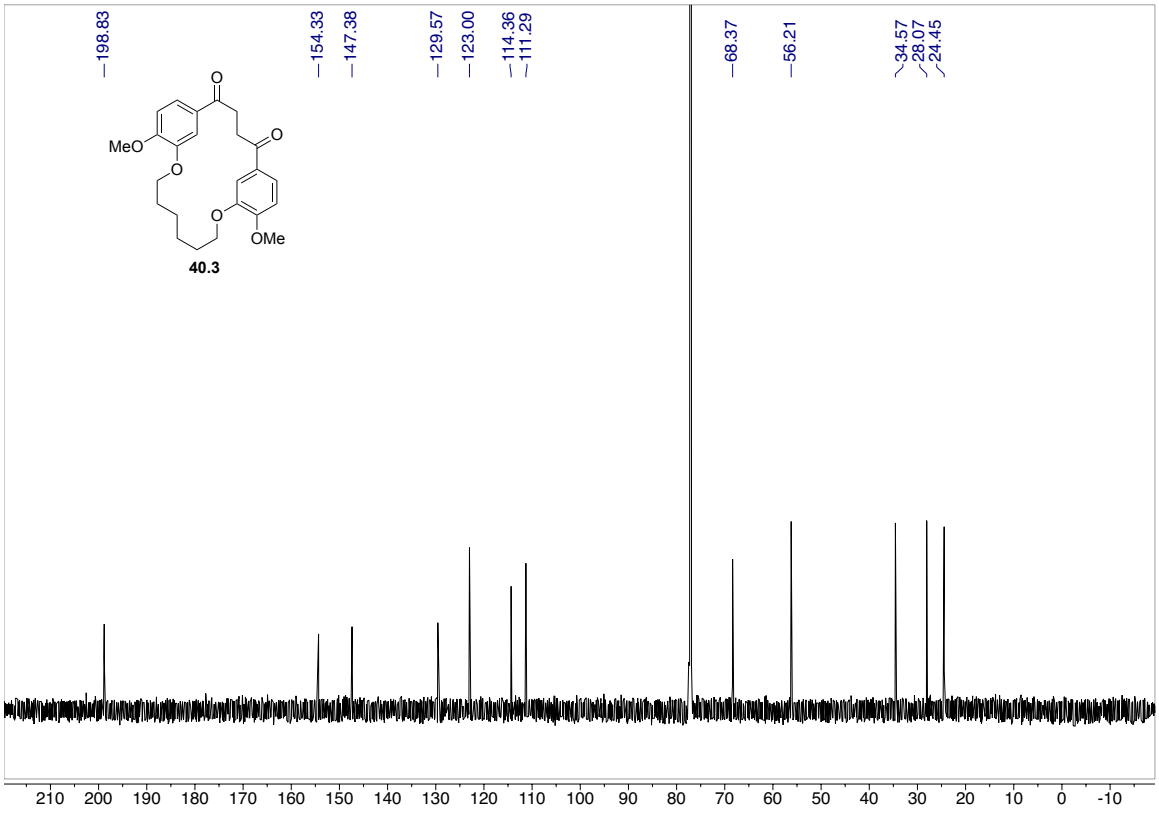
198.83
154.33
147.38
129.57
123.00
114.36
111.29
68.37
56.21
34.57
28.07
24.45
MeO
O
O
O
O
OMe
40.3
210 200 190 180 170 160 150 140 130 120 110 100 90 80 70 60 50 40 30 20 10 0 -10

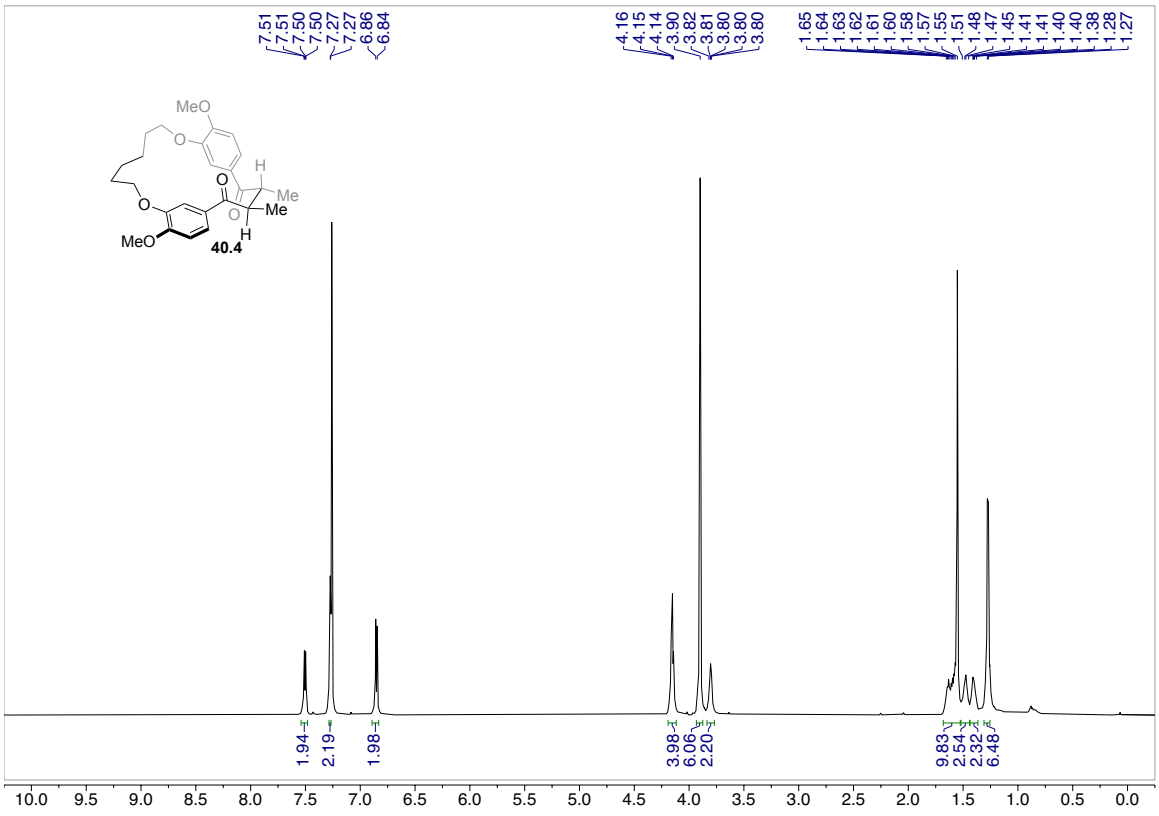
7.51
7.51
7.50
7.50
7.27
7.27
6.86
6.84
4.16
4.15
4.14
3.90
3.82
3.81
3.80
3.80
3.80
1.65
1.64
1.63
1.62
1.61
1.60
1.58
1.57
1.55
1.51
1.48
1.47
1.45
1.41
1.41
1.40
1.40
1.38
1.28
1.27
MeO
O
H
O
Me
Me
O
O
MeO
H
40.4
1.94
2.19
1.98
3.98
6.06
2.20
9.83
2.54
2.32
6.48
10.0
9.5
9.0
8.5
8.0
7.5
7.0
6.5
6.0
5.5
5.0
4.5
4.0
3.5
3.0
2.5
2.0
1.5
1.0
0.5
0.0

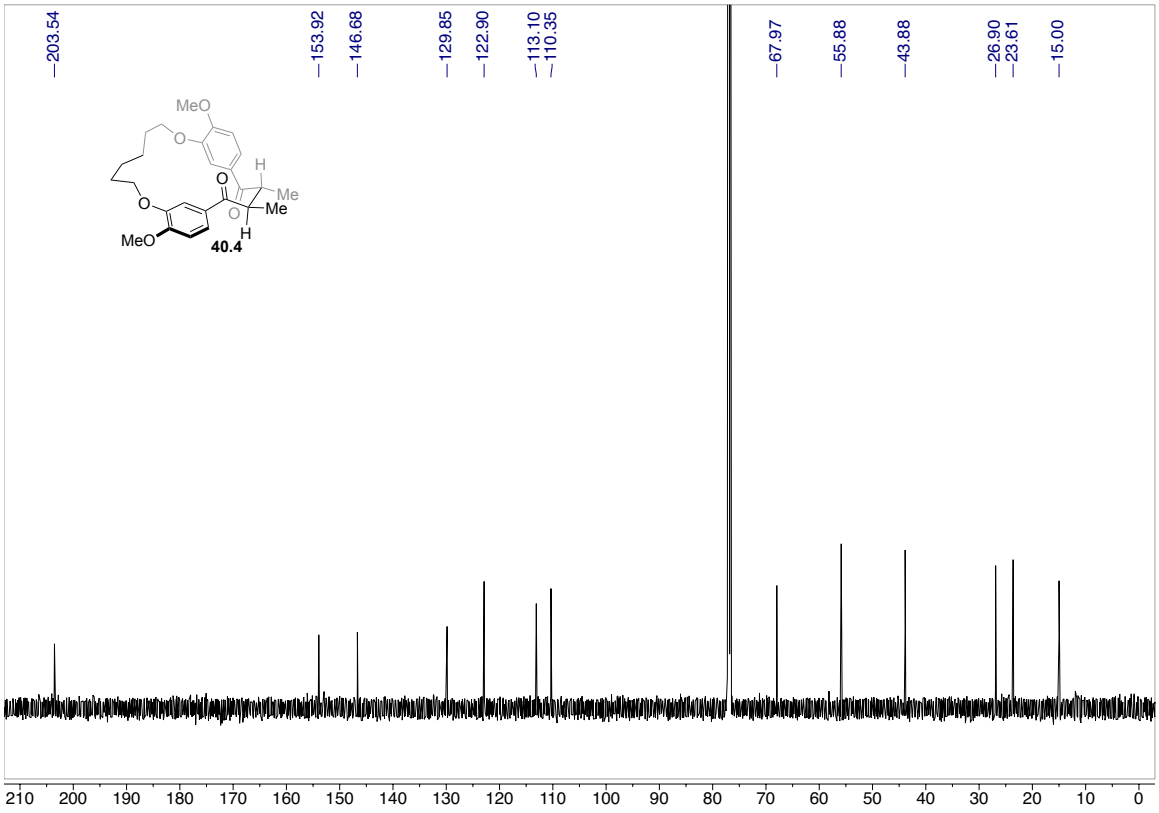
203.54
153.92
146.68
129.85
122.90
113.10
110.35
67.97
55.88
43.88
26.90
23.61
15.00
MeO
O
H
O
Me
Me
O
O
MeO
H
40.4
210
200
190
180
170
160
150
140
130
120
110
100
90
80
70
60
50
40
30
20
10
0

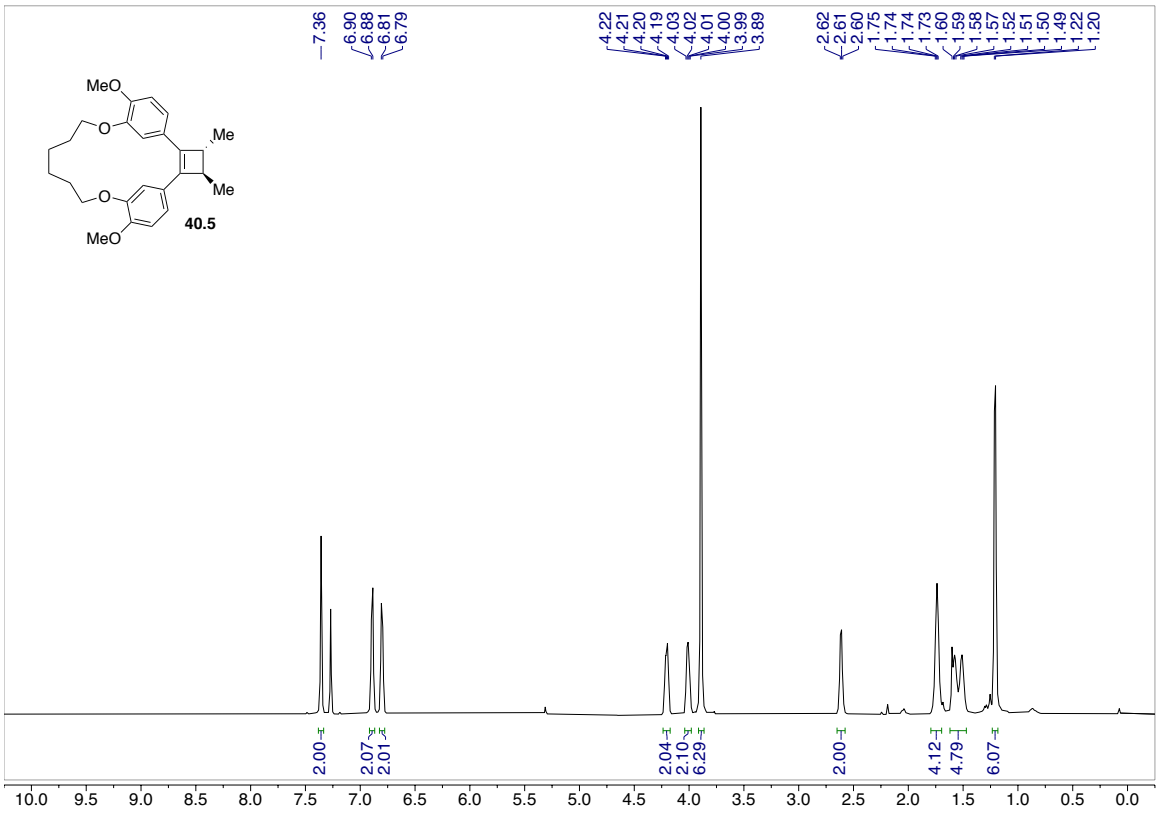
7.36
6.90
6.88
6.81
6.79
4.22
4.21
4.20
4.19
4.03
4.02
4.01
4.00
3.99
3.89
2.62
2.61
2.60
1.75
1.74
1.74
1.73
1.60
1.59
1.58
1.57
1.52
1.51
1.50
1.49
1.22
1.20
MeO
O
Me
Me
O
MeO
40.5
2.00
2.07
2.01
2.04
2.10
6.29
2.00
4.12
4.79
6.07
10.0 9.5 9.0 8.5 8.0 7.5 7.0 6.5 6.0 5.5 5.0 4.5 4.0 3.5 3.0 2.5 2.0 1.5 1.0 0.5 0.0

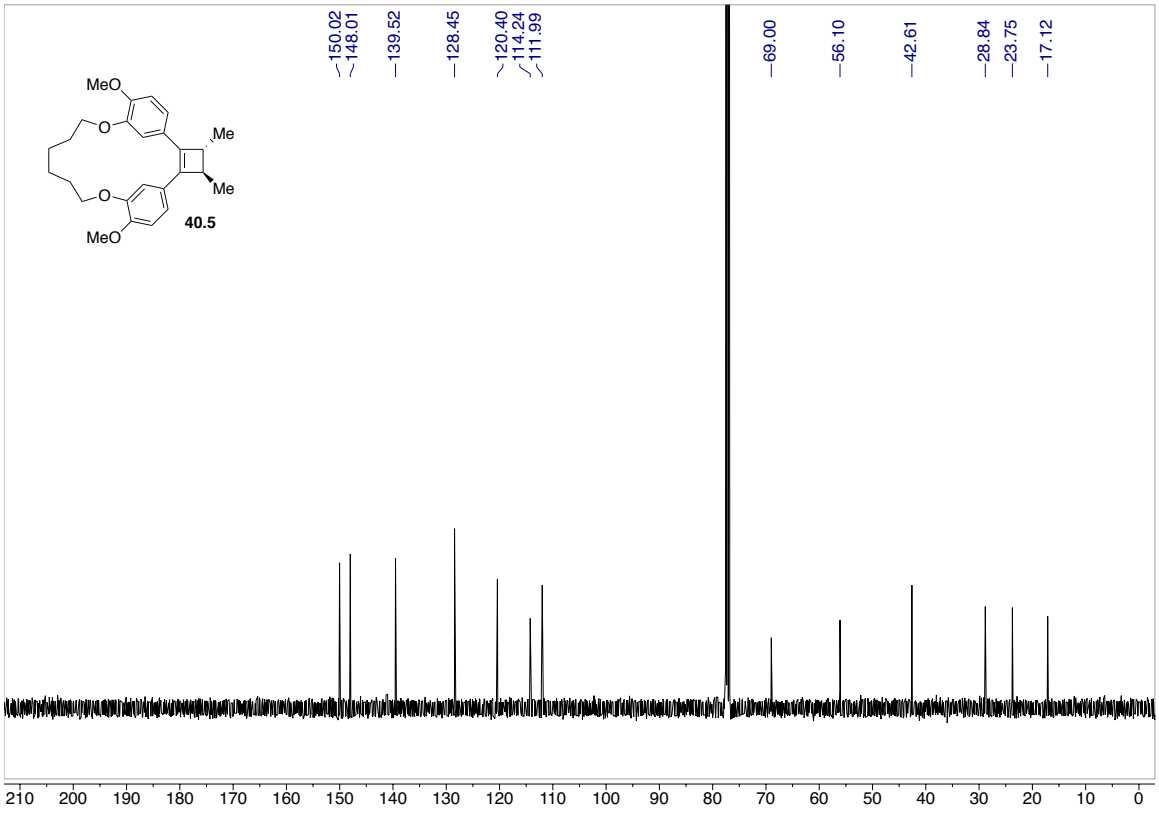
150.02
148.01
139.52
128.45
120.40
114.24
111.99
69.00
56.10
42.61
28.84
23.75
17.12
MeO
O
Me
Me
O
MeO
40.5
210 200 190 180 170 160 150 140 130 120 110 100 90 80 70 60 50 40 30 20 10 0

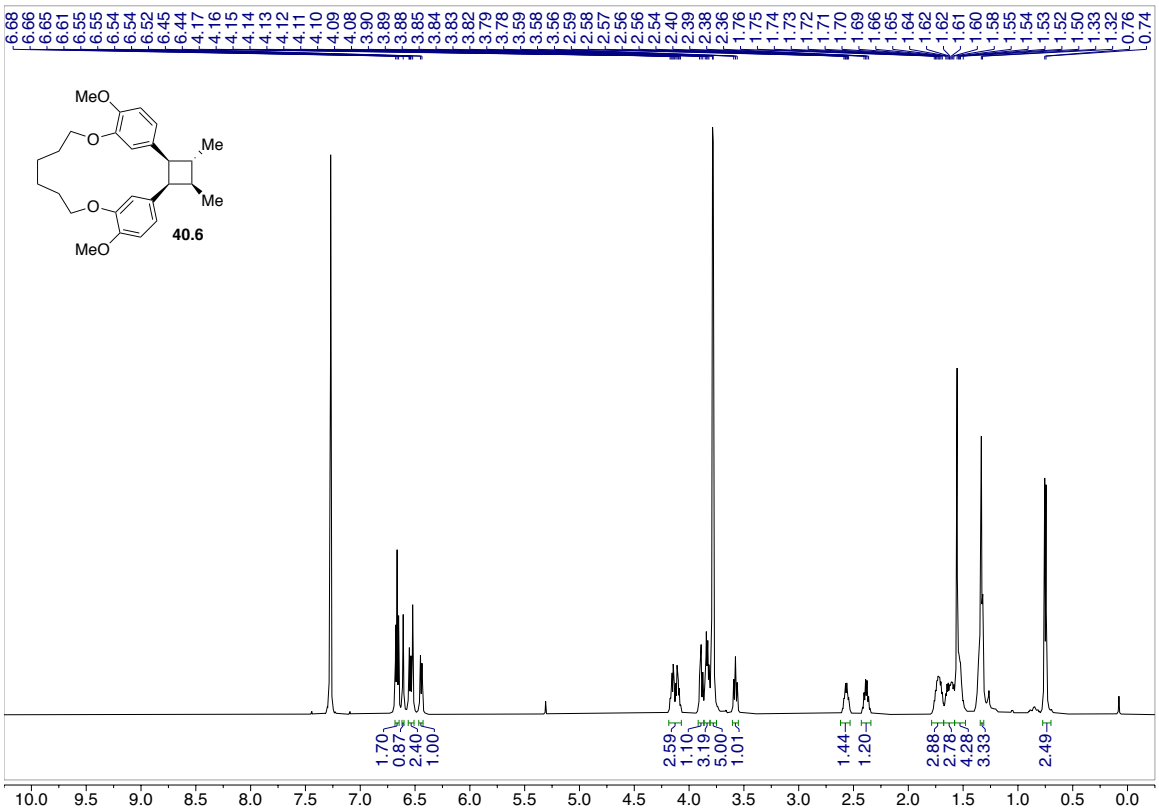
MeO
O
Me
Me
O
MeO
40.6

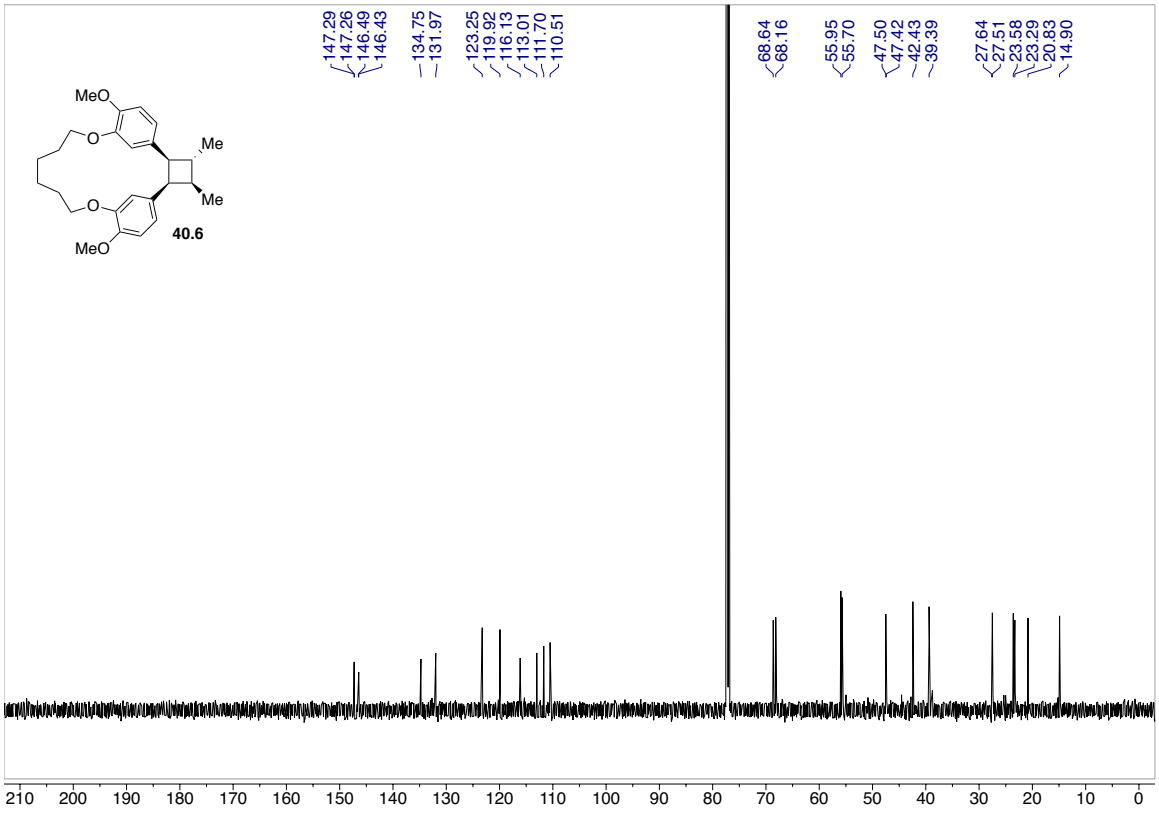
MeO
O
Me
Me
O
MeO
40.6

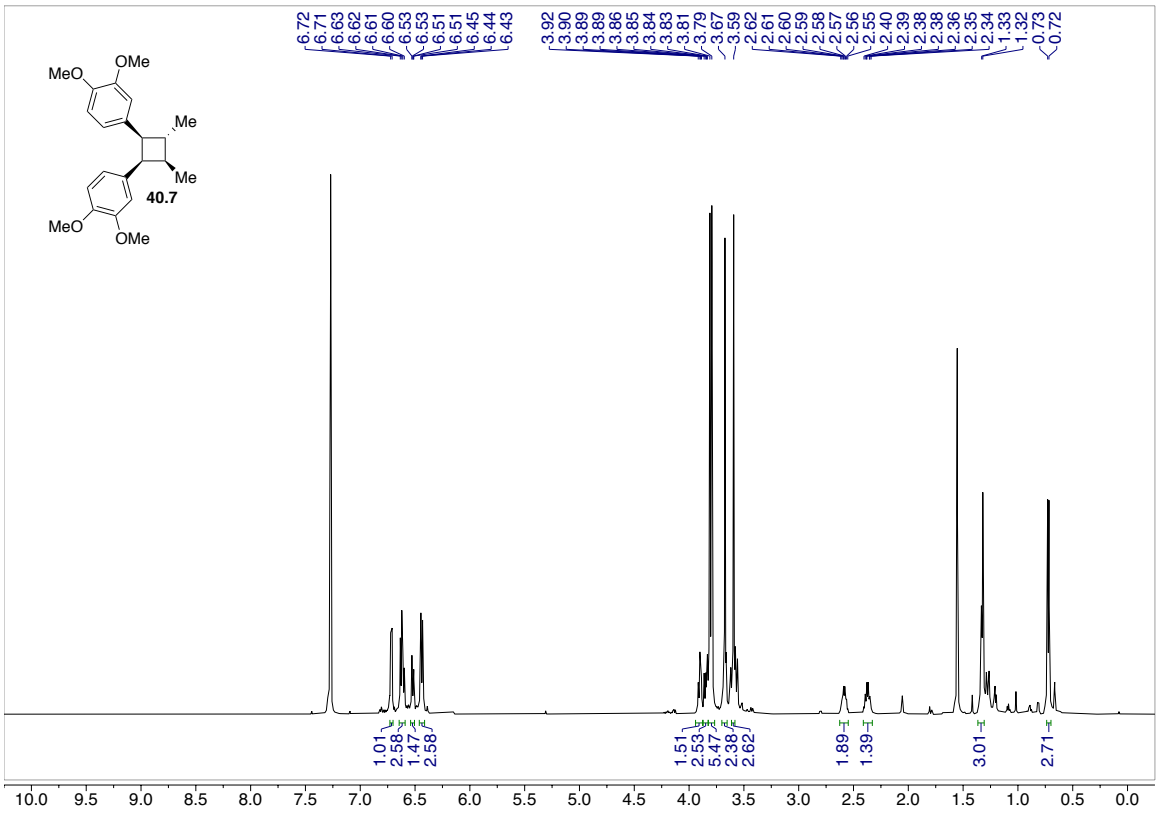
6.72
6.71
6.63
6.62
6.61
6.60
6.53
6.53
6.51
6.51
6.45
6.44
6.43
3.92
3.90
3.89
3.89
3.86
3.85
3.84
3.83
3.81
3.79
3.67
3.59
2.62
2.61
2.60
2.59
2.58
2.57
2.56
2.55
2.40
2.39
2.38
2.38
2.36
2.35
2.34
1.33
1.32
0.73
0.72
OMe
MeO
Me
Me
40.7
MeO
OMe
1.01
2.58
1.47
2.58
1.51
2.53
5.47
2.38
2.62
1.89
1.39
3.01
2.71
10.0
9.5
9.0
8.5
8.0
7.5
7.0
6.5
6.0
5.5
5.0
4.5
4.0
3.5
3.0
2.5
2.0
1.5
1.0
0.5
0.0

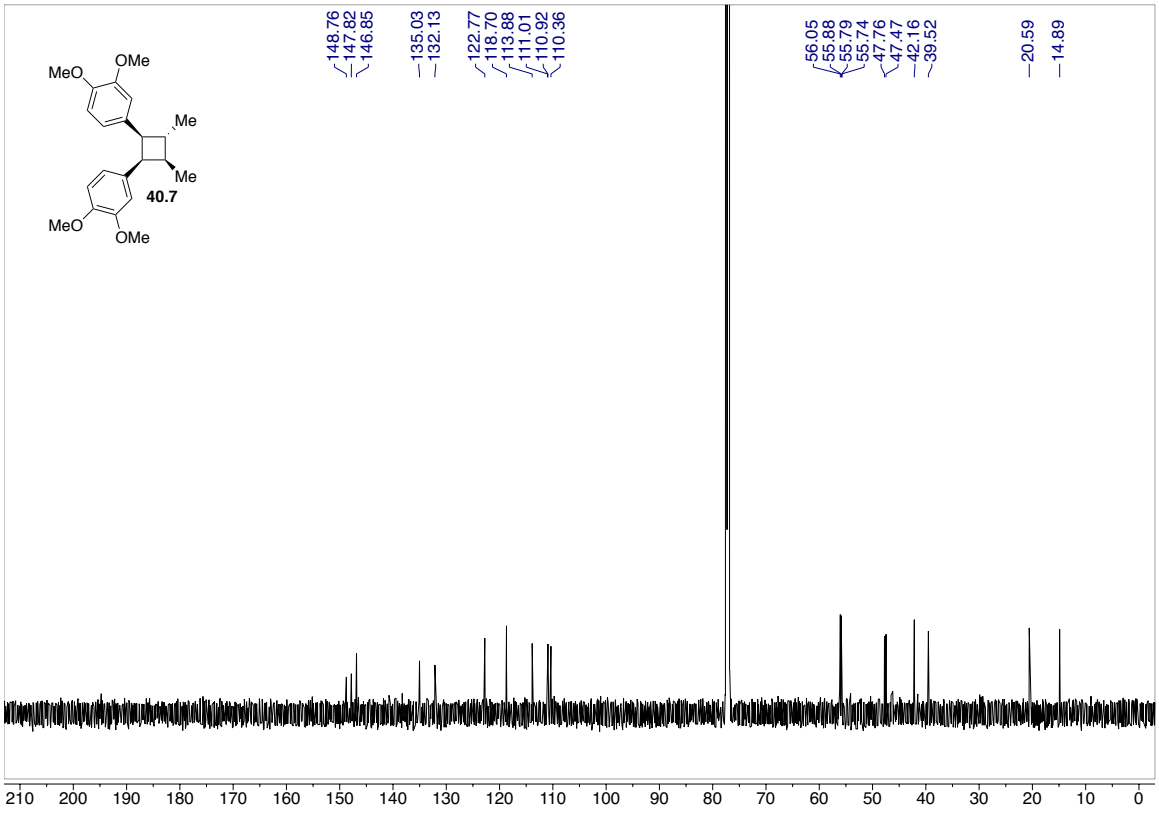
148.76
147.82
146.85
135.03
132.13
122.77
118.70
113.88
111.01
110.92
110.36
56.05
55.88
55.79
55.74
47.76
47.47
42.16
39.52
20.59
14.89
OMe
MeO
Me
Me
40.7
MeO
OMe
210
200
190
180
170
160
150
140
130
120
110
100
90
80
70
60
50
40
30
20
10
0

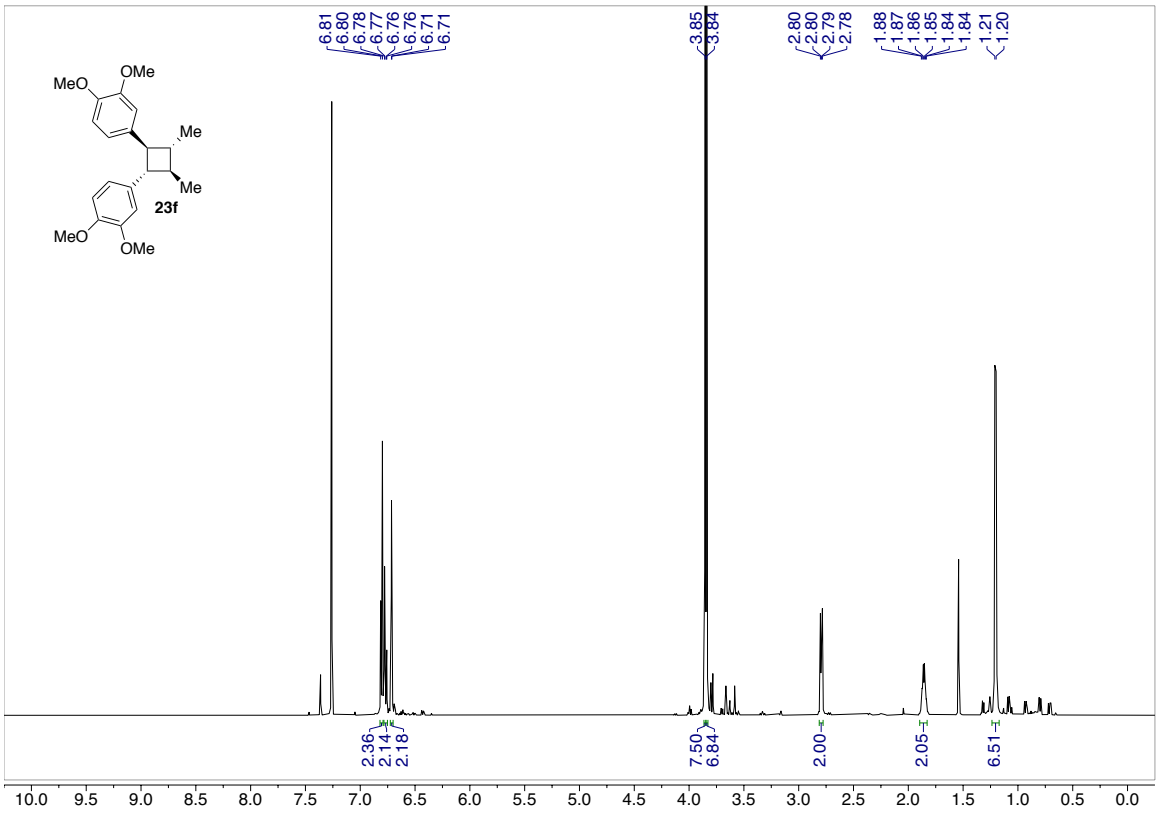
6.81
6.80
6.78
6.77
6.76
6.76
6.71
6.71
3.85
3.84
2.80
2.80
2.79
2.78
1.88
1.87
1.86
1.85
1.84
1.84
1.21
1.20
MeO
OMe
Me
Me
23f
MeO
OMe
2.36
2.14
2.18
7.50
6.84
2.00
2.05
6.51
10.0 9.5 9.0 8.5 8.0 7.5 7.0 6.5 6.0 5.5 5.0 4.5 4.0 3.5 3.0 2.5 2.0 1.5 1.0 0.5 0.0

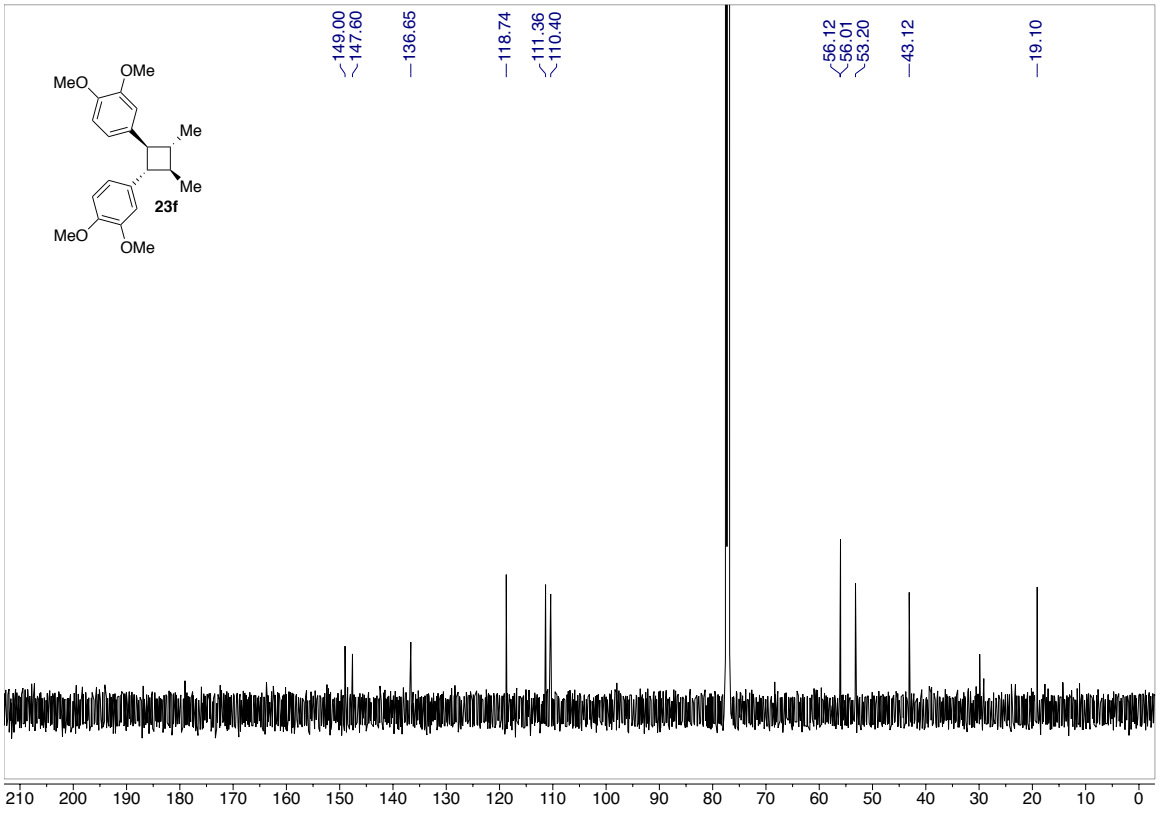
149.00
147.60
136.65
118.74
111.36
110.40
56.12
56.01
53.20
43.12
19.10
MeO
OMe
Me
Me
23f
MeO
OMe
210 200 190 180 170 160 150 140 130 120 110 100 90 80 70 60 50 40 30 20 10 0